# The Expression of ADAM-9 and -10 in Prostate Cancer and Their Regulation by Dihydrotestosterone, Insulin-like Growth Factor-1 and Epidermal Growth Factor.

**A thesis submitted to the Queensland University of Technology, Brisbane, Queensland, Australia by:**

**Daniel R. McCulloch.**

BAppSc (Hons), AD Biol. Lab. Tech.



To fulfil the requirements of the degree of Doctor of Philosophy in the Science Research Center, School of Life Sciences.

June 2003

**QUEENSLAND UNIVERSITY OF TECHNOLOGY**

**DOCTOR OF PHILOSOPHY THESIS EXAMINATION**

| | |
|---|---|
| **CANDIDATE NAME:** | *Daniel McCulloch* |
| **CENTRE/RESEARCH CONCENTRATION:** | *Hormone Dependent Cancer* |
| **PRINCIPAL SUPERVISOR:** | *Prof Adrian Herington* |
| **ASSOCIATE SUPERVISOR(S):** | *Dr Dimitri Odorico* |
| **THESIS TITLE:** | *The Expression of ADAM-9 and –10 in Prostate Cancer and their Regulation by Dihydrotestosterone, Insulin-like Growth Factor-1 and Epidermal Growth Factor* |

*Under the requirements of PhD regulation 16.8, the above candidate presented a Final Seminar that was open to the public. A Faculty Panel of three academics attended and reported on the readiness of the thesis for external examination. The members of the panel recommended that the thesis be forwarded to the appointed Committee for examination.*

*Name:* PROF A. HERINGTON ..... *Signature:* .... QUT Verified Signature .....
***Panel Chairperson*** *(Principal Supervisor)*

*Name:* Dr Eliza J Whiteside ..... *Signature:* QUT Verified Signature .....
*Panel Member*

*Name:* DR. JOHN P. HOOPER ..... *Signature:* QUT Verified Signature.....
*Panel Member*

*Name:* ASSOC PROF C. Phillips Morris ..... *Signature:* QUT Verified Signature .....
*Panel Member*

*Under the requirements of PhD regulations, Section 16, it is hereby certified that the thesis of the above-named candidate has been examined. I recommend on behalf of the Examination Committee that the thesis be accepted in fulfilment of the conditions for the award of the degree of Doctor of Philosophy.*

*Name:* PROF P. TIMMS ..... *Signature:* QUT Verified Signature *Date:* 22/10/2003
***Chair of Examiners (Head of School or nominee)*** *(Examination Committee)*

## STATEMENT OF AUTHORSHIP

The work presented in this thesis is to the best of my knowledge and belief original, except when acknowledged within the text. This material has not been submitted in part or in whole for a degree at this or any other university.



**Daniel R. McCulloch.**

## KEY WORDS

A Disintegrin and Metalloprotease domain (ADAM), Prostate Cancer, Metastasis, Matrix Metalloprotease, Integrin, Dihydrotestosterone, Insulin-like Growth Factor-1, Epidermal Growth Factor, Extracellular Matrix, Androgen.

## ABSTRACT

Prostate cancer (PCa) is the most common cause of cancer death amongst Western males. PCa occurs in two distinct stages. In its early stage, growth and development is dependent primarily on male sex hormones (androgens) such as testosterone, although other growth factors have roles maintaining PCa cell survival in this stage. In the later stage of PCa development, growth and maintenance is independent of androgen stimulation and growth factors including Insulin-like Growth Factor -1 (IGF-1) and Epidermal Growth Factor (EGF) are thought to have more crucial roles in cell survival and PCa progression.

PCa, in its late stages, is highly aggressive and metastatic, that is, tumorigenic cells migrate from the primary site of the body (prostate) and travel via the systemic and lymphatic circulation, residing and colonising in the bone, lymph node, lung, and in more rare cases, the brain. Metastasis involves both cell migration and tissue degradation activities. The degradation of the extracellular matrix (ECM), the tissue surrounding the organ, is mediated in part by members of a family of 26 proteins called the Matrix Metalloproteases (MMPs), whilst cell adhesion molecules, of which proteins known as Integrins are included, mediate cell migration. A family of proteins known as the ADAMs (A Disintegrin And Metalloprotease domain) were a recently characterised family at the commencement of this study and now comprise 34 members. Because of their dual nature, possessing an active metalloprotease domain, homologous to that of the MMPs, and an integrin-binding domain capable of regulating cell-cell and cell-ECM contacts, it was thought likely that members of the ADAMs family may have implications for the progression of aggressive cancers such as those of the prostate.

This study focussed on two particular ADAMs -9 and -10. ADAM-9 has an active metalloprotease domain, which has been shown to degrade constituents of the ECM, including fibronectin, *in vitro*. It also has an integrin-binding capacity through association with key integrins involved in PCa progression, such as $\alpha 6\beta 1$. ADAM-10 has no such integrin binding activities, but its bovine orthologue, MADM, is able to degrade collagen type IV, a major component of basement membranes. It is likely human ADAM-10 has the

same activity. It is also known to cleave L1 - a protein involved in cell anchorage activities - and collagen type XVII - which is a principal component of the hemidesmosomes of cellular tight junctions. The cleavage of these proteins enables the cell to be released from the surrounding environment and commence migratory activities, as required in metastasis.

Previous studies in this laboratory showed the mRNA expression of the five ADAMs -9, -10, -11, -15 and -17 in PCa cell lines, characteristic of androgen-dependent and androgen-independent disease. These studies were furthered by the characterisation of ADAM-9, -10 and -17 mRNA regulation by Dihydrotestosterone (DHT) in the androgen-responsive cell line (LNCaP). ADAM-9 and -10 mRNA levels were elevated in response to DHT stimulation. Further to these observations, the expression of ADAM-9 and -10 was shown in primary prostate biopsies from patients with PCa. ADAM-10 was expressed in the cytoplasm and on the cell membrane in epithelial and basal cells of benign prostate glands, but in high-grade PCa glands, ADAM-10 expression was localised to the nucleus and its expression levels appeared to be elevated when compared to low-grade PCa glands. These studies provided a strong background for the hypothesis that ADAM-9 and -10 have key roles in the development of PCa and provided a basis for further studies.

The **aims** of this study were to: 1) characterise the expression, localisation and levels, of ADAM-9 and -10 mRNA and protein in cell models representing characteristics of normal through androgen-dependent to androgen-independent PCa, as well as to expand the primary PCa biopsy data for ADAM-9 and ADAM-10 to encompass PCa bone metastases 2) establish an *in vitro* cell system, which could express elevated levels of ADAM-10 so that functional cell-based assays such as cell migration, invasion and attachment could be carried out, and 3) to extend the previous hormonal regulation data, to fully characterise the response of ADAM-9 and -10 mRNA and protein levels to DHT, IGF-1, DHT plus IGF-1 and EGF in the hormonal/growth factor responsive cell line LNCaP.

For aim 1 (expression of ADAM-9 and -10 mRNA and protein), ADAM-9 and -10 mRNA were characterised by RT-PCR, while their protein products were analysed by Western blot. Both ADAM-9 and -10 mRNA and protein were expressed at readily detectable

levels across progressively metastatic PCa cell lines model that represent characteristics of low-grade, androgen-dependent (LNCaP and C4) to high-grade, androgen-independent (C4-2 and C4-2B) PCa. When the non-tumorigenic prostate cell line RWPE-1 was compared with the metastatic PCa cell line PC-3, differential expression patterns were seen by Western blot analysis. For ADAM-9, the active form was expressed at higher levels in RWPE-1, whilst subcellular fractionation showed that the active form of ADAM-9 was predominantly located in the cell nucleus. For ADAM-10, in both of the cell lines, a nuclear specific isoform of the mature, catalytically active ADAM-10 was found. This isoform differed by ~2 kDa in Mr (smaller) than the cytoplasmic specific isoform. Unprocessed ADAM-10 was readily detected in RWPE-1 cell lines but only occasionally detected in PC-3 cell lines. Immunocytochemistry using ADAM-9 and -10 specific antibodies confirmed nuclear, cytoplasmic and membrane expression of both ADAMs in these two cell lines. To examine the possibility of ADAM-9 and -10 being shed into the extracellular environment, membrane vesicles that are constitutively shed from the cell surface and contain membrane-associated proteins were collected from the media of the prostate cell lines RWPE-1, LNCaP and PC-3. ADAM-9 was readily detectable in RWPE-1 and LNCaP cell membrane vesicles by Western blot analysis, but not in PC-3 cells, whilst the expression of ADAM-10 was detected in shed vesicles from each of these prostate cell lines.

By Laser Capture Microdissection (LCM), secretory epithelial cells of primary prostate gland biopsies were isolated from benign and malignant glands. These secretory cells, by Western blot analysis, expressed similar Mr bands for ADAM-9 and -10 that were found in PCa cell lines *in vitro*, indicating that the nuclear specific isoform of ADAM-10 was present in PCa primary tumours and may represent the predominantly nuclear form of ADAM-10 expression, previously shown in high-grade PCa by immunohistochemistry (IHC). ADAM-9 and -10 were also examined by IHC in bone metastases taken from PCa patients at biopsy. Both ADAMs could be detected at levels similar to those shown for Prostate Specific Antigen (PSA) in these biopsies. Furthermore, both ADAM-9 and -10 were predominantly membrane- bound with occasional nuclear expression.

For aim 2, to establish a cell system that over-expressed levels of ADAM-10, two full-length ADAM-10 mammalian expression vectors were constructed; ADAM-10 was cloned into pcDNA3.1, which contains a CMV promoter, and into pMEP4, containing an inducible metallothionine promoter, whose activity is stimulated by the addition of $CdCl_2$. The efficiency of these two constructs was tested by way of transient transfection in the PCa cell line PC-3, whilst the pcDNA3.1 construct was also tested in the RWPE-1 prostate cell line. Resultant Western blot analysis for all transient transfection assays showed that levels of ADAM-10 were not significantly elevated in any case, when compared to levels of the housekeeping gene β-Tubulin, despite testing various levels of vector DNA, and, for pMEP4, the induction of the transfected cell system with different degrees of stimulation with $CdCl_2$ to activate the metallothionine promoter post-transfection. Another study in this laboratory found similar results when the same full length ADAM-10 sequence was cloned into a Green Fluorescent Protein (GFP) expressing vector, as no fluorescence was observed by means of transient transfection in the same, and other, PCa cell lines. It was hypothesised that the Kozak sequence included in the full-length construct (human ADAM-10 naturally occurring sequence) is not strong enough to initiate translation in an artificial system, in cells, which, as described in Aim 1, are already expressing readily detectable levels of endogenous ADAM-10. As a result, time constraints prevented any further progress with Aim 2 and functional studies including cell attachment, invasion and migration were unable to be explored.

For Aim 3, to characterise the response of ADAM-9 and -10 mRNA and protein levels to DHT, IGF-1, DHT plus IGF-1 and EGF in LNCaP cells, the levels of ADAM-9 and -10 mRNA were not stimulated by DHT or IGF-1 alone, despite our previous observations that initially characterised ADAM-9 and -10 mRNA as being responsive to DHT. However, IGF-1 in synergy with DHT did significantly elevate mRNA levels of both ADAMs. In the case of ADAM-9 and -10 protein, the same trends of stimulation as found at the mRNA level were shown by Western blot analysis when ADAM-9 and -10 signal intensity was normalised with the housekeeping protein β-Tubulin. For EGF treatment, both ADAM-9 and -10 mRNA and protein levels were significantly elevated, and further investigation

found this to be the case for each of these ADAMs proteins in the nuclear fractions of LNCaP cells.

These studies are the first to describe extensively, the expression and hormonal/growth factor regulation of two members of the ADAMs family (-9 and -10) in PCa. These observations imply that the expression of ADAM-9 and -10 have varied roles in PCa whilst it develops from androgen-sensitive (early stage disease), through to an androgen-insensitive (late-stage), metastatic disease. Further studies are now required to investigate the several key areas of focus that this research has revealed, including:

- Investigation of the cellular mechanisms that are involved in actively transporting the ADAMs to the cell's nuclear compartment and the ADAMs functional roles in the cell nucleus.
- The construction of a full-length human ADAM-10 mammalian expression construct with the introduction of a new Kozak sequence, that elevates ADAM-10 expression in an *in vitro* cell system are required, so that functional assays such as cell invasion, migration and attachment may be carried out to find the functional consequences of ADAM expression on cellular behaviour.
- The regulation studies also need to be extended by confirming the preliminary observations that the nuclear levels of ADAMs may also be elevated by hormones and growth factors such as DHT, IGF-1 and EGF, as well as the regulation of levels of plasma membrane vesicle associated ADAM expression.

Given the data presented in this study, it is likely the ADAMs have differential roles throughout the development of PCa due to their differential cellular localisation and synergistic growth-factor regulation. These observations, along with those further studies outlined above, are necessary in identifying these specific components of PCa metastasis to which the ADAMs may contribute.

## TABLE OF CONTENTS

## LIST OF FIGURES

## LIST OF TABLES

## LIST OF ABBREVIATIONS

| | |
|---|---|
| ADAM | A Disintegrin And Metalloprotease domain |
| β-APP | Beta Amyloid Precursor Protein |
| bp | Base Pairs |
| BCA | Bicinchoninic Acid |
| BM | Basement Membrane |
| BSA | Bovine Serum Albumin |
| cDNA | Complimentary DNA |
| CIP | Calf Intestinal Phosphatase |
| DHT | Dihydrotestosterone |
| DIG | Digoxygenin |
| DNA | Deoxyribonucleic Acid |
| DTT | Dithiothreitol |
| ECM | Extracellular Matrix |
| EDTA | Ethylenediamine Tetraacetic Acid |
| EGF | Epidermal Growth Factor |
| EST | Expressed Sequence Tag |
| EtBr | Ethidium Bromide |
| EtOH | Ethanol |
| gDNA | Genomic DNA |
| H&E | Hematoxylin and Eosin |
| HRP | Horse Radish Peroxidase |
| ICC | Immunocytochemistry |
| IHC | Immunohistochemistry |
| IGF-1 | Insulin-like Growth Factor-1 |
| kDa | Kilodaltons |
| LB | Luria Broth |
| LCM | Laser Capture Microdissection |
| MMP | Matrix Metalloprotease |
| Mr | Molecular Weight |

| | |
|---|---|
| MT-MMP | Membrane-Type MMP |
| mRNA | Messenger Ribonucleic Acid |
| NLS | Nuclear Localisation Sequence |
| OCT | Optimal Cutting Temperature compound |
| PAGE | Polyacrylamide Gel Electrophoresis |
| PCa | Prostate Cancer |
| PCNA | Proliferating Cell Nuclear Antigen |
| PMSF | PhenylMethylSulphonylfluoride |
| POD | Peroxide Dismutase |
| PSA | Prostate Specific Antigen |
| RT-PCR | Reverse Transcription - Polymerase Chain Reaction |
| SDS | Sodium Dodecyl Sulphate |
| SDW | Sterile Distilled Water |
| STP | Synthetic Transfer Polymer |
| TACE | TNF α Converting Enzyme |
| TIMP | Tissue Inhibitor of MMPs |
| TNF α | Tumour Necrosis Factor Alpha |
| uPA | Urokinase Plasminogen Activator |
| UV | Ultra Violet |
| WCL | Whole Cell Lysate |
| WSS | Whole Section Scrape |

## PUBLICATIONS ARISING FROM THIS STUDY

McCulloch, D.R., Akl, P., Samaratunga, H., Herington, A.C. and Odorico, D.M. (2003) The expression of ADAM-10 in prostate tumour biopsies and its regulation by DHT, IGF-1 and EGF in the LNCaP cell model. *In Press*, **Clin Cancer Res**

McCulloch, D.R., Odorico, D.M. and Herington, A.C. (2003) The expression of ADAM-9 in prostate tumour biopsies and its regulation by DHT, IGF-1 and EGF in the LNCaP cell model. **In Prep**

McCulloch, D.R., Odorico, D.M., Herington, A.C., Thompson, E.W. and Williams, E.D. (2003) The detection of ADAM-9 and -10 proteins by Western blot analysis from prostate gland epithelial cells isolated by laser capture microdissection. **In Prep**

## PUBLICATIONS RELATED TO BUT NOT ARISING FROM THIS STUDY

McCulloch, D.R., Harvey, M. and Herington, A.C. (2000) Expression of the ADAMs family of proteases in prostate cancer cell lines and their regulation by dihydrotestosterone. **Mol Cell Endocrinol** 167(1-2), 11-21.

Manzetti, S., McCulloch, D.R., Herington, A.C. and Van der Spoel, D. (2003) Computer modelling of substrate homology between stromolysin (MMP-3), ADAM-9 and ADAM-10. *In Press*, **J Comp Aided Molec Design**

## ACKNOWLEDGEMENTS

I would like to thank Prof. Adrian Herington for providing me with every opportunity to move forward in my pursuit to be a Research Scientist. Dr. Dimitri Odorico for Co-supervision including guidance in strategic planning and experimental design. Dr. Mark Harvey and Dr. Eliza Whiteside from whose initial input of work and ideas created the opportunity for this project. Dr. Chris Collet for the award of a QUT Biotechnology Innovation Scholarship allowing a major part of this thesis (Laser Capture Microdissection) to be carried out with Dr. Elizabeth Williams (thankyou Elizabeth), in a collaborative laboratory. Dr. Ying Dong for paying particular interest in my progress and leading me in the right direction during tough times. Dr. Zee Upton and Dr. David Leavesley, who have shown me what true inspiration and a high level of motivation to succeed is. I would like to make a special mention of Prof. Erik Thompson, my mentor, who has guided me in the very special skill of effective networking.

I would like to acknowledge my laboratory peers, Dr. Tara Veveris-Lowe for taking time out to teach me basic laboratory techniques upon the commencement of my scientific research at QUT. Ms. Rachael Collard, Ms. Carolyn Chan and Dr. Lisa Chopin for their continuing moral support throughout the entirety of my Ph.D studies. Mr. Sergio Manzetti for inspiring conversation and brainstorming, Mr. Christian Gruber and Mr. Santy Pereza for mateship and good conversation, Ms. Jennifer Kricker and Ms. Carolyn Hyde (the terrible two!), also for good conversation and great social laughs, temporarily forgetting the pressures bestowed upon us.

Finally, I would like to thank Ms. Alison Teh for truly believing in my abilities to succeed in my chosen career and giving me unquestionable support at those much needed times. Thankyou.

# CHAPTER ONE

## 1.0 INTRODUCTION AND LITERATURE REVIEW

## THE ADAMS FAMILY OF PROTEASES AND PROSTATE CANCER: A POTENTIAL ROLE IN EXTRACELLULAR MATRIX REMODELLING

## *1.1 Introduction*

The extracellular matrix (ECM) comprises a number of proteins including collagen, fibronectin, vitronectin, laminin and proteoglycans that act as a supportive network of tissue surrounding organs within the body. An equally important specialised ECM is the basement membrane (BM) (Rucklidge et al. 1994), of which a major protein component is collagen type IV. The BM forms a barrier between cells in a confined organ and the ECM. When cells of a particular organ become tumorigenic in nature, the surrounding BM and ECM proteins are degraded to allow room for those cells to 1) divide, thus enlarging the organ, and 2) to migrate through the surrounding tissue. These two key mechanisms are central to the multistep process known as metastasis.

A family of 26 proteins called the matrix metalloproteases (MMPs) are currently subdivided into 5 categories depending on substrate specificity and preference, the gelatinases, stromelysins, collagenases, membrane-type MMPs (MT-MMP) and a heterogeneous subgroup (Egeblad and Werb, 2002;Sternlicht and Bergers, 2000). Collectively they mediate the degradation of most BM and ECM proteins; therefore these proteases are key facilitators of metastasis. Cell adhesion molecules (CAMs) including glycoproteins known as integrins, regulate the migration of tumorigenic cells through the degraded ECM. A recently characterised family of 34 predominantly membrane - bound proteins called the **ADAM**s (**A** **D**isintegrin **A**nd **M**etalloprotease domain) have the potential to act both as ECM degrading enzymes and integrin-binding/dissociation molecules for cell migration activity. Hence, the expression of the ADAMs by tumour cells may have implications in these two steps of metastasis.

Classically, the role of the ADAMs family is to cleave/solubilise and/or activate membrane bound growth factors and cytokines on the cell surface. However, particular members of the ADAMs have also shown metalloprotease activity specifically toward BM and ECM proteins. With respect to cell migration, members of the ADAMs family bind key integrins via a conserved tri-peptide motif of an integrin - binding loop in their disintegrin

domain. Given these characteristics, we hypothesise that the ADAMs family may be mechanistic contributors to the process of metastasis.

The expression of the ADAMs family is not well characterised in metastatic cancers such as lung, colon, breast and prostate. The latter two cancers, breast and prostate, are hormone-dependent in that key hormones such as estrogen and testosterone respectively, assist in their growth, development (progression) and maintenance. These hormones and other contributing growth factors are thought to regulate cancer progression by regulating the expression of proteins such as the MMPs that are involved in the metastatic process.

This study focuses on the potential for the ADAMs family of proteins to 1) be expressed in prostate cancer (PCa) and 2) be regulated by testosterone and key growth factors, namely Insulin-like Growth Factor-1 (IGF-1) and Epidermal Growth Factor (EGF), known to contribute to PCa progression and cell survival.

Therefore, the purpose of this literature review is to outline:

1) PCa and the process of metastasis,
2) The expression of MMPs, their regulation and function,
3) The biology and role of integrins in cell migration, and,
4) The biology of the ADAMs and their link with MMPs and integrins.

## *1.2 Prostate Cancer*

"Prostate cancer (PCa) is the sixth most common cancer in the world, the third most common cancer in men, and the most common cancer in men in Europe, North America, and some parts of Africa" (Gronberg, 2003). Risk factors for the development of PCa include genetic, environmental, dietary, social and hormonal factors (Haas, 1997), whilst the incidence of PCa is strongly correlated with increasing age. A patient suspected of suffering from PCa, may have benign prostate hyperplasia (BPH) (enlarged but not malignant prostate gland), low or high-grade prostatic intraepithelial neoplasia (PIN) or low, medium or high-grade PCa. BPH has not been linked directly to PCa although androgen metabolism and increasing age are two common risk factors in both diseases (Boyle, 1994).

To quantify and describe the progression of PCa disease, the Gleason grading system (Gleason, 1966) has been implemented. A numerical value is assigned to the prostate glands of the biopsy. Grade 1 is the lowest score reflecting the least aggressive, highly differentiated form of PCa whilst grade 5 is the highest score reflecting the most aggressive, poorly differentiated form of PCa. Two Gleason grades are given to any particular biopsy examined; the first number describes the most dominant type of prostate gland whilst the second is the next frequently occurring type of gland. An example of a Gleason score is 3+4=7 where most of the glands seen are Gleason grade 3, moderately differentiated, whilst the next frequently occurring gland is Gleason grade 4, poorly differentiated.

Clinical tests for the presence of PCa often include the intrusive procedure of Digital Rectal Examination (DRE) and, a less intrusive serum test for the marker Prostate Specific Antigen (PSA). Both methods of screening can effectively detect PCa, however the efficiency of each is suboptimal. The sensitivity of DRE examination has been reported to be as low as 18 - 22 % (Vihko et al. 1985; Optenberg and Thompson, 1990). In the case of PSA screening, a serum value of > 4.0 ng/ml indicates an associative risk of having PCa. The sensitivity of PSA evaluation reports is as high as 80 % in some studies, whilst others

report as low as 29 %. Grossly elevated PSA levels are often indicative of more aggressive PCa. PSA specificity is however limited, as men with benign disease such as BPH and prostatitis often screen positive for elevated PSA serum values (Catalona et al. 1993; Mettlin et al. 1994; Scaletscky et al. 1994; Humphrey et al. 1994). It is controversial whether the early detection of PCa lowers mortality, although the incidence of metastatic disease over time has decreased where regular screening occurs (Labrie et al. 1996). These initial screening methods often lead to more invasive screening, including biopsies such as 'transurethral resection of the prostate' (TURP), or 'transrectal guided ultrasound' (TRUS) biopsies as well as repeat screening of all invasive and non-invasive methods.

Treatment regimes for PCa include androgen ablation therapy, radiation therapy and radical prostatectomy. Androgen ablation therapy gives some respite from the suffering of PCa morbidity. However, commonly the cancer still progresses through late-stage to an aggressive metastatic phenotype. The benefits of radical treatment are often not seen in patients with a life expectancy of less than 10 years (Adolffson, 1993; Chodak et al. 1994; Warner and Whitmore, 1994; Johansson et al. 1997). Radiation therapy and radical prostatectomy often lead to severe side effects such as erectile dysfunction and urinary incontinence, considerably affecting the patient's quality of life.

### *1.2.1 Metastasis*

PIN (prostatic intra-epithelial neoplasia) is a condition that is believed to precede cancer of the prostate gland. Development of a neoplasia such as PIN involves two factors affecting cellular behaviour, that is the disruption of cellular differentiation and the development of abnormal relationships between the cells and their microenvironment (Pusztai et al. 1996). Once neoplastic cells develop into a primary tumour, the cells may acquire the ability to migrate from their primary organ to a distant organ in the body, a process referred to as metastasis (Figure 1.1).

"Tumour metastases have proved to be the major cause of death in cancer patients" (Zern and Reid, 1993). Migration of tumour cells involves a plethora of biological interactions at

the molecular and cellular level. The tumour cell first loses cell-cell contact by altering the expression of cell surface molecules known as cell adhesion molecules (CAMs) allowing subsequent cell separation (Edelman, 1984). Epithelial cells must invade local tissue before migration occurs. Components of local tissue invasion include the lysis of the surrounding healthy cells, the degradation of the BM and invasion (Figure 1.1) through the ECM. Proteolytic enzymes such as metalloproteases, of which the MMPs are the major contributing enzymes, are believed to be responsible for the invasive event (Chang and Werb, 2001).

**Figure 1.1:** The various stages a primary tumour must undergo for complete metastasis, ECM = vitronectin, collagen, fibronectin, laminin, other glycoproteins.

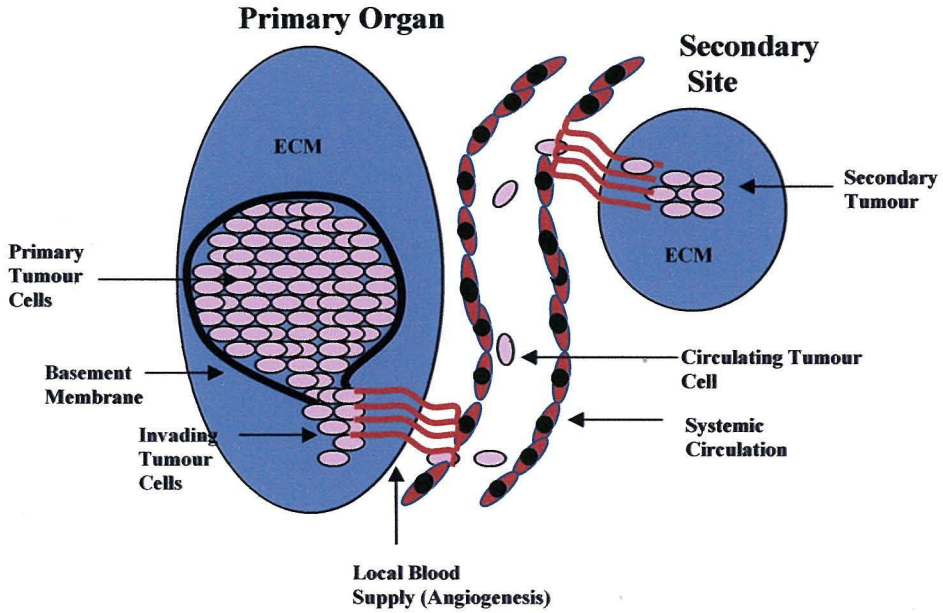


Once a path of degradation is established through the BM and the ECM, the tumour cells can undergo migration from their primary location (Figure 1.1). CAMs, which include cell surface proteins such as cadherins and the cell surface glycoproteins, integrins, are modulators of this process (Holly et al. 2000).

In addition to the loss of cell-cell contact, invasion and migration, tumour cells sustain their growth by vascularising their local environment (angiogenesis - Figure 1.1).

Vascularisation is brought about by the secretion of growth factors such as Vascular Endothelial Growth Factor (VEGF) and basic Fibroblast Growth Factor (bFGF) (Sato and Rifkin, 1988; Keck et al. 1989) and is necessary to supply oxygen and nutrients otherwise present at insufficient levels via diffusion (Vile, 1995). The capillary endothelial cells must also invade through the ECM and migrate to the site of the tumour. Again the MMPs and CAMs are believed to mediate this important step in metastasis (Pusztai et al. 1996).

Angiogenesis provides a transport medium, in the form of capillaries, for the tumour cells to utilise. The tumour cells invade into the bloodstream via angiogenic capillary invasion (intravasation) or into the lymphatic system. Once in the blood stream, many cells escape immune surveillance and arrest in downstream organs. An arresting tumour cell again makes use of CAMs enabling its adhesion to the wall of a blood vessel. Subsequent extravasation occurs allowing the cell to leave the bloodstream and colonise an entirely different organ (Figure 1.1). Both intravasation and extravasation involve proteolytic activity for BM degradation, again mediated by the MMPs. Hence, CAM modification and proteolysis are two major events mediating cancer metastasis. Thus, it is imperative to further our knowledge of these two particular molecular mechanisms so that a greater understanding of cancer progression can be acquired.

High-grade PCa commonly metastasises to bone (Carlin and Andriole, 2000) and lymph nodes (Bader et al. 2003) whilst other less common sites include the lung and brain (Levi et al. 2003; Castro et al. 2003). In the case of patients with bone metastasis, for example, severe morbidity, which entails painful osteosclerotic lesions and fractures, prevails. This may lead to nerve compression, paralysis and eventually death (Rubens, 1998). Once tumour cells have colonised in the bone, the normal remodelling between osteoclast bone resorption and osteoblast bone deposition is disrupted. In the case of PCa, there is evidence suggesting that both osteolysis and osteosclerosis activities (bone resorption and deposition, respectively) are enhanced, presumably initial colonisation requiring the former and subsequent growth and progression requiring the latter (Mundy and Yoneda, 1996). With respect to the underlying mechanisms involved in this process, like metastasis, little to date is known.

### *1.2.2 Growth factors involved in prostate cancer progression and metastasis*

Early stage PCa growth and progression is dependent on male sex hormones (androgens), predominantly testosterone. Testosterone, secreted by the male testis, is converted intracellularly to 5-α-dihydrotestosterone (DHT), which binds, activates, and translocates the androgen receptor (AR) to the cell nucleus. The AR binds androgen response elements in the promoter region of genes (Reinikainen, 1996), which in turn regulate the transcriptional activity of many proteins involved in PCa growth. In the prostate, the AR is found predominantly in the secretory epithelial cells of prostate glands (Chung, 1991; Lee, 1996). The transition from androgen sensitive (low-grade PCa) and androgen insensitive (high-grade PCa) is not well understood. Along with evidence suggesting that the AR is subject to point mutations so that it is no longer able to bind, or has reduced signalling in response to DHT binding (Veldscholte et al. 1990; Bentel and Tilley, 1996), there is also evidence that suggests particular mutations in the AR confers hypersensitivity to other hormones such as estrogen leading to an increase in AR transactivation (Thin et al. 2003). The AR mutations are predominantly found in metastatic disease but not in cases of primary prostate tumours (Marcelli et al. 2000).

Other growth factors involved in the regulation of PCa growth include the Fibroblast Growth Factors (FGFs), IGFs, Transforming Growth Factor α (TGF α) (Russell et al. 1998) as well as Interleukin-6 (IL-6) (Chung et al. 1999), Leukaemia Inhibitory Factor (LIF) and EGF (Jarrad et al. 1994). Past studies suggest IGF-1, EGF and IL-6 are enhancers of the transactivation and stimulation of the sensitivity of the AR, when in the presence of DHT (Culig et al. 1994; Chan et al. 1998; Ueda et al. 2001; Orio et al. 2002). Levels of growth factors such as these are also themselves regulated by androgens. Stromal cells surrounding prostate epithelia commonly express these growth factors, which act in a paracrine manner (Figure 1.2), diffusing through the ECM. Cell proliferation and transformation in the glandular epithelium of the prostate is thought to be dependent on these stromal growth factor secretions (Ware, 1994; Farnsworth, 1999). Figure 1.2 outlines schematically the interactions of DHT and growth factors on prostate stroma and epithelia, and their consequences on cell behaviour.

The IGFs are peptide GFs that share homology with insulin. They are produced by the liver and circulated in the blood, as well as being locally secreted from the prostate and exerting their effects in both an autocrine and paracrine manner. Their binding proteins (BPs), of which there are 6 described to date (Baxter, 2001), can regulate IGF bioavailability by binding free IGF-1, reducing the levels of the bioactive peptide. High levels of IGF-BPs are known to have an apoptotic effect on PCa cells (Rajah et al. 1997). The IGFs are thought to be the major regulators of PCa growth in its later, more metastatic stage, and indeed stimulates PCa cell proliferation (Daughady and Rotwein, 1989). Recent studies show higher serum levels of IGF-1 in PCa patients when compared to healthy controls (Peng et al. 2002) giving IGF-1 the potential to be a new biomarker for the development of PCa. The levels of IGF-1 and its BPs were examined in patients after prostatectomy and unexpected significantly elevated levels of IGF-1 and its BPs were found (Bubley et al. 2002).

**Figure 1.2:** DHT can act directly on the prostate epithelia or on the surrounding stroma to stimulate the secretion of various growth factors. Both DHT and the growth factors act in a paracrine and/or autocrine fashion to allow the tumorigenic epithelial cell to undergo the various stages of metastasis, in red.

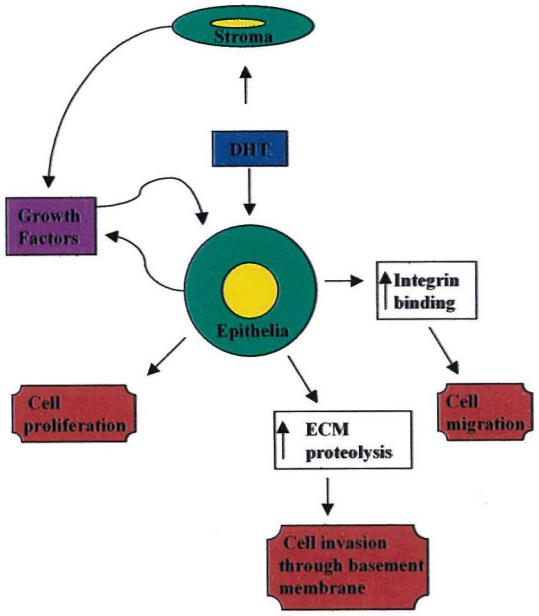

This indicates that the levels of IGF-1 in the serum are not contributed by the secretion of IGF-1 from PCa cells but rather from another endocrine source, perhaps the liver. Therefore, elevated levels of IGF-1 may be a causative PCa agent and major risk factor rather than a result of PCa itself.

EGF is expressed more highly in PCa as opposed to the prostate in its benign state (Harper et al. 1993; Glynne-Jones et al. 1996) and has been shown to increase PC-3 cell (a late stage PCa cell line derived from a bone metastasis) cell invasion *in vitro* (Jarrad et al. 1994). EGF has notable effects on the activation of DNA repair genes in PCa cell lines through its receptor (EGFR) transactivation and subsequent Mitogen Activated Protein Kinase (MAPK) signalling (Yacoub et al. 2003). Targeting EGFR and inhibiting its phosphorylation can achieve significant therapeutic effects against PCa bone metastasis, as was shown in a mouse model where this approach induced PCa cell apoptosis (Kim et al. 2002). EGF and IGF-1 are important for regulating protease expression involved in cell invasion and EGF is known to interact with, and regulate, the IGF axis (Jarrad et al. 1994; Russell et al. 1998).

Both stromal and epithelial prostate cells express bFGF and, as PCa progresses to late-stage, the levels of bFGF, like EGF in the epithelial cells, increase. The underlying mechanisms of bFGF stimulation are thought to mediate angiogenesis enabling metastasis to occur (Folkman, 1990). IL-6 also has a high level of expression in PCa cell lines and is thought to contribute to PCa morbidity (Siegsmund et al. 1994). IL-6 can regulate cell growth by activating signalling pathways such as Signal Transducer and Activator of Transcription (STAT) and MAPK in many cell types (Steiner et al. 2003).

Growth factors involved in the development of PCa, such as those described above, regulate cell signalling processes, cell migration and ECM proteolysis through the regulation of the levels and activation of proteins such as the MMPs and integrins, factors highly implicated in the successful metastasis of PCa cells.

## *1.3 The Matrix Metalloproteases (MMPs)*

The MMPs, which belong to the 'metzincin' superfamily, have been extensively studied and play a major role in the process of tissue degradation (Nagase, 1997). They are believed to mediate the initial ECM degradation of metastasising tumour cells (Matrisian, 1990). MMPs are distinguished from other metalloproteases by two unique motifs. The PRCG [V/N] PD motif (single letter amino acid code) found in the pro or unprocessed, inactive form of MMPs, and the HEXGHX[L/M]G[L/M]XH motif responsible for binding zinc in the catalytic domain (Nagase, 1997). Within the MMP family a relatively new set of six closely related MMPs has been characterised, the Membrane-Type MMPs (MT-MMP). As its name suggests MT-MMPs are bound to the cell membrane via a transmembrane domain (Nagase, 1997). A short cytoplasmic tail, which may be involved in cell signal processes, is also common to all six MT-MMPs. Pro-MMPs are directed through the endoplasmic reticulum, and most MMPs are then directed to the outside of the cell into the ECM, whilst the MT-MMPs remain on the cell surface. (Sternlicht and Bergers, 2000).

### *1.3.1 Activation and regulation of the catalytic activity of MMPs*

The activation mechanism of pro-MMPs is explained by a cysteine switch hypothesis (Springman et al. 1990; Van Wart and Birkedal-Hansen, 1990). It is proposed that the cysteine residue in the unique PRCG[V/N]PD motif in the pro-domain provides a sulfhydryl (-SH) group, which interacts with zinc preventing its association with water. Once the cysteine residue is removed, either proteolytically or by an SH reactive agent, the zinc ion is free to associate with water molecules. The association of water molecules provides the catalytic activity (acid-base catalysis) needed for subsequent breakdown of MMP substrates (Springman et al. 1990). The high enzymatic activity portrayed by fully active MMPs is believed to arise by the interaction of N-terminal Y or F residues with a conserved D residue, (Benbow et al. 1996) of particular importance for collagenase activity (Suzuki et al. 1990; Knauper et al. 1993; Reinemer et al. 1994). The pro-domain of the MMPs is made up of three alpha helices followed by the cysteine switch (discussed above). MMPs are thought to be activated in a two step, calcium dependent, mechanism where an

active intermediate is formed by the removal of the first alpha helix (Nagase et al. 1990; Cameron et al. 1995).

Several proteases are involved in the process of proteolytically activating the pro-MMPs. These include the plasminogen activator system, tissue kallikreins (Clements, 1997), other MMPs and MT-MMPs (Nagase, 1997). For example, MT1-MMP and MT2-MMP have been shown to activate proMMP-2 (gelatinase A) (Will et al. 1996; Butler et al. 1997). Particular residues in the alpha helices are thought to mediate which proteases can activate individual MMPs, for example, proMMP-3 can be activated by leukocyte elastase whereas proMMP-10 cannot, due to its lack of a V at position 35 (Suzuki et al. 1990). Urokinase plasminogen activator (uPA) is perhaps the most characterised and most prominent MMP activator. uPA activates the serine protease plasminogen to form active plasmin. Plasmin has a very broad substrate specificity and converts zymogens (of which most of the MMPs are included) to active proteases.

Activation studies have also shown that non-proteolytic reagents including mercurial compounds such as HgCl and 4-aminophenylmercuric acetate (APMA) (Okada et al. 1988; Suzuki et al. 1990), thiol-modifying agents including iodoacetate, oxidised glutathione, and denaturants such as urea and SDS (Koklitis et al. 1991) are all capable of converting proMMPs to their active form. Although the mechanism of activation via these synthetic compounds is not entirely understood, they are believed to activate MMPs in a stepwise manner, generating several active intermediates, as is the case when proMMP-3 is activated by APMA (Okada et al. 1988) ultimately dissociating the cysteine residue from the zinc ion in the catalytic motif.

### *1.3.2 Regulation of MMP catalytic activity*

To date, major inhibitors of all MMPs are the Tissue Inhibitors of MMPs or TIMPs (Matrisian, 1990; Mignatti and Rifkin, 1993). TIMPs are synthesised locally and inhibit MMP activation by binding in a 1:1 stoichiometry extracellularly (Murphy and Docherty, 1992). The TIMPs comprise two distinct domains, the N-terminal domain, which is

responsible for the physical inhibition of metalloprotease activity, and the C-terminal domain, thought to confer the TIMPs binding specificity (Stetler-Stevenson et al. 1996). Most activated MMPs will interact with TIMPs, however, inactive MMP pro-forms are selective with respect to the type of TIMP they will bind to. Activated MMP-2, for example, is inhibited by TIMP-1 and TIMP-2. However, inactive proMMP-2 interacts selectively with TIMP-2 but not TIMP-1 (Goldberg et al. 1989, 1992; Stetler-Stevenson et al. 1996). Additionally, there is evidence to suggest that the proMMP-2/TIMP-2 complex can interact with activated MMP-9, also inhibiting its activity, introducing a new degree of regulation in the form of ternary complexes (Murphy et al. 1989; Moll et al. 1990; Stetler-Stevenson et al. 1996). In most cells, MMP-9 is secreted as a complex with TIMP-1, which inhibits its activity. Interestingly, TIMPs have recently been implicated in cell proliferation and survival, unrelated to their MMP inhibitory role (Blavier et al. 1999).

### *1.3.3 MMP activity in cancer - The Gelatinases and MT-MMPs*

Collectively, the MMPs are able to cleave a broad spectrum of collagen substrates and other ECM components (see Appendix one A). Of the numerous MMPs illustrated in Appendix one, the more predominant MMPs that have been studied to date, in the process of metastasis, are MMP-2 and -9 or Gelatinases A and B respectively. Alongside these studies, there is emerging evidence that the MT-MMPs are likely candidates for cancer cell invasion and migration. MMPs -2 and -9 contain a cysteine rich repeat in their catalytic domain required for the binding of collagen (Sternlicht and Bergers, 2000) and both have type I, IV, V and X collagenase activity (Kleiner et al. 1999). In addition, MMP-2 can act to degrade laminin, another component of the ECM. MMP-2 and -9 also bind the integrins $\alpha V\beta 3$ (Brooks, et al. 1996) and $\alpha 3\beta 1$ (Yu and Stamenkovic, 1999) respectively. The importance of integrin association in cancer is outlined below in section 1.4 'The biological role of integrins.'

The gelatinases have also been implicated in the process of embryo implantation. The developing embryo must invade into the uterine lining for further development and survival. This process can be likened to that of cancerous cells invading into surrounding

tissues. The expression of MMP-9 in mouse blastocyst outgrowth is thought to be critical for this event both *in vitro* and *in vivo* (Alexander et al. 1996; Das et al. 1997; Whiteside et al. 2001).

Gelatinase expression has been shown in several cancers including prostate, gastric, colorectal and pancreatic. In gastric cancer, for example, the active form of MMP-2 is found in malignant tissue but not in normal tissue (Yamagata et al. 1991). In addition to this finding, Sato et al. (1994) showed MT1-MMP to be an important activator of MMP-2 and further, MT1-MMP expression correlates with activated MMP-2 in gastric cancer tissues (Nomura et al. 1995). Completing the regulation of MMP-2 mediated cell invasion, several studies have concluded that TIMP-2, artificially over-expressed in invasive cell types, reduces the cell's metastatic potential due to its inhibition of MMP-2 activity (Kawamata et al. 1995).

In breast cancer, the tumour itself expresses the MMPs. In many cases the expression of MMP-9, in particular, is only found at the interface between the tumour and the surrounding stroma (Ueda et al. 1996). A pertinent study of breast tissue carcinoma observed, by *in situ* hybridisation, the localisation of MMP-9 gene expression in inflammatory and neoplastic cells of malignant tumours, suggesting a direct correlation between MMP-9 expression and this cell phenotype. Moreover, there is evidence for elevated levels of circulating MMP-9 in the plasma of breast cancer patients (Zucker et al. 1993). Cells surrounding tumours are also found to express MMP-9, as is the case with colorectal adenocarcinoma and prostate carcinoma, where the surrounding macrophages and neutrophils express this MMP (Pyke et al. 1993; Jeziorska et al. 1994; Nagle et al. 1994; Gallegos et al. 1995; Zeng and Guillem, 1995). Recently, MMP-2, MMP-9 and MT1-MMP expression has been found in the membrane associated vesicles shed from endothelial cells (Taraboletti et al. 2002), giving endothelial cells a mechanism by which they can degrade the ECM for subsequent migration and formation of new blood vessels (angiogenesis). Thus it is clear that the metalloprotease activity of the MMPs is localised to the site of, and has major implications for, the process of tissue invasion.

### *1.3.4 MMPs and prostate cancer*

There is growing evidence that the MMPs are implicated in PCa, with respect to their expression and function. MT1-MMP expression was characterised in the PCa cell lines DU-145 and PC-3 (androgen insensitive cell lines), the TSU-1 cell line, previously thought to be a PCa cell line but later found to have originated from a bladder cancer (van Bokhoven et al. 2001), whilst LNCaP (androgen sensitive) showed very low levels of expression (Nagakawa et al. 2000). This is an interesting observation, given its role in the activation of MMP-2 (discussed above) and existing evidence showing MT1-MMP can degrade some collagens, fibronectin, laminin and vitronectin (Ohuchi et al. 1997). MMP-2 has also been characterised in DU-145 and BPH-1 along with TIMP-2. Further, Macrophage Inhibitory Factor (MIF), a cytokine expressed by prostatic glandular epithelial cells (Meyer-Seigler, 2000), up regulated MMP-2. MMP-2, but not MMP-9 levels are also elevated in response to androgens in the PCa cell line LNCaP (Liao, 2003).

The gelatinases have also been identified, by *in-situ* hybridisation, in prostate pre-surgery biopsy samples. Specimens from 40 patients were analysed and MMP-2 and -9 were found to be at their highest expression at the leading (invasive) edge of the tumour irrespective of the tumour grade (Kuniyasu et al. 2000). Parallel research investigated the expression of MT1-MMP and MMP-2 in 50 radical prostatectomy samples characteristic of benign and high-grade PIN glands. The basal cells in this case immunostained principally for MT1-MMP in benign glands, as opposed to secretory cell staining in the case of high grade PIN. A similar pattern was observed in the case of MMP-2 (Upadhyay et al. 1999). Another investigation used 42 samples from men representing both malignant and benign tumours and examined the mRNA expression pattern for MMP-2 and TIMP-2. Still et al. (2000), by quantitative analysis, concluded that with an increase in cancer severity, there was an increase in MMP-2 expression as compared to the expression of TIMP-2, thereby tipping the balance in favour of MMP-2 proteolytic activity.

In an *in-vitro* study (Inoue et al. 2000) PC-3P cells (usually poorly metastatic) were transfected with Interleukin-8 (IL-8) resulting in up-regulation of MMP-9 and increased

collagenase activity as measured by Matrigel (synthetic ECM). PC-3 cells have been shown to degrade mineralised and non-mineralised bone using MMP activity stimulated by phorbol esters (Sanchez-Sweatman et al. 1999) - not surprising considering these cells were originally derived from a PCa metastasis to the bone.

MMP-7 (Matrilysin) was found to be over expressed in PCa by Pajouh et al. (1991). More recently, MMP-7 has been shown by quantitative RT-PCR to be up regulated by the FGF family in LNCaP cells whilst FGF had no effect on MMP-7 expression in the normal prostate cell line PrEC (Klein et al. 1999). Additionally, EGF is also a regulator of MMP-7 at least in the LNCaP cell line (Sundareshan et al. 1999). Membrane vesicle associated uPA, an activator of the MMPs (discussed above) promotes the invasion of the poorly metastatic PCa cell line LNCaP and the metastatic cell line PC-3 (Angelucci et al. 2000). The addition of plasminogen, the substrate for uPA and a subsequent activator of the MMPs (discussed above), increased the adhesion to, and degradation of, collagen IV and Matrigel in both PC-3 and LNCaP cell cultures. Angelucci et al. (2000) also showed the effect of the addition of membrane vesicles collected from PC-3 cells, added to LNCaP cell cultures. The LNCaP cells displayed a significant amount of increased invasion through Matrigel, indicating that these vesicles may have a role in increased tumorigenesis, presumably via MMP activation.

### *1.3.5 Synthetic inhibitors of the MMPs*

Many synthetic MMP inhibitors (MMP-I) have been designed to counter the detrimental effects of MMP expression in cancer progression and severity. Common inhibitors include batimastat and marimastat of which the latter reached phase III trials for treatment of colorectal cancer (Sternlicht and Bergers, 2000). Rabbani et al. (2000) evaluated an MMP-I called A-177430, previously described to block the progression of cancer (Steinman et al. 1998) in a metastasising rat prostate model. After injecting PCa cells into the flanks of 6 Copenhagen rats, tumour size was measured between 8 and 16 days. A-177430 induced a 10-fold decrease in tumour growth. Another compound, Alendronate, was shown to decrease the secretion of the gelatinases in human PC-3 ML tumours, preventing bone

destruction (Stearns and Wang, 1998). This type of bone degrading activity was also suppressed using the MMP-I 1,10-phenanthroline (Sanchez-Sweatman et al. 1999). The drug tetracycline has also been shown to inhibit MMP secretion in PC-3 cells (Duivenvoorden et al. 1999).

By 1996, over 25 pharmaceutical companies were involved in MMP-I trials (Beckett, 1996). Common inhibitors of MMP activity, such as those mentioned above have undergone phase II and III clinical trials (Zucker et al. 2000; Coussens, et al. 2002). Problems associated with achieving specific MMP inhibition have been encountered, although in some cases specificity of inhibiting target MMPs has been achieved (Shalinsky et al. 1999). The lack of specificity has led to severe side effects in patients involved in clinical trials, rendering these approaches detrimental (Zucker et al. 2000; Coussens et al. 2002). Often, if the pathological state was being treated in its early stages, it regressed somewhat in the first instance but the disease eventually advanced. Treatments were not effective once the pathological conditions were well established (Bergers et al. 2000; Zucker et al. 2000). A greater understanding of the underlying mechanisms of MMP action is required to further develop more successful drugs for the treatment of diseases such as cancer. Further development and refinement of these inhibitors, and a better understanding of the role and regulation of key MMPs for each cancer type, continues to hold promise for a new series of therapeutics.

### *1.4 Integrins*

Integrins are a large family of cell membrane spanning glycoproteins capable of binding to structural proteins of the ECM including vitronectin, collagen, fibronectin and laminin (Hynes, 1992; Hans, 1995). Several integrins are expressed in each cell type (Hynes, 1992). There are over twenty characterised integrins, each consisting of non-covalently bonded $\alpha$ and $\beta$ subunits. Each $\alpha$ subunit is able to complex with a number of $\beta$ subunits introducing a further degree of diversity (Matsumoto et al. 1995). Currently, 15 $\alpha$ and 9 $\beta$ subunits have been characterised. The $\alpha/\beta$ arrangement diversifies integrin functionality. Furthermore, splice variants of both $\alpha$ and $\beta$ subunits exist (Hynes, 1992). Integrin

nomenclature is based on the naming of the α subunit first, followed by the β subunit - for example, α2β1 appearing in lymphocytes and αIIbβ3, a platelet specific integrin (Hynes, 1992).

Integrins are major adhesion foci for cell-cell and cell-ECM contacts. They are also implicated in intracellular signal transduction via the binding of ligands. Most integrins have a defined recognition-binding site. Commonly, this site is recognised by a protein containing an RGD peptide sequence. Variations of integrin recognition sequences include DGEA, EILDV, GPRP and KQAGDV (Hynes, 1992). Interestingly, more than one integrin can be recognised by the same ligand. An example of this is that each of the integrins α2β1, α3β1 and α6β1 binds the ECM protein laminin (Wayner et al. 1991). Also, individual integrins often have the capability of binding more than one ligand. Integrins can be receivers or generators of signals. In both outcomes, cell adhesion characteristics are changed and cell-cell or cell-ECM contacts may be promoted or disrupted.

### *1.4.1 The biological role of integrins*

Essentially, integrins can provide a link between cells or between cells and the ECM through focal adhesions. It is suggested that focal adhesions form as a result of intracellular signalling, possibly by protein kinase C (PKC) and the small G protein *rho* (Keck et al. 1989) as well as *rac* and cdc42 (Horwitz and Parsons, 1999). The binding of a ligand stimulates intracellular events such as the tyrosine phosphorylation of paxillins and focal adhesion kinase (FAK). Integrins are believed to undergo conformational changes upon the initial ligand binding and activation, subsequently altering their binding affinity. Therefore, an integrin may remain in an inactive state until its affinity is altered, conferring upon it the ability to bind several ligands (Gumbiner, 1996). This is exemplified by the classical major platelet integrin αIIbβ3 where, upon activation it is converted to a high affinity receptor for binding soluble fibrinogen, involved in the blood clot pathway (Gumbiner, 1996). At least seven different integrin alpha subunits contain a 200 amino acid "I" domain called the metal ion-dependent adhesion site (MIDAS), important for cell adhesion. MIDAS-like domains are also found in some beta subunits and are thought to be a type of divalent cation

chelator, regulating the type and abundance of particular divalent cations, which in turn, regulate integrin binding affinity (Gumbiner, 1996).

An important role in cancer metastasis is that of modulating cell migration due to the cell contact characteristics described previously. It is speculated that FAK phosphorylation is necessary for anchorage-dependent cellular growth (Presta et al. 1989; Pepper et al. 1990) illustrating the concept of integrin binding leading to the correct intracellular environment to stimulate cell proliferation. Cells that are attached to the ECM use focal adhesions to which integrins are the major receptor. Focal adhesions provide a contact between the extracellular environment and the cell cytoskeleton or actin filaments. Ligand binding and signalling events regulate these types of adhesions both intracellularly and extracellularly. Not all integrins are in focal contact with the cytoskeleton however, for example, $\alpha5\beta1$ is in focal contact whereas $\alpha3\beta1$ is not (Gumbiner, 1996) perhaps further diversifying the function of integrin binding. A study investigating the role of the integrin $\alpha3\beta1$ found that the addition of monoclonal antibodies raised to an $\alpha3\beta1$-tetraspanin protein complex and thought to biologically activate this integrin, increases the invasive potential of cells (Sugiura and Berditchevski, 1999).

The importance of integrins in the metastatic process is also reflected by studies showing that synthetic peptides containing RGD sequences can block experimental metastasis (Folkman and Klagsburn, 1987). Integrins that are able to bind ECM proteins include the $\alpha2$, $\alpha3$ and $\alpha6$ subunits, all of which bind laminin when individually bound to the $\beta1$ subunit. Both $\alpha V\beta3$ and $\alpha5\beta5$ are able to bind vitronectin (Felding-Habermann and Cheresh, 1993; Horton, 1997; Schvartz et al. 1999). This type of binding event in the case of lung carcinoma H2981 and human melanoma M21 cells, can mediate different post-ligand binding and hence different cellular responses (Wayner et al. 1991). $\alpha5\beta1$ is recognised by the RGD peptide sequences in vitronectin (Wayner et al. 1988) and IGF-BP1 (Jones et al. 1993), which stimulates the migration of Chinese Hamster Ovary (CHO) cells *in vitro* by activating the $\alpha5\beta1$ cell surface integrin signalling (Jones et al. 1993). The binding of integrins may be imperative for the attachment of a circulating tumour cell to an endothelial cell before extravasation can occur. Therefore, integrin binding may be largely

responsible for the re-establishment of a colony of primary tumour cells to a distant organ and the formation of a secondary tumour (Fidler and Ellis, 1994; Matsumoto et al. 1995).

### *1.4.2 Integrins and prostate cancer*

As with most highly aggressive cancers, integrin expression and function has been characterised in PCa. The diversity of integrin expression was illustrated by Haywood-Reid et. al. (1997) where the α subunits 1 through 6 and V as well as the β subunits 1 through 5, IIb and 7 were found in a cohort of PCa cells. Using PC-3 cells in a cell adhesion model, antibodies raised to the α2 and β1 subunits inhibited binding to type I collagen. Further investigation concluded the integrin α2β1 is a major collagen receptor that is up regulated by TGF β (Kostenuik et al. 1997). The integrin αIIbβ3 is also expressed in PC-3 and DU-145 cells as well as clinical prostate tumour specimens (Trikha et al. 1996). When this integrin was inhibited by a monoclonal antibody in DU-145 cells, migration through reconstituted basement membranes was abolished. The above examples demonstrate the necessity of integrins for both attachment and migration.

Other integrins involved in PCa development include the α6 subunit (laminin receptor) which, in the case of DU-H cells (derived from DU-145 cells), complex with β1 and β4 subunits whilst in DU-L cells, only complex with the β4 subunit. When both cell lines are injected into SCID (immuno-comprimised) mice DU-H cells showed a higher degree of invasive potential and were also 3-times more mobile on laminin (Rabinovitz et al. 1995). A recent study outlining the importance of the integrin α6β4 showed this integrin to be more highly expressed in PC-3 cells when compared to LNCaP cells. Upon the transfection of PC-3 cells with the androgen receptor, the expression of α6β4 was markedly reduced. Further treatment of these cells with the synthetic androgen R1881 markedly decreased the existing levels of α6β4 and inhibited the attachment of these cells to laminin and the invasion through matrigel (Bonaccorsi et al. 2000).

Another comparison between LNCaP and PC-3 cell lines demonstrated the expression of αVβ3 in the more metastatic PC-3 cells only. Whilst androgen-insensitive PC-3 cells easily adhered to, and migrated on vitronectin, androgen-sensitive LNCaP cells were only able to display this quality when transfected with αVβ3 integrin. (Zheng et al. 1999). The same study reported FAK phosphorylation as a response to αVβ3 induction. FAK is up regulated in prostate carcinoma (Kornberg, 1998). These studies provide an important link between the loss of androgen sensitivity and a more metastatic cellular phenotype in PCa. The above examples are just a few pertinent studies conducted in this area of cancer research and outline the true functional consequences of particular integrins expressed in the prostate and their important contribution to metastasis.

### *1.5 A Disintegrin And Metalloprotease domain (ADAMs) proteins*

ECM degradation is mediated in part by the MMPs, whilst integrin binding/dissociation is a key regulator of cell adhesion, both of which are important processes in metastasis. The **ADAM**s family of proteins comprise **A D**isintegrin **A**nd **M**etalloprotease domain, acting as integrin binding ligands and representing metalloprotease-mediated proteolytic activity. Thus, the ADAMs have the potential to play major roles in tissue/cell invasion processes. This recently characterised group of 34 proteins, described to date (Appendix one B), are closely related to the reprolysins (snake venom metalloproteases). A subset of the ADAMs family called ADAM-TS, of which there are 12, has also been described (Appendix one B), differing from the ADAMs by the presence of a thrombospondin-like repeat that likely functions in binding to substrates such as those found in the ECM (Cal et al. 2001). Like the reprolysins, the ADAMs are synthesised as inactive zymogens, having a pro-domain that is proteolytically processed to yield an active enzyme. This mechanism is thought to function in a stepwise activation mechanism with a cysteine switch such as that described for the MMPs (Jia et al. 1996) (see evidence for this below).

The ADAMs family differ from reprolysins by the addition of an EGF like domain, a transmembrane domain and a C-terminal cytoplasmic domain (Figure 1.3). Some members of the ADAMs also have a sequence homologous to viral fusion peptides (Huovila et al.

1996), important in cell attachment. The ADAMs proteolytic domain displays a catalytic motif homologous to that found in MMPs (Figure 1.4) and the disintegrin domain contains an integrin binding loop region with a consensus integrin-binding motif.

As the pro-domain of the MMPs inhibits their metalloprotease activity, it has been shown, by expression in insect cells, the pro-domain of ADAM-17 also inhibits its metalloprotease activity. Further, the cysteine-rich domain was found to be pertinent in the release of the pro-domain, as is the case for MMP activation. The pro-domain of ADAM-17 is thought to be imperative for the intracellular secretion of functional ADAM-17 from the Golgi apparatus (Milla et al. 1999).

ADAM-12 is also synthesised as an inactive zymogen and there is evidence that its activation mechanism is via a cysteine switch mechanism. Supporting this hypothesis includes a study that replaced the cysteine residue in the pro-domain of ADAM-12 with other residues. This yielded an active pro-form of ADAM-12 and the latency was restored by the replacement of a cysteine at various positions in the pro-domain (Loechel et al. 1999).

There is evidence that the ADAMs contain a functional furin cleavage site, raising the possibility of intracellular maturation, as occurs for the MT-MMPs (Schlondorff et al. 2000). Within the ADAM family, mature proteins appear to be localised in different cellular compartments. ADAM-10 and -15, for example, are localised to the intracellular compartment as well as the cell surface, whilst ADAM-28 is on the cell surface only (Schlondorff et al. 2000). ADAM-12, when over-expressed in skeletal muscle cells, is retained in the trans-Golgi network in its unprocessed form (Kadota et al. 2000). Little mature ADAM-17 seems to accumulate in the intracellular compartment, although it is cleaved by a furin-type pro-protein convertase in the secretory pathway (Schlondorff et al. 2000). The emerging evidence for quite similar mechanisms of regulating the metalloprotease activity between the ADAMs and MMP classes of the metzincin superfamily, suggests that these two classes may have similar biological roles in normal and pathological cell types.

**Figure 1.3:** A typical ADAM and its domain assembly. ss=signal sequence, tm=transmembrane domain (Huovila et al. 1996; Jia et al. 1996).

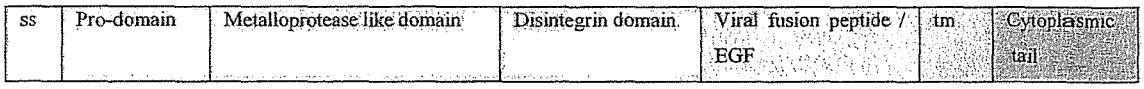


The metalloprotease domain of the ADAMs contains an active site predicted to bind zinc in the consensus sequence HEXGHNLGXXHD (Alfandari et al. 1997). The three histidine residues bind a zinc ion in the same manner as the MMPs. The glycine residues allow a turn, reducing conformational strain, the glutamic acid is the catalytic residue and the aspartic acid residue is a fingerprint for all reprolysins (Wolfsberg et al. 1995). The similarities between the ADAM metalloprotease catalytic site and an MMP catalytic site (Figure 1.4) suggest the same functionality, although the structural domain components differ between the ADAMs and MMPs (Appendix one B) with the ADAMs having the additional, abovementioned disintegrin, EGF-like, transmembrane and cytoplasmic tail domains.

**Figure 1.4** The ADAMs and MMPs have strikingly similar zinc-binding catalytic motifs.

| | | | | | | | | | | | | |
|---|---|---|---|---|---|---|---|---|---|---|---|---|
| **ADAMs** catalytic motif | **H** | **E** | X | **G** | **H** | N | L | **G** | X | X | **H** | D |
| **MMPs** catalytic motif | **H** | **E** | X | **G** | **H** | L/M | | **G** | L/M | X | **H** | |

ADAMs with the metalloprotease active site sequence HEXGHXXGXXHD (across all known orthologues) are: ADAMs 1, 8-10, 12, 13, 15, 16, 17, 19, 20, 21, 24, 25, 26, 28, 30, 33, and 34 (http://www.people.virginia.edu/~jw7g/Table_of_the_ADAMs.html, and Appendix one C). Some ADAMs are also found as soluble active metalloprotease variants, not unlike the MMPs. Among these, ADAM-9, -12, -17, -28 and some of the ADAM-TS family are included (outlined below). It is not yet clear as to the extracellular role these particular forms of the ADAMs may have.

### *1.5.1 The biological roles of the ADAMs*

The metalloprotease domain of the highly characterised reprolysins has been shown to contribute to the haemorrhagic response to basal lamina degradation (Kini et al. 1992; Alfandari et al. 1997). Classically, the ADAMs are characterised as cell surface sheddases, able to cleave and activate and/or solubilise cell surface growth factors and cytokines. The reader is referred to Appendix one (C) for a more comprehensive list of ADAMs and their characterised substrates. Of these, the more characterised cytokine and one of the first whose solubilisation was identified to be by an ADAM, is tumour necrosis factor α (TNF α). Pro-TNF α is a 26 kDa membrane spanning protein which has an intracellular N - terminus. Human ADAM-10 demonstrates, along with ADAM-17 (TACE - TNF α converting enzyme) the proteolytic cleavage of proTNF α to yield soluble TNF α (Blobel, 1997; Rosendahl et al. 1997). It is suggested that an inhibitor of TACE expression or metalloprotease activity would prevent its cleavage, reducing the levels of soluble TNF α (Cerretti, 1999). ADAM-17 also has Growth Hormone Binding Protein (GHBP) sheddase activity, regulating the release of GHBP from the cell surface (Zhang et al. 2000). ADAM-17, as well as ADAM-10, is responsible for the cleavage of the Cellular Prion Protein (Vincent et al. 2001) and the Amyloid Precursor Protein (β-APP), a protein that is upregulated in the brain of Alzheimer patients (Buxbaum et al. 1998; Lammich et al. 1999). The ADAM-17 catalytic domain has been crystallised and the deduced structure yields a remarkable resemblance to adamalysin (a reprolysin) and to the predicted structure of the ADAM-10 catalytic domain (Maskos et al. 1998). Hence, it is not surprising that these two proteins have substrate specificity overlap.

ADAM-9 (MDC9) demonstrates cleavage of peptide sequences homologous to TNF α, β-APP, P75 TNFR, and KL-1 as well as the MMP substrate peptide (P-Cha-G-) (Roghani et al. 1999). The same study also demonstrated that an array of MMP inhibitors successfully inhibited ADAM-9 proteolytic activity. Further, ADAM-9 is thought to be involved in TPA-induced shedding of Heparin Binding EGF like growth factor (HB-EGF) via its metalloprotease domain and activation of its C-terminal located PKC response sites. This

is supported by the lack of HB-EGF cleavage upon the mutation of the metalloprotease catalytic motif (Izumi et al. 1998). Additionally, ADAM-9 has recently been shown to be proteolytically active against fibronectin and gelatin (Schwettmann and Tschesche, 2001) and it is likely that the soluble form of this metalloprotease is active against the same substrate, likening this ADAM to a secreted MMP.

MADM (Bovine ADAM-10) isolated from bovine kidney, has been shown to have human placental type IV collagenase activity (Millichip et al. 1998). ADAM-10 thus represents an ADAM having the same catalytic activity as MMP-2, -3, -9, -7, -10 and -11 with a similar membrane-spanning domain as the MT-MMPs (Nagase, 1997). ADAM-10 also cleaves the protein L1, which has been proposed to promote cell migration via signalling events with the αVβ3 integrin (Mechtersheimer et al. 2001).

The ADAM-TS subfamilies, which are ADAMs containing thrombospondin-like motifs, have also been characterised as active metalloproteases. ADAM-TS1 cleaves aggrecan, a cartilage proteoglycan (Kuno et al. 2000). This study found the C-terminal of ADAM-TS1 to be necessary for aggrecan degradation presumably through an attachment/binding role. Interestingly, ADAM-TS3 and 4, also called aggrecanases, have presumed proteolytic activity against this substrate (Tang, 2001). ADAM-TS2 has now been identified as a pro-collagen N proteinase whose activity is important in the cleavage of pro-collagen for the formation of collagen for the basement membrane and the ECM (Blelloch et al. 1999).

### *1.5.2 ADAM metalloprotease activities and their regulation by TIMPs*

Recently, both ADAMs -10 and -17 have been shown to be inhibited by TIMPs. MMP tissue inhibitor TIMP-3 but not TIMP-1, -2 and -4 has been shown to inhibit ADAM-17 (Amour et al. 1998). The same group showed that TIMP-1 and TIMP-3 but not TIMP-2 and -4 inhibited ADAM-10 metalloprotease activity *in vitro* (Amour et al. 2000). ADAM 12 (meltrin α) also demonstrates metalloprotease activity as described by Loechel *et al.* (1998) using α2 macroglobulin as a substrate. TIMP-1, -2, and -3 do not inhibit the metalloprotease activity of ADAM-12 (Loechel et al. 1999). ADAM-12 also exists in a

soluble form called ADAM-12s. This form of ADAM-12 lacks a transmembrane domain and is secreted from the cell representing a potential soluble metalloprotease, not unlike the MMPs (Gilpin et al. 1998). TIMP-3 is able to inhibit the protease activity of ADAM-12s; no other TIMPs were examined in this study (Loechel et al. 2000). It could be inferred that the above TIMPs inhibit ADAM-10, -12s and -17 via the same mechanism as they inhibit the MMPs. Recently, the TIMPs have been shown not to inhibit the activity of ADAM-8 and -9 (Amour et al. 2002).

### *1.5.3 ADAMS and integrin binding/cell adhesion*

Because not all ADAMS are proteolytically active (Huovila et al. 1996; Jia et al. 1996; Blobel, 1997), it is likely that there are significant differences between the physiological roles of individual ADAMs. The snake venom reprolysins bind integrin $\alpha 2\beta 3$ and inhibit platelet aggregation (Kini et al. 1992; Alfandari et al. 1997). The integrin-binding domain of the reprolysins includes a hairpin loop with the integrin ligand sequence RGD (Blobel, 1997). Although all ADAMs contain a predicted integrin binding site, ADAM-2, -5, -7, -9, -11 and -15 are the only ADAMs which possess a negatively charged residue in the third position of the ligand binding sequence motif (Huovila et al. 1996). This characteristic has been conserved across species and suggests differential integrin binding potential within the ADAMs family.

Perhaps the most studied ADAMs are mouse ADAM-1 and -2 (fertilin $\alpha$ and $\beta$ respectively). Both ADAMs have integrin-binding activities that have major implications for the fundamental physiological event - the process of sperm-egg fusion in the mouse (Cho et al. 1996). A monoclonal antibody raised against fertilin $\beta$ has been found to block sperm-egg fusion in the mouse. Also blocking this process were peptides designed against the predicted integrin-binding site of Fertilin (fertilin $\alpha$ /$\beta$ heterodimer) (Inoue et al. 1998). The integrin found on the egg, $\alpha 6\beta 1$, has been identified as a receptor for sperm, suggesting this integrin to in fact be the Fertilin receptor. Chen et al. (1999) further investigated this interaction and confirmed that the ADAM-2 disintegrin loop binds this integrin. In humans, ADAM-1 appears to be a pseudogene. However, human ADAM-20

and -21 show high similarity to ADAM-1 and -2 and are thought to be testis specific, suggesting that these ADAMs are the human homologues of mouse ADAM-1 and -2 (Hooft, 1998).

As some ADAMs, for example, ADAM-11, only contain an active disintegrin domain and not an active protease domain (Huovila et al. 1996) it is possible that such ADAMs may be solely involved in cell attachment. ADAMs possessing metalloprotease and integrin domains, ADAM-9, -12, -15 and -17, may contribute to either, or both, mechanisms. Additionally, ADAM-9, -11 and -15 have the conserved negatively charged peptide in the predicted integrin-binding domain, potentially enhancing integrin-binding affinity. Eto et al. (2000) have shown RGD-independent binding of human and mouse ADAM-12 and mouse ADAM-15 to the integrin $\alpha 9\beta 1$. Although mouse ADAM-15 does not contain an RGD sequence, it still possesses the negatively charged putative integrin-binding residue at the third position in the motif.

The specific role in attachment that ADAM-12 portrays has become increasingly evident. Iba et al. (2000) described the role of ADAM-12 in binding to cell surface syndecans and demonstrated that syndecans and the integrin $\beta 1$, respectively, support cell adhesion and cell spreading during the binding event. The tumour cells in this study, however, did not spread unless the $\beta 1$ integrins were activated, via an activating monoclonal antibody. Another group reported similar findings with respect to the attachment of myoblast and fibroblast cells to the recombinant ADAM-12 cysteine-rich/disintegrin domain in a disulphide-bond dependent manner (Zolkiewska, 1999). Iba et al. (1999) had previously outlined that the cysteine-rich domain can exclusively mediate the adhesion of a number of cells *in vitro* in cell attachment assays. The same study observed that the disintegrin-like domain did not support adhesion of the panel of carcinoma cells tested.

Zhang et al. (1998) found that a recombinant ADAM-15 disintegrin domain has a specific interaction with the integrin $\alpha V\beta 3$. Nath et al. (1999) found ADAM-15 to have specific binding to this integrin also, whilst Cal et al., (2000) showed ADAM-23 to have RGD-independent binding to the same integrin. This group also demonstrated ADAM-15

specific binding to integrin α5β1. ADAM-9, which lacks an RGD, but has a negatively charged residue at the third position of the integrin-binding peptide motif, binds the integrins α6β1 and αVβ5, with a similar cation dependence as needed for integrin to ECM interaction (Zhou et al. 2001). Within the ADAM-TS subfamily, ADAM-TS1 has been shown to induce a tight anchorage interaction with ECM proteins, possibly through the same type of integrin-binding mechanisms (Kouji and Kouji, 1998).

### *1.5.4 ADAMs and Cancer - Expression and Function*

ADAMs -9, -10, -11 and -15 mRNA transcripts are expressed in the haematological malignant cell lines HL60, Jurkat, K562, U266B1, U937 and Cippullo (Wu et al. 1997), and ADAMs -10 and -17, were found to be expressed in the choriocarcinoma cell lines JEG-3, JAR and BeWo (Whiteside et al. unpublished data from our laboratory) as well as the ADAM-12 splice variants ADAM-12S (short, soluble form) and ADAM-12L (long, membrane-bound form) in the human tumour cell lines HU-1 (lung adenocarcinoma), undifferentiated RD (rhabdosarcoma) and A204 rhabdomyosarcoma (Gilpin et al. 1998).

Furthermore, ADAM-12L appears to be up regulated in breast, colon and gastric carcinoma when compared to normal controls, both by PCR and IHC. Further, it was found to support the attachment of αVβ3-expressing A375 melanoma cells (Iba et al. 1999) in *in vitro*, cell attachment assays. Interestingly, the recombinant cysteine-rich domain but not the disintegrin domain was found to support cell adhesion of various tumour cells including breast carcinoma. This group further suggests attachment to be via cell surface heparin sulphate proteoglycans instead of integrins. ADAM-10 has been shown to cleave collagen XVII (Labrousse et al. 2002), disrupting hemidesmosome complexes, which have been shown to be intact in the normal prostate gland but disrupted in PCa (Nagle et al. 1995). Also, a disintegrin-metalloprotease like protein, which was later identified as ADAM-11, was shown to be rearranged somatically in two primary breast cancers and has thus been labelled a potential tumour suppressor gene (Emi *et al.* 1992).

Our laboratory has further characterised the ADAMs in PCa showing the expression of ADAM-9, -10, -11, -15 and -17 mRNA in the cell lines LNCaP, ALVA-41, DU-145 and PC-3 (McCulloch et al. 2000). The prostatic localisation of ADAM-9 and -10 was also determined previously by IHC in primary tumour biopsy sections from patients with PCa (Akl, unpublished data and McCulloch et al. *in press* 2003). Both ADAM-9 and -10 proteins were expressed in the glandular epithelial cells of the prostate in all samples tested. Occasionally, expression was also seen in scattered stromal fibroblasts. A less intense signal was observed for ADAM-9 in higher-grade cancer glands compared to benign glands in the same section. Such a reduction in the levels of ADAM-9 as PCa progresses may indicate that its role is unrelated to metalloprotease degradation of the ECM, which one would predict to be greater in metastatic cells, but is more closely aligned with modulation of cell-cell or cell-ECM contacts via its disintegrin domain. A role for ADAM-9 in cell adhesion would be consistent with a decrease in expression in cancer cells, *in vivo*, as those cells gain a capacity to break free and dissociate from the primary tumour mass.

ADAM-10, on the other hand, while present in the same cell types as ADAM-9, appeared to be unchanged or to increase slightly in cancer glands. This would be consistent with a role for ADAM-10 in ECM degradation and facilitation of subsequent invasion of metastatic cells. However, ADAM-10 showed marked nuclear localisation in all cancer glands when compared to benign glands. What role ADAM-10 has in the nucleus is unclear and requires further investigation. The co-expression but somewhat contrasting levels of ADAM-9 and -10 in the transition from benign glands to cancer glands may reflect distinct but complementary roles in regulation of tumour metastasis.

### *1.5.5 The hormone/growth factor regulation of the ADAMs*

As mentioned previously, ADAM-9, -10 and -17 mRNA expression in LNCaP cells was found to be regulated by DHT in our laboratory (McCulloch et al. 2000). Contrary to ADAM-9 and -10, ADAM-17 mRNA levels were down regulated with the addition of DHT. Whether the declining levels of ADAM-17 have an effect on the levels of soluble TNF $\alpha$ remains to be investigated. PC-3 cells produce TNF $\alpha$ (McCulloch et. al. 2000) but

display cytotoxic effects when treated exogenously with this cytokine (Fong et al. 1992). A recent finding however, concluded PC-3 cell growth, along with another androgen-independent PCa cell line DU-145, was not affected by treatment with TNF α (Sumitomo et al. 1999). In contrast, a study by Chung et al. (1999) concluded there were no detectable levels of TNF α in PC-3 cells or indeed any of the PCa cell lines screened, including LNCaP-ATCC, LNCaP-GW and DU-145, a cohort of androgen-sensitive and androgen-insensitive cell lines. Soluble TNF α levels have also been examined in the systemic circulation of patients suffering from various grades of PCa before surgery or androgen ablation. Adler et al. (1999) found that TNF α levels increased with age but not with PCa severity or metastatic occurrence.

The presence or absence of TNF α in PCa cell lines and their sensitivity to this important cytokine is clearly different in the hands of individual research groups. A definitive role for TNF α in PCa however, is not clear. Its association with the ADAMs and evidence of at least one link to regulation may suggest that fluctuations of TNF α, via the regulation of ADAM-17, can have implications in PCa progression and requires further investigation.

Given the preliminary observation that levels of the ADAMs are regulated by DHT in PCa, their regulation may also be controlled by other growth factors such as IGF-1, the phorbol ester PMA, the androgen DHT, bFGF and EGF, which affect growth rate and cell motility, although there is limited data available in this respect.

The androgen DHT is implicated in the proliferation of androgen-dependent carcinomas including the prostate. Tumour cells in the early stages of prostate cancer are androgen dependent. Tumours that become more aggressive and metastatic, are often androgen insensitive. Therefore, factors affecting metastasis, potentially ADAMs, may well be regulated by androgens in the early stages of disease development and regulated by other growth factors at later stages. As mentioned above, our laboratory has shown that some ADAM mRNA levels are regulated by DHT in the LNCaP PCa cell line (McCulloch et al. 2000). Alongside these observations, the expression of ADAM-7 mRNA has been shown to be responsive to DHT in castration studies in the mouse (Cornwall and Hsia, 1997).

IGF-1, a known growth promoter of the PCa cell lines LNCaP, PC-3 and DU-145 (Iwamura et al. 1993) elevates the expression of MMP-2 (Long et al. 1998). The prostate has a fully functional IGF-1 axis responsible for growth of normal and tumorigenic cell types (Cohen et al. 1994). Also, IGF-1 mediates cell motility regulation (Matsumoto et al. 1995; Leventhal et al. 1997). The MMPs have IGF-BP protease activity, processing these binding proteins, releasing IGF-1 and presumably increasing the bioavailability of IGF-1 (Fowlkes et al. 1994, 1995, 1997). Kubler et al. (1998) identified an IGF-BP protease in human pregnancy serum with disintegrin/metalloprotease properties providing preliminary evidence that ADAMs may be important regulators of IGF-1 mediated activities. More recently ADAM-12 has been shown to associate with IGF-BP3, partially purified ADAM-12s was able to cleave IGF-BP3, whilst only ADAM12s and IGF-BP3 were co-precipitated when IGF-BP3 and -BP5 was incubated with ADAM12s conditioned media (from ADAM-12s transfected COS1 cells), suggesting no interaction with IGF-BP5 (Loechel et al. 2000). Recently, ADAM-9 was shown to cleave IGF-BP5 in a human osteoblast cell line (Mohan et al. 2002), potentially elevating levels of bioactive IGF-1, which may be important in stimulating bone deposition and resorption, processes thought to be important in PCa bone metastasis.

The phorbol ester, PMA, has also demonstrated the ability to regulate MMP expression (Mackay et al. 1992). Additionally, PMA stimulates the expression of the integrin subunit β3 (Zhu, 1996). Phorbol esters are also known to activate signalling pathways through enzymes of the Protein Kinase C (PKC) family. Blobel (1997) suggests that at least some ADAMs have PKC response sites in the cytoplasmic domain. Potentially, they are involved in intracellular signalling. Therefore, PMA is a good candidate for regulating both the expression and activity of the ADAMs and has already been shown to decrease cell surface staining for ADAM-17, shown by immunofluorescence microscopy and cell surface biotinylation (Doedens and Black, 2000).

Further hormonal/growth factor responsive studies are needed to better our understanding of how the ADAMs are regulated and the potential impact on their role/s in cancer. Because of the potentially 'dual functionality' of these proteins, the hormonal and growth

factor regulation of ADAMs may have major mechanistic consequences, important for tumorigenic cell types to metastasise.

### *1.6 Conclusion*

Prostate cancer is a step-wise, progressive hormone dependent cancer, which often develop a highly aggressive, metastatic phenotype. The underlying molecular mechanisms of metastasis are unclear. However, the MMPs have key ECM proteolysis properties that can effectively assist in cell invasion through the BM and ECM. Cell migration is mediated, in part, by integrin activation and cell signalling events allowing tumorigenic cells to move through the degraded ECM. The ADAMs proteases share a functional catalytic motif homologous to the MMPs and also have integrin binding activities. Hence the ADAMs are potential key contributors toward the successful and effective metastasis of cancer cells.

Hormones and growth factors involved in PCa cell proliferation and survival regulate levels of proteins such as the MMPs. Therefore, given the similarities between the properties of the ADAMs and MMPs, and their key interactions with integrins, it is likely the ADAMs will be regulated in the same manner in PCa. Limited data is available to date, on the expression and regulation of ADAMs in any cancer type. There is however, a wide range of preliminary evidence and functional characteristics implicated, to propose that ADAMs have a potential hormonal/growth factor-regulated role in cancer metastasis.

### *1.7 Project Aims*

Using PCa cell lines characteristic of normal prostate, from low-grade, androgen sensitive to high-grade, androgen-insensitive PCa, and prostate tissue biopsies from both primary tumours and metastatic, secondary site tumours, the overall **aims** of this study are:

1. To characterise potential changes in the expression of both ADAM-9 and -10 proteins in normal, low through high-grade and metastatic examples of PCa.

2. To establish a PCa cell line model that over-expresses ADAM-10 by way of transfection with a mammalian expression construct, in anticipation of further use in functional *in vitro* assays such as cell attachment, migration and proliferation, and
3. To examine the regulation of the levels of both ADAM-9 and -10 by the prostate cancer growth promoters DHT, IGF-1 and EGF in an androgen/growth factor responsive PCa cell model.

Chapters 3 and 4 will examine potential differences in the levels of expression of both ADAM-9 and -10 proteins in a progressively metastatic PCa cell line model, the C4 series of cell lines. Protein expression of both ADAMs will also be examined in cellular compartments (cytoplasm and nucleus) between two contrasting cell models, RWPE-1, a non-tumorigenic prostate cell model, and PC-3, a late-stage metastatic PCa cell model. Additionally, PCa bone metastases will be examined for ADAM-9 and -10 protein expression and localisation. These studies will build on preliminary expression data indicating that ADAM-9 and -10 mRNA are present in PCa cell lines and ADAM-9 and -10 proteins are present in prostate primary tumour biopsies.

To find a functional consequence of the expression of ADAM-10 in the prostate, Chapter 5 will focus on the construction of a full-length human ADAM-10 construct and its subsequent transfection in PC-3 and RWPE-1 cells. ADAM-10 was chosen at the outset of this study based on the previous observations in our laboratory, discussed above, that the expression of this ADAM appeared elevated in high-grade PCa when compared to glands diagnosed with a lower Gleason grade in primary prostate tumour biopsies. Carrying out functional cell-based assays with cell lines over-expressing ADAM-10 protein is an integral part of elucidating the function of ADAMs such as ADAM-10 in PCa, although due to technical difficulties and time-constraints this aspect of the study needs further development.

Lastly, Chapter 6 will extensively characterise the regulation of both ADAM-9 and -10 mRNA and protein levels by the androgen DHT and the growth factors IGF-1 and EGF in the androgen/growth factor responsive cell model LNCaP. This chapter builds on our

laboratory's previous data, showing both ADAM-9 and -10 mRNA levels are elevated in response to DHT stimulation (McCulloch et al. 2000). Additional preliminary data also shows that ADAM-9 protein expression is lower in high-grade PCa when compared to low-grade and benign prostate glands. ADAM-10 expression, on the other hand, appears increased in late-stage PCa glands, and its expression is differentially localised to the cell nucleus when compared to low-grade cancer glands, where it appears to be localised to the membrane/cytoplasm. A change in levels of ADAM protein as PCa progresses from androgen-dependent through androgen-independent characteristics suggests hormones and growth factors, also involved in cancer progression, regulate these protein levels.

# CHAPTER TWO

## 2.0 MATERIALS AND METHODS

**Chemicals and Reagents:** All chemicals and reagents used throughout this study were of analytical grade and purchased from common companies such as: APS Finechem - Asia Pacific Speciality Chemicals Limited, Seven Hills, NSW, Australia; MERK Pty. Ltd. Kilsyth, Vic. Australia; Sigma RBI, Castle Hill, NSW, Australia, unless otherwise specified.

## *2.1 Cell Culture*

### *2.1.1 Resuscitation of cells from liquid nitrogen ($N_2$) storage*

Each ampoule, containing the cell line of interest, was retrieved from a liquid $N_2$ canister, thawed in a 37 °C water bath, and transferred to 50 ml tissue culture medium (specific for the cell line undergoing resuscitation) in a Falcon tube (Becton Dickinson, Franklin Lakes, NJ, USA). The Falcon tube containing the medium and cells was inverted gently three times and centrifuged at 1000 X G for 3 min. The medium was aspirated leaving the cell pellet, which was re-suspended in 5 ml medium and transferred to a standard T25 tissue culture flask (Nunc Nalge International, Naperville, IL, USA). Cells were allowed to attach to the flask and grow at 37 °C in 5 % $CO_2$ in an IR sensor incubator (Sanyo scientific, Bensenville, IL, USA).

### *2.1.2 Routine passage of cell lines*

Once each cell line reached approximately 70 - 90 % confluency, as determined by visualisation under an inverted light microscope (Olympus Australia Pty. Ltd. Mount Waverely, Vic, Australia), the cells were washed with warm (37 °C) phosphate buffered saline (PBS) (tissue culture grade, Oxoid, Brisbane, Australia). The cells were treated with 1 X trypsin/versine (Invitrogen Australia Pty. Ltd. Mount Waverely, Vic, Australia) (0.2 ml for T25, 0.5 - 1 ml for T75 and 1 - 2 ml for T175 or T225 $cm^2$ flasks) and were incubated for up to 5 min (depending on the cell type) at 37 °C. The culture vessels were gently tapped to dislodge any remaining cells from the bottom of the flask. The appropriate medium, which contained serum, was used to wash and re-suspend the cells for transfer into new culture vessels containing the appropriate amount of medium.

### *2.1.3 Cyropreservation of cell lines cultured*

Each cell line was harvested with trypsin/versine as described above for routine passage of cells. Harvested cells were pelleted by centrifugation at 1000 X G in a 15 ml Falcon tube. Cell pellets were resuspended in media containing 10 % Dimethyl Sulfoxide (DMSO) and transferred to 1.5 ml cryotubes (Nunc) in 1.0 ml aliquots. The cryovessels were put in an ice-cold isopropanol bath at -80 °C for at least 6 h. Each cryotube was then transferred to a liquid $N_2$ canister and logged in a tissue culture logbook for long-term storage.

### *2.1.4 Cell counting*

The cell type of interest was cultured to ~70 % confluency in either a T25 or T75 tissue culture vessel as described above, trypsin/versine treated and resuspended in either 5 ml (for T25) or 10 ml (for T75) tissue culture medium. 0.2 ml of cell suspension was combined with 0.2 ml 0.4 % trypan blue and transferred to a haemocytometer. Viable cells (not stained blue) were counted in 2 X 1 $mm^2$ counting chambers under an inverted light microscope (Olympus) under the 10X objective, ensuring that the number of cells in each counting square was at least 100 (for statistical viability) and that the total cell count between the counting squares differed by less than 10 %. Cell number/ml was calculated and the appropriate dilution was made for downstream experiments requiring a pre-determined cell density.

## *2.2 Reverse Transcription - Polymerase Chain Reaction (RT-PCR)*

### *2.2.1 General RNA extraction method*

Total RNA was extracted from the 90% confluent, growth factor treated LNCaP cells using either the RNAgents Total RNA Isolation System (Promega, Annandale, NSW, Australia), Trizol reagent (Life Technologies, Mulgrave, Vic, Australia) or QIAGEN (Fairfield, Vic, Australia) column purification kit, according to the specific manufacturer's protocol. RNA concentrations and purity were determined using a DU 640 Beckman (La Jolla, CA) spectrophotometer wavelength scanning analysis from 220 nm - 320 nm or a RNA/DNA calculator (Amersham Biosciences Pty Ltd. Castle Hill, NSW, Australia). The relative

purity of each sample was determined by A260/A280 ratios and was accepted as satisfactory in the range 1.8 - 2.0.

### *2.2.2 Reverse Transcription (RT)*

Reverse transcription (RT) was carried out using 5 µg of total RNA, 5 µg of oligodT primer and 1U superscript II RNAse H⁻ reverse transcriptase (Invitrogen). RT was carried out at 43 °C for 90 min. All cDNA was screened by PCR using β-actin primers, which span a β-actin intron 5'-CGTGGGCCGCCCTAGGCACCA-3' (forward) and 5'-GGGGGGACTTGGGATTCCGGTT-3' (reverse) yielding a 234 bp cDNA PCR product and a 330 bp gDNA PCR product, as an indicator of possible genomic DNA (gDNA) contamination (Telford et al., 1990). PCR was performed in a 50 µl volume containing 5 µl 10 x PCR buffer (with a final reaction concentration of; 1.5 mM $MgCl_2$, 50.0 mM KCl, 10.0 mM Tris-HCL, pH 8.0) (Roche Diagnostics, Brisbane, QLD, Australia), 0.3 mM dNTP mix, 1U DNA Taq polymerase (Roche) and 1 µl cDNA made up to 50 µl with sterile distilled water.

### *2.2.3 Polymerase Chain Reaction (PCR)*

PCR was carried out on a DNA Thermal Cycler (Perkin Elmer, Brisbane, QLD, Australia) using the following protocol; 95 °C 5 min (initial denaturation), followed by 35 cycles at: 95 °C 30 sec (denaturation), (annealing temperature specific for each primer used) 30 sec, 72 °C (10 sec/ 100 bp PCR product) (extension) with the final cycle at 72 °C for 10 min (final extension). Primers were purchased from Proligo (Southern Cross University, Lismore, NSW, Australia). All PCR products underwent electrophoresis at 100 volts for 45 min on a 2% agarose/Tris-acetate-EDTA (TAE) gel containing 1 µg/ml ethidium bromide (EtBr). DNA molecular weight marker IX or X (Roche) was used as a guide for PCR product size. DNA bands were visualised under a UV lamp, photographed and excised from the gel with a sterile scalpel blade. Excised samples were purified using either Wizard PCR Preps DNA Purification System (QIAGEN) or Clontech Gel Purification Kit (Invitrogen) using the manufacturer's protocol.

### *2.2.4 Sequencing using Big Dye$^{tm}$*

Automated DNA sequencing using Big Dye$^{tm}$ versions I through III technology was carried out at the Australian Genome Research Facility, (University of Queensland, Brisbane, Australia).

## *2.3 Western Blot Analysis*

### *2.3.1 Protein extraction*

*Whole cell lysate*

Cell pellets of the PCa cell lines from a ~70 to 90 % confluent T75 tissue culture flask were resuspended in 500 ul Triton X-100 lysis buffer (50 mM Tris pH 7.5, 150 mM NaCl, 1% Triton X-100, 0.1 mM PMSF, 10 mM EDTA pH 8.0, 1 tablet Roche complete protease inhibitor cocktail/25 ml). The cell lysate was frozen on dry ice, thawed in ice-cold water then passed through a 26-gauge needle twice to shear high molecular weight gDNA. The cell lysate was then centrifuged at 12000 X G for 30 min at 4 °C. The resultant supernatant was collected and whole cell protein was quantitated in triplicate using the BCA protein assay reagent (Pierce, Rockford, IL) as per the manufacturer's 'microwell' protocol using serial dilutions of 2 mg/ml Bovine Serum Albumin (BSA) as a reference standard. Yields between 1 and 6 µg/µl were obtained as determined by absorbance at 545 nm on a multi-well plate reader (Beckman).

*Nuclear / Cytoplasmic fractions*

Cellular compartmentalisation was achieved by using the NePer nuclear/cytoplasmic fractionation kit (Pierce) as per manufacturer's recommendations. Briefly, cell pellets of LNCaP, RWPE-1 or PC-3 cells from a ~70 to 90 % confluent T25 or T75 tissue culture flask were resuspended in a 5 ml/mg volume of buffer CERI. Buffer CERII was added, followed by a centrifugation step, which pelleted the intact cell nuclei. By removing the supernatant the cytoplasmic fraction was isolated. Buffer NERI was added to the nuclear-

membrane pellet, lysing the nuclear membrane. An additional centrifugation step pelleted unwanted nucleic acid, lipids, carbohydrates and cell debris. The supernatant from this step contained protein isolated from the cell nucleus. Each buffer was adapted to contain a final concentration of 0.1 mM PMSF, 10 mM EDTA pH 8.0 and 1X complete protease inhibitor cocktail (Roche) was added to inhibit protease activity, as recommended by the manufacturer.

### *2.3.2 Sodium Dodecyl Sulphate - Polyacrylamide Gel Electrophoresis (SDS-PAGE)*

10 % PAGE (29:1) Acrylamide: Bis-acrylamide (Biorad, Hercules, CA) gels (0.75 mm thick x 83 mm x 73 mm) were used for all Western blot analyses, as the proteins detected were acceptably resolvable with this percentage of acrylamide. For the resolving gel, a final concentration of 0.01 % SDS, 1.5 M Tris-HCl, 10 % acrylamide, was polymerised with 50 ul 10 % ammonium persulfate (APS, Biorad) and 10 µl N,N,N,N-tetra-methyl-ethylonediamine (TEMED, Biorad) at room temperature. The stacking gel contained a final concentration of 0.01 % SDS, 0.5 M Tris-HCl, 3.8 % acrylamide, polymerised with 30 µl 10 % APS and 5 µl TEMED at room temperature.

Protein was loaded into each well of the stacking gel alongside a pre-stained protein molecular weight marker (Biorad) and electrophoresed at ~15 mA per gel until the dye front, and hence the protein, had run into the resolving gel, at which point the current was boosted to ~20 mA per gel. Each gel was run for 1 - 1.5 h or until the dye front was as close as possible to the bottom edge of the resolving gel.

### *2.3.3 Standard protein transfer*

After electrophoresis, each gel was equilibrated in 1 X Carbonate transfer buffer (10 mM $NaHCO_3$, 3 mM $Na_2CO_3$, 20 % Methanol, pH 9.9), pre-cooled at - 20 °C, for 1 min. The 'blot' was built on the negative side of the Western blot transfer cassette in the following order: sponge, 3 X 3 sheets of blotting paper, PAGE gel, 0.2 µm pore size nitrocellulose membrane (Protran, Schleicer & Schuell, Dassel, Germany) 3 X 3 sheets of blotting paper,

sponge. Building of the blot took place submerged in blot buffer so as to reduce possible air bubbles interfering with efficient transfer. Protein electro-transfer was run at ~150 mA per gel for 1 h at 4 °C. The nylon membrane was removed from the gel and stained with Ponceau S (Biorad) (2 min) at room temperature on a bench top shaker, for protein visualisation so that transfer efficiency could be assessed.

### *2.3.4 Standard Western blot detection*

The nitrocellulose membrane containing transferred protein was blocked for 1 - 2 h at room temperature in 5 % Blotto (5 % Skim milk powder in TBS-Tween-0.05%). The membrane was then incubated with the antibody of interest either overnight at 4 °C or 2 h at room temperature in 0.8 % Blotto followed by 4 X 5 min washes in TBS-Tween (10 mM TrisHCl pH 8.0, 150 mM NaCl, 0.05 % Tween-20) at room temperature. Next, the membrane was incubated with the appropriate secondary antibody (1-2 h, room temperature) followed by another 4 X 5 min wash in TBS-Tween. For detection of signal, the membrane was incubated in Femto (Pierce) chemiluminescence substrate and exposed to X-ray film for the appropriate amount of time before developing on an automatic developer (Curix-60 AGFA, Agfa Gaveart, Australia). All films were re-aligned with the membranes and the protein marker was traced onto the X-ray film so that the size of the signal developed could be estimated.

For the subsequent detection of additional proteins, the membrane was stripped with a first wash 4 X 5 min in TBS-Tween and an incubation for 15 min at room temperature in Western blot stripping buffer (Pierce) followed by another 4 X 5 min wash in TBS-Tween. The membrane was subsequently incubated in Femto and underwent detection by X-ray film to ensure no signal was developed. An additional 4 X 5 min in TBS-Tween was carried out to remove the chemiluminescence; the primary antibody was then applied to the membrane.

### *2.3.5 Antibodies used in Western blotting*

For ADAM-9, two different antibodies were used throughout this study, 1) ADAM-9Dis was raised against the recombinant disintegrin domain of ADAM-9 (Chemicon, Temecula, CA, USA) and 2) ADAM-9Cterm was raised against a C-terminal specific peptide (Biomol Plymouth Meeting, PA, USA) (See Figure 2.1A). For ADAM-10, two antibodies were also used throughout this study, 1) ADAM-10Cterm was raised against a C-terminal specific peptide to ADAM-10 (Chemicon) and 2) ADAM-10Met, was raised against a peptide sequence at the N-terminal of the mature, active metalloprotease region of ADAM-10 (see Figure 2.1B). For housekeeping proteins, an antibody against β-Tubulin (Labvision-Neomarkers, Fremont, CA, USA) was used in the case of whole cell lysate and cytoplasmic fractions, and an antibody against Proliferating Cell Nuclear Antigen (PCNA) (Zymed South San Francisco, CA, USA) was used in the case of nuclear cell fractions.

**Figure 2.1** Schematic representations of ADAM-9 and -10 antibodies used throughout this study:

**A) ADAM-9 antibodies:**

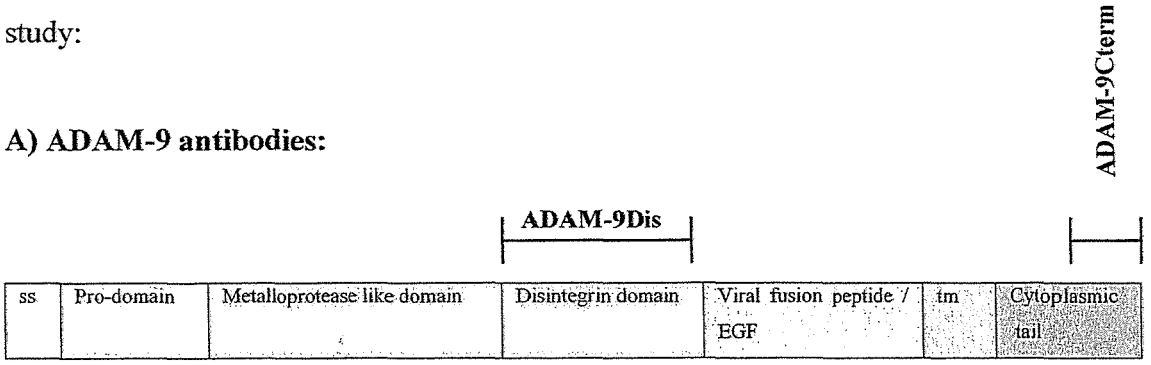


**B) ADAM-10 antibodies:**

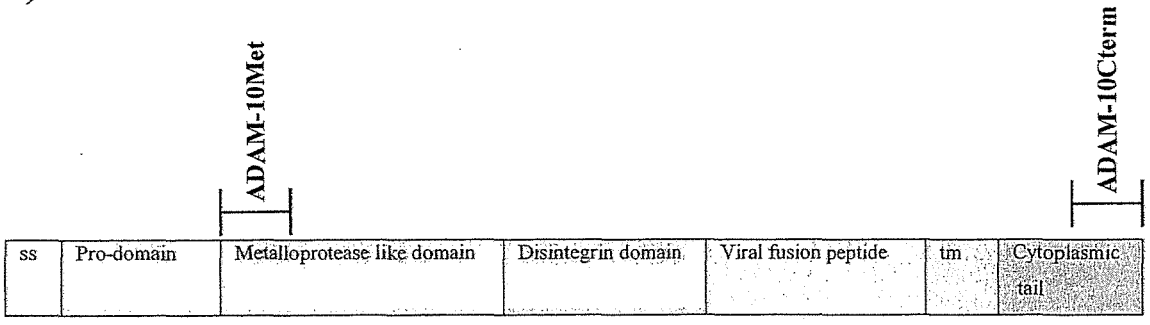

## *2.4 Prostate biopsy tissue section analysis*

### *2.4.1 Hematoxylin and Eosin (H&E) Staining*

Formalin fixed, paraffin embedded tissue sections underwent routine H&E staining for pathological examination and assessment in the following protocol: Deparaffinisation schedule: 100 %Shellex/Xylene 3 X 5 min, 2 X 100 % ethanol (EtOH) 1 min, 70 % EtOH 1 min, distilled water ($dH_20$) 1 min, Staining schedule: Mayers hematoxylin 4.5 min, Scotts water (water, pH 8.0) 1 min, 3 X $dH_20$ 30 sec, Eosin 1 min, 3 X $dH_20$ 30 sec, Dehydration schedule: $dH_20$ 1 min, 70 % EtOH 1 min, 2 X 100 % EtOH 1 min, Shellex/Xylene 3 X 5 min followed by the application of a coverslip using DEPEX, which was allowed to set for 24 h before visualising the stained section under a light microscope. For fresh frozen tissue sections, the slide was introduced at the first 100 % EtOH incubation and underwent the subsequent steps of staining as outlined above.

# CHAPTER THREE

## 3.0 THE EXPRESSION OF ADAM-9 AND -10 PROTEASES IN PROSTATE CANCER

*3.1* ***Introduction:***

The key components, which contribute to the mechanisms of successful metastasis, include extracellular matrix (ECM) invasion, mediated in part by matrix metalloprotease (MMP) proteolysis (Bergers and Coussens, 2000) and cell migration, assisted by cell surface molecules including the integrins (Gumbiner, 1996). It was hypothesised that the **ADAMs** proteases were likely to be additional key mediators of this process, as they comprise **A** **D**isintegrin **A**nd **M**etalloprotease domain. These proteins exist predominantly as membrane bound proteases that have the potential to degrade ECM components via their extracellular active metalloprotease domain and to regulate cell-cell and cell-ECM contacts via their integrin binding/dissociation capabilities.

Both ADAM-9 and -10 are active metalloproteases (Skovronsky et al. 2000; Blobel 1997; Rosendahl et al. 1997) and are able to degrade ECM substrates *in vitro,* including gelatin, fibronectin (Schwettmann et al. 2001) and collagen type IV (Millichip et al. 1998). ADAM-9 is also known to bind key integrins involved in cell-cell and cell - ECM contacts such as $\alpha 6\beta 1$, which maintains expression throughout the various stages of PCa development (Rabinovitz et al. 1995).

Previously, this laboratory has described the mRNA expression of ADAM-9, -10, -11, -15 and -17 in PCa cell lines characteristic of androgen-sensitive disease (LNCaP and ALVA-41) and androgen-insensitive disease (DU-145 and PC-3) (McCulloch et al. 2000). In the same study the regulation of three of these ADAMs (-9, -10 and -17) by the androgen dihydrotestosterone (DHT) was examined at the mRNA level. ADAM-9 and -10 mRNA levels were responsive to and significantly up-regulated by DHT. Given this type of regulation, it is possible that these two ADAMs will be involved in PCa development and progression. Indeed, closely related MMPs, for example, MMP-7 are regulated in this fashion in PCa (Sundareshan et al. 1999).

In order to study this, the use of an *in vitro* cell model representative of PCa progression would be helpful. The C4 series of cell lines - C4, C4-2 and C4-2B, which were derived

from the co-culture of LNCaP cells with a bone cell line in athymic mice (Chung et al. 1997; Zhau et al. 2000) are reported to reflect changes in androgen sensitivity. The LNCaP and C4 cell lines are androgen sensitive and poorly metastatic whilst the C4-2 and C4-2B cell lines are androgen insensitive and moderately metastatic. Thus, this series of cell lines may represent a good model for the examination of ADAM-9 and -10 expression and their relationship to PCa progression.

Recent studies in our laboratory have examined the expression of ADAM-9 and -10 at the mRNA and protein level in primary prostate tumour biopsies by *in situ* hybridisation (ISH) and immunohistochemistry (IHC) respectively (reviewed in Chapter 1). This provided data regarding the expression and localisation patterns of these particular ADAMs in differing prostate diseases, from benign/hyperplastic states, to low through high-grade cancer. To extend those immunohistochemical studies further, several bone metastases taken from late-stage PCa patients at biopsy have also been examined as part of this study of ADAM-9 and -10 expression, to determine whether these two ADAMs may have a role in these later stages of carcinoma.

In the earlier more comprehensive prostate biopsy IHC studies, strong membrane/cytoplasmic staining was seen for ADAM-9 in the benign type of prostate gland. However, glands characteristic of low to high-grade cancer showed weaker staining in comparison. In the case of ADAM-10, the intensity of IHC staining was strong in the benign situation, apparently weaker in low-grade cancer glands but strong in high-grade cancer glands. The most striking observation however, was that within high-grade cancer glands, ADAM-10 appeared to be localised to the perinuclear and/or nuclear compartment of the cell as compared to benign and low-grade cancer glands where membrane staining was more apparent.

These novel observations led to the hypothesis that the ADAMs might have differential functions depending on their cellular localisation - cytoplasmic/membrane bound versus nuclear. To test this, it was envisaged that there might be a nuclear-predominant expression of ADAM-10 in PC-3 cells, representing late-stage PCa, whereas this may not be apparent

in RWPE-1 cells, which represent a normal prostate cell model. In the case of ADAM-9, it was hypothesised that nuclear expression in one or both of these cell lines may be observed, given the occasional perinuclear expression observed in primary prostate glands within prostate tissue biopsies.

Additionally, recent studies have examined the event of membrane vesicle shedding from the cell surface, releasing membrane-associated proteins into the extracellular environment (Angelucci et al. 2000; Taraboletti et al. 2002). These studies observed MMP activity associated with shed membrane vesicles as well as illustrating that more tumorigenic cell types had a higher occurrence of shed membrane vesicles. It is therefore likely, given both ADAM-9 and -10 are membrane bound, that these two ADAMs are also present in shed membrane vesicles from PCa cell lines and their metalloprotease activity perhaps contributes to ECM degradation activities.

Thus, the **aims** of this chapter were:

1) a) To extend the RT-PCR expression data previously published (McCulloch et al. 2000) to assess the mRNA expression of ADAM-9 and -10 in the C4 series of the prostate cancer cell lines: C4, C4-2, and C4-2B.
   b) To examine possible changes in the expression of ADAM-9 and -10 at the protein level in each of the LNCaP metastatic variant cell lines.
2) To examine the protein expression pattern of ADAM-9 and -10 in prostate cancer bone metastases obtained at biopsy.
3) To examine the nuclear/cytoplasmic expression patterns of ADAM-9 and -10 in RWPE-1 and PC-3 prostate cell lines.
4) To examine possible membrane-vesicle associated ADAM-9 and -10 protein expression using the RWPE-1, LNCaP and PC-3 cell lines.

## *3.2 Materials and Methods*

### *3.2.1 Reverse Transcription-Polymerase Chain Reaction (RT-PCR)*

*Reverse transcription (RT)*

Total RNA was obtained from cell pellets, from each of the PCa cell lines: LNCaP, C4, C4-2 and C4-2B and reverse transcribed as described in Chapter 2. All cDNA was screened by PCR using β-actin primers (Table 3.1), which span a β-actin intron, as an indicator of possible genomic DNA (gDNA) contamination.

*Polymerase Chain Reaction (PCR)*

PCR was performed as described in Chapter 2 using each of the primers and their corresponding annealing temperatures illustrated in Table 3.1, with 1 µl cDNA as a template from each of the cell lines LNCaP, C4, C4-2 and C4-2B in separate PCRs, made up to 50 µl with sterile distilled water.

**Table 3.1:** Oligonucleotide primers for ADAM-9, -10 and β-actin used in PCR analysis, and their corresponding PCR product sizes and annealing temperatures.

| mRNA Transcript | Primer Sequences | PCR Product Size (bp) | Annealing Temp. (C) | Reference |
|---|---|---|---|---|
| ADAM-9 | 5' AGTGCAGAGGACTTTGAGAA (Forward)<br>5' TGCCGTTGTAGCAATAGGCT (Reverse) | 391 | 56 | Wu et al. 1997 |
| ADAM-10 | 5' TGGATTGTGGCTTCATTGGTG (Forward)<br>5' TGCAGTTAGCGTCTCATGTGTC (Reverse) | 236 | 55 | Wu et al. 1997 |
| β-actin | 5'CGTGGGCCGCCCTAGGCACCA (Forward)<br>5'GGGGGGACTTGGGATTCCGGTT (Reverse) | 234(cDNA)<br>330(gDNA) | 55 | Telford et al. 1990 |

### *3.2.2 Protein Extraction*

Protein was extracted from cell pellets lysates of the LNCaP, C4, C4-2 and C4-2B cell lines whilst nuclear/cytoplasmic fraction protein was extracted from cell pellets of the RWPE-1 and PC-3 cell lines. All cell pellets were derived from ~70 to 90 % confluent T75 tissue culture flasks as described in Chapter 2. Each protein extract was quantified using the BCA method also described in Chapter 2.

*Membrane Vesicle Isolation*

Serum-free media (RPMI-1640) were collected (10 ml) from RWPE-1, PC-3 and LNCaP confluent T75 cell cultures after 24 h incubation. The media were centrifuged at 1200 X g for 10 min, the resultant supernatants collected and centrifuged at 8000 X g for 20 min at 4 °C. The supernatant after the 2nd centrifugation should be free of any contaminating cells and cellular debris (Taraboletti, et al. 2002). The supernatants were then subjected to a high-speed ultra-centrifugation (100,000 X g) on an Ultracentrifuge (Beckman) using an SW41.1 rotor to pellet the cell membrane vesicles as per methods outlined in Taraboletti, et al. (2002). The supernatants were removed and each membrane vesicle pellet was resuspended in 200 µl of Triton X-100 protein lysis buffer (Chapter 2).

### *3.2.3 Western Blot*

10 µg of protein from each whole cell lysate of LNCaP, C4, C4-2, and C4-2B or 5 µg cytoplasmic or nuclear fractions of RWPE-1 and PC-3 cells or 20 µl of membrane vesicle lysate was suspended in a reducing loading buffer and boiled for 3 min prior to loading onto a 10 % SDS-PAGE gel, followed by a standard Western blotting procedure – outlined in Chapter 2. The blocked membrane (5 % Blotto) was incubated with either ADAM-9Dis, (0.5 µg/ml), ADAM-9Cterm (0.25 µg/ml), ADAM-10Cterm (0.5 µg/ml) or ADAM-10Met (0.05 µg/ml) rabbit polyclonal antibody (see Figure 2.1) or human anti-β-Tubulin, or PCNA (0.2 µg/ml) mouse monoclonal antibody, in 0.8 % Blotto: TBS/Tween-20 (0.05 %) at 4 °C overnight. The primary antibody was collected and re-used up to three times without loss of efficiency. The membrane was incubated for 2 h at room temperature in anti-rabbit HRP (DAKO, Carpintera, CA), 0.2 µg/ml or anti-mouse POD (Roche), 0.2 µg/ml in 0.83% Blotto: TBS/Tween-20 (0.05%). For detection, the membrane was incubated in 2 ml Femto (Pierce). The resultant signal was detected on X-ray film by autoradiography and developed on an automatic developer (Curix-60 AGFA, Agfa-Gaveart, Australia).

### *3.2.4 Immunohistochemistry (IHC) & Immunocytochemistry (ICC)*

*Bone metastasis tissue samples (IHC)*

Paraffin embedded, EDTA-decalcified, prostate bone metastasis tissue blocks with embedded tissue acquired from men with high-grade, metastatic PCa at biopsy were obtained from the Bernard O'Brien Institute of Microsurgery (BOBIM), St. Vincent's Hospital, Melbourne, Vic. via collaborations undertaken with Dr. Elizabeth Williams (Senior Research Scientist).

*Cell line culture (ICC)*

The normal but transformed, non-tumorigenic prostate cell line RWPE-1 and the metastatic PCa cell line PC-3 were cultured in standard T25 tissue culture vessels to 70 % confluency and harvested with trypsin/versine as described in Chapter 2. The cells were counted on a haemocytometer and seeded onto a 12 well tissue culture microscope slide at a concentration of 5000 cells/well and allowed to grow overnight.

*Fixation and processing*

For IHC, the tissue blocks were sectioned at 4-5 μm thickness on a standard bench-top microtome and the sections were mounted on APES (3-aminopropyl triethoxysilane) coated slides and dried at 37 °C overnight. The sections were then dewaxed and rehydrated as described in Chapter 2. H&E - as described in Chapter 2 was used for routine histological examination. For ADAM-10, antigen retrieval was necessary, the tissue sections were immersed in 0.1 M citrate buffer, enclosed in a microwave proof pressure cooker and heated on high setting (650 Watt microwave) 2 X 4 min. The pressure cooker was cooled on ice for 20 min and the slides allowed to cool in Citrate buffer to room temperature. For ICC, the medium was aspirated and the cells were washed with warm (37 °C) Phosphate Buffered Saline (PBS) and fixed by immersion in ice-cold methanol at -20 °C for 5 min. The fixed sections/cells were incubated in 10% methanolic peroxide, 2 X 20min or 2 X 15 min (IHC and ICC respectively) at room temperature to block any endogenous peroxidase

activity, which may be present in the samples. Non-specific antigenic sites were blocked by incubation with 5 % BLOTTO for 1 hour (IHC) or 30 min (ICC) at room temperature. The optimal antibody dilution for IHC (ADAM-10Cterm: 5 µg/ml, ADAM-9Dis: 4 µg/ml) or ICC (ADAM-9Dis & ADAM-10Cterm: 10 µg/ml) or Prostate Specific Antigen (PSA) (pre-optimised immune rabbit anti-sera - DAKO), in the case of IHC, was applied and incubated overnight at 4 °C.

The slides were washed for 3 X 5 min in TBS-Tween. The signal was detected using the DAKO Envision plus detection kit which involves a 30 min incubation with a HRP-conjugate antisera followed by a 3 X 5 min wash in TBS-Tween and detection using diaminobenzine (DAB) chromogenic substrate, which was monitored for optimal incubation time (1 - 10 min) under a light microscope. The DAB was inactivated by a $dH_20$ bath. The nuclei were counterstained with Hematoxylin (5 min) followed by several washes in tap water and dehydration through graded ethanol (70 % and 100 %) and cleared in Xylene, cover-slipped using DEPEX and allowed to dry overnight in a fume hood before microscopic examination. The mounted slides were viewed under a light microscope and with the use of a digital camera (Kodak) images could be directly downloaded and saved as a Tagged Image File Format (TIFF) picture file.

As a positive control for IHC, paraffin embedded prostate tissue blocks from men with BPH, non-malignant conditions and various stages (Gleason scores) of cancerous prostate tissues were obtained via collaboration with Dr. Hema Samaratunga from the Pathology Department, Royal Brisbane Hospital, Australia. As a negative control for the immunostaining, the primary antiserum (either ADAM-9 or ADAM-10) was omitted from the staining schedule. ADAM-10 primary antibody was also pre-absorbed with a purified blocking peptide (Chemicon) to detect non-specific binding. No blocking peptide, or its precise sequence was commercially available for the ADAM-9 primary antibodies. The PSA negative control (non-immune rabbit serum) was supplied as a pre-optimised solution by DAKO. As a negative control for the ICC, the primary anti-serum was omitted from the staining schedule.

## *3.3 Results*

### *3.3.1 The expression of ADAM-9 and -10 mRNA and protein in the LNCaP metastatic variants C4, C4-2 and C4-2B*

*mRNA expression by RT-PCR*

Expression of PCR products, the expected size for ADAM-9 and -10 were found in cDNA from each of the LNCaP PCa cell line metastatic variants C4, C4-2 and C4-2B (Figure 3.1). As the PCR protocol was not quantitative no comparison of expression levels is possible in this case. The LNCaP cell line was used as a positive control in all steps as ADAM-9 and -10 mRNA was previously identified in this cell line (McCulloch et al. 2000) and it is the parent cell line of the subsequent metastatic variants analysed. Each cell line cDNA was free of gDNA contamination as determined by β-Actin primers.

*Protein expression by Western blot*

A qualitative measure of protein expression was undertaken by Western blot analysis and showed ADAM-9 and -10 protein expression in the LNCaP, C4, C4-2 and C4-2B whole cell lysate (Figure 3.2). ADAM-9 was detected in all of the PCa cell lines tested with a single band at ~84 kDa (Figure 3.2A), the anticipated size of the inactive pro-form of ADAM-9. Very faint bands at ~60 kDa were occasionally observed (too faint to be shown) and may indicate the mature active form of ADAM-9 protein. ADAM-10 protein bands were visualised at ~100 kDa representing the unprocessed, pro-form of ADAM-10 and ~60 kDa, the expected size of the mature, catalytically active form of ADAM-10 (Figure 3.2B). A positive control (as recommended by Chemicon), using JURKAT (Human Acute T-cell leukaemia) whole cell lysate run alongside LNCaP cell protein, showed bands of the same size for unprocessed and processed ADAM-10 forms (Figure 3.2C).

**Figure 3.1:** RT-PCR of ADAM-9 and -10 mRNA transcripts in the increasingly metastatic prostate cancer cell lines LNCaP, C4, C4-2 and C4-2B

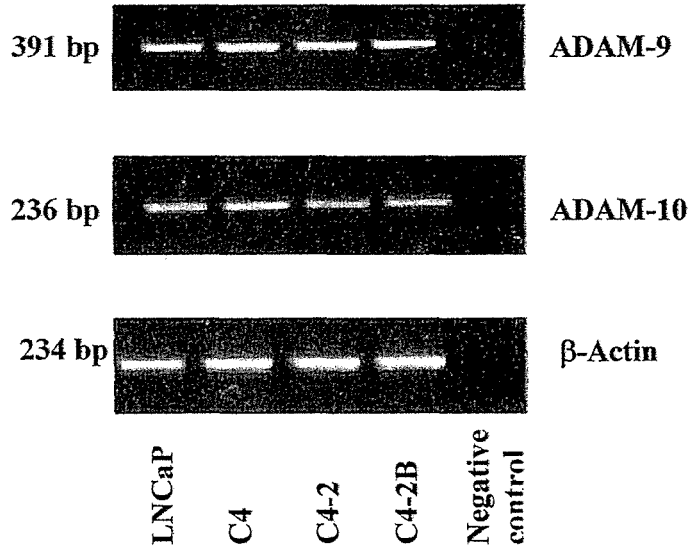


Each cell line was cultured to 70 - 90 % confluency, harvested, and their total RNA extracted of which 5 µg was reversed transcribed as described in Materials and Methods. ADAM-9 and -10 gene specific primers (Table 3.1) were used in subsequent PCR analysis. The size of the PCR product was determined by direct comparison of molecular weight marker IX (Roche - not shown) run alongside each PCR product on a 2 % agarose gel containing 1 µg/ml EtBr. The PCR product was visualised under a UV lamp. β-Actin primers, which span an intron, were used to ensure the cDNA in each cell line was free of gDNA contamination. The LNCaP cell line, known to express both ADAM-9 and -10 mRNA transcripts was used as a positive RT-PCR control whilst a PCR with no cDNA template was used as the negative control. Identical results were found for three separate RNA preparations of each C4 series cell line.

**Figure 3.2:** Western blot analysis of ADAM-9 and -10 protein in the increasingly metastatic prostate cancer cell lines LNCaP, C4, C4-2 and C4-2B

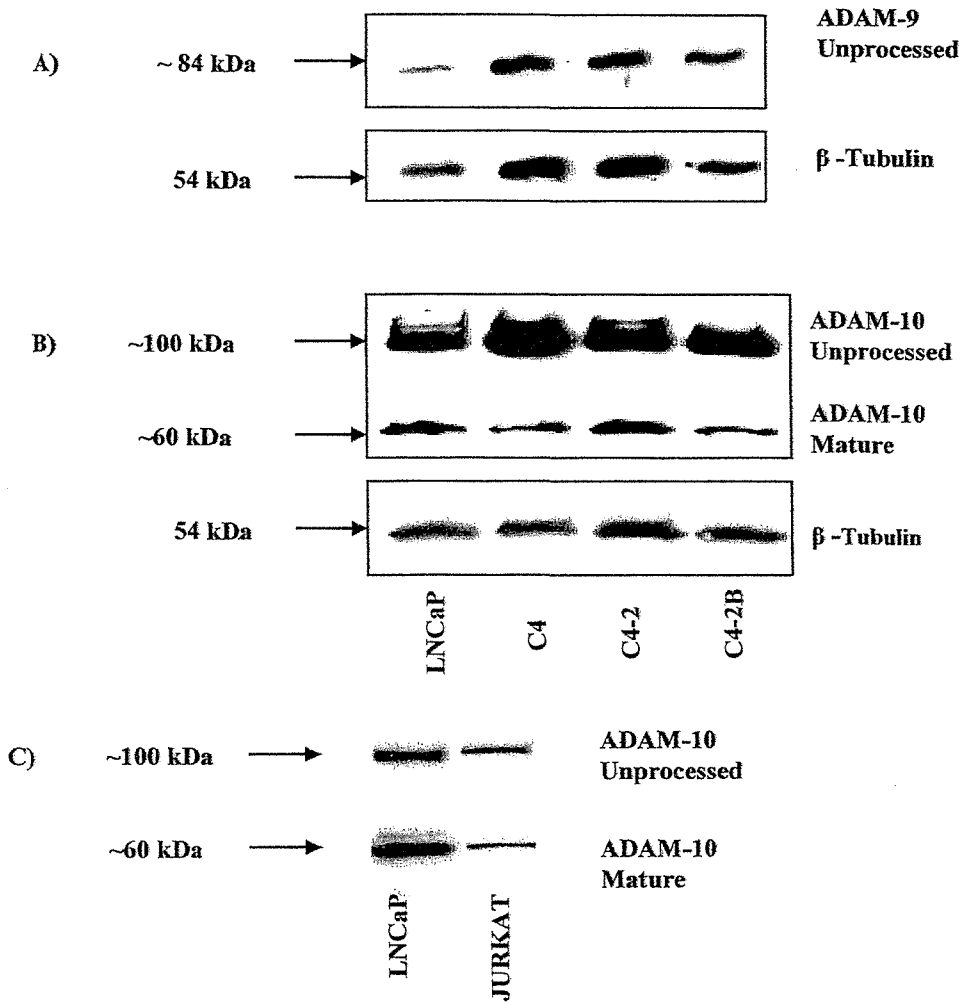


Each cell line was cultured to 70 - 90 % confluency, harvested, and their total protein extracted with protein extraction lysis buffer. 10 μg of protein was loaded onto a 10 % PAGE gel followed by standard Western blot procedure (Chapter 2). The size of each ADAM product was determined by comparison of Biorad pre-stained protein marker run on the same PAGE gel (not shown). The housekeeping gene β-Tubulin was used in a subsequent Western blot on the same membrane to visualise protein loading variability between cell lines. Similar results were found in three separate whole cell lysate protein preparations for each C4 series cell line. As a positive control for ADAM-10, LNCaP whole cell lysate was run alongside the JURKAT cell line whole cell lysate.

### *3.3.2 The expression of ADAM-9 and -10 in bone metastases obtained at biopsy from prostate cancer patients*

*Immunohistochemistry (IHC)*

ADAM-9 and -10 protein expression was observed by IHC in prostate tissue taken from patients undergoing bone metastasis biopsies. Expression of both ADAM-9 and -10 proteins was clearly detected in the epithelial cells of prostate origin within each biopsy (Figure 3.3 A - ADAM-9 & Figure 3.3 B - ADAM-10) with little or no bone or bone fibroblast cell staining. In the case of both ADAM-9 and -10, levels comparable to those in primary prostate tumours (eg. Figure 3 E & F) were detected in the cytoplasm and on the cell membrane with expression also seen in the perinuclear/nuclear region. As a positive control, PSA was detected using immune rabbit anti-sera (DAKO), in the same type of cells of prostate origin in which ADAM-9 and -10 were detected, in serial sections (Figure 3.3 G). H & E (Chapter 2) stained serial sections were reviewed by a pathologist and the different cell types within each bone metastasis section were identified. Negative controls for both ADAM-9 and -10 included the omission of each primary antibody (Fig. 3.3 E). Positive controls included the detection of ADAM-9 (Figure 3.3 G) and ADAM-10 (Figure 3.3F) and PSA (Figure 3.3G) in primary prostate tumours taken from PCa patients at biopsy, performed in the same IHC experiment. Negative controls for primary prostate tumours for ADAM-9, -10 and PSA included the omission of the primary antibody (Fig. 3.3 H). These observations were the same in at least five independent patient bone metastasis biopsies.

**Figure 3.3:** Immunohistochemistry for ADAM-9, -10 and PSA on bone metastases, obtained from prostate cancer patients at biopsy

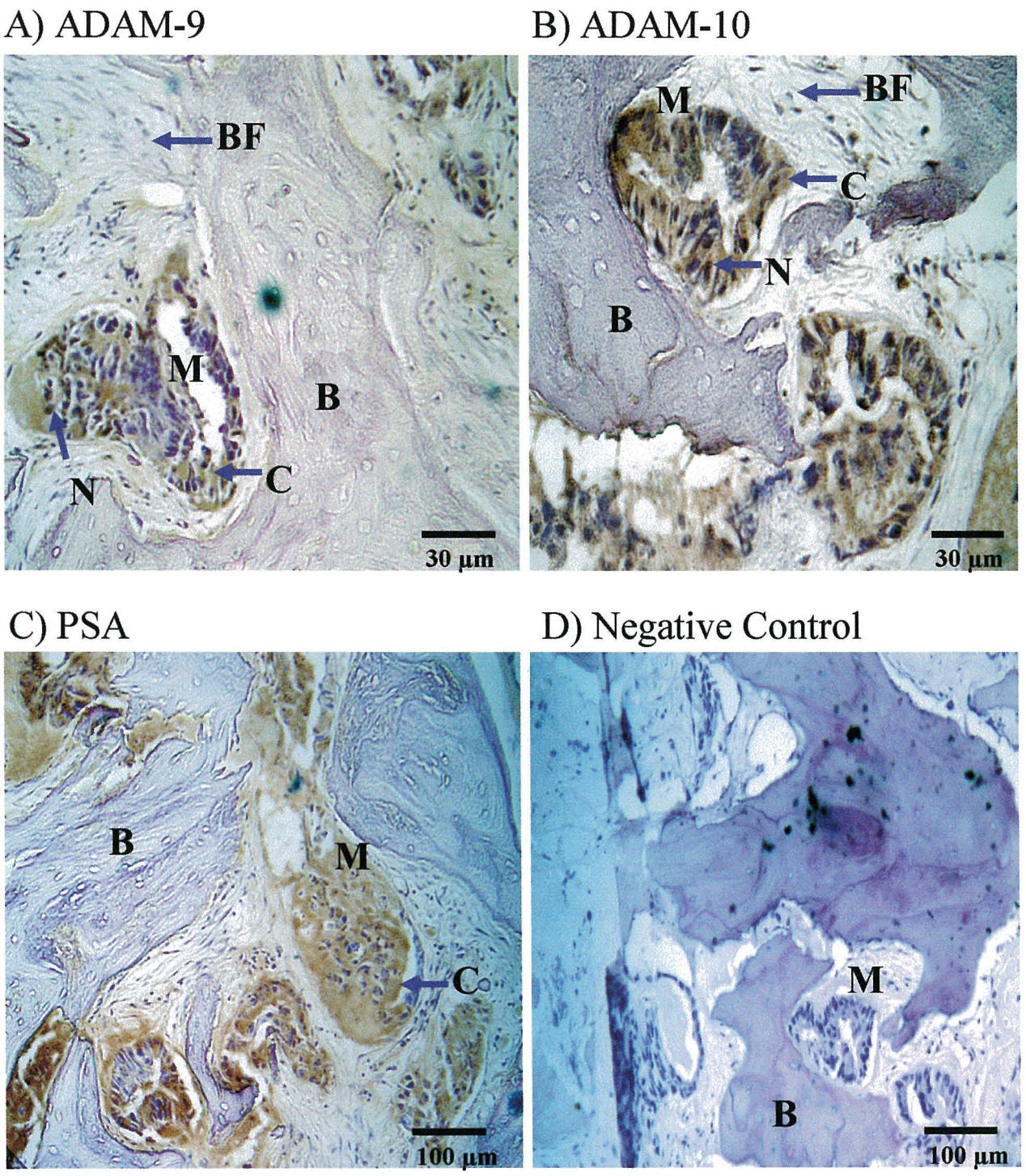


Immunohistochemistry for ADAM-9, -10 and PSA on bone metastases, obtained from prostate cancer patients at biopsy: ADAM-9Dis and ADAM-10Cterm antibodies show staining in prostate cancer cells in bone metastases. ADAM-9 (A) and ADAM-10 (B) are predominantly expressed in the cell cytoplasm, cell membrane and occasionally in the cell nucleus. PSA was detected in the same cell types in adjacent bone sections from the same bone metastases (C). In the case of ADAM-9 and -10, both antibodies were omitted to serve as the same negative control (D) Legend: **M** - Metastasis, **B** - Bone, **BF** - Bone Fibroblast, **C** - Cytoplasmic staining, **N** - Nuclear staining.

**Figure 3.3cont:** Immunohistochemistry for ADAM-9, -10 and PSA (positive controls), for primary prostate tissue obtained from prostate cancer patients at biopsy

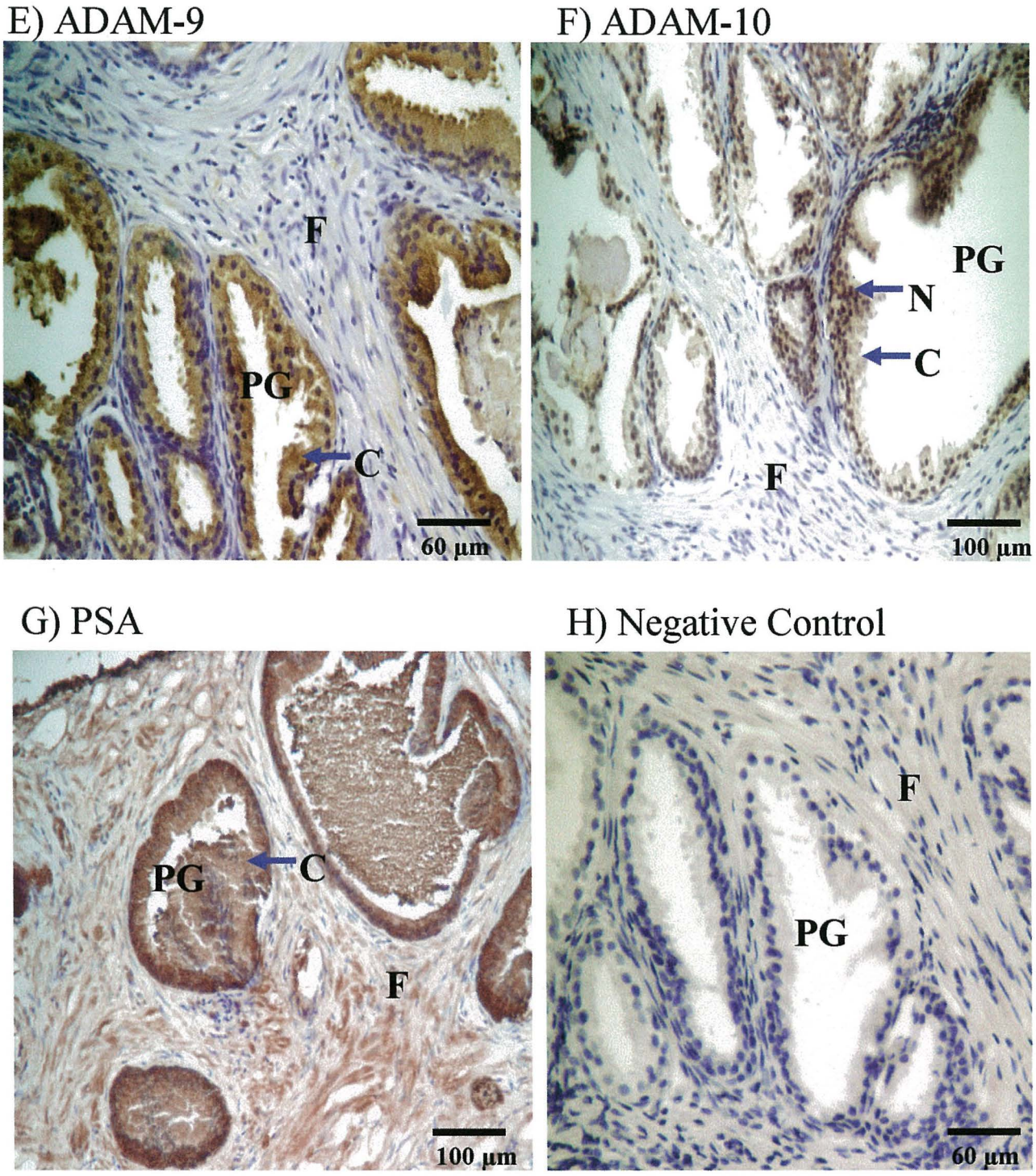


Immunohistochemistry for ADAM-9, -10 and PSA on prostate primary tumours, obtained from prostate cancer patients at biopsy: ADAM-9 (E), ADAM-10 (F) and PSA (G) were detected in the same IHC run as the bone metastases (Fig. 3A, B, C & D - previous page). In the case of ADAM-9 and -10, both antibodies were omitted to serve as the same negative control, for PSA, non-immune primary rabbit antisera (DAKO) was used (H). Legend: **C** - Cytoplasmic staining, **N** - Nuclear staining, **F** - Fibroblast, **PG** - Prostate Gland .

### *3.3.3 The nuclear and cytoplasmic expression of ADAM-9 and -10 in the prostate cell lines RWPE-1 and PC-3*

*Nuclear localisation signal (NLS)*

Previous observations in this laboratory using IHC showed strong nuclear expression for ADAM-10 in high-grade PCa and occasional nuclear/perinuclear expression for ADAM-9 throughout all stages of PCa (discussed in Chapter 1). This, along with the apparent nuclear expression of both these ADAMS in bone metastases (shown above) provides a good rationale for further investigation of this phenomenon. An active transport mechanism is required to import larger molecular weight proteins, such as ADAM-9 and -10 into the nucleus of a cell. The mechanisms often depend on the presence of a consensus nuclear localisation signal (NLS). Therefore, the primary amino acid sequence of the coding region of ADAM-9 and -10, Genbank (NCBI, NIH) accession numbers NP_003816 and NP_001110 respectively, were imported into the World Wide Web based search engine PSORT and analysed for likely NLS consensus sequences. Table 3.2 shows the numerous NLSs found in both ADAM-9 and -10, which are consensus sequences for the α/β Importin active nuclear transport system (Catimel et al. 2001).

*Immunocytochemistry*

Similar observations regarding cellular localisation were made for both ADAM-9 and -10 in both the RWPE-1 and PC-3 cell lines. ADAM-9 was expressed in the cytoplasm, on the cell membrane and in the nucleus in both PC-3 (Figure 3.4 A & B) and RWPE-1 cell lines (Figure 3.4 D & E). In the case of ADAM-10, cytoplasmic and membrane staining was observed in both the PC-3 (Figure 3.4 G & H) and RWPE-1 (Figure 3.4 J & K) along with strong perinuclear/nuclear staining in both cell types. No staining was visualised in the case of each negative control (primary antibody omitted) for ADAM-9 (Figure 3.4 C & F) and ADAM-10 (Figure 3.4 I & L).

**Table 3.2:** Consensus Nuclear Localisation Sequences (NLSs) found in the primary amino acid sequence of ADAM-9 and -10.

| **Sequence Pattern (Origin)** | **Consensus Motif** | **ADAM 9 Sequences** | **ADAM 10 Sequences** |
|---|---|---|---|
| Pat 4<br>(SV40 Large T antigen) | 4 basic amino acids - K or R (or 3 basic aa plus H or P) | RRRR (residues 202-)<br>RRRH (295-)<br>RKKR (729-) | RKKR (residues 210-)<br>KRRR (721-)<br>RRRP (722-) |
| Pat 7<br>(SV40 Large T antigen) | PX1-3 plus 3(K/R) out of next 4 residues | | PELLRKK (206-)<br>PEGRKCK (490-)<br>PLARLKK (653-)<br>PGTLKRR (717-) |
| Bi-Partite<br>(Xenopus) | 2 basic residues, 10 residue spacer, 3 basic in next 5 residues 2 K/RX10(3/5 K/R) | | RR RPPQPIQQPQ RQRPR (722-) |

The primary amino acid sequences of ADAM-9 and -10 were analysed in PSORT for the consensus NLS for the α/β importin system. Several NLS were identified in the case of ADAM-9 and more so in ADAM-10.

**Figure 3.4:** Immunocytochemistry analysis of ADAM-9 & ADAM-10 in RWPE-1 and PC-3 cells

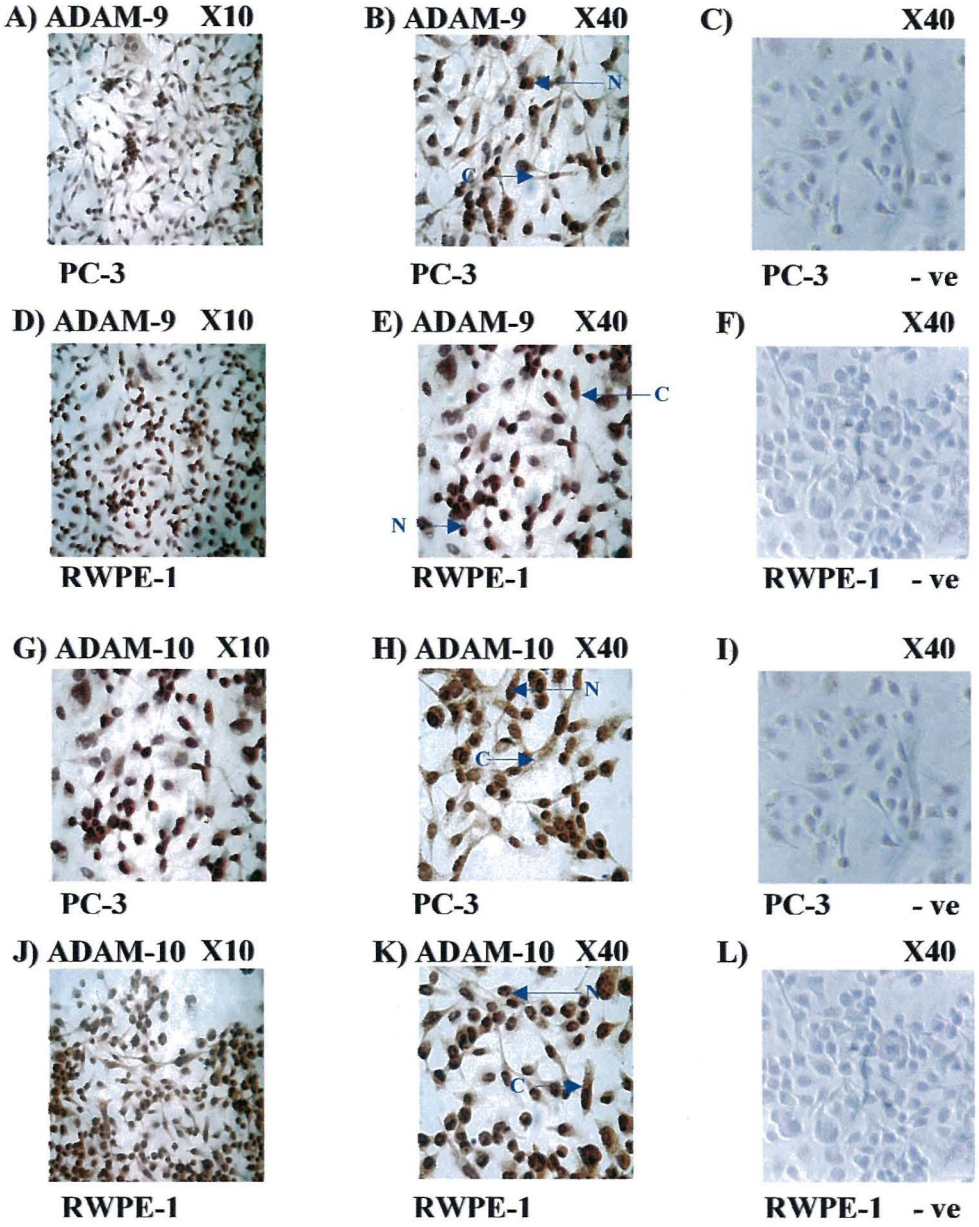


Immunocytochemistry using ADAM-9Dis and ADAM-10Cterm antibodies. ADAM-9 (A & B - PC-3, D & E - RWPE-1), -10 (G & H - PC-3, J & K - RWPE-1) was shown in the cytoplasm and nucleus of each cell line. Negative controls: omission of each primary antibody (ADAM-9 - PC-3, C & RWPE-1, F) (ADAM-10 - PC-3, I & RWPE-1, L). Legend: **N** = Nucleus, **C** = Cytoplasm.

*Western blot analysis*

For the ADAM-9Dis antibody, a band at the predicted size of the unprocessed pro-form, ~84 kDa was expressed across all cellular fractions and whole cell lysate in both RWPE-1 and PC-3 cell lines (Figure 3.5). A lower band ~60 kDa, the predicted active form of ADAM-9, was expressed highly in RWPE-1, but weakly in PC-3 cell lines to the point that it was not detectable when 5 μg of whole cell lysate was analysed by Western blot (Figure 3.5 A). Further, this potentially mature active form of ADAM-9 could be seen in whole cell lysate and nuclear fractions but only faintly in the cytoplasmic fraction of the RWPE-1 cell line. A smaller doublet of ~34 kDa of unknown identity but previously detected in other studies with antibodies raised to similar regions of ADAM-9 (Weskamp et al. 1996) was detected in the cytoplasmic fractions of RWPE-1 and PC-3 cells but not in the nuclear fractions. As a control for the efficiency of subcellular fractionation, the cytoplasmic specific protein β-Tubulin (54 kDa) and the nuclear specific protein Proliferating Cell Nuclear Antigen (PCNA) (34 kDa) was detected by Western blot in each cell line fraction (Figure 3.5 B - Tubulin & 3.5 C - PCNA). Although slight cross-contamination was observed, ~10 % as expected and stated by the manufacturer of the subcellular fractionation kit (NePer – Pierce), the subcellular fractionation was found to be sufficient and acceptable for the purposes of analysis in this study using these particular markers. The cross-contamination observed in this case was indicative of each subsequent sub-cellular fractionation carried out for replication purposes of each ADAM-9 and -10 protein expression experimental data.

For ADAM-10, the ADAM-10Cterm antibody detected a ~100 kDa band (unprocessed form) in RWPE-1 cells, whilst weak expression of this band was occasionally seen in PC-3 cells (Figure 3.6 A). Two lower bands, ~54 and ~56 kDa, likely representing mature active forms, were expressed in both RWPE-1 and PC-3 cells (Figure 3.6 A). Examination of cellular fractions showed, with the ADAM-10Cterm antibody, the higher ~56 kDa band was expressed in the cytoplasmic fraction of each cell line whilst the lower ~54 kDa band was present only in the nuclear fraction of RWPE and PC-3 cells. These lower molecular weight bands were also detected by the ADAM-10Met antibody, which was raised to the N-terminal of the processed, mature catalytically active form of ADAM-10 (Figure 3.6 B),

indicating the presence of the N-terminal of the active ADAM-10 protein sequence in each of these isoforms. In the case of Figure 3.6 B, both the 54 kDa and 56 kDa bands were detected in the nuclear fraction of both of the cell lines, unlike the previous analysis using the ADAM-10Cterm antibody, which detected the clear differential localisation described above. It is possible that, given the ADAM-10Met antibody is raised to the N-terminal sequence of mature ADAM-10; its affinity for processed ADAM-10 might be stronger than that of the ADAM-10Cterm antibody. Hence, lower levels of ADAM-10 protein present, possibly, but not necessarily due to cross-contamination might be easily detected. Nonetheless, the lower 54 kDa band still appears to be exclusively expressed in the nuclear fraction of each of the RWPE-1 and PC-3 cell lines. The expression of the unprocessed form of ADAM-10 was not readily detected with the ADAM-10Met antibody in this case, which again reflects the possibility of the differing binding preferences/affinities of this antibody between the ADAM-10 processed and unprocessed forms.

### *3.3.4 The expression of ADAM -9 and -10 in isolated membrane vesicles from the prostate cell lines RWPE-1, LNCaP and PC-3*

For ADAM-9, a qualitative membrane vesicle protein content from the normal prostate cell line RWPE-1 and the PCa cell lines LNCaP and PC-3 was analysed by Western blot with the ADAM-9Dis and the ADAM-9Cterm antibody. The ADAM-9Dis antibody detected a band in RWPE-1 (60 kDa) and LNCaP (60 kDa) vesicles but not in the PC-3 cell vesicles (Figure 3.7), whilst the ADAM-9Cterm antibody detected bands in the LNCaP cell vesicles (84 kDa and 60 kDa) whilst no bands were detected in the PC-3 or the RWPE-1 cell vesicles (Figure 3.7). A higher band ~100 kDa of unknown identity was, in this case, also detected with the ADAM-9Dis but not the ADAM-9Cterm antibody in the LNCaP whole cell lysate preparation, as well as the expected 84 kDa and 60 kDa bands (positive control) along with the additional 34 kDa band of unknown identity, as found previously in RWPE-1 and PC-3 cell extracts described above.

For the qualitative assessment of ADAM-10 membrane vesicle protein content, the ADAM-10Met antibody detected an intense signal at ~60 to ~80 kDa in PC-3, whilst for

RWPE-1 a less intense signal was detected at approximately the same size (Figure 3.8). For LNCaP, two major bands (~100 kDa and ~60 kDa) were detected in close vicinity to the bands detected in the LNCaP whole cell lysate (positive control) run on the same gel (Figure 3.8) and may represent unprocessed and processed, catalytically active proteins respectively.

**Figure 3.5:** Western blot analysis of ADAM-9 in the nuclear and cytoplasmic fractions of the normal but transformed prostate cell line RWPE-1 and the metastatic prostate cancer cell line PC-3

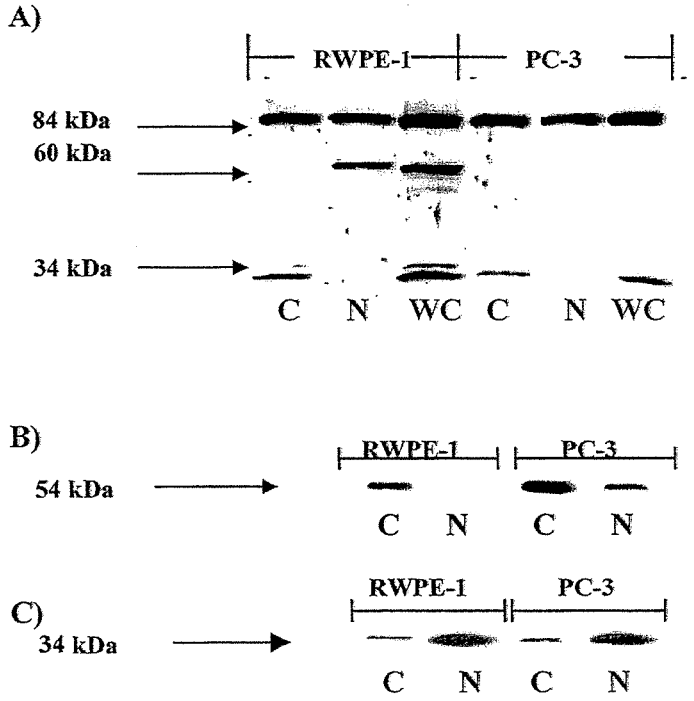


A) Cell pellets of RWPE-1 and PC-3 cells were collected from a ~70 - 90 % confluent T75 tissue culture flask and subcellular fractionation was subsequently carried out. 5 µg of protein from each nuclear (**N**), cytoplasmic (**C**) cell fraction or whole cell (**WC**) lysate was run on an SDS-PAGE followed by standard Western blot procedure as described in Chapter 2. β-Tubulin (cytoplasmic specific) (B) and PCNA (nuclear specific) (C) were detected by standard Western blot procedure as controls for the efficiency of subcellular fractionation. Similar observations were observed in three separate cellular fractionation preparations.

**Figure 3.6:** Western blot analysis of ADAM-10 in the nuclear and cytoplasmic fractions of the normal but transformed prostate cell line RWPE-1 and the metastatic prostate cancer cell line PC-3

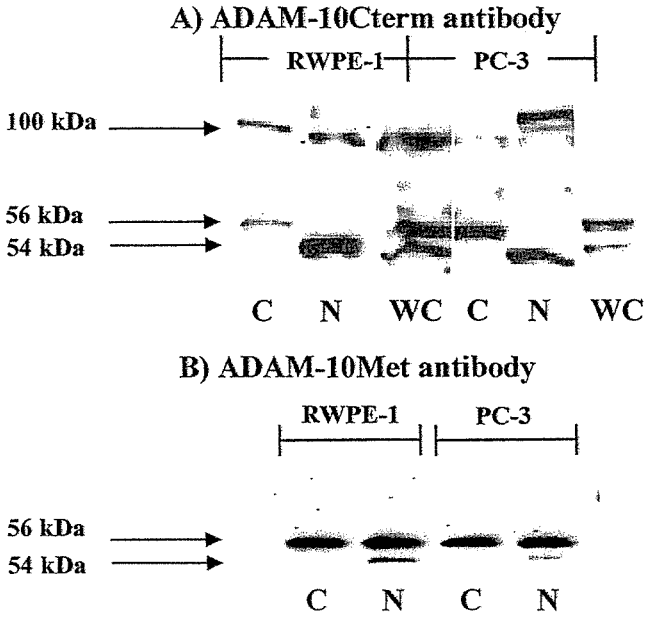


Cell pellets of RWPE-1 and PC-3 cells were collected from a ~70 - 90 % confluent T75 tissue culture flask and subcellular fractionation was subsequently carried out. 5 µg of protein from each nuclear (**N**), cytoplasmic (**C**) cell fraction or whole cell (**WC**) lysate was run on an SDS-PAGE followed by standard Western blot procedure as described in Chapter 2. A) The ADAM-10Cterm antibody detected a differential expression pattern for the predicted active form, whilst the unprocessed form was not readily detected in the whole cell lysate of PC-3 cells and may indicate a higher level of expression of this form in the nuclear protein fraction of this cell line. In the case of the ADAM-10Met antibody (B), both bands were detected in each fraction, confirming the presence of the active N-terminal metalloprotease sequence. The lower 54 kDa band was exclusively confined to the nuclear compartment in both cases, in both cell lines. This was indicative of results seen between more than three separate nuclear/cytoplasmic fractions of each cell line.

**Figure 3.7:** Western blot analysis of ADAM-9 in the membrane vesicle fractions of the normal but transformed prostate cell line RWPE-1, and the prostate cancer cell lines LNCaP and PC-3

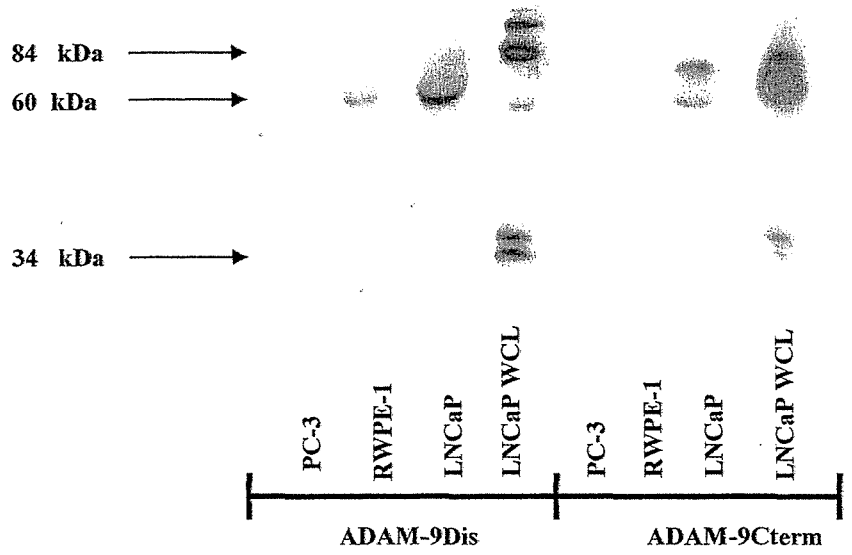


Qualitative Western blot analysis of protein isolated from membrane vesicles released into the media of each of the cell cultures PC-3, RWPE-1 and LNCaP. LNCaP whole cell lysate was run alongside the membrane vesicle protein lysate as a positive control, with the expected 84 kDa and 60 kDa bands being detected with each antibody. These results are indicative of one preliminary membrane vesicle isolation experiment, which now needs to be confirmed.

**Figure 3.8:** Western blot analysis of ADAM-10 in the membrane vesicle fractions of the normal but transformed prostate cell line RWPE-1, and the prostate cancer cell lines LNCaP and PC-3

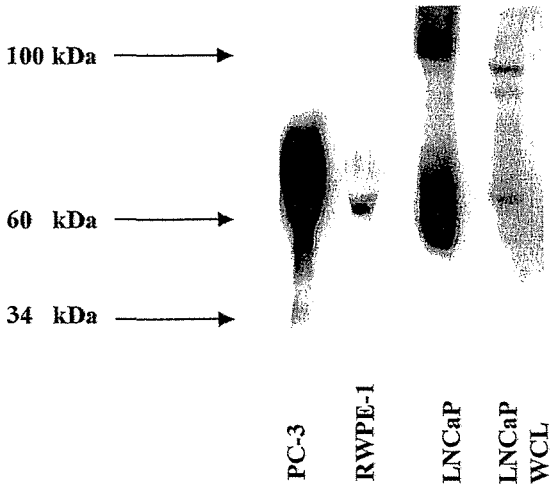


Qualitative Western blot analysis of protein isolated from membrane vesicles released into the media of each of the cell cultures PC-3, RWPE-1 and LNCaP. The ADAM-10Met antibody was used for this experiment. LNCaP whole cell lysate was run alongside the membrane vesicle protein lysate as a positive control, and showed the expected 100 kDa and 60 kDa bands. These results are indicative of one preliminary membrane vesicle isolation experiment, which now needs to be confirmed.

### *3.4 Discussion*

The development and progression of prostate cancer (PCa) involves a plethora of molecular events, which seemingly act in synergy, eventually enabling metastasis to occur. PCa commonly metastasises to the lymph node and bone where the colonisation of prostate secretory epithelial cells takes place. The process of PCa metastasis, specifically to the bone is poorly understood. However, it is thought that tumour cells are attracted to bone by growth factors and cytokines activated or released upon osteoclast bone reabsorption, from bone marrow and stroma (Roodman, 2001). The processes of ECM and bone matrix degradation, and cell migration are key mechanisms for establishing secondary site metastatic tumours.

ADAM-9 and -10 are potential candidates for assisting the type of activity required for metastasis - firstly, via their active extracellular metalloprotease domains and secondly by the ability, in the case of ADAM-9, to interact with integrins, potentially regulating cell-cell and cell-ECM contact and adhesive capabilities.

The expression of ADAM-9 and -10 was examined in an *in vitro* metastatic cell line model (the C4 series), derived from the PCa cell line LNCaP, which was originally isolated from a lymph node metastasis. The C4 cell line was derived from the primary tumour and C4-2 cell line from the lymph node metastasis resulting from the LNCaP cell line being co-cultured with the human bone fibroblast cell line (MS) in male athymic mice (Wu et al. 1994) whilst the C4-2B cell line is a bone metastasis derivative from the C4-2 cell line (Chung et al. 1997), again established by passage in male athymic mice. The LNCaP and C4 cell lines are proliferatively responsive to androgen stimulation, whilst the latter C4-2 and C4-2B cell lines are not, giving these derivatives the characteristics of PCa progression and providing a good theoretical model to characterise the expression of potential mediators of metastasis to the lymph node and more so, given the co-culture conditions with bone fibroblast cells, to the bone.

Expression of both ADAM-9 and -10 proteins was found in the parent LNCaP cell line and its metastatic derivatives: C4, C4-2 and C4-2B cell lines. The Western blots revealed an ADAM-9 band at ~84 kDa under reducing conditions, a size which agrees with that of

latent pro-forms of ADAM-9 expression in rodent kidney-derived extracts (Weskamp et al., 1996) and with recombinant expression in COS-7 cells (Mahimkar et al., 2000). Faint bands were occasionally seen at about ~60 kDa (too faint to be shown) suggesting that mature ADAM-9 is present at very low levels in these PCa cell lines. For ADAM-10, two distinct bands were observed at ~100 kDa and ~60 kDa. The larger band likely represents the unprocessed pro-form of ADAM-10, whilst the ~60 kDa band corresponds to that found in plasma membrane preparations from bone MG-63 cells (Dallas et al., 1999) and is believed to represent the mature, active form of ADAM-10. The predicted sizes of each ADAM-9 and -10 protein from their primary amino acid sequence is illustrated in Figure 3.9 A & B respectively. The observed Mr of ADAM-9 and -10 protein by Western blot was a close match to that of the predicted size, although the ADAM-10 pro-form ranged 18 kDa higher than the predicted 82 kDa most likely due to post-translational modification such as N- or O-glycosylation (Colciaghi et al. 2002).

Despite no obvious changes in levels of either ADAM, when compared to the levels of the housekeeping gene β-Tubulin, detection of endogenous levels of the active form of ADAM-10 (~60 kDa) indicates a potentially intrinsic role for ADAM-10 in each of these cell lines. ADAM-9, on the other hand, was not routinely detected in its predicted active form (~60kDa), although the parent latent form could be readily detected in each of the cell lines tested. Western blots are at best semi-quantitative, suffering from a limited dynamic range. With the use of recently developed, commercially available, recombinant ADAM-9 and -10 (R & D systems), Western blot efficiency of each of the antibodies used in this study could be assessed as a measure of linearity for a more efficient quantitative assessment.

To further these observations, the possibility of finding the expression of ADAM-9 and -10 outside of the cell in the extracellular environment was explored by way of isolating cell membrane vesicles. Previous studies have found that for some cell types the cell membrane tends to constitutively 'bud' and shed parts of its membrane and cellular/membrane bound protein content into the extracellular environment (Angelucci et al. 2000; Taraboletti et al. 2002).

**Figure 3.9:** Schematic representation of ADAM-9 and -10 showing the predicted molecular weights of the unprocessed and processed forms as determined from their primary amino acid sequence

**A) ADAM-9**

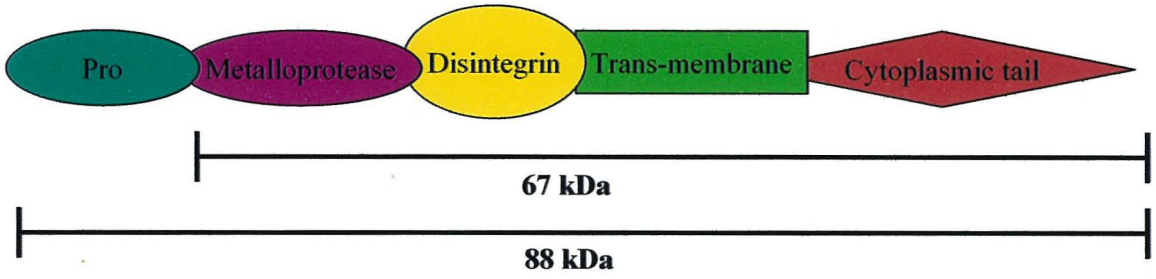


**B) ADAM-10**

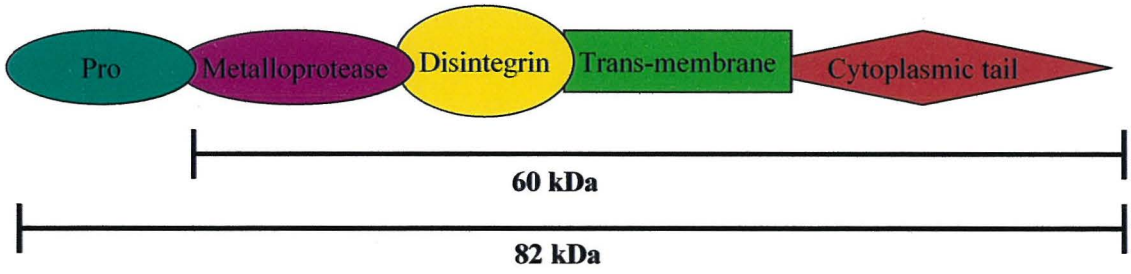


It has also been previously observed that cell lines of a tumorigenic nature undergo more frequent membrane budding (Angelucci et al. 2000) and ECM proteases such as the MMPs have been found in these membrane vesicles (Taraboletti et al. 2002). Furthermore, these vesicles have been found to facilitate cell migration of other cell types, when added in cell culture media in *in vitro* cell migration assays (Angelucci et al. 2000). These observations suggest an important potential role for membrane vesicles in the early stages of metastasis. The presence of ADAM-9 and -10 in these vesicles suggests that they might also be involved in this activity.

The expression of the presumably active ADAM-9 and -10 was found in isolated membrane vesicles from LNCaP and PC-3 cell lines, and ADAM-10 was also found in the RWPE-1 cell line. Interestingly, the active form of ADAM-9 was readily detected in shed membrane vesicles of the LNCaP cell line as opposed to not routinely being detected in

LNCaP whole-cell lysate, this observation needs to be explored further to assess absolute amounts of ADAM-9 (and -10) within and between cell types varying from normal to a metastatic phenotype. These data give evidence that ADAM-9 and -10, as potentially active ECM proteases, may exert their activity extracellularly.

Although earlier studies from this laboratory have examined ADAM-9 and -10 protein expression in primary tumour biopsies from the prostate (McCulloch et al. *in press, 2003*, see Chapter 1), nothing was known about their expression in secondary tumours or metastasis. Thus, the present study extended these observations by characterising the expression of both ADAM-9 and -10 protein by IHC, in bone metastases donated by PCa patients at biopsy. Levels of expression comparable to the expression levels in primary tumours were detected, for ADAM-9 and -10 in colonised tumorigenic prostate cells within the bone, which were also found to co-express PSA, confirming their origin as prostate-derived. Both ADAM-9 and -10 were predominantly expressed in the cytoplasm and on the cell membrane and in some cases, the nucleus. These data suggest the ADAMs continue to have roles late in the process of metastasis, perhaps important in the colonisation process involving bone matrix degradation, cell migration and proliferation. This and our previously described data outlining the presence of both ADAM-9 and -10 in normal through hyperplastic and low to high-grade cancer glands, and their apparent differential cellular localisation - membrane-bound, cytoplasmic and nuclear - suggests that ADAM-9 and -10 have important intrinsic, perhaps varied roles, in the various stages of PCa development.

The nuclear presence of ADAMs -9 and -10 was particularly interesting - raising questions about how it gets there and what it does. To gain some further insight as to how ADAM-9 and -10 might enter the nucleus the primary amino acid sequence of ADAM-9 and -10 was analysed in PSORT, a World Wide Web based analytical search engine which analyses primary protein sequences for consensus motifs of interest, to look for possible nuclear localisation signals (NLS). The NLS consensus sequences identified are homologous to those sequences implicated in the nuclear import pathway mediated by the Importin $\alpha/\beta$ heterodimer (Gorlich, 1998). This pathway is strongly implicated in the post-translational nuclear import/translocation of many proteins, each containing such NLSs (Catimel et al.

2001). Hence, this is a possible nuclear import mechanism for the nuclear translocation of ADAM-9 and -10. The perinuclear/nuclear localisation of ADAM-10 has been previously reported in human articular cartilage (Dallas et al. 1999) whilst closely related ADAM-17, has also been reported to be localised to perinuclear regions in other cell types, although these were not tumorigenic in origin (Roghani et al. 1999; Schlondorff et al. 2000).

Given the strong evidence that points to both ADAMs -9 and -10 being nuclear localised in clinical prostate tumour samples, their cellular localisation was further investigated in two prostate cell lines; by immunocytochemistry (ICC), and secondly by subcellular fractionation and Western blot analysis. Both RWPE-1, which is a normal but transformed prostate cell line and PC-3, which is a high-grade, androgen-insensitive PCa cell line derived from a PCa metastasis to the bone, were utilised as cell line models to differentiate potential changes in expression patterns between a normal prostate situation and a high-grade metastatic PCa cell.

For ICC, strong cytoplasmic/membrane and nuclear/perinuclear expression was found for both ADAM-9 and -10 in both RWPE-1 and PC-3 cell lines. For subcellular fractionation, the processed, ~60 kDa mature form of ADAM-9 was expressed in both the cytoplasmic and nuclear fractions of RWPE-1 and PC-3 cells, although the lower 60 kDa form is not apparent in PC-3 cells when lower amounts of protein are loaded and detected by Western blot. These observations strengthen the data obtained by ICC with respect to observed nuclear expression.

For ADAM-10 expression, the ~100 kDa pro-form was not as frequently observed across different PC-3 cell lysate preparations as it was in RWPE-1 cell lysate. The subcellular fractionation revealed quite a distinct pattern of the mature isoform expression between the cytoplasm and the nucleus. The smaller form (~54 kDa) was exclusively localised in the cell nucleus in both cell types whilst the slightly larger (~56 kDa) form appeared initially to be cytoplasmic/cell membrane specific, although further analysis with a second ADAM-10 antibody showed expression of this form in the nuclear fractions of each of the two cell lines. Whether this observation is a result of cytoplasmic fraction contamination in the

nuclear fraction remains to be investigated. Therefore, at this point in time it cannot be fully concluded that the 56 kDa form of ADAM-10 is specifically localised to the cell cytoplasm/membrane. The presence of ADAM-10 in the nucleus raises new questions as to what possible role the ADAMs, and in particular ADAM-10, might have in PCa. Further, it led to the new hypothesis that as PCa progresses, the nuclear localisation observed by IHC, might be attributed to the smaller ~54 kDa isoform of mature ADAM-10 as well as the unprocessed form of ADAM-10.

For both ADAM-9 and -10 protein expression, their unprocessed higher molecular weight forms were universally expressed across each of the cell fractions and in the whole cell lysate of each cell line. However, their processed, presumably catalytically active lower molecular weight forms appeared differentially expressed as described above. This observation suggests the possibility that, after these ADAMs are processed through the Golgi apparatus, they are differentially transported to either the cell membrane or the nucleus. Presumably, a pool of ADAM protein might be available after processing and a portion of this pool of ADAM protein, depending on its location, might be bound by the α/β-importin protein complex via their NLS (discussed above, Table 3.2), and actively transported into the nucleus.

In the case of ADAM-9, the mature processed form appears to be the same molecular weight whether appearing in the cell cytoplasm or in the nucleus. ADAM-10 processed mature form, on the other hand, appears to be a different size in different locations within the cell. A contributing factor to differential molecular weight analysis is often glycosylation. In this study, differentially glycosylated ADAM-10 might as a consequence be transported to different cellular locations if, for example, such glycosylation determined specific nuclear import system recognition, or where ADAM-10 is secreted from the Golgi apparatus, to a potential docking rendezvous with nuclear import systems. The unprocessed form of ADAM-10 would also be indicative of a slightly higher or lower molecular weight, depending on its extent of glycosylation. As this may be the case, data generated to date in this study has not uniformly depicted definitive sizes of unprocessed ADAM-10 across separate cellular fractions. Both N- and O- sugar linkages have been

characterised on the mature, catalytically active region of ADAM-10 (Colciaghi et al. 2002), see Figure 5.1 for putative glycosylation sites on the ADAM-10 primary amino acid sequence. Attempts in our laboratory have been made to N-deglycosylate proteins within each cellular fraction. However, no changes in molecular weight of either of the isoforms in question were seen in subsequent Western blot analysis (data not shown), although these experiments need further investigation, as they were not conclusive.

Another possible explanation for the differences in molecular weights of each ADAM-10 isoform might be due to differential splicing events, whereby one or more exons might be spliced during translation. As the ~54 kDa and ~56 kDa forms are smaller than the predicted Mr of processed ADAM-10 (60 kDa - Figure 3.9 B) this may well be the case. Examination of the exon arrangement of ADAM-10 gDNA shows that some exons are in the correct reading frame that, if removed, the primary amino acid sequence would not be altered down-stream and both the ADAM-10Met and ADAM-10Cterm antibodies would still efficiently detect potential splice variants.

The observations made across the RWPE-1 and PC-3 cell line models, whilst novel, are limited with respect to extrapolating the data generated to the 'in tissue' observations made with prostate tissue biopsies. RWPE-1, although derived from normal prostate tissue has undergone the usual 'crisis' event involved in the cell immortalisation process. Hence its genome consists of greater than 50 chromosomes (Bello et al. 1997), it is an infinite cell line in terms of population doublings and its population displays a mixed genotype when karyotyping is carried out (Bello et al. 1997). Despite this, RWPE-1 is non-tumorigenic when seeded into NUDE mouse models (Bello et al. 1997), unlike PC-3 which forms primary tumours (Kim et al., 2003) setting these two cell types apart sufficiently for the purposes of these studies. Given this information, the presence of ADAM-10 in the nucleus of RWPE-1 may not truly be a reflection of the localisation pattern seen in normal prostate epithelial secretory cells as the nuclear expression of this ADAM is less commonly seen in normal/hyperplastic prostate glands by IHC.

For the first time the expression of ADAM-9 and -10 at the protein level has been shown in prostate cell lines indicative of normal (RWPE-1), androgen sensitive PCa (LNCaP, C4) and androgen-insensitive PCa (C4-2, C4-2B and PC-3). These studies also extended our previous data pertaining to the expression of ADAM-9 and 10 in primary prostate tumours to prostate cancer bone metastases. Furthermore, the cellular localisation of ADAM-9 and -10 *in vitro* in the contrasting cell line models RWPE-1 and PC-3 has been characterised; the potential active forms of both ADAMs are present in the nuclear compartment of both of these cell lines. These data suggest both ADAMs to have intrinsic and varied roles in normal and pathological states of the prostate. Further investigation is required to identify and correlate the molecular size of each ADAM found *in vitro* to the prostate gland secretory epithelial cells *in vivo*.

# CHAPTER FOUR:

## 4.0 THE DETECTION OF ADAM-9 AND -10 mRNA AND PROTEIN IN CELLS ISOLATED BY LASER CAPTURE MICRODISSECTION FROM PROSTATE GLANDS OBTAINED AT BIOPSY

## *4.1 Introduction*

Laser Capture Microdissection (LCM) is a state of the art technique useful for the isolation of a homogeneous cell population from a heterogeneous tissue sample. LCM enables the user to scrutinise gene expression within and between individual cell types from tissue sections 5 to 8 μM in thickness (Rubin, 2001). In the case of PCa, which is commonly found in small foci in the prostate, the glands within a tissue sample obtained at biopsy may be classified by a pathologist as containing normal, hyperplastic and/or tumorigenic cells/glands. However, as not every gland within that particular tissue sample will be of a common diagnosis, this introduces variability when downstream molecular screening of the presence, abundance and different potential alternative transcripts of mRNA, and isoforms of proteins of interest is carried out. With the use of LCM, one can isolate individual glands of each type for subsequent analysis of their pattern of specific proteins, in this case ADAM expression - and minimize the error that cellular/glandular heterogeneity may contribute in this type of study.

The basic principle of LCM, illustrated in Figure 4.1, involves placing a Synthetic Transfer Polymer (STP), made of Ethylene Vinyl Acetate, in direct contact, overlaying the tissue section. With the aid of an appropriate cytological stain, for example, Hematoxylin, the epithelial cells of each type of gland can be viewed on a monitor attached to a laser-fitted, inverted light microscope. The user is able to guide the laser around each single gland. Each time the laser is pulsed, the STP is activated and the cells on the tissue section adhere to the polymer. Once the polymer is lifted from the tissue section only the activated/adhered region of the tissue, that is, the cells of the gland type of interest, are removed. The polymer/adhered cells can then be placed in an eppendorf tube and the downstream application of choice (RNA, DNA or protein extraction) can be carried out.

Previously, ADAM-9 and -10 expression has been examined, firstly by RT-PCR and Western blot in normal prostate and prostate cancer (PCa) cell lines (Chapter 3) and secondly, by Immunohistochemistry (IHC) in prostate tissue (Reviewed in Chapter 1) and bone metastases obtained from PCa patients at biopsy (Chapter 3).

**Figure 4.1:** Schematic representation of the principle of Laser Capture Microdissection

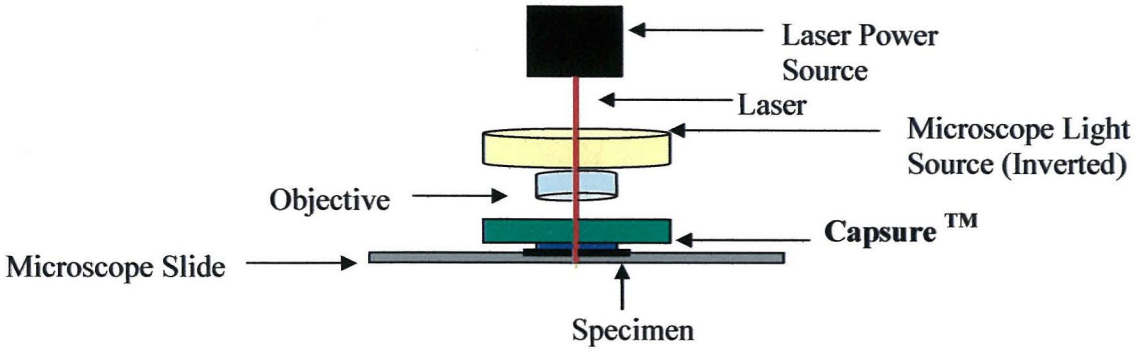


In the case of the prostate cell lines, readily detectable levels of unprocessed and processed, presumably catalytically active, forms of ADAM-9 and -10 were found in cells representing normal prostate, androgen-sensitive and late stage androgen-insensitive PCa. Examination of expression in tissue sections by IHC suggested that for ADAM-9 a decrease in protein levels could be seen as a general trend from prostate glands of the benign state to low, through to high-grade carcinoma. In contrast, for ADAM-10, the same or increasing levels of protein could be seen from low through to high-grade PCa. Furthermore, along with the changes in staining intensity, ADAM-10 showed specific nuclear localisation in high grade PCa. Further examination of the expression of both ADAM-9 and -10 in prostate secretory epithelial cells might provide more specific information as to exactly which isoforms of each ADAM found in prostate cell lines *in vitro* may be present in a prostate gland of a normal, benign, PIN or low to high-grade malignant state.

It was primarily hypothesised that the nuclear expression of ADAM-10, seen in high-grade prostate cancer by IHC, is the same ADAM-10 isoform (54 kDa) as that seen in the nuclear fractions of both RWPE-1 and PC-3 cell lines, whilst the benign cells of the prostate gland might express the isoform found in the cytoplasmic fraction (56 kDa) of these two cell lines (Chapter 3). A secondary hypothesis was that the two forms of ADAM-9 previously detected in prostate cell lines, would also be present in clinical PCa samples. Using LCM followed by Western blot analysis, one could elucidate the molecular size of both ADAMs - to date only observed *in vitro* - in tissue from PCa patient biopsies. Further, with respect

to our existing IHC data, the particular isoform of each ADAM, to date only observed by immunostaining in prostate tissue, may be resolved.

Therefore, the **aims** of this chapter were:

1) To optimise a system using LCM technology to isolate both hyperplastic and malignant prostate cells from patients who underwent radical prostatectomy or TURP biopsy, suitable for subsequent protein analysis by Western immunoblotting and mRNA analysis by RT-PCR, and
2) To determine whether ADAM-9 and -10 mRNA and/or protein was detectable in material captured from the optimised LCM assays and to examine the molecular weight of the subsequently detected protein from homogeneous LCM samples.

## *4.2 Methodology and Results*

### *4.2.1 The optimisation of processing and fixation of prostate tissue obtained at biopsy for LCM analysis.*

*Processing of prostate tissue obtained at biopsy*

Prostate tissue obtained at biopsy was either formalin-fixed and paraffin embedded and stored at ambient room temperature or snap-frozen in Optimal Cutting Temperature (OCT) compound, in liquid $N_2$ and stored at -80 °C. A board-certified pathologist assessed each biopsy as a particular percentage of benign, PIN or a particular Gleason score of cancer (outlined in Chapter 1). The paraffin-embedded prostate tissue was cut into 8 µm sections on a microtome and mounted on uncoated microscope slides, dried overnight at 60 °C and stored at room temperature to be used for further analysis.

The OCT embedded frozen tissue was sectioned on a cryotome as follows: Each specimen was kept on dry ice until it was transferred into the cryotome cold chamber (-20 °C); the cutting temperature of the specimen block was set at -15 °C. Up to 10 sections (8 µM thick) were cut from any given prostate specimen. The sections were transferred and adhered to uncoated microscope slides, returned to a slide box embedded and pre-cooled in

dry ice. All of the mounted tissue sections collected were transferred to -80 °C to await further processing. Mounted specimens were not used after 7 days of mounting to ensure the specimen did not 'over-adhere' to the slide due to dehydration, rendering it not useful for LCM applications.

*Western blot analysis of ADAM-9 and -10 from 8 μM tissue sections*

To ensure it was possible to detect the small amounts of protein contained in 8 μM sections of tissue by Western blot, an initial 'Whole Section Scrape' (WSS) was performed by scraping an 8 μM frozen section off its slide with the sterile edge of another microscope slide, into a 1.5 ml eppendorf tube. 60 μl of protein lysis buffer (50 mM Tris pH 7.5, 150 mM NaCl, 1% Triton X-100, 0.1 mM PMSF, 10 mM EDTA pH 8.0, 1 tablet Roche complete EDTA-free protease inhibitor cocktail/25 ml) was added to the eppendorf tube and the tissue was homogenised by pipette and vortexed vigorously creating a crude extract. 20 μl of the crude extract was combined with 5 μl of 5X Western blot reducing loading buffer, boiled for 5 min and loaded on a 10 % PAGE gel followed by standard Western blot procedure for both ADAM-9 and -10 as outlined in Chapter 2. Figure 4.2A & B shows that bands representing ADAM-9 (50 and 70 kDa) and -10 (50 and 82 kDa) are readily detectable from an 8 μm WSS, with the preliminary observation that each of the ADAM-9 and -10 isoforms is present in heterogeneous clinical PCa specimen tissue.

*Fixing and re-hydration of fixed prostate tissue*

The usefulness of formalin-fixed, paraffin embedded tissue for the analysis of ADAM-9 and -10 protein was assessed by testing two conditions. Two tissue sections were de-waxed with Shellex, 2 X 5 min, followed by dehydration, 100 % EtOH for 2 min. One of the sections underwent further rehydration in 70 % EtOH, 1 min and water. Both sections underwent a WSS and were resuspended in lysis buffer. No bands were detected for either ADAM-9 or ADAM-10 in subsequent Western blot analysis (Figure 4.2 C&D)

For fresh frozen prostate tissue, each section was fixed for 5 min in ice-cold acetone. One was subjected to the re-hydration schedule through to water, as described above, whilst a second section was immediately homogenised in protein lysis buffer. Each of these procedures was performed in duplicate so that both ADAM-9 and -10 could be examined on separate membranes by subsequent Western blotting (Figure 4.2 C&D).

**Figure 4.2:** The detection of ADAM-9 and -10 by Western immunoblot and the subsequent effect of fixation and rehydration schedules from formalin fixed and fresh frozen prostate tissue sections

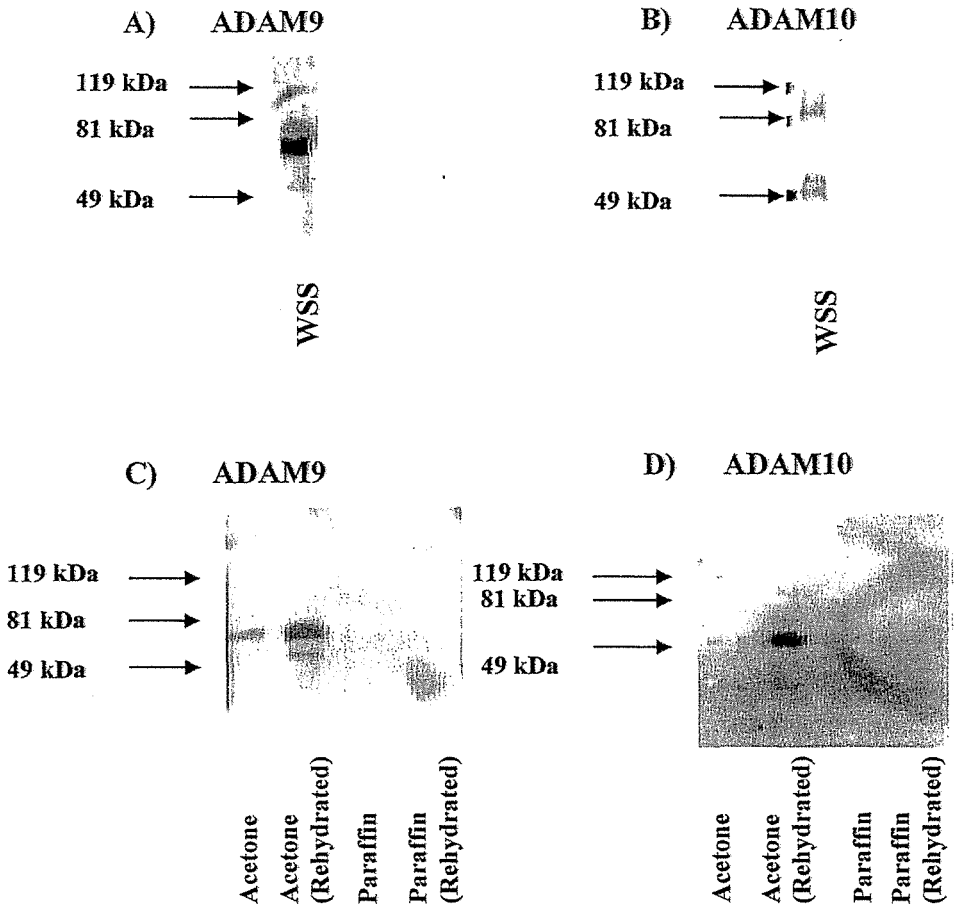


A) & C) The detection of ADAM-9, ~70 & 50 kDa (using the ADAM-9Dis antibody) and B) & D) the detection of ADAM-10, ~54, 56 and 100 kDa (using the ADAM-10Cterm antibody) on protein from a whole section scrape (WSS) of a fresh frozen prostate tissue section followed by Western blot analysis, described previously. For A) & B), no fixative was used, whilst for C) and D), fresh frozen tissue was fixed in ice-cold acetone, whilst paraffin embedded tissue was dewaxed in Shellex. Both tissues underwent differential rehydrating schedules as described previously. No signal was detected for either ADAM-9 or -10 from the paraffin embedded prostate tissue sections.

### *4.2.2 The optimisation of histological staining of fixed prostate tissue sections obtained at biopsy for LCM analysis.*

Subsequently, only ADAM-10 was used for optimisation of Western blot protocols as the previous data showed both ADAM-9 and -10 to be comparably detectable from fresh frozen prostate tissue sections.

Although acetone was a successful fixative on fresh frozen tissue for subsequent Western blot analysis, ice cold ethanol (EtOH) fixation was subsequently chosen as the preferred method, as this is more commonly used for LCM and it was anticipated that it would give a better histological resolution with subsequent staining protocols. A fresh frozen tissue section was fixed in 70 % ice cold EtOH, 15 sec followed by a WSS and Western blot analysis. Figure 4.3A shows that ADAM-10 was detectable after EtOH fixation and further staining schedules using this type of fixation were therefore carried out.

In order to optimise the staining of ethanol fixed fresh frozen tissue sections several different staining schedules were examined, including the following stains: Methylene blue, H&E and Histogene, a commercial stain available from Arcturis Engineering.

*Methylene blue & H&E staining*

EtOH fixed fresh-frozen sections (described above) were subjected to staining with Methylene blue dye according to the following schedule 70 % EtOH, 15 sec, sterile distilled water (SDW), 15 sec, 1 % Methylene blue, 30 sec, 70 % EtOH, 15 sec, 90 % EtOH, 15 sec, 100 % EtOH, 15 sec.

The above Methylene blue staining schedule was performed alongside a rapid H&E stain whereby the following protocol for H&E staining was performed; 15 second steps were used for all of the following reagents in the order, 70 % EtOH, SDW, Mayers Hematoxylin, SDW, Scotts water ($dH_2O$, pH 8.0), SDW, Eosin, SDW, 70 % EtOH, 90 % EtOH, 100 % EtOH.

**Figure 4.3:** Detection of ADAM-10 protein from fresh frozen prostate tissue sections, which underwent differential histological staining treatments

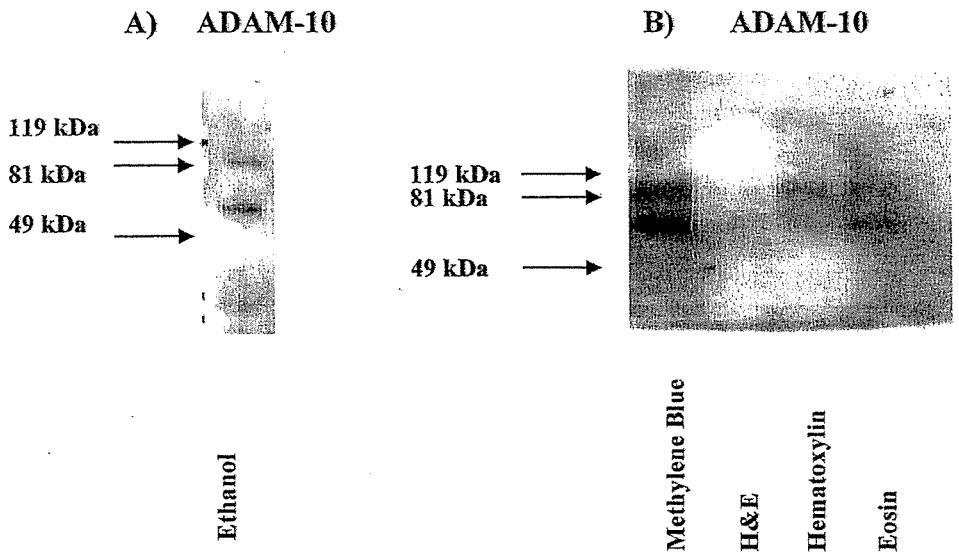


Western blot analysis of ADAM-10 (ADAM-10Cterm antibody) on protein from fresh frozen prostate tissue sections fixed in ice-cold ethanol (A) or Methylene blue, in comparison with H&E staining schedule (B). The Methylene blue staining schedule, as described above, was found to be the optimal stain for ADAM-10 detection as clearer bands could be detected than those after H&E staining (B).

One section was processed through the whole H&E protocol, whilst one omitted the Hematoxylin step and another omitted the Eosin step. One slide was cover-slipped (DEPEX) for visualisation under the light microscope whilst the other slides were subjected to a WSS and Western blot analysis (Figure 4.3 B). All of the solutions used for Methylene blue and H&E staining contained 50 mM EDTA, 0.1 mM PMSF and 1X EDTA free complete protease cocktail inhibitor (Roche).

*Histogene*

Histogene (Arcturis Engineering), a commercially available stain of which the contents are a trade secret, was purchased. Histogene was designed for the application of rapid staining for LCM applications, specifically for subsequent RNA extraction. The following Histogene staining schedule was carried out; all steps had an incubation time of 30 sec except for the Histogene stain, which was 20 sec: 75 % EtOH, SDW, Histogene, SDW, 75 % EtOH, 95 % EtOH, 100 % EtOH followed by WSS and Western blot analysis (Figure 4.4 A). Slides were mounted with DEPEX and cover-slipped for pathologist review.

Introducing a 'quick-dip' method whereby all of the above reagents were used except the SDW, which was omitted in both cases, optimised the Histogene stain further. The fresh frozen specimen was immersed and immediately removed from each solution. In the case of the Histogene stain, 20 to 100 ul (depending on the size of the section) was applied by pipette directly onto the tissue section, incubated at room temperature for 5 to 30 seconds before the slide was passed to the next solution. All solutions contained 0.1 mM PMSF, 10 mM EDTA pH 8.0 and 1 X Roche complete EDTA-free protease inhibitor cocktail.

Having established that both the Methylene blue and Histogene stains gave similar, acceptable levels of the detection of ADAM-10 by Western blot (see Figure 4.3 & Figure 4.4), each of these two staining schedules were repeated, and the stained sections were coverslipped with DEPEX and reviewed by a pathologist. Dr. Kennith Opeskin (Department of Pathology, St. Vincent's Hospital, Melbourne) deemed the Methylene blue stained prostate tissue section unacceptable to successfully determine prostate pathology,

whilst the Histogene stained section was found to be satisfactory (Figure 4.4B) and was consequently used in the subsequent experiments in this study.

### *4.2.3 LCM*

A fresh frozen tissue section was removed from -80 °C and immediately processed through the rapid Histogene staining protocol described above, followed by 2 X 5 min incubation in Xylene. The slide was allowed to air dry in a fume hood for ~5 min before being transported in a closed container to the LCM station.

The LCM microscope (PixCell® II), manufactured by Arcturus Engineering (California, USA), consists of an inverted microscope (Olympus IX-50 Binocular), a class IIIB variable output laser (0 - 100 mW), a video imaging camera (High Resolution Panasonic GP-KR222) and monitor (High Resolution Sony, PVM-1350). An inbuilt vacuum assists in holding the slide in place on the microscope stage and a stage joystick enables the stage, and hence, the slide to be easily manoeuvred in an X-Y plane.

The Histogene stained, slide-mounted prostate tissue section was placed on the microscope stage and the vacuum was activated. A 'Capsure' (see Figure 4.1) was placed over, and lowered onto, the tissue section with a mechanical arm so that handling of the STP could be avoided. Once the prostate glands of the tissue were focussed on the monitor the laser was switched to the on position. Three settings: spot size (diameter of the laser fired), amplitude (milliwatts) and pulse width (milliseconds) were optimised according to which combination of settings gave the best 'wetting' effect (Figure 4.5). Wetting is best described in terms of refractive index where, before the transfer polymer is activated, the light passing through the specimen is slightly distorted by the transfer polymer giving a well resolvable but not optimal image. Once the laser is fired, the polymer is activated and it adheres to the cells on the specimen improving the refractive index (amount of light distorted) closer to 1.0 (no distortion of light). The image where

**Figure 4.4:** Morphological examination of Histogene stained fresh frozen prostate tissue sections and subsequent Western blot analysis of ADAM-10 from protein extracted from a similarly stained tissue section

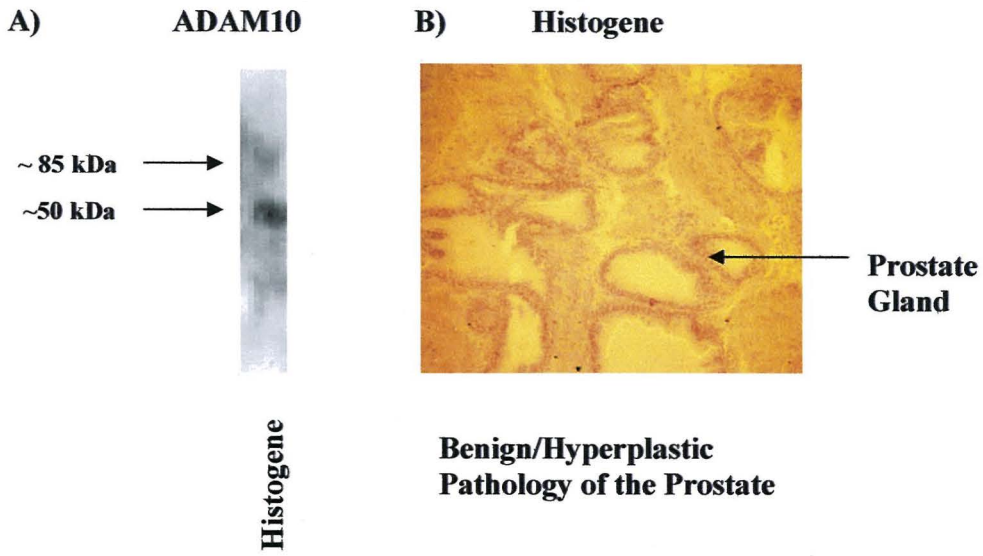


A) The detection of ADAM-10 by Western blot from an EtOH fixed, Histogene- stained, fresh-frozen prostate tissue section. B) Morphological examination of fresh frozen, ethanol fixed, Histochioce-stained prostate tissue section deemed acceptable by a pathologist to assess the pathological state of the prostate glands within.

the polymer is activated becomes sharp and crisp and appears 'wet' in contrast to areas not activated by the laser. The optimum setting was determined to be: 60 μm spot size, amplitude 40 milliwatts and the pulse width 110 milliseconds.

Once the area of interest, in this case, the epithelial cells around a given prostate gland, were adhered to the STP, the Capsure was simply lifted off the tissue section with the mechanical arm. The cells from the prostate gland were removed from the tissue section (Figure 4.6 A & B) with a lifting motion. The STP was briefly placed on the sterile, sticky back of an adhesive paper (as recommended by Arcturis Engineering) to remove any non-specific stromal adhesion (Figure 4.6 B).

**Figure 4.5:** The 'wetting effect' is indicative of optimised LCM settings

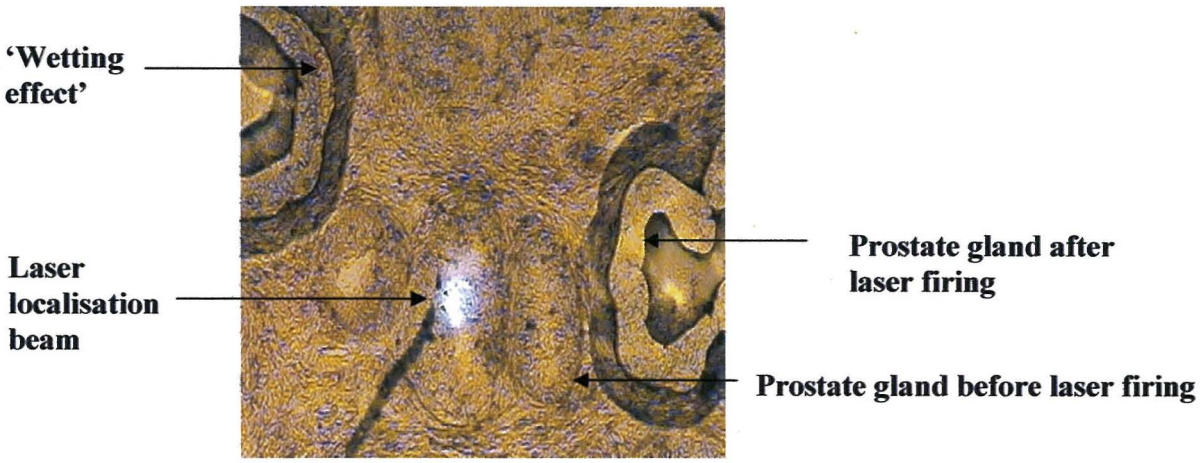


A photomicrograph of a fresh-frozen tissue, Ethanol fixed and Histogene stained as described previously, depicting cancerous glands of the prostate, as determined by a pathologist. Note the 'wetting effect', which was achieved by firing overlapping laser spots and activating the STP to give a well-resolvable image.

**Figure 4.6:** Photomicrographs of prostate gland secretory epithelial cells before and after removal by LCM

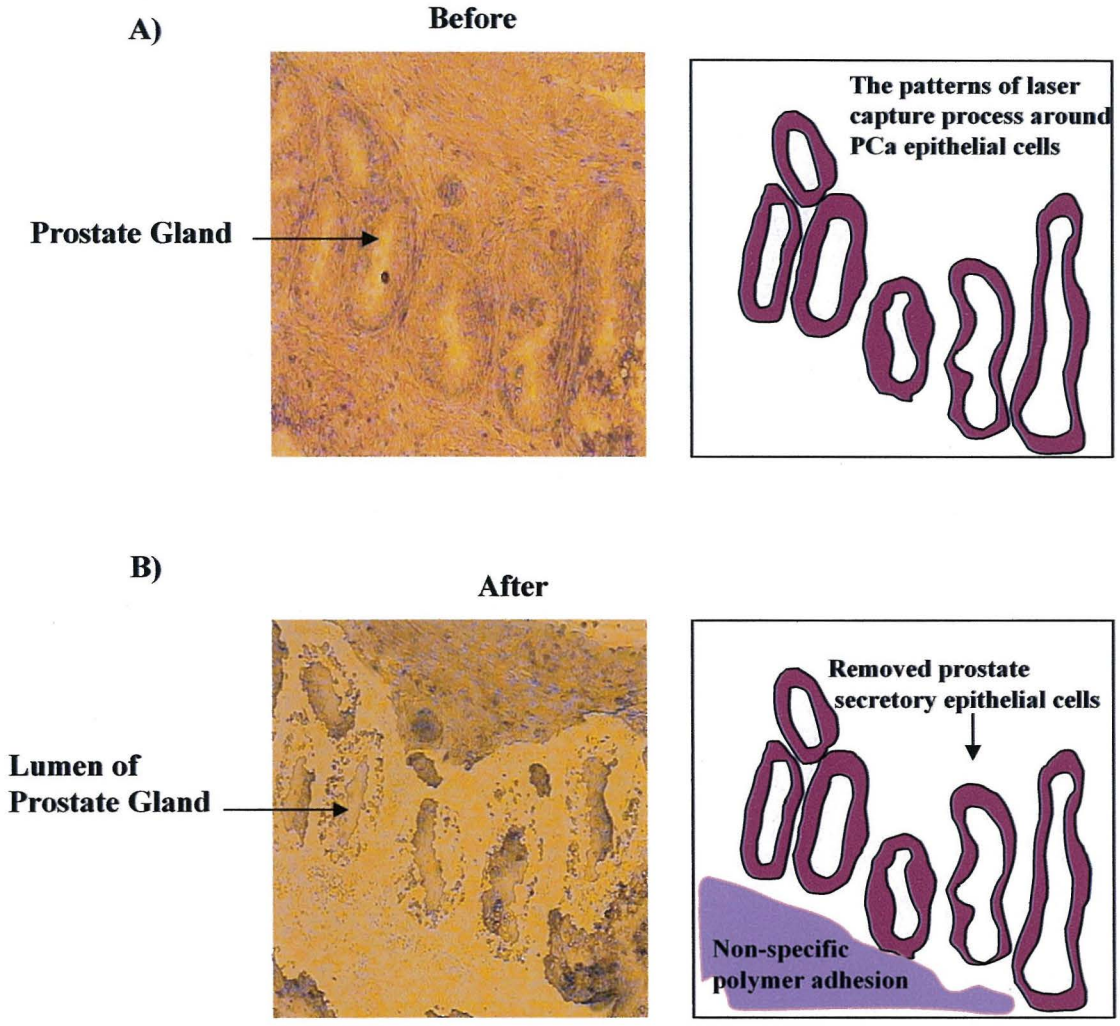


Photomicrographs of A) Gleason Grade 3 prostate glands, as determined by a pathologist before LCM and B) after the secretory cells of the prostate glands were removed by LCM. The lumen of the prostate glands and their surrounding stroma remain on the tissue section illustrating the capturing of a homogeneous cell population from a heterogeneous tissue sample. Stroma that adhered to the polymer non-specifically (B) was removed with a sterile sticky back adhesive paper before the specifically adhered tissue underwent downstream processing. Diagrammatic representation of the captured PCa glands and the non-specific adhesion of stromal tissue are depicted beside each photomicrograph.

### *4.2.4 The cryotomy and LCM of prostate samples obtained at biopsy.*

*Prostate tissue biopsies*

Fresh frozen prostate tissue biopsies were obtained from the Bernard O'Brien Institute of Microsurgery (BOBIM), St. Vincent's Hospital, Melbourne, Vic. tissue bank or from Dr. RA (Frank) Gardiner, Royal Brisbane Hospital, Brisbane Qld. The following table is a summary of tissues obtained for LCM studies.

**Table 4.1:** A summary of prostate tissue obtained at biopsy.

| **Sample ID** | **Pathologists Opinion** | **Location and Volume If Indicated In Pathology Report of Cancer in Prostate Gland** |
|---|---|---|
| ***02R4*** | Gleason 3+3=6 | Approximately 8 % volume of the left lateral lobe |
| ***02R6*** | Gleason 3+4=7 | Up to 35 % of the total prostate gland |
| ***02R9*** | Gleason 3+3=6 | Left lateral lobe |
| ***02R12*** | Gleason 3+4=7 | 15 % right lateral lobe, 10 % left lateral lobe |
| ***02R13*** | Gleason 4+3=7 | 15 % right lateral lobe, 10 % left lateral lobe |
| ***RC4-00*** | Gleason 4+3=7 | Up to 30% of the total prostate gland |
| ***RC9-00*** | Gleason 4+5=9 | Poorly differentiated adenocarcinoma through entire core |
| ***RC9-99*** | Gleason 3+3=6 | Moderately differentiated carcinoma in 5 % |

Table 4.1 indicates each of the fresh frozen tissue samples used in this study, the grade of cancer diagnosed, the anatomical location, and the predicted % volume of cancer within the prostate.

*Cryotome sectioning and routine H&E staining of fresh frozen prostate tissue*

The appropriate prostate lobe (if indicated) for each tissue outlined in Table 4.1 was subjected to cryotome sectioning as described previously. 25 sections were cut in series, mounted on non-coated microscope slides and stored at -80 °C. The first and last section from each serial was fixed in ice cold 75 % EtOH, 1 min and underwent routine H&E staining as described in Chapter 2. The slides were cover-slipped and mounted using DEPEX and examined by a pathologist. Table 4.2 is a summary of the pathologists' opinion pertaining to the glands within the initial sectioning of each tissue.

**Table 4.2:** The pathologist's histological examination of 8 um sections initially cut from fresh, frozen tissue.

| **Sample ID** | **Pathologists Opinion** |
|---|---|
| *02R4* | Hyperplasia |
| *02R6* | Hyperplasia |
| *02R9* | Gleason 3+3=6 |
| *02R12* | Seminal Vesical |
| *02R13* | Hyperplasia |
| *RC4-00* | Hyperplasia |
| *RC9-00* | Artefact - Diathermic |
| *RC9-99* | Hyperplasia |

As illustrated in Table 4.2, only the 02R9 sample had cancerous glands within the tissue section, all the other samples contained hyperplastic glands, contrary to the previously reported presence of high grade cancer illustrated in Table 4.1. The RC9-00 sample was artefactual due to incorrect temperature processing at biopsy (in the pathologists opinion).

Each lobe of interest except 02R9 was subjected to further cryotomy using the opposite side of the tissue as the cutting template, than was used previously. Again, 25 more sections were cut in serial from each tissue of which the first and last section was EtOH fixed and underwent routine H&E staining followed by examination by a pathologist. Table 4.3 summarises the pathologist's second report.

**Table 4.3:** The pathologist's histological examination of 8 μm sections subsequently cut from fresh, frozen tissue.

| Sample ID | Pathologists Opinion |
|---|---|
| ***02R4*** | Hyperplasia |
| ***02R6*** | Hyperplasia |
| ***02R9*** | Gleason 3+3=6 |
| ***02R12*** | Gleason Grade 3+3=6 |
| ***02R13*** | Hyperplasia |
| ***RC4-00*** | Hyperplasia |
| ***RC9-99*** | Hyperplasia |

As shown in Table 4.3, cancer glands were present in an additional sample 02R12, and still present in 02R9, whilst the glands in the rest of the samples remained diagnosed as hyperplastic.

Further cryotomy was performed on biopsies from both the same and opposite lateral lobes for samples 02R4, 02R6 and 02R13. Although additional tissue for RC4-00 and RC9-99 was not available, the remaining tissue was sectioned through to completion. Surprisingly, no cancer glands were subsequently found in any of the lobes subjected to further examination. These observations are indicative of the very small foci in which PCa glands are located within the prostate tissue as a whole. Only a small amount of the available biopsy material actually contained prostate glands tumorigenic in nature. This result was somewhat surprising and limited this particular study. In this particular archive, ~40 % of samples taken from the whole prostate are found to contain PCa by the pathology department (Personal Communication, Dr. Elizabeth Williams, Senior Scientist, BOBIM). Although it was now not plausible to anticipate a sound comparison of expression analysis of either ADAM-9 or -10 between prostate glands of differing pathological states, important information regarding the molecular size of both ADAMs in a homogeneous population of secretory epithelial cells from prostate glands could still be obtained.

### *4.2.5 LCM, protein and RNA extraction from cryosectioned prostate tissue*

*Isolation of protein from tissue sections by Laser Capture Microdissection*

Tissue sections from each of the samples represented in Table 4.3 underwent rapid Histogene staining as described above, followed by subsequent LCM processing. Before and after photomicrographs were taken of the process of capturing and removing the secretory epithelial cells from the prostate glands of interest in each section. This enabled the assessment of efficiency of the removal of these cells from each microdissected tissue section as well as reference photographs for a pathologists review at a later date. Once the STP was lifted from the tissue section, the mechanical arm was swung on a hinge to a 'vial capping station' where a 0.5 ml eppendorf tube containing 40 µl of protein lysis buffer was loaded. The Capsure was clipped into the top of the eppendorf tube creating an airtight seal, inverted so that the lysis buffer was in direct contact with the captured cells on the STP and placed immediately on ice. The whole procedure, from Histogene staining to placing the captured cells on ice, took approximately 1 h. The eppendorf tube was stored on ice for up to 3 hours to await further processing whilst subsequent tissue underwent LCM. Initially the eppendorf tube containing the Capsure was vortexed vigorously for 5 min followed by centrifugation at 10 000 X G for 10 min.

Examination of the Capsure under a light microscope revealed that a high percentage of tissue remained adhered to the transfer film. Therefore, an additional sonication step (high frequency water bath sonication) by the submersion of the Capsure/eppendorf tube, 2 min was performed at room temperature, followed by vigorous vortexing, 2 min and a 30 min centrifugation (10 000 X G), 4 °C. Examination of the Capsure under the light microscope showed that 100 % of the captured cells had been removed from the transfer film by this method. Once the Capsure was removed from the eppendorf tube, the captured cells were briefly homogenised by pipette. The resultant protein extract was stored at -80 °C to await further analysis.

*Isolation of RNA from tissue sections by Laser Capture Microdissection*

The prostate samples 02R9 and 02R12 were processed through rapid Histogene staining as described above and subjected to LCM, with benign and cancer glands from the same tissue section being isolated in two separate LCM runs. Two paraffin embedded, formalin fixed tissue sections were de-waxed in xylene 2 X 5 min and also rapid stained with Histogene and subjected to the same kind of LCM processing. Upon isolation of each prostate gland/cell type, the Capsure was placed into a 0.5 ml eppendorf tube containing RNA extraction buffer (XB) (PicoPure Isolation Kit, Arcturus Engineering). Total RNA was extracted as per the manufacturer's protocol. Briefly, the eppendorf tube was inverted so that the XB covered the transfer film and incubated at 42 °C for 30 min. A centrifugation step collected the XB containing the LCM material from the transfer film into the bottom of the eppendorf tube. Ethanol was added to the RNA extract and the solution was applied to a spin column, provided by the manufacturer. The column containing bound RNA was washed 3 times by centrifugation with provided wash buffers and eluted into a separate eppendorf tube by centrifugation, 2 times each with 11 µl of elution buffer, collected in the same eppendorf tube (total volume = 22 µl) and stored at -80 °C to await further analysis.

*Protein and RNA material available for downstream LCM analysis*

The small number and amount of initial sample available from this study, followed by the clear absence of cancer in many of the available lobes of the prostate tissue, infringed on solid outcomes of this study. Nonetheless Table 4.4 summarises the samples that were obtained from LCM. These samples were used for optimisation and examination in the appropriate downstream processing (Western blot analysis or RT-PCR) described above.

Enough material was available to carry out pilot experiments for Western blot and RT-PCR analysis of ADAM-9 and -10. Availability was however, limited and as this experiment was performed in a collaborative laboratory, geographically distant from QUT, time did not permit the collection and analysis of further prostate tissue biopsies.

**Table 4.4:** Samples obtained from LCM for use in downstream applications.

| Sample ID | # Benign Protein Samples | # Cancer Protein Samples | # Benign RNA Samples | # Cancer RNA Samples |
|---|---|---|---|---|
| ***02R4*** | 4 | - | - | - |
| ***02R6*** | 2 | - | - | - |
| ***02R9*** | 1 | 4 | 1 | 1 |
| ***02R12*** | 4 | 2 | 2 | 2 |
| ***02R13*** | 2 | - | - | - |
| ***RC4.00*** | 1 | - | - | - |
| ***RC9.99*** | 4 | - | - | - |
| ***Wax Embedded A*** | - | - | 1 | 1 |
| ***Wax Embedded B*** | - | - | 1 | 1 |

Table 4.4 represents the material collected from LCM experiments performed at BOBIM, Melbourne, Vic. Australia.

The material outlined in Table 4.4 was, however, enough to determine the possibility of detecting each ADAM of interest in LCM acquired material and to make preliminary observations as to the corresponding molecular weight of ADAM-9 and -10 in a homogeneous cell population of prostate glands.

### *4.2.6 Downstream processing of protein and RNA isolated from prostate tissue samples by LCM.*

*Western blot analysis of ADAM-9 and -10*

20 µl of protein extract isolated from each sample described above was combined with 5 µl 5 X Western blot reducing loading buffer and boiled for 3 min, loaded onto an SDS-PAGE gel followed by standard Western blot procedure (Chapter 2). ADAM-9Cterm (0.025 µg/ml), ADAM-9Dis (0.5 µg/ml) and ADAM-10Met (0.05 µg/ml) or ADAM-10Cterm (0.5 µg/ml) was used as primary antibody. Each blot was incubated with primary antibody overnight at 4 °C, followed by 4 X 5 min washes in TBS Tween20 (0.05%). Anti-rabbit

HRP (Dako) was used at the concentration of 0.2 µg/ml in a 2 h incubation at room temperature, followed by a further 4 X 5 min wash in TBS Tween20 (0.05%). FEMTO (Pierce) chemiluminescent substrate was used to detect signal by autoradiography on an X ray film. RWPE-1 or PC-3 prostate cell lines were run on each Western blot to serve as a positive control. A pre-stained protein marker (Biorad) was used to determine molecular weight by direct comparison of migration distances.

*Reverse Transcription – Polymerase Chain Reaction (RT-PCR) of β-actin, ADAM-9 and -10 expression from LCM RNA samples*

9 µl of each RNA extraction sample, described above, was reversed transcribed with Superscript II (Invitrogen) using random decamers and oligodT priming. 5 µg of LNCaP total RNA was used as a positive RT control. Reverse transcription was carried out at 43 °C for 2.5 h. PCR was carried out using β-actin, ADAM-9 or ADAM-10 primers (McCulloch et al. 2000) in a standard PCR reaction (Chapter 2) increasing the amount of cycles to 60 and using 2 µl of cDNA as a template. The PCR product was run on a 2 % agarose EtBr gel and visualised under a UV lamp. The size of the PCR product was determined by comparison to molecular weight marker IX (Roche) run alongside the PCR products on the same gel.

### *4.2.7 Western blot analysis of ADAM-9 and -10*

ADAM-9 and -10 proteins were both detected in protein samples obtained by LCM. For ADAM-9, bands at ~70 kDa and ~50 kDa were detected in the 02R9 (cancer) sample with the ADAM-9Cterm antibody (Figure 4.7 A) which correspond to some of the bands detected in the RWPE-1 whole cell lysate (positive control), whilst higher molecular weight bands ~85 - 90 kDa were detected in RC4.00 and 02R4 (benign) samples (Figure 4.7 B) using the ADAM-9Dis antibody. Unlike the previous ADAM-9 Western blots performed with the ADAM-9Dis antibody in the previous chapter, the ADAM-9Cterm antibody showed additional higher molecular weight bands in the RWPE-1 whole cell lysate preparation used in this experiment. The identity of these bands is not yet known.

For the ADAM-10Met antibody, clear bands were detected at ~54 kDa and ~56 kDa in the 02R12 and 02R4 (benign) samples (Figure 4.7 C) and the 02R9 cancer sample (not shown - too faint), which correspond to bands detected in the RWPE-1 positive control cell line, as well as bands detected in WSS specimens run alongside the LCM protein extracts. Additional lower molecular weight bands ~30 kDa could also be seen in each WSS and may represent smaller processed ADAM-10 fragments possibly found in the stroma but not in the epithelial cells of the prostate gland. Higher molecular weight bands ~100 kDa were also detected, although very faintly (Figure 4.7 C). The ADAM-10Cterm antibody detected bands of similar size in RC4.00 and 02R12 (benign protein samples) (Figure 4.7 D).

### *4.2.8 RT-PCR analysis of β-Actin, ADAM-9 and ADAM-10*

Using β-Actin primers, which span an intron, clear PCR products were detected in 02R12 (benign), 02R9 (benign) and 02R9 (cancer) samples, however, no PCR product was visualised from RNA extracted from formalin fixed, paraffin wax embedded prostate tissue or from 02R12 (cancer) (Figure 4.8 A). The cDNA was free of genomic DNA (gDNA) contamination as determined by the absence of a higher molecular weight band, which would otherwise represent an intronic sequence in the β-Actin gene. PCR products of the expected size for both ADAM-9 and -10 (Figure 4.8 A & B) were successfully detected in the same samples as the β-Actin PCR products, using primers described previously (McCulloch et al. 2000).

**Figure 4.7:** Western Immunoblot of LCM acquired protein for ADAM-9 and -10

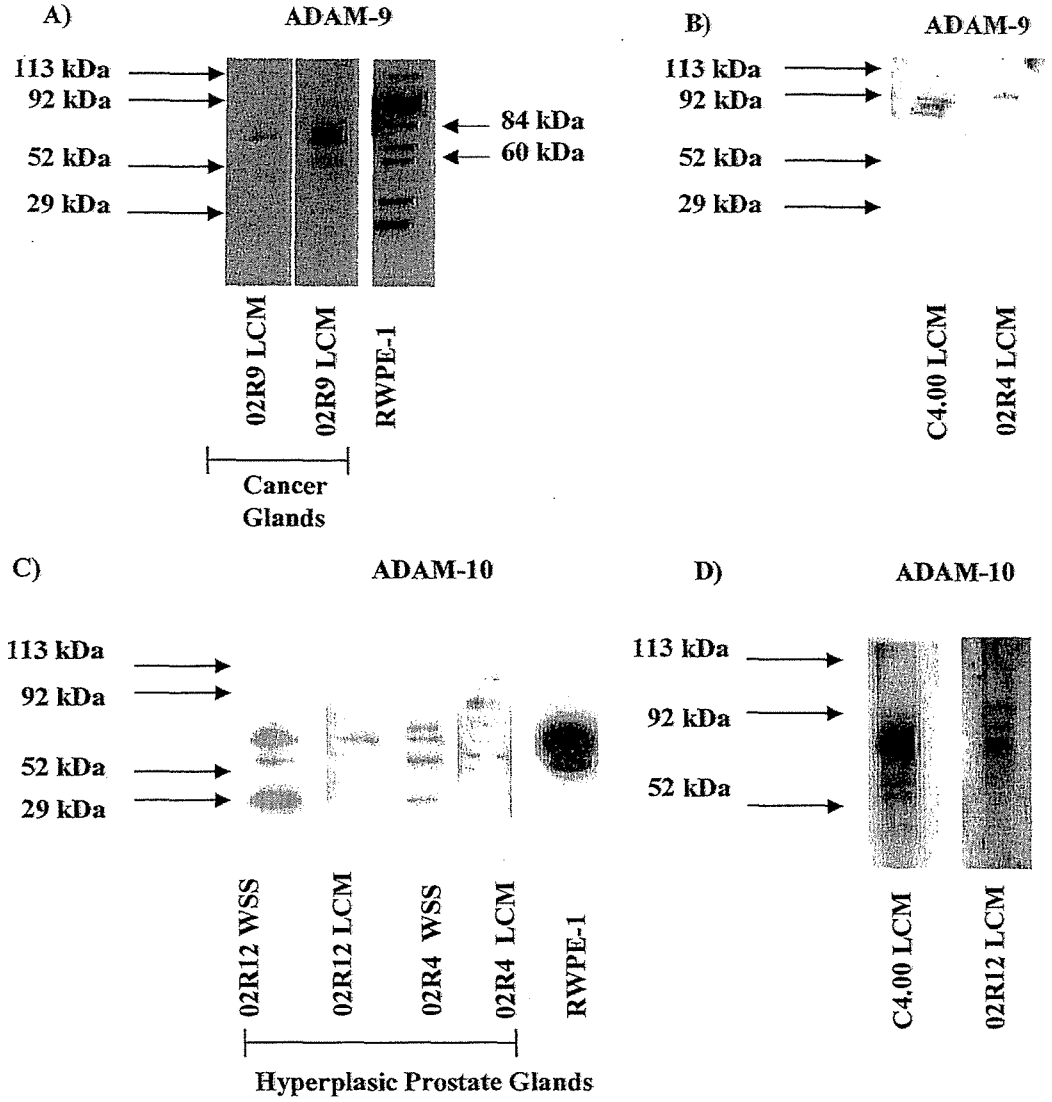


Western blot analysis for LCM samples (Table 4.4) for ADAM-9: A) bands were detected ~50 to ~70 kDa with the ADAM-9Cterm antibody and B) ~85 to ~90 kDa with the ADAM-9Dis antibody. RWPE-1 was used as a positive control. For ADAM-10: C) bands were detected ~54 kDa and ~56 kDa and 100 kDa with the ADAM-10Met antibody and D) bands of similar sizes were detected with the ADAM-10Cterm antibody. Corresponding WSS were run alongside the LCM material as well as the positive control cell line RWPE-1.

**Figure 4.8:** RT-PCR showing β-Actin, ADAM-9 and ADAM-10 cDNA transcripts from LCM acquired RNA

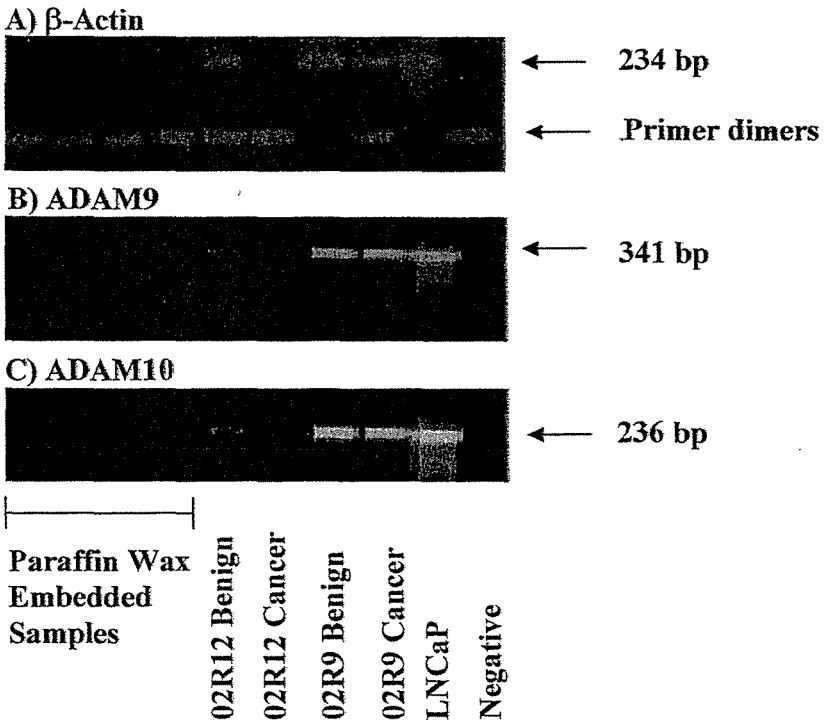


**Figure 4.8:** All PCR products for β-Actin (A), ADAM-9 (B) and ADAM-10 (C) were successfully detected in cDNA from LCM processed fresh-frozen tissue except 02R12 (Cancer). No PCR products could be detected from cDNA from LCM processed formalin fixed, paraffin embedded tissue. The size of the PCR product was determined by molecular weight marker IX (Roche) run alongside each PCR product on a 2 % agarose EtBr gel and visualised under a UV lamp. Each cDNA sample positive for β-Actin was free of gDNA contamination as determined by the β-Actin primers that cross an intron. LNCaP cell total RNA was used as a positive RT-PCR control in which all three genes were also successfully detected.

### *4.3 Discussion*

Laser Capture Microdissection (LCM) enables the isolation and enrichment of specific cell types within a heterogeneous tissue sample. This approach has been previously used successfully to identify differences in gene expression profiles between hyperplastic and cancer glands from the prostate (Paweletz et al. 2001). These studies used subsequent downstream analysis such as 2-D PAGE gel analysis, SELDI- and MALDI-TOF (protein molecular weight spectra analysis), mRNA expression by real time PCR and Microarray analysis (Xu et al. 2002; Rubin et al. 2001). Despite the abovementioned protein analytical approaches, the application of the Western blot used in conjunction with LCM, is relatively uncommon, despite the information this type of analysis may add to studies such as these. Just two studies, by a single research group, have used LCM in this fashion to examine the detectability of the well-characterised PCa marker Prostate Specific Antigen (Ornstein et al. 2000). The current study represents the first demonstration of ADAM family members at both the mRNA and protein level, in LCM-derived prostate epithelial glands.

PCa glands are commonly present in small, defined foci within prostate tissue. At the time of biopsy, several tissue samples are taken from anatomically different locations within the prostate so as to increase the chances of the successful detection of any PCa, which may or may not be confined within the prostate. The extensive cryotome sectioning of the prostate tissue obtained at biopsy in this study, reinforced the difficulty of locating cancerous glands within the prostate. Despite having available several tissue samples from each of the left and right lateral lobes of the prostate, which were initially diagnosed with the presence of high-grade PCa glands, cancer could be found in only two out of an initial eight biopsies. A requirement for this type of study is the analysis of carefully defined specific regions within the diseased prostate. Nonetheless, eight separate biopsies provided a good source of normal/hyperplastic prostate glands, and on occasion, cancerous glands, sufficient to develop a suitable approach for analysing gene expression by LCM in the secretory epithelial cells of prostate glands.

A LCM protocol was developed which enabled the isolation of both protein and RNA from homogeneous cell types in PCa glands from prostate tissue characteristic of the benign and malignant disease. Further, it was demonstrated that mRNA could be detected at suitable levels for subsequent real time PCR analysis. Importantly, the detection of ADAM-9 and -10 protein from LCM samples by Western blot analysis was also effectively achieved, although the molecular weights of the bands detected in some cases, outlined below, varied somewhat from those molecular weights detected in cell lines previously studied in Chapter 3 and may represent processing that has occurred throughout the LCM procedure.

To this stage, this particular study has not had access to enough individual fresh frozen prostate patient specimens, nor sufficient material to allow for adequate replicates to provide a valid comparison of ADAM-9 or -10 between benign and malignant states of the prostate. However, preliminary data obtained clearly indicates that the protocol developed will be suitable to extend this study further. The current data obtained by Western immunoblot analysis, however, do provide information as to the molecular size of each ADAM present in homogeneous cell populations of the prostate gland and warrants a short discussion.

For ADAM-9, a clear band was detected, firstly with the ADAM-9Cterm antibody at ~60 and ~70 kDa and subsequently with the ADAM-9Dis antibody at ~85 to ~90 kDa. Each of these bands corresponded to bands detected in the RWPE-1 prostate cell line. The larger molecular weight bands may represent the unprocessed, inactive form of ADAM-9 whilst the intermediate and lower molecular weight bands may represent partly processed and fully processed mature active forms of ADAM-9 respectively.

No specific role for ADAM-9 has been determined as yet, although it has been shown to be an active membrane-bound metalloprotease, as well in being secreted as a soluble form. As outlined in Chapter 1, ADAM-9 is able to cleave peptide sequences mimicking cell surface protein cleavage sites such as those in p75 TNFR, TNF α and β-Amyloid Precursor Protein (β-APP) (Roghani et al. 1999). However, *in vivo* data has not yet been obtained in respect to this proposed role. ADAM-9 is also able to degrade gelatin and fibronectin

(extracellular matrix substrates) *in vitro* (Schwettmann and Tschesche, 2001). Additionally, its disintegrin domain is able to bind particular integrins involved in cell-cell and cell-ECM interactions such as α6β1 (Zhou et al. 2001). It is therefore entirely possible that ADAM-9 and other ADAMs, due to their multifunctional domain composition, may perform a variety of roles in PCa cells and that those roles may differ during the multiple stages of PCa progression.

In the case of ADAM-10, the ADAM-10Met antibody detected clear bands at ~54 and ~56 kDa, which corresponded to the size of ADAM-10 found in nuclear and cytoplasmic fractions, respectively, of both RWPE-1 and PC-3 prostate cell lines (Chapter 3). Larger molecular weight bands up to ~100 kDa were also detected with both the ADAM-10Cterm and ADAM-10Met antibodies possibly representing unprocessed, partly processed or different isoforms of unprocessed ADAM-10.

Active ADAM-10 is known to carry out the definitive but shared task *in vivo* (with ADAM-17), of solubilising proTNF α (Blobel, 1997; Rosendahl et al. 1997) and the cleavage of β-APP (Buxbaum et al. 1998; Lammich et al. 1999). Another study has shown that bovine ADAM-10 can cleave collagen type IV (a basement membrane and extracellular matrix protein) (Millichip et al. 1998). Each of these roles, and others outlined in Chapter 1, has so far focussed on metalloprotease activity on the cell surface.

It was found by LCM that the secretory epithelial cells of prostate glands express what appear to be cytoplasmic and nuclear specific isoforms of ADAM-10, as detected in previous subcellular fractionation studies (Chapter 3). These isoforms each contain the N-terminal domain of the mature, catalytically active protein, as determined by a site-specific antibody. A new question has now arisen as to what roles active ADAM-10 may have in the cell nucleus. Given the consistent observation by IHC that ADAM-10 re-localises to the nucleus in high-grade cancer, when compared to benign and low-grade cancer glands in the same tissue section (See Chapter 1), it is likely that, as discussed for ADAM-9, ADAM-10 may have differential roles through the stages of PCa development.

LCM has enabled us to directly compare observations from prostate cell lines *in vitro* to homogeneous cell populations from glands of the prostate in clinical specimens. Also, especially with respect to ADAM-10, LCM has allowed us to correlate data acquired by IHC and sub-cellular fractionation and its apparent nuclear ADAM-10 localisation, to the molecular size of the ADAM-10 protein found in the secretory cells of the prostate glands. Further studies using a larger population set and more replicates are required, so that any difference in the pattern of expression for both ADAM-9 and -10 mRNA and protein can be properly examined between homogeneous populations of normal, hyperplastic and cancerous secretory cells of the prostate gland.

LCM is a powerful tool, which gives rise to important information with respect to gene profiling between differing normal and pathological states of glands within tissues and organs. Although the optimisation of such assays is a lengthy process and the mRNA or protein yield can be very limiting, the investment in time is worth the acquisition of novel data, such as those acquired by this technique in this particular study. With more sensitive and effective methods of molecular analysis emerging, LCM has sound applications in downstream processing and gene profiling experiments and perhaps the diagnosis of pathological disease states.

# CHAPTER FIVE:

## 5.0 THE CLONING AND OVER EXPRESSION OF FULL LENGTH ADAM-10 IN PROSTATE CELL LINES

## *5.1 Introduction*

The previous two chapters have established the expression status of both ADAM-9 and -10 in a range of normal prostate and prostate cancer (PCa) cell lines, prostate tissues and bone metastases. Both ADAM-9 and -10 were expressed at readily detectable levels in PCa cell line models that mirror characteristic of androgen-sensitive and androgen insensitive prostate cancer. The processed forms corresponding to the molecular weight of catalytically active ADAM-9 and -10 were detected by Western blot analysis in both the normal prostate and PCa cell lines and were also found to be variously localised in the cell nucleus, cytoplasm/membrane and in extracellular, plasma membrane vesicles. These observations provide significant but as yet poorly studied opportunities for both ADAMs to display many potential functions within and outside the cell.

As reviewed in Chapter 1, the functions of ADAM-10 that have been described to date, include "sheddase" activity at the cell surface, whereby ADAM-10 can cleave the ectodomains of membrane-bound proteins such as TNF α and βAPP (Blobel, 1997; Rosendahl et al. 1997; Lammich et al. 1999). Given that we have described the localisation of both ADAM-9 and -10 in the cell nucleus and in extracellular membrane vesicles, it is likely that these ADAMs have additional but distinct functional roles, beyond cell surface sheddase activities. The presence of metalloprotease activity, essentially as a soluble protease in the case of membrane vesicle expression, gives rise to potential ECM degradation activity, which may impact on cell invasive and migratory properties. This is especially pertinent with respect to ADAM-9 and -10, which, as reviewed in Chapter 1, can degrade fibronectin and collagen respectively, *in vitro* (Schwettmann and Tschesche, 2001; Millichip et al. 1998). With respect to the nuclear localisation, the function of ADAM-9 or -10 proteins is not yet known.

A common and accepted approach for showing the functional consequences of proteins with respect to cellular behaviour is to under - or over-express them in suitable, relevant cell models. In the case of the prostate, the normal (RWPE-1) and the metastatic (PC-3) prostate cell lines, in which we have already described both ADAM-9 and -10 localisation

to the nucleus, cytoplasm/membrane and shed membrane vesicles, provide good *in vitro* models to examine the function of both of these ADAMs.

ADAM-10 was chosen in this particular study because of the previous observations that ADAM-10 appears to show increased expression in high-grade cancer glands. Further to this, a clear shift in localisation from the cell membrane to the nucleus of prostate tumour cells suggests that ADAM-10 has roles in late-stage cancer that may be related to transcriptional events, which may lead to abnormal cellular behaviour. Full-length ADAM-10 mammalian expression constructs should provide good molecular tools for stimulating cell lines to express elevated levels of this protein. Over-expression of active ADAM-10 in differing non-tumorigenic and tumorigenic PCa cell lines will provide information about the function of these proteins in PCa through the use of subsequent functional assays such as cell invasion, adhesion and migration, as well as micro-array analysis.

The **aims** of this chapter were

1) To clone full length ADAM-10 cDNA into non-inducible and inducible mammalian expression vectors, and
2) To test each full length clone's efficiency, with respect to its ability to be over expressed in prostate cell lines by means of transient transfection.

A number of technically challenging problems were encountered at the onset of, and throughout, this part of the overall study. Such problems included, initially, difficulty in obtaining enough ADAM-10 PCR product for subsequent cloning activities, followed by the failure of several different cloning strategies, which were attempted numerous times. Through a logical approach to these problems, two ADAM-10 full-length mammalian expression vector constructs were eventually created. These were used to test for ADAM-10 over-expression in prostate cell lines by way of transient transfection. Hence, this chapter describes the optimisation activities carried out for the successful attainment of each aim. Due to time constraints the studies could not be extended to the ultimate intended goal - of carrying out ADAM-10 functional studies in cell invasion, adhesion and

migration assays. Information obtained from the current studies does however, set a basis for future studies to be carried out in this area.

## *5.2 Methodology and Results*

### *5.2.1 The design of ADAM-10 primers for full length cDNA amplification and sequencing*

The primary mRNA sequence for ADAM-10 was retrieved from Genbank (accession number NM_001110) and subjected to restriction enzyme site analysis (WEB ANGIS) to determine which common restriction enzyme sites did and did not fall within its primary sequence. The restriction enzymes *HindIII* and *Xho1* were chosen for the forward and reverse primers respectively, as they did not cut full length ADAM-10 and were matched to the multiple cloning sites (MCS) of the chosen mammalian expression vectors pcDNA3.1 and pMEP4 (Appendix Two). The forward (sense) primer for ADAM-10 was designed 5' to the naturally occurring Kozak sequence of ADAM-10 (GAAAGaugG); and the reverse primer (antisense) encompassing the upstream natural 3' stop codon. The appropriate restriction enzyme sites were incorporated in each primer by mutating the minimum number of bases in the primary mRNA sequence of ADAM-10 (Figure 5.1). Forward and reverse sequencing primers were also designed every 300 bp along the full-length ADAM-10 primary sequence for subsequent PCR and sequencing analysis (Figure 5.1).

### *5.2.2 ADAM-10 full-length transcript PCR*

Initially, 5 μg of mRNA from PC-3 cells was reversed transcribed with 500 ng oligodT or 500ng gene specific (ADAM-10XhoR) priming. The oligodT primed RT was screened for gDNA contamination as described in Chapter 2. A lambda prostate library was also purchased (Promega). To check for the attainment of amplifiable full-length cDNA, platinum Taq DNA polymerase (Life Technologies) was used initially, with the understanding that once the PCR was optimised, a proof reading system would be employed. Each of the two templates (PC-3 cDNA and the prostate library) was used in

the following PCR protocol: 95 °C (5 min), 40 cycles: 95 °C (30 sec), 50 °C (30 sec), 72 °C (3 min), with a final incubation of 72 °C (10 min) with the final magnesium concentration of 1, 2, 3 or 4 mM with 200 nM forward and reverse primer. No bands were seen for either of the templates PC-3 cDNA (Figure 5.2), or the lambda prostate cDNA library (Figure 5.3).

### *5.2.3 ADAM-10 cDNA cloning*

The result from Table 5.1 and Figure 5.4, allowed the reasonable assumption that a) both A10*HindIII*F and A10*XhoR* efficiently bound to the full length ADAM-10 transcript and b) internal sequences of ADAM-10 are present in each of the templates tested. It was a surprise however, that full length ADAM-10 could not be amplified from either of the templates. Given this information, a variety of templates were tested from mRNA extracted from other PCa cell lines including: LNCaP, ALVA-41 and DU-145 cDNA by the PCR protocol described above.

For the PCa cDNAs outlined above, a faint band was seen in ALVA-41 cDNA (too faint to be shown). A re-amplification of this PCR product - ALVA-41 (a) was carried out using that particular PCR product as a template in one reaction, and the original cDNA, using 4 µl instead of 1 µl in a separate PCR reaction. A band at the expected molecular weight, 2.4 Kb was clearly visualised in the ALVA-41 (a) PCR product re-amplification and only faintly visualised in the original ALVA-41 (a) cDNA (Figure 5.5 A). Each band was subsequently gel purified (Life Technologies). The gel-purified products were subjected to a nested PCR to confirm the authenticity of the transcript. The nested PCR from internal ADAM-10 primers was successful (Figure 5.4 B). Although these bands could be gel purified for nested PCR, not enough DNA could be recovered from the gel to be successfully quantitated by spectrophotometric analysis, for subsequent cloning activities. We did not pursue a re-amplification step as this would greatly increase the risk of introducing errors into the cDNA sequence given existing sequence had already been amplified through at least 40 cycles.

**Figure 5.1** Primary sequence of full length ADAM-10 (Genbank accession number NM_001110) showing the position of forward and reverse full length and sequencing primers

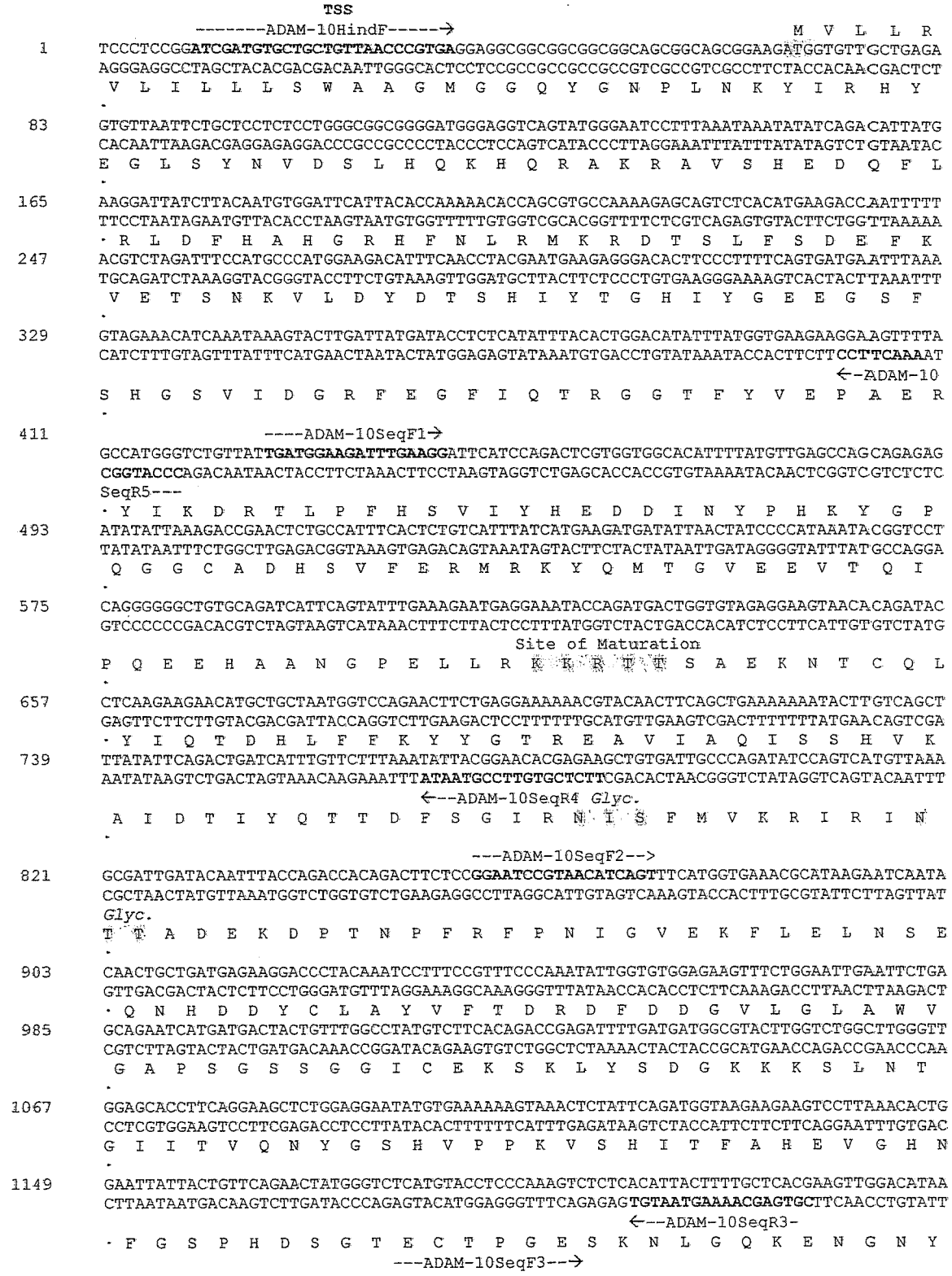

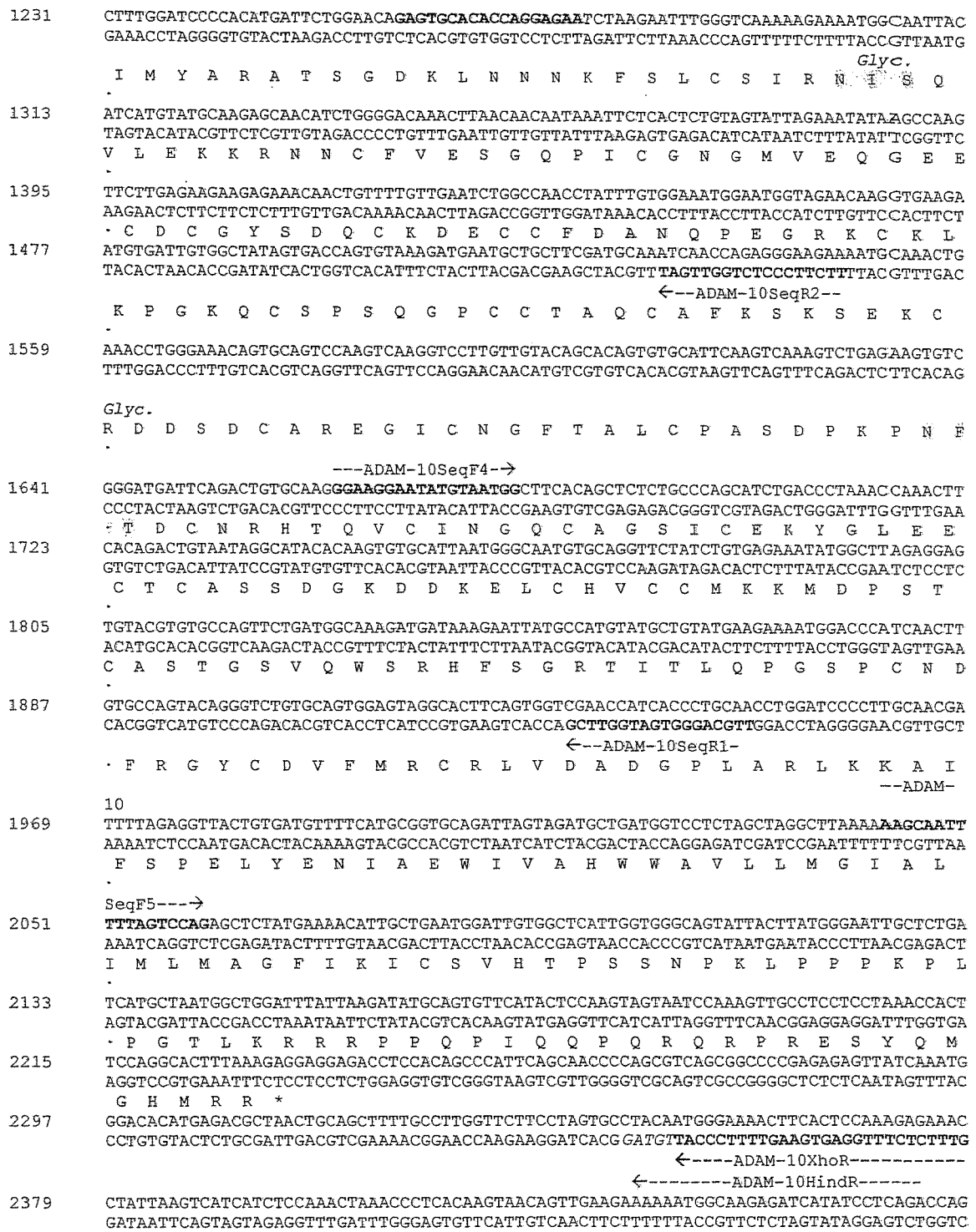
1231
CTTTGGATCCCCACATGATTCTGGAACAGAGTGCACACCAGGAGAATCTAAGAATTTGGGTCAAAAAGAAAATGGCAATTAC
GAAACCTAGGGGTGTACTAAGACCTTGTCTCACGTGTGGTCCTCTTAGATTCTTAAACCCAGTTTTTCTTTTACCGTTAATG
Glyc.
I M Y A R A T S G D K L N N N K F S L C S I R N I S Q
1313
ATCATGTATGCAAGAGCAACATCTGGGGACAAACTTAACAACAATAAATTCTCACTCTGTAGTATTAGAAATATAAGCCAAG
TAGTACATACGTTCTCGTTGTAGACCCCTGTTTGAATTGTTGTTATTTAAGAGTGAGACATCATAATCTTTATATTCGGTTC
V L E K K R N N C F V E S G Q P I C G N G M V E Q G E E
1395
TTCTTGAGAAGAAGAGAAACAACTGTTTTGTTGAATCTGGCCAACCTATTTGTGGAAATGGAATGGTAGAACAAGGTGAAGA
AAGAACTCTTCTTCTCTTTGTTGACAAAACAACTTAGACCGGTTGGATAAACACCTTTACCTTACCATCTTGTTCCACTTCT
C D C G Y S D Q C K D E C C F D A N Q P E G R K C K L
1477
ATGTGATTGTGGCTATAGTGACCAGTGTAAAGATGAATGCTGCTTCGATGCAAATCAACCAGAGGGAAGAAAATGCAAACTG
TACACTAACACCGATATCACTGGTCACATTTCTACTTACGACGAAGCTACGTTTAGTTGGTCTCCCTTCTTTTACGTTTGAC
←--ADAM-10SeqR2--
K P G K Q C S P S Q G P C C T A Q C A F K S K S E K C
1559
AAACCTGGGAAACAGTGCAGTCCAAGTCAAGGTCCTTGTTGTACAGCACAGTGTGCATTCAAGTCAAAGTCTGAGAAGTGTC
TTTGGACCCTTTGTCACGTCAGGTTCAGTTCCAGGAACAACATGTCGTGTCACACGTAAGTTCAGTTTCAGACTCTTCACAG
Glyc.
R D D S D C A R E G I C N G F T A L C P A S D P K P N F
---ADAM-10SeqF4-→
1641
GGGATGATTCAGACTGTGCAAGGGAAGGAATATGTAATGGCTTCACAGCTCTCTGCCCAGCATCTGACCCTAAACCAAACTT
CCCTACTAAGTCTGACACGTTCCCTTCCTTATACATTACCGAAGTGTCGAGAGACGGGTCGTAGACTGGGATTTGGTTTGAA
T D C N R H T Q V C I N G Q C A G S I C E K Y G L E E
1723
CACAGACTGTAATAGGCATACACAAGTGTGCATTAATGGGCAATGTGCAGGTTCTATCTGTGAGAAATATGGCTTAGAGGAG
GTGTCTGACATTATCCGTATGTGTTCACACGTAATTACCCGTTACACGTCCAAGATAGACACTCTTTATACCGAATCTCCTC
C T C A S S D G K D D K E L C H V C C M K K M D P S T
1805
TGTACGTGTGCCAGTTCTGATGGCAAAGATGATAAAGAATTATGCCATGTATGCTGTATGAAGAAAATGGACCCATCAACTT
ACATGCACACGGTCAAGACTACCGTTTCTACTATTTCTTAATACGGTACATACGACATACTTCTTTTACCTGGGTAGTTGAA
C A S T G S V Q W S R H F S G R T I T L Q P G S P C N D
1887
GTGCCAGTACAGGGTCTGTGCAGTGGAGTAGGCACTTCAGTGGTCGAACCATCACCCTGCAACCTGGATCCCCTTGCAACGA
CACGGTCATGTCCCAGACACGTCACCTCATCCGTGAAGTCACCAGCTTGGTAGTGGGACGTTGGACCTAGGGGAACGTTGCT
←--ADAM-10SeqR1-
F R G Y C D V F M R C R L V D A D G P L A R L K K A I
--ADAM-
10
1969
TTTTAGAGGTTACTGTGATGTTTTCATGCGGTGCAGATTAGTAGATGCTGATGGTCCTCTAGCTAGGCTTAAAAAAGCAATT
AAAATCTCCAATGACACTACAAAAGTACGCCACGTCTAATCATCTACGACTACCAGGAGATCGATCCGAATTTTTTCGTTAA
F S P E L Y E N I A E W I V A H W W A V L L M G I A L
SeqF5---→
2051
TTTAGTCCAGAGCTCTATGAAAACATTGCTGAATGGATTGTGGCTCATTGGTGGGCAGTATTACTTATGGGAATTGCTCTGA
AAATCAGGTCTCGAGATACTTTTGTAACGACTTACCTAACACCGAGTAACCACCCGTCATAATGAATACCCTTAACGAGACT
I M L M A G F I K I C S V H T P S S N P K L P P P K P L
2133
TCATGCTAATGGCTGGATTTATTAAGATATGCAGTGTTCATACTCCAAGTAGTAATCCAAAGTTGCCTCCTCCTAAACCACT
AGTACGATTACCGACCTAAATAATTCTATACGTCACAAGTATGAGGTTCATCATTAGGTTTCAACGGAGGAGGATTTGGTGA
P G T L K R R R P P Q P I Q Q P Q R Q R P R E S Y Q M
2215
TCCAGGCACTTTAAAGAGGAGGAGACCTCCACAGCCCATTCAGCAACCCCAGCGTCAGCGGCCCCGAGAGAGTTATCAAATG
AGGTCCGTGAAATTTCTCCTCCTCTGGAGGTGTCGGGTAAGTCGTTGGGGTCGCAGTCGCCGGGGCTCTCTCAATAGTTTAC
G H M R R *
2297
GGACACATGAGACGCTAACTGCAGCTTTTGCCTTGGTTCTTCCTAGTGCCTACAATGGGAAAACTTCACTCCAAAGAGAAAC
CCTGTGTACTCTGCGATTGACGTCGAAAACGGAACCAAGAAGGATCACGGATGTTACCCTTTTGAAGTGAGGTTTCTCTTTG
←----ADAM-10XhoR----------
←---------ADAM-10HindR------
2379
CTATTAAGTCATCATCTCCAAACTAAACCCTCACAAGTAACAGTTGAAGAAAAAATGGCAAGAGATCATATCCTCAGACCAG
GATAATTCAGTAGTAGAGGTTTGATTTGGGAGTGTTCATTGTCAACTTCTTTTTTACCGTTCTCTAGTATAGGAGTCTGGTC

| Primer | Sequence |
|---|---|
| ***A10HindF*** | 5' ATCGAT***AAGCTT***CTGTTAACCCGTGA 3' |
| *A10SeqF1* | 5' TGATGGAAGATTTGAAGG 3' |
| *A10SeqF2* | 5' GGAATCCGTAACATCAGT 3' |
| *A10SeqF3* | 5' GAGTGCACACCAGGAGAA 3' |
| *A10SeqF4* | 5' GGAAGGAATATGTAATGG 3' |
| *A10SeqF5* | 5' AAGCAATTTTTAGTCCAG 3' |
| *A10SeqR1* | 5' CCCATGGCTAAAACTTCC 3' |
| *A10SeqR2* | 5' TTCTCGTGTTCCGTAATA 3' |
| *A10SeqR3* | 5' CTGTAGCAAAAGTAATGT 3' |
| *A10SeqR4* | 5' TTCTTC CCTCTGGTTGAT 3' |
| *A10SeqR5* | 5' TTGCAGGGTGATGGTTCG 3' |
| ***A10XhoR*** | 5' GGTTT***CTCGAG***GGAGTGAAGTTTTCCCAT 3' |
| ***A10HindR*** | 5' CTCTTTGGAGTG***AAGCTT***TCCCATTGTAG 3' |

ADAM-10 forward and reverse primers designed for the full-length amplification of ADAM-10 cDNA together with internal primers along the full-length sequence for subsequent nested PCR and sequencing analysis. The restriction enzyme sites are indicated in bold/italic in each A10*HindIII*F and A10*Xho*R primer sequence. *Glyc.* indicates putative glycosylation sites. The site of maturation is a furin-recognition cleavage site at which ADAM-10 is processed.

**Figure 5.2:** Effects of magnesium titration on PCR amplification of full length ADAM-10 in PC-3 cells

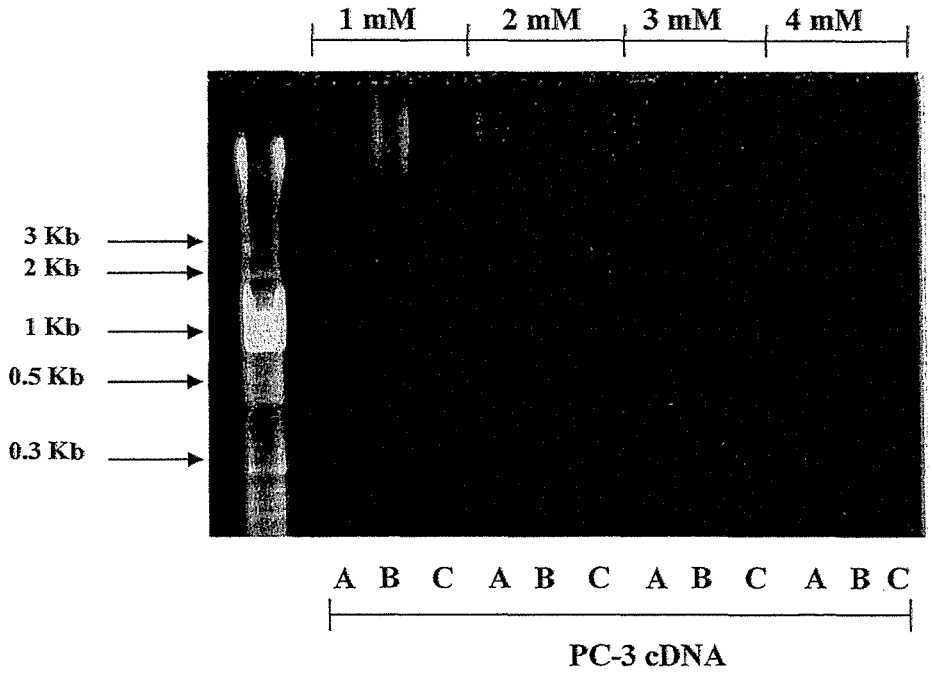


No bands were obtained for full length ADAM-10 at any of the final magnesium concentrations of 1, 2, 3 or 4 mM. Each lane represents A (PC-3 cDNA by oligodT priming), B (PC-3 cDNA by gene-specific reverse priming with ADAM-10XhoR) and C (no template - negative control). See Figure 5.3 for positive control detecting the presence of internal sequence of ADAM-10 in PC-3 cDNA.

**Figure 5.3:** Full length ADAM-10 amplification using a Lambda prostate library as a template

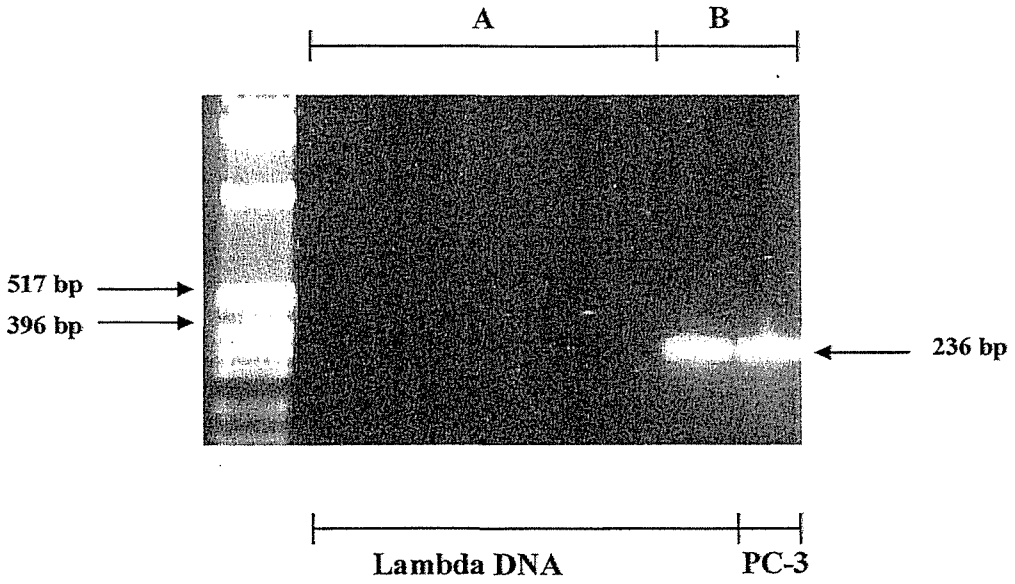


No PCR product was obtained from the Lambda prostate library for full length ADAM-10 (A). Positive controls included internal ADAM-10 primers used previously (Table 3.1) in the same PCR (B) in which clear PCR products were seen in both the Lambda prostate cDNA library and in PC-3 cDNA at the expected 236 bp, indicating the presence of ADAM-10 transcript in both templates used.

The efficiency of hybridisation of the two restriction enzyme incorporated primers ADAM-10*Hind*F and ADAM10*Xho*R used for ADAM-10 full length amplification was tested by combining each with sequencing primers outlined in Figure 5.1. Table 5.1 (below) summarises each primer set used, their expected size in base pairs and a summary of the results obtained and illustrated in Figure 5.4.

**Table 5.1:** ADAM-10 full-length forward and reverse primer binding efficiency by PCR

| **Forward Primer (ADAM-10)** | **Reverse Primer (ADAM-10)** | **Expected Size (Base Pairs)** | **PC-3 Template** | **Lambda Prostate Library Template** |
|---|---|---|---|---|
| A10HindF | A10SeqR1 | 380 | √ | × |
| A10SeqF5 | A10XhoR | 338 | √ | √ |
| A101SeqF1 | A10SeqR5 | 1522 | √ ? | √ ? |

Table 5.1: √ indicates that a clear PCR product was visualised at the expected molecular weight, × indicates no PCR product, and ? indicates that non-specific binding was seen.

**Figure 5.4** PCR of internal sequences of ADAM-10 full-length transcript in each of the Lambda prostate library and PC-3 templates

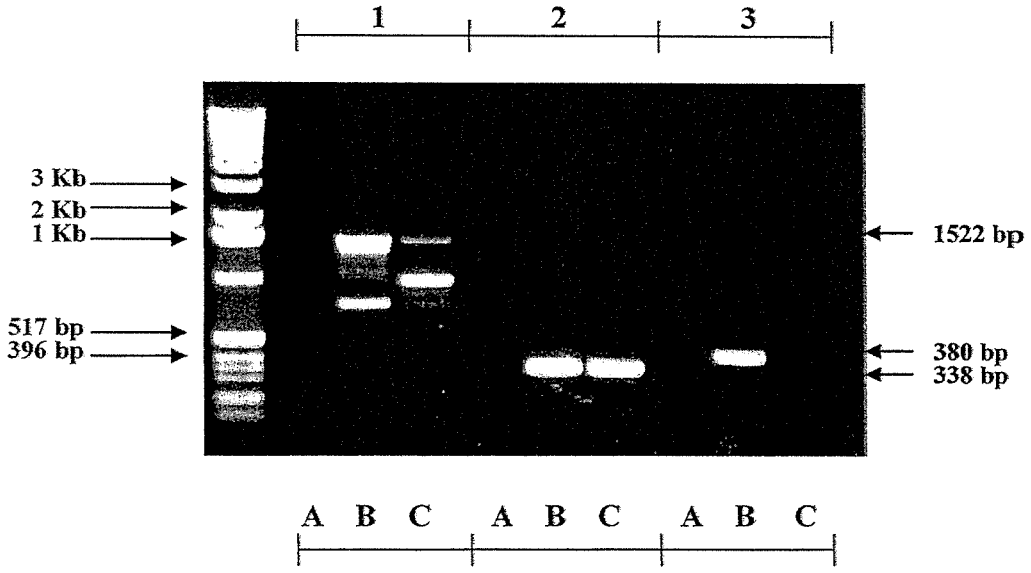


Bands of expected size for each of the templates A (negative control), B (PC-3) and C (Lambda prostate library) for the primer sets outlined in Table 5.1 were visualised. The expected PCR products were seen in 1 (1522 bp, templates B & C), 2 (338 bp, templates B & C) and 3 (380 bp, template B only).

**Figure 5.5:** PCR of full length ADAM-10 using ALVA-41 and DU-145 cDNA as a template

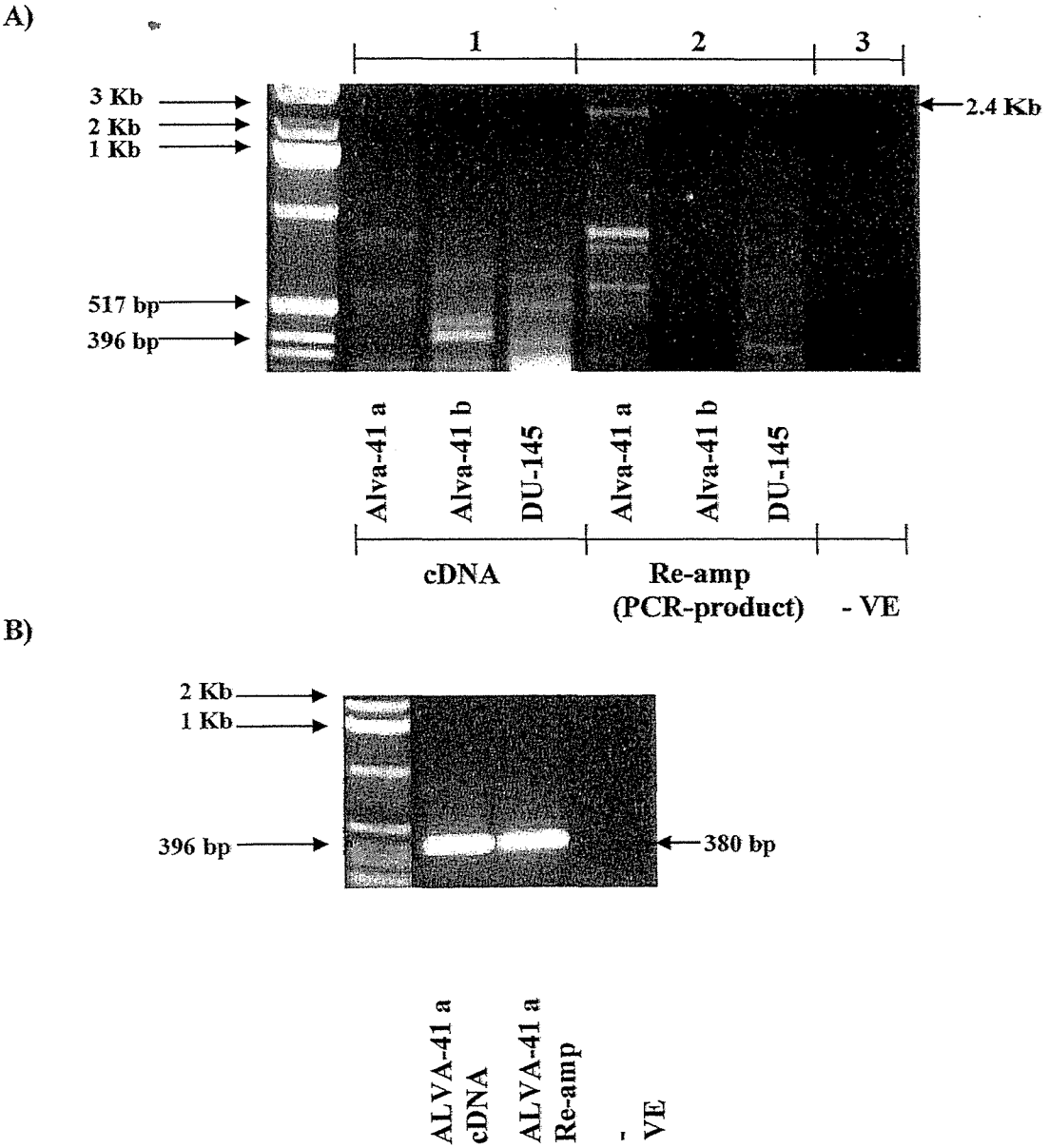


Full length ADAM-10 (A) by PCR could be obtained from one of two separate RT-PCR preparations of the ALVA-41 (a and b) prostate cancer cell line cDNA (ALVA-41 a) but not the ALVA-41 b or DU-145 prostate cancer cell line. The bands shown at ~2.4 Kb (A) were gel purified and analysed by subsequent nested primers (B), A10Seq1F and A10Seq4R confirming the identity of the ~2.4 Kb transcript as ADAM-10. For negative controls, no template was added to the PCR.

Next, the EST database (Genbank) was searched and an EST that contained the full-length ADAM-10 sequence (Genbank accession number AI 680390, I.M.A.G.E clone I.D number 2264325) was found and subsequently purchased from Insight Genomics (St. Louis, USA). The proof reading enzyme system, EXPAND$^{tm}$ (Roche), was initially tested using the following PCR protocol: Two separate master mixes were made, the first containing 700 µM dNTP, 200 nM each 5' ADAM-10*Hind*F and 3' ADAM-10*Xho*R full length transcript primers, 56 ng template (EST) in a final volume of 25 µl per reaction. The second master mix contained 5 µl 10X Buffer (supplied by the manufacturer), 0.75 µl Expand enzyme in a final volume of 25 µl per reaction. Each master mix was combined and the following PCR protocol was run: 94 °C 3 min, 35 cycles; 94 °C 30 sec, 55 °C 30 sec, 68 °C 3 min followed by 68 °C 10 min.

The PCR product (2.4 Kb) (Figure 5.6 A) was column purified (QIAGEN) and ligated into pGEMTEasy (Promega) (Appendix 2) as per the manufacturer's protocol (no A-tailing was necessary as the EXPAND system incorporates an A-tailing polymerase). 1 ml of competent JM-109 cells (Life Technologies) was transformed with the resultant ligation; 43 °C for 50 sec, and incubated at 37 °C / 2500 rpm on a table-top shaker, for 2 hours (recovery) followed by plating out onto XGAL/IPTG LB-Ampicillin (1 µg/ml) blue/white selective agar. White colonies were selected and cultured in 6 ml LB-Ampicillin 37 °C, on a platform shaker, 2500 rpm for 16 h. Subsequent cultures were mini-prepped (QIAGEN miniprep columns) and the concentration determined on a DNA/RNA calculator (Pharmacia). Yields between 100 and 200 µg/ml were obtained. To check for the efficient introduction of each restriction enzyme site incorporated in the forward and reverse primers, 1µg of each mini-prepped clone was subjected to a *HindIII/Xho1* (1U each) double digest in a final volume of 20 µl at 37 °C, 2 h. Clone#4, one of the successfully digested clones (Figure 5.6 B) was selected and its full length ADAM-10 insert was sequenced using each of the forward and reverse sequencing primers in Figure 5.1.

**Figure 5.6:** Full length ADAM-10 PCR product from an ADAM-10 EST template and the restriction digest of this product once cloned into pGEMTeasy

A)

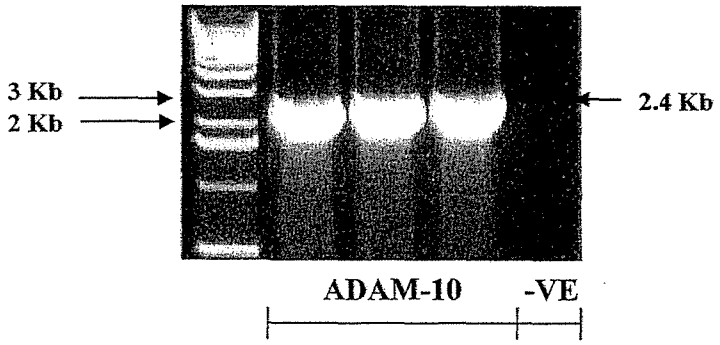


B)

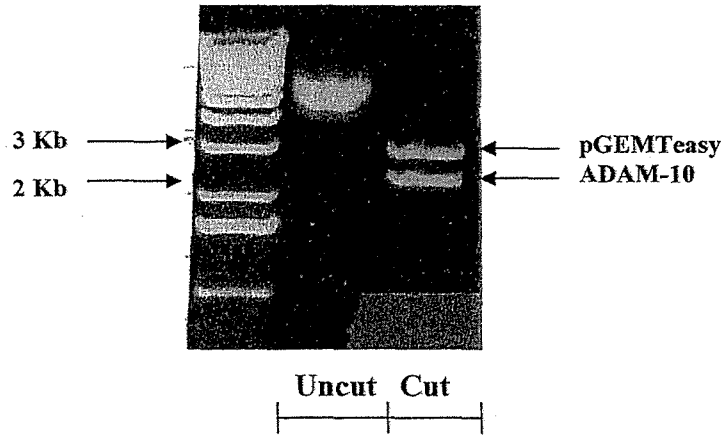


A) Full length ADAM-10 amplified from an ADAM-10 EST using the proofreading enzyme system EXPAND$^{tm}$ and B) *HindIII*/Xho1 double restriction enzyme digest of one pGEMTeasy clone#4 containing the ADAM-10 full-length insert. Bands at the expected size of linear pGEMTeasy (3 Kb) and full length ADAM-10 (2.4 Kb) were clearly seen, indicating the successful cloning of the full length ADAM-10 insert.

### *5.2.4 Sub-cloning of full length ADAM-10*

Full length sequencing data was analysed using Seqman (DNAStar Software). A single contig was constructed from each of the sequences generated by the forward and reverse sequencing primers (Figure 5.1) and aligned with the full-length ADAM-10 cDNA sequence imported from Genbank. A point mutation was found in the cloned ADAM-10 primary DNA sequence. Co-incidentally, the Met-Ala mutation occurred at a point in the primary amino acid sequence, which is crucial for a Met-turn (Val434-Met435-Tyr436) that aligns the substrate-binding pocket with the catalytic centre in all metalloproteases. Hence, this site was crucial for catalytic function (Gall et al. 2001). Attempts to sub-clone this insert into the mammalian expression vectors pcDNA3.1 and pMEP4 were made as it was anticipated that a one base mutation could be corrected by site directed mutagenesis. This clone also provided, by chance, a potentially non-functional mutant.

*Construction of an ADAM-10 DIG-labelled probe*

A DIG-labelled ADAM-10 probe was constructed using the ADAM-10 EST as a template with the sequencing primers A10Seq1F and A10Seq5R, by incorporating DIG-labelled UTP into the PCR reaction (annealing temperature 50 °C), extension time 1 min 30 sec with platinum Taq DNA polymerase. The DIG labelled probe was gel purified and quantitated by dot-blot alongside a known amount of DIG-labelled DNA. A concentration of 100 pg/µl was calculated. This probe was intended for use in a colony blot fashion for the colonies that grew as a result of the sub-cloning activities. Full length ADAM-10 was used as the positive control whilst the vector pcDNA3.1 was used as a negative control in each dot-blot.

*Sub-cloning of ADAM-10pGEMT#4*

Double digests (*HindIII/XhoI*) of A10pGEMTeasy#4 (Figure 5.6B), pcDNA3.1 and pMEP4 were performed as described above. The purified, digested products were column purified. Each vector was either treated with Calf Intestinal Phosphatase (CIP) (1U/50pmol

vector free ends for 2 h at 37 °C to remove free phosphates from the digested ends) or not. The CIP treated and non-treated vectors underwent a further column purification (QIAGEN) to remove any free CIP and/or restriction enzymes from the solution. A ligation schedule was set up using three different insert:vector ratios, 5:1, 3:1 and 1:1 ng DNA with T4 ligase at 4 °C for 16 h. JM109 *E.coli* cells were transformed as described above. The resultant colonies were screened both by PCR and by colony dot-blot analysis, positive colonies were picked, cultured overnight and subsequently mini-prepped, followed by double digestion with *HindIII*/Xho1 as described above and analysed by full length PCR. Each of these methods, plus further sequencing analysis, confirmed the vectors did not contain inserts, confirming that this cloning method was not suitable. Other competent *E.coli* cells used included Top10, in which no results were obtained and, previous DH5 α competent *E.coli* preparations (supplied courtesy of Dr. Dimitro Odorico) showed, when transformed with pGEMTeasy containing full-length ADAM-10, that this strain of *E.coli* cells inserted a transposon into the ADAM-10 insert.

*Sub-cloning of ADAM-10 full-length PCR product*

Several attempts were made to clone the full-length ADAM-10 PCR product not contained within a vector, 'directionally' into pcDNA3.1 and pMEP4. ADAM-10 was amplified from the EST using the ADAM-10*HindIII*F and ADAM-10*Xho*R full-length primers with the PCR protocol describe above (EXPAND$^{tm}$) followed by column purification. The concentrations of DNA obtained were between 2.7 - 11.3 μg/ml.

To test restriction enzyme efficiency, 1 μg of pcDNA3.1 was digested with 1U *HindIII* or Xho1 (there were enough base pair overhangs on either side of the restriction site of the full-length PCR product as recommended for these restriction digest enzymes) at 37 °C for 2 hours. The subsequent digest was run on a 1% agarose gel containing EtBr. Linear vector was visualised at the expected size in each case confirming the efficacy of each restriction digest. 1 μg of pcDNA3.1 or pMEP4 or ~400 ng of purified full length ADAM-10 was double digested with *HindIII* and *Xho1* overnight at 37 °C.

Each restriction digest was column purified (QIAGEN) and quantitated. Digested pcDNA3.1 and pMEP4 were treated with or without CIP 1U/50 pmol vector for 2 h at 37 °C to remove the free phosphates from the digested ends. Double digested/CIP treated or non-treated expression vectors were again column purified and quantitated. Three different ligation schedules were set up for each vector using 50 ng, 100 ng and 200 ng of vector with ratios of vector:insert 1:1 and 3:1 in each case. T4 ligase was used in an overnight ligation reaction at 4 °C. JM-109 *E.coli* were transformed by heat shock (43 °C, 50 sec) with the resultant overnight ligation reaction. The cells were suspended in 1 ml LB-broth and left to recover on a shaker at 37 °C for 2 h. Each transformed *E.coli* culture was plated out on LB-agar containing 1ug/ml ampicillin and cultured for 16 h at 37 °C.

Typically, ~30 colonies were screened by PCR using ADAM-10 nested primers. Clones that screened positive (Figure 5.7 A, for example) appeared to yield the correct PCR product size. Each of these colonies was picked and cultured for 16 h in 5 ml LB/Ampicillin broth at 37 °C on a shaker and subsequently mini-prepped (QIAGEN). 1 μg of the vector was double-digested and run on an agarose gel; only linear vector at the expected size of the empty vector could be seen (Figure 5.7 B). Other additional colonies were screened with different sets of ADAM-10 nested primers. Those that screened positive had the same process repeated, with the same negative result. Similar results were seen in each of the cases of pMEP4 and pcDNA3.1.

**Figure 5.7:** PCR screens of potential pcDNA3.1/ADAM-10 clones and their subsequent mini-prep digests

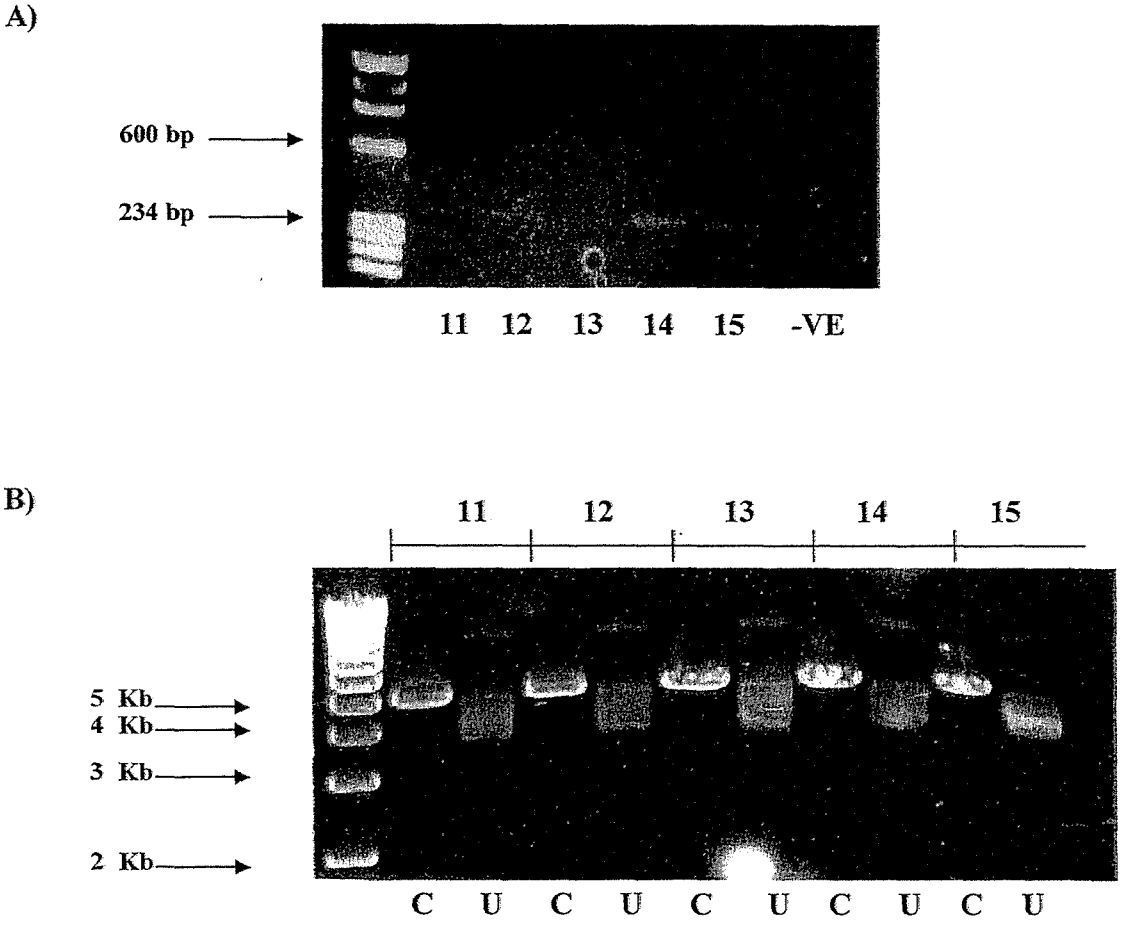


A) A representative PCR screen of colonies which were transformed with potential pcDNA3.1/A10 ligation products. Each colony which screened positive was miniprepped and underwent a subsequent *HindIII*/*Xho*1 double digest. Each potential clone was also sequenced. B) No ADAM-10 insert was present (C = Cut or digested with *HindIII* and *Xho*1, U= uncut or not digested). Similar results were obtained for the vector/ligation carried out with pMEP4/ADAM-10.

*Cloning with one restriction enzyme site*

Having established the directional cloning strategy to be sub-optimal either by sub-cloning or directly from amplified PCR product, an ADAM-10 full length PCR was carried out using the new proofreading enzyme *Pfx* (as a mutation was previously encountered with the use of the EXPAND system), primers ADAM-10*Hind*F (Figure 5.1) and a new ADAM-10*Hind*R (Figure 5.1) and the ADAM-10 EST as a template was carried out. The purified PCR product was A-tailed using *Taq* DNA polymerase (Roche) and ligated into pGEMTEasy. JM109 competent cells were transformed and taken through to the miniprep stage as described above. Full length sequencing of resultant clones in both the forward and reverse direction revealed no errors in the full-length transcript insert when analysed by the DNAStar software as described above.

The insert was digested from the pGEMTEasy vector with 1 U *HindIII*, alongside a *HindIII* digest of each of the expression vectors pcDNA3.1 and pMEP4. Each vector was CIP treated as described above, column purified and subsequently ligated with the ADAM-10 *HindIII* digested insert. Colonies that screened positive by PCR on LB-Ampicillin agar plates were picked and cultured. Subsequent minipreps were screened for the selection of clones with the ADAM-10 insert in the forward direction (the ADAM-10 5' Kozak sequence closest to the vector promoter) by restriction digest mapping. Four clones were chosen for further use in the laboratory: pcDNA3.1#6.2, pcDNA3.1#6.4, pMEP4 #4.1 and pMEP4 #4.2 (Figure 5.8). Each clone was fully sequenced to confirm the insert orientation and an error free primary DNA sequence.

**Figure 5.8:** *HindIII* digest of pcDNA3.1/A10 and pMEP4/A10

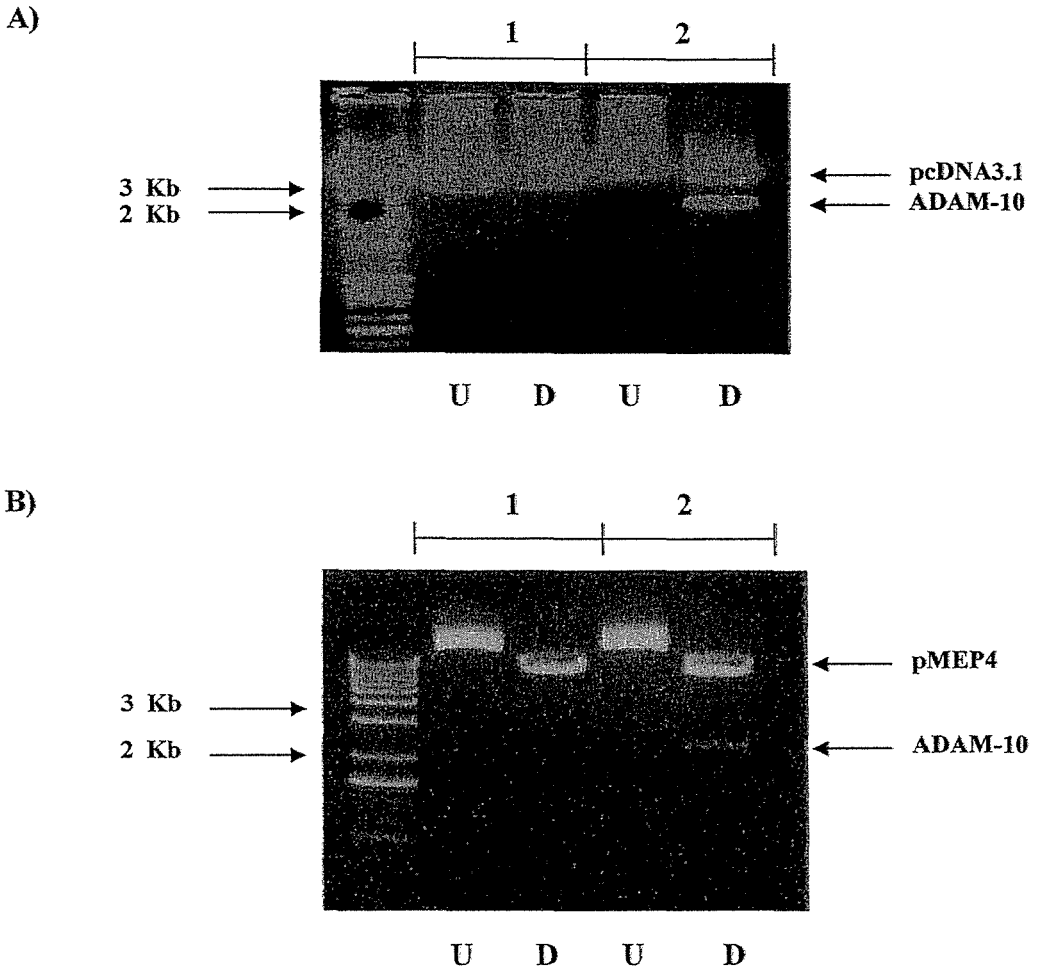


Representative restriction enzyme digest using *HindIII* for A1) pcDNA3.1 without ADAM-10 insert and A2) with ADAM-10 insert and B1) pMEP4 without ADAM-10 insert and with ADAM-10 insert (B2), D = Digested, U = Undigested. These vectors were used for subsequent transient transfection studies.

### *5.2.5 Transient transfection of prostate cell lines with pcDNA3.1 and pMEP4 mammalian expression vectors containing full length ADAM-10*

*Cell culture*

The prostate cell lines PC-3 and RWPE-1 were resuscitated from liquid $N_2$ and grown to 90 % confluency in a T75 standard tissue culture flask as described in Chapter 2. The PC-3 cells were harvested with trypsin/versine and counted on a haemocytometer using trypan blue as described in Chapter 2. 36 wells of 2 X 24 well plates were seeded with 100,000 cells/well in RPMI1640/10 % FBS and allowed to attach and grow to ~90 % confluency.

*Transient transfection*

Each of the vectors illustrated in Table 5.2 were transiently transfected into PC-3 cells using the following Vector: Lipofectamine ratios respectively: 0.9 µg:2 µl, 1 µg:3 µl and 1.2 µg:3.6 µl. These ratios were recommended by the manufacturer of the transfection reagent Lipofectamine 2000 (Invitrogen) and were shown previously, to give a greater than 60 % transfection efficiency for GFP expressing vectors in PC-3 cell cultures (courtesy of Dr. Dimitri Odorico). The following transfection protocol was used. Each vector was diluted in 50 µl Opti-MEM media (Life Technologies), mixed gently by pipette and allowed to incubate for 5 min at room temperature. Alongside this, Lipofectamine 2000, as per manufacturers recommendations, was also diluted into a separate tube (See amounts in Table 5.3) in a final volume of 50 µl Opti-MEM. Both 50 ul aliquots of Opti-MEM (one containing the vector, the other containing Lipofectamine 2000) were combined, mixed gently by pipette and allowed to incubate at room temperature for a further 20 min.

The PC-3 cells plated in the 24 well plates as described above, were washed twice with warm PBS just before the 100 µl aliquots containing both vector and lipofectamine were added to duplicate wells. The volume in each well was made up to 1 ml with antibiotic free RPMI-1640/10 % FBS.

**Table 5.2:** Transient transfection protocol for full-length ADAM-10 mammalian expression vector constructs

| Vector/Clone | Insert and Direction | µl Lipofectamine/ 0.9 µg vector | µl Lipofectamine/ 1 µg vector | µl Lipofectamine/ 1.2ug vector |
|---|---|---|---|---|
| *pMEP4 4.1* | ADAM-10 Forward | 2 | 3 | 3.6 |
| *pMEP4 4.2* | ADAM-10 Forward | 2 | 3 | 3.6 |
| *pcDNA3.1 6.1* | ADAM-10 Forward | 2 | 3 | 3.6 |
| *pcDNA3.1 6.2* | ADAM-10 Forward | 2 | 3 | 3.6 |
| *pMEP4* | No Insert Control | 2 | 3 | 3.6 |
| *pcDNA3.1* | No Insert Control | 2 | 3 | 3.6 |

The PC-3 cells were incubated for 18 h at 37 °C and the medium was aspirated, the cells were then washed twice with warm PBS. For the inducible vector, pMEP4 transients, RPMI-1640/10 % FBS containing 5 µM of the metallothionine promoter activator $CdCl_2$ (as per previous studies – Kazmi et al. 1996) was added (1 ml/well) whilst media without $CdCl_2$ was added to the pcDNA3.1 vectors. The cells underwent further 16 h incubation at 37 °C.

*Western blot analysis*

Each cell population was washed twice with warm PBS and harvested with 200 ul ice cold cell lysis buffer (50 mM Tris pH 7.5, 150 mM NaCl, 1% Triton X-100, 0.1 mM PMSF, 10 mM EDTA pH 8.0, 1 tablet Roche complete EDTA-free protease inhibitor cocktail/25 ml). The crude cell extract was quantitated using the BCA assay 'micro-well protocol' (Pierce). Equal amounts of protein for each vector containing ADAM-10 insert and its appropriate control (each vector without the ADAM-10 insert) were loaded onto a 10 % PAGE gel, followed by standard Western blot procedure (Chapter 2) using 0.5 µg/ml ADAM-10Met antibody. After the detection of ADAM-10 by X-ray autoradiography, using Femto (Pierce) chemiluminescence, the membrane was stripped as described in Chapter 2 and the levels of the housekeeping gene tubulin-β (0.2 µg/ml, Neomarkers) were detected to allow normalisation for any differences in protein loading. Figure 5.9 shows clearly, that little or

no increase in ADAM-10 protein levels could be seen in any of the cases tested by Western blot analysis.

It was then decided to 'scale up' our cell population number and test for transient transfection efficiency in RWPE-1 and PC-3 cells in T25 tissue culture flasks. Both cell lines were cultured to 90 % confluency, at which point transient transfection was carried out as described above. For pMEP4, differing incubation times with 5 μM $CdCl_2$ were also tested with 4 μg vector: 10 μl Lipofectamine-2000 ratio in the hope that we might optimise the induction of expression (Figure 5.10). Previous optimisation activities found that > 5 μM $CdCl_2$ induced cell death within 8 h. Further, differing amounts of each expression vector, were introduced in several transient transfection attempts in each prostate cell line (Figure 5.11). Again, it was previously determined the upper limit of DNA concentration that did not result in cell death 16 h post transfection in each of the cases of RWPE-1 (9000 ng) and PC-3 (5000 ng). 1000 ng lower than that determined to induce cell death was used. In no cases were significant increases in ADAM-10 protein levels seen.

**Figure 5.9:** Transient transfection of pcDNA3.1 and pMEP4 containing a full length ADAM-10 insert in PC-3 cells

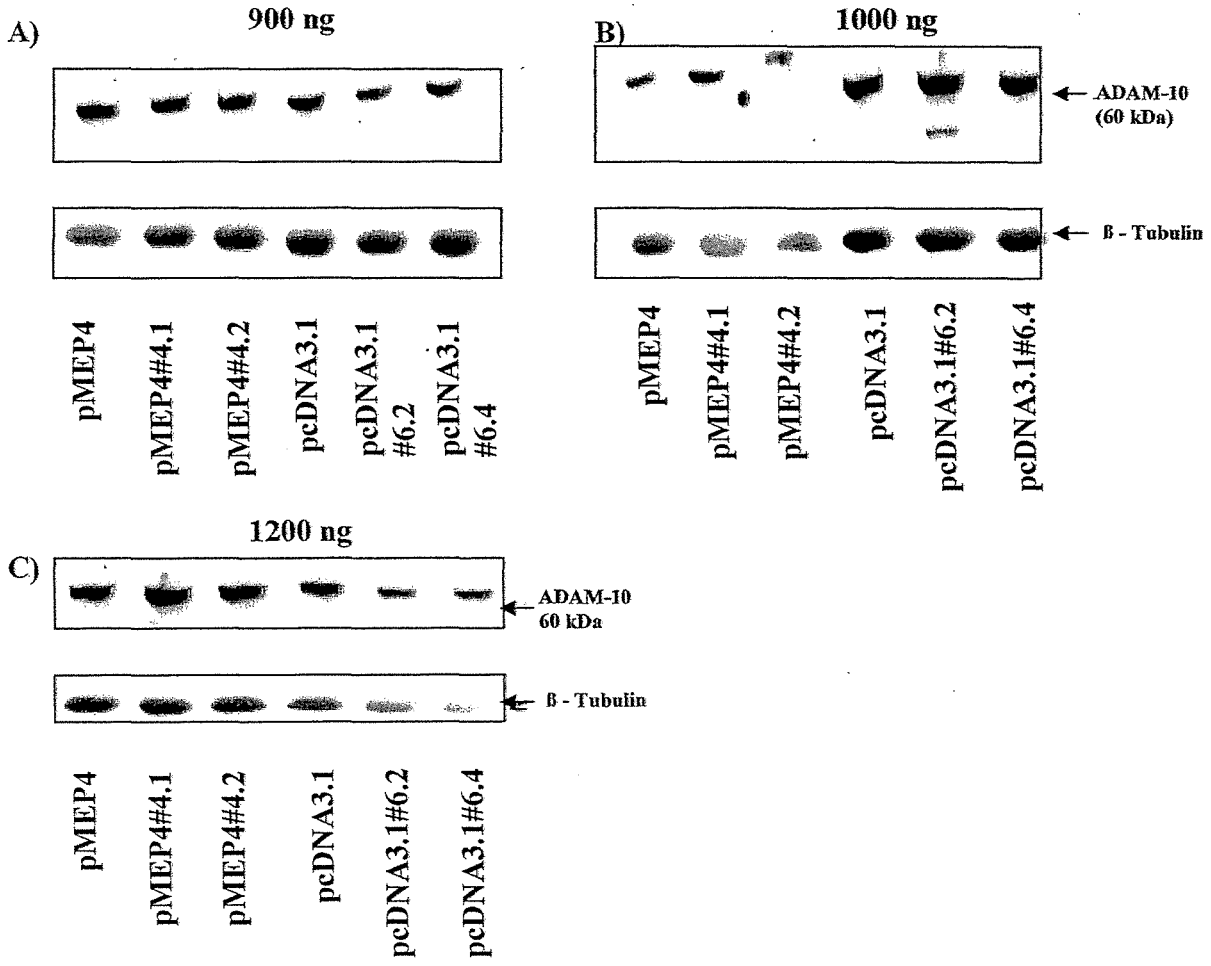


PC-3 cells were transiently transfected with the two separate full-length ADAM-10 clones of pcDNA3.1 or pMEP4 with increasing amounts of vector DNA: A) 900 ng, B) 1000 ng and C) 1200 ng. pcDNA3.1 transients were harvested 34 h post transfection, whilst for pMEP4 clones: 18 h post transfection, 5 μM $CdCl_2$ was added and cells were incubated for a further 16 h prior to harvesting. No significant increase in ADAM-10 expression could be seen in any of the transfection conditions tested when compared to levels of the housekeeping gene β-Tubulin. Negative controls included transfection of PC-3 cells with the respective vectors, which do not contain the ADAM-10 insert. These particular blots only revealed signal for mature ADAM-10, possibly due to the lower levels of protein having to be loaded onto the PAGE gel (2 – 3 μg), a result of a low protein yield, due to a small population of cells from one well, in a 24-well plate.

**Figure 5.10:** Transient transfection of pMEP4 containing a full length ADAM-10 insert in PC-3 cells

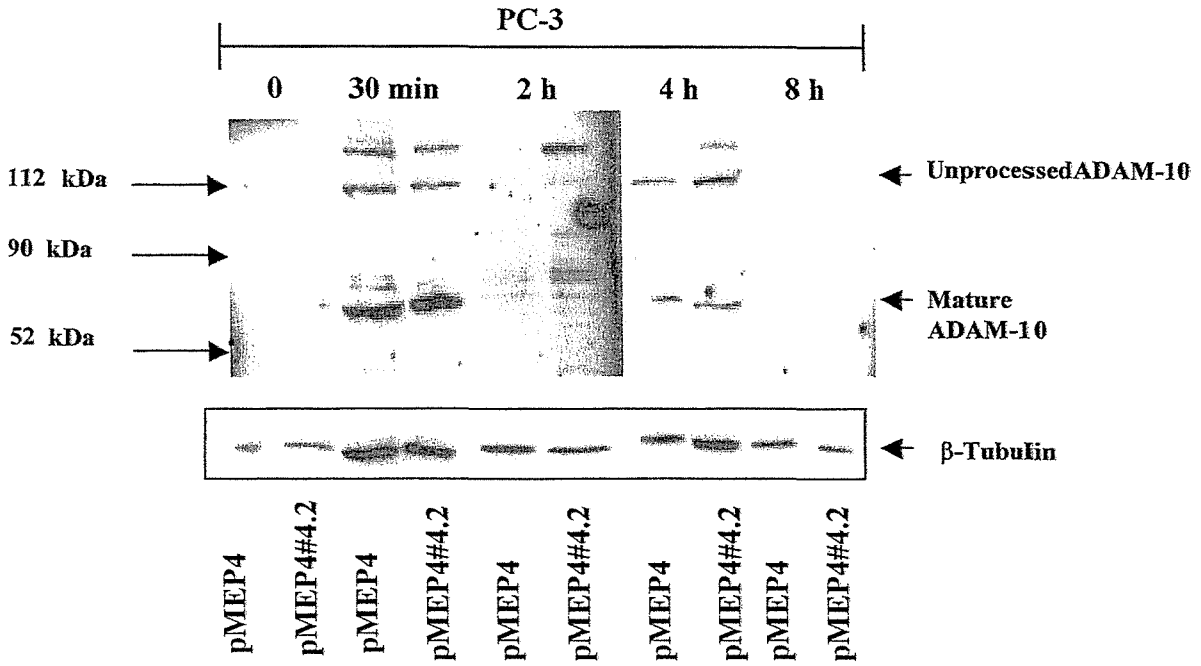


PC-3 cells were transiently transfected with 4000 ng of pMEP4/ADAM-10#4.2 clones. 18 h post transfection 5 μM $CdCl_2$ was added and cells were incubated for each of the times outlined above, prior to harvesting. No significant increase in ADAM-10 expression could be seen in any of the transfection conditions tested when compared to the levels of the housekeeping gene β-Tubulin. Negative controls included the transfection of PC-3 cells with the same amount of pMEP4 empty vector, which did not contain the ADAM-10 insert. Each time point was determined in anticipation that functional cell assays would be performed within or close to this range of times.

**Figure 5.11:** Transient transfection of pcDNA3.1 containing a full length ADAM-10 insert in RWPE-1 and PC-3 cells

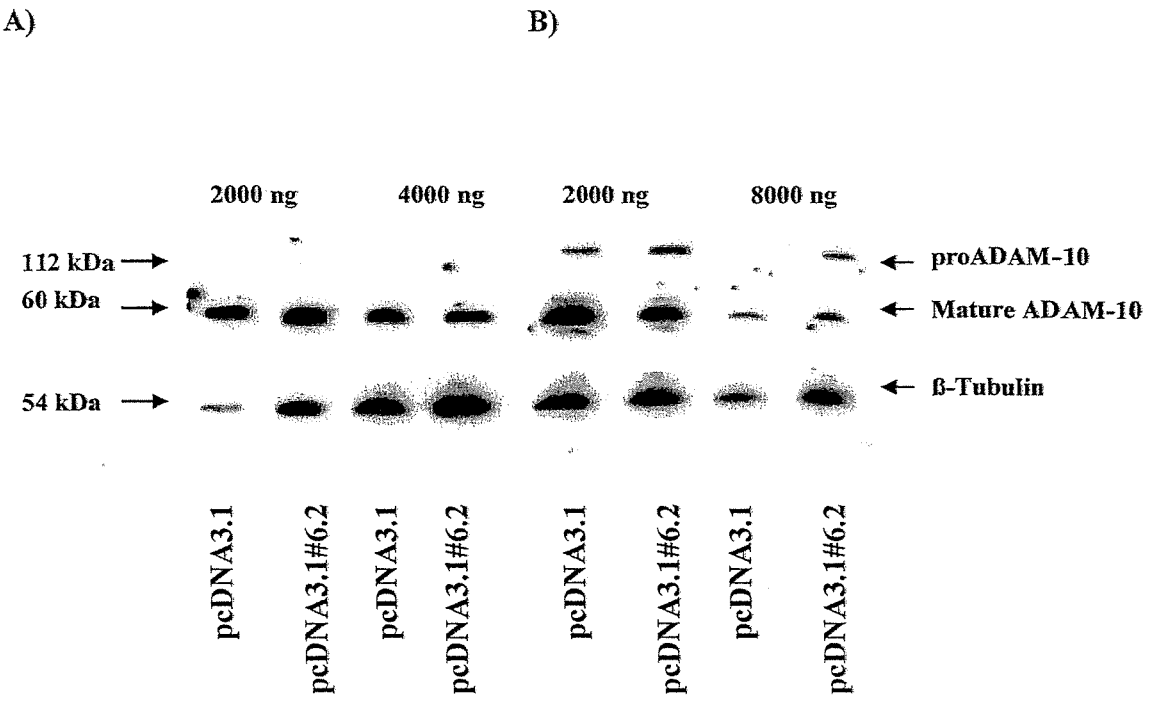


RWPE-1 or PC-3 cells were transiently transfected with A) 2000 ng or 4000 ng pcDNA3.1#6.2 for PC-3, or B) 2000 ng or 8000 ng pcDNA3.1#6.2 for RWPE-1. Cells were harvested 40 h. post transfection. No significant increase in ADAM-10 expression could be seen in any of the transfection conditions tested when compared to the levels of the housekeeping gene β-Tubulin. Negative controls included the transfection of both RWPE-1 and PC-3 cells with the same amount of pcDNA3.1 empty vector, which did not contain the ADAM-10 insert.

*5.3 **Discussion***

At the commencement of this part of the thesis, such a tool as an ADAM-10 mammalian expression construct containing human ADAM-10 was unavailable despite exhaustive efforts including personal communication with international laboratories that study ADAM-10. It was decided to attempt to clone full-length human ADAM-10 (hADAM-10) cDNA by PCR amplification and insertion into each of the mammalian expression vectors pcDNA3.1 and pMEP4. The pcDNA3.1 mammalian expression vector contains a CMV viral promoter element upstream of the Kozak sequence and the translation start site included in the full-length hADAM-10 insert for potential efficient transcription. The pMEP4 mammalian expression vector is an inducible vector that has a metallothionine promoter element upstream of the hADAM-10 Kozak sequence. Its activity is induced by the introduction of $CdCl_2$ into the cell system (Kazmi et al. 1996).

Initially, obtaining full-length hADAM-10 by PCR from cDNA of several PCa cell lines proved unrewarding. The presence of an EST, which contained the full-length sequence, provided a more suitable template. However, the directional cloning strategy of the full-length hADAM-10 PCR product, or the sub-cloning of this product directionally, from the intermediate vector pGEMTeasy, was not successful. Therefore, a new strategy using a single restriction enzyme site, where an error free insert could be ligated in either the forward or the reverse direction, was used. This method led to successful sub-cloning from pGEMTeasy into each of the vectors pcDNA3.1 and pMEP4. Subsequently, forward direction clones were screened and selected by restriction digest mapping and confirmed by sequencing.

Once full-length clones were established, the efficiency of the vector/ADAM-10 clones to induce levels of hADAM-10 in a transient transfection system was tested. By Western blot analysis in the prostate cell line PC-3, neither the pcDNA3.1 clone, nor the inducible pMEP4 clone, led to enhanced hADAM-10 protein production. A similar result was obtained in the non-tumorigenic prostate cell line RWPE-1. A separate study in this laboratory has cloned the same full-length transcript in-frame in a Green Fluorescent

Protein (GFP) expression vector. Like the results presented in this study, the GFP clone did not fluoresce, as one would have expected, in a transient transfection system in the PCa cell lines LNCaP and PC-3 (data not shown).

Given that in three different vectors the same lack of expression was shown, it was hypothesised that the natural Kozak sequence, which is encompassed by the forward primer binding sites chosen in this study, may not be strong enough to promote any significant translation. We chose to use the natural Kozak sequence as the bases known to be crucial within a Kozak sequence for strong promotion of translation (A at -3, and G at +4) (Kozak, 1997) were indeed conserved in human ADAM-10, suggesting this to be a 'strong' Kozak sequence.

A study recently published (Anders et al. 2001) cloned full length bovine ADAM-10 (MADM) into pcDNA-HA, a vector which post-dates pcDNA3.1, with a Hemagglutinin (HA) tag, and selected stably transfected HEK293 cells. This study demonstrated the expression of ADAM-10-HA by affinity chromatography using an anti-HA antibody and further demonstrated an increase in β-APP processing in this cell system by measuring the levels of secreted β-APP. As seen in Table 5.3 (below) the Kozak sequence for MADM varies slightly from that of hADAM-10. This may be functionally relevant and may, in part, explain the inability of our mammalian expression constructs to stimulate ADAM-10 expression in prostate cell lines. Interestingly, this study only showed over-expression by using the HA-tag antibody in Western immunoblots and no indication of a fold increase of overall (endogenous plus HA-tagged ) ADAM-10 production within the cell system was presented. In our cell system, translation of ADAM-10 from our vector templates may well have taken place. However, a tagged vector was not used, so the introduced ADAM-10 protein could not be distinguished from endogenous ADAM-10 protein, as it was in the above study using MADM.

Another recent study (Yan et al. 2002) showed, by transfection, that ADAM-10 but not ADAM-9 or -17 was able to mediate the transactivation of the EGFR. This study used an expression construct with full-length mouse ADAM-10, which as illustrated below (Table

5.3) has a Kozak sequence almost identical to MADM. Yet another group showed that the introduction of ADAM-9 and -10 expression vectors to a keratinocyte cell line, lead to the enhanced cleavage of Collagen XVII (Franzke et al. 2002). In Franzke's study, human ADAM-9 was used, but in the case of ADAM-10, the bovine orthologue MADM was again used for these purposes.

**Table 5.3** ADAM-10 orthologue Kozak sequences

| | | | | | | | | | | | |
|---|---|---|---|---|---|---|---|---|---|---|---|
| Consensus Kozak | C | C | *A* | C | C | *A* | *U* | *G* | *G* | *G* | Kozak, 1984 |
| hADAM-10 Kozak | G | A | *A* | A | G | *A* | *U* | *G* | *G* | *G* | Genbank Accession # NM_001110 |
| MADM Kozak | G | G | *A* | A | G | *A* | *U* | *G* | *G* | *G* | Genbank Accession # NM_174496 |
| Mouse ADAM-10 | G | G | *A* | A | G | *A* | *U* | *G* | *G* | T | Genbank Accession # NM_007399 |

Table 5.3 illustrates the differences in the Kozak sequence of human ADAM-10 (hADAM-10), bovine ADAM-10 (MADM), mouse ADAM-10 and the consensus Kozak sequence (Kozak, 1984).

Given that studies such as these have chosen to use MADM or mouse ADAM-10 rather than human ADAM-10, to generate functional data in human cell lines, it is likely that these and other groups may have also experienced the same technical difficulties, with respect to the generation of functional hADAM-10 mammalian expression vectors. Because the transient transfections were unsuccessful in stimulating ADAM-10 production it was decided, due to time constraints, not to pursue this part of the study further at this time, since the next stages anticipated were to 1) to make stably transfected over-expressing ADAM-10 prostate cell lines and 2) to perform functional assays including cell migration, attachment and invasion on both transiently transfected and stably transfected prostate and PCa cell lines.

To progress this study, which is intrinsically important, firstly, a strategy whereby primers are designed against a small 5' untranslated sequence of each pcDNA3.1 or pMEP4 vector sequence, between the promoter region and the ADAM-10 gene, followed by PCR analysis should be carried out. This approach, which was not carried out in this study, might confirm the expression or otherwise of exogenously produced ADAM-10. Failing this, a

new Kozak sequence should be introduced, which exactly matches the consensus Kozak sequence CCACCaugG (Kozak, 1984) or that of MADM and mouse ADAM-10 primary DNA Kozak sequence (Table 5.3). Recently developed mammalian expression systems, with detectable tags, as well as the existing two used (pcDNA3.1 and pMEP4) in this particular study would be used. Additionally, the use of a cell line that does not express ADAM-10 would also be advantageous in distinguishing exogenously expressed protein. Although no such cell line was available in this study, such a cell line could easily be derived from an ADAM-10 knockout mouse, for example. No full-length human ADAM-10 mammalian expression vector, to date, to our knowledge, is available for this kind of research. With the added knowledge this study has provided, key areas have been identified, which require attention when attempting to establish such a hADAM-10 over-expressing system.

# CHAPTER SIX:

## 6.0 THE REGULATION OF ADAM-9 AND -10 mRNA AND PROTEIN EXPRESSION BY THE PROSTATE GROWTH PROMOTERS DHT, IGF-1 AND EGF IN THE LNCaP PROSTATE CANCER CELL LINE

## *6.1 Introduction*

As reviewed in Chapter 1 prostate cancer (PCa) occurs in two distinct stages, 'early' and 'late'. In the early stages, cell growth and proliferation is sensitive to androgen stimulation (Lee, 1996). IGF-1 and EGF are thought to help maintain cell survival and growth during this early stage of PCa development (Lee, 1996). As the cancer progresses into a more aggressive, metastatic phenotype (late stage), cell proliferation becomes insensitive to androgens. IGF-1 and EGF and other growth factors/cytokines, such as IL-6 are thought to act in an autocrine and paracrine manner to maintain the cancer cells survival and progression (Russell et al. 1998).

Normal prostate and PCa cell models are widely used to characterise the growth factor responsiveness and expression profile of candidate genes, which are potential contributors to PCa progression. The LNCaP cell line, previously used in our earlier expression studies (McCulloch et al. 2000), is a particularly good model as its proliferation can be stimulated by androgens such as DHT, synthetic androgens, for example, R1881, and other growth factors, including IGF-1 and EGF (Iwamura et al. 1993; Culig et al. 1994; Russell et al. 1998), enabling the effective assessment of the growth factor responsiveness of ADAM protein levels.

The extensive ADAM expression profiling outlined in Chapters 3 and 4 showed the presence and localisation of both ADAM-9 and -10 throughout the stages of PCa development. Additionally, preliminary data suggested that the LNCaP cell line, like the RWPE-1 and PC-3 cell lines used in Chapter 3, expressed both ADAM-9 and -10 in the nuclear compartment. Given the readily detectable levels of ADAM-9 and -10 in cell models of normal, androgen-dependent and androgen-independent PCa, and in primary and secondary/metastatic tumours, and the previous observation that ADAM-9, -10 and -17 mRNA levels are regulated by DHT (McCulloch et al. 2000), it is reasonable to hypothesise that the expression of ADAM-9 and -10 mRNA and protein may be regulated by a cohort of other hormones, growth factors and cytokines which stimulate PCa cell growth,

proliferation, invasion and migration. This provides a rational basis for the further characterisation of the growth factor and hormonal regulation of these particular ADAMs.

The three pertinent and extensively studied hormone/growth factors DHT, IGF-1 and EGF were chosen for this study. This set of hormone/growth factors are already implicated in the regulation of PCa cancer development and the induction of specific enzyme expression in the prostate, including the well characterised serine protease Prostate Specific Antigen (PSA) and the Matrix Metalloproteases (MMPs), in particular MMP-7 and -2 (Montgomery et al. 1992; Sundareshan et al. 1999; Liao, 2003).

Thus, the **aims** of this chapter were:

1) To assess the responsiveness of ADAM-9 and -10 mRNA levels to DHT, IGF-1, DHT plus IGF-1 and EGF alone in LNCaP cells.
2) To assess the responsiveness of ADAM-9 and -10 proteins levels in the whole cell lysate of LNCaP cells by DHT, IGF-1, DHT plus IGF-1 and EGF alone.
3) To assess the responsiveness of ADAM-9 and -10 protein levels in the nucleus of LNCaP cells to EGF.

This chapter builds on work previously published from this laboratory (McCulloch et al., 2000), which found ADAM-9 and -10 mRNA to be significantly up regulated by varying levels of DHT in the LNCaP PCa cell model. It is important to examine whether the levels of these potentially active proteases fluctuate in response to hormone/growth factor regulation in order to understand the roles the ADAMs may have throughout the progressive stages of PCa.

## 6.2 *Materials and Methods*

### *6.2.1 Cell culture*

*For characterisation of ADAM-9 and -10 mRNA and protein expression*

The PCa cell line LNCaP was obtained from ATCC (Rockville, MD) and cultured in standard T75 culture flasks to ~60-70 % confluency, as described in Chapter 2. The cells were transferred into serum-free (SF) RPMI-1640/ 0.01% Bovine Serum Albumin (BSA)/50 U/ml Penicillin/50 µg/ml Streptomycin sulphate for 24 h. Test medium was then added to the cells after a warm wash (37 °C) with Phosphate Buffered Saline (PBS) (tissue culture grade; Oxoid, West Heidelberg, Australia). To test for androgen regulation 5α-dihydrotestosterone (DHT) (Sigma, St Louis, MO) was added at concentrations of 0 (control), 0.1, 1.0 or 10 nM. For IGF-1 regulation, human recombinant IGF-1 (Gropep, Adelaide, Australia) was added at concentrations of 0 (control), 10 or 50 ng/ml in the presence or absence of 10 nM DHT in SF-RPMI-1640/Phenol Red (PR) free/0.01% BSA/ Penicillin/Streptomycin. A maximal dose of 10 nM DHT was chosen based on previous ADAM-9 and -10 mRNA regulation data (McCulloch et al. 2000) so that any additional regulatory effects could be attributed to IGF-1 acting in synergy with DHT. For EGF regulation, human recombinant EGF (Gropep) was added at concentrations of 0 (control) or 50 ng/ml. In a preliminary experiment, ADAM-10's responsiveness to EGF was tested at concentrations of 5, 10, 50 and 100 ng/ml (data not shown), 50 ng/ml was found to have the maximal stimulatory effect with ADAM-10 protein levels declining at 100 ng/ml. Hence, 50 ng/ml EGF was chosen for subsequent mRNA and protein regulation experiments. The cells were cultured for a further 48 h under test conditions, with a change of medium to replenish the appropriate growth factors after 24 h. Cells were harvested with ice-cold PBS and a cell scraper, pelleted by centrifugation at 175g (1000 rpm, CS-6R Centrifuge, Beckman) for 3 min and stored at -80 °C until further processing.

*Cell proliferation assay using the MTT dye method*

A 90% confluent cell culture of LNCaP was trypsin/versine treated and seeded into a 96-well tissue culture plate (Medos) at a pre-determined optimal density of 10 000 cells/well (as determined on a haemocytometer - Chapter 2) in 200 µl RPMI-1640/10% HI-FBS/PR free/Penicillin/Streptomycin medium. Cells were allowed to attach for 24 h, washed with 200 µl warm PBS (37 °C) and serum starved for 24 h in SF-RPMI-1640/PR-free/0.01% BSA/Penicillin/Streptomycin medium. Test medium containing DHT concentrations of 0 (control) 1.0 and 10 nM +/- 10 or 50 ng/ml IGF-1 or EGF 0 (control) 5, 10 and 50 ng/ml was added and replaced every 24 h for a period of 96 h. A total of 16 wells per concentration were used. Each replacement of medium included a warm wash with 200 µl PBS. The MTT dye method was carried out as previously described (McCulloch et al. 2000). Briefly, a standard curve was constructed by seeding doubling increases in LNCaP cell number into a 96-well tissue culture plate (Medos) in PR-free/10% HI-FBS/ RPMI-1640. The cells were allowed to plate down for 6 h followed by treatment with MTT. Absorbance was plotted against cell number to ensure linearity of the MTT assay across the range of cell numbers used (4000 - 40,000 cells). The absorbances obtained at the completion of the proliferation assays were extrapolated to cell number using this standard curve. Statistical analysis was carried out by one-way ANOVA, followed by a Tukey Post-Hoc analysis to determine significance between all treatments and respective controls.

### *6.2.2 Quantitative RT-PCR analysis*

*Primer design*

Full-length sequences for both ADAM-9 and -10 were downloaded from the Genbank database, accession numbers NM_003807 and NM_001110, respectively, and saved as a text (.txt) file. Each sequence was individually imported into the software application Primer Express (PE Biosystems). The parameters for primer design were set according to the manufacturer's default setting recommendations. Primer Express automatically generated primers deemed suitable for downstream real-time PCR application. More optimal primers, as determined again by Primer Express software using a 'penalty score'

system, were individually analysed for primer-dimer and hairpin formation. Primers with little or no secondary structure or complementary binding were chosen (Table 6.1) and subsequently purchased from Proligo (Southern Cross University, Australia). PSA primers (Table 6.1) were designed in a similar fashion by Dr. Jin Gao and the 18s housekeeping gene primer set (Table 6.1) was already in routine use in this laboratory.

**Table 6.1** Primer sets for Quantitative PCR

| **Primer** | **Sequence** | **PCR Product Size (bp)** |
|---|---|---|
| ADAM-9Fprexp (Forward) | 5'-GGACCAATGGAAACCTGATCAA-3 | 106 |
| ADAM-9Rprexp (Reverse) | 5'-ACTGTCATGTCTCCGACGTGTG-3' | |
| ADAM-10Fprexp (Forward) | 5'-TCCACAGCCCATTCAGCAA-3' | 105 |
| ADAM-10Rprexp (Reverse) | 5'-AGGCACTAGGAAGAACCAA-3' | |
| PSA-F | 5'-AGTGCGAGAAGCATTCCCAAC-3' | 140 |
| PSA-R | 5'-GACCCAGCAAGATCACGCTTT-3' | |
| 18s rRNA (Forward) | 5'-TTCGGAACTGAGGCCATGAT-3' | 151 |
| 18s rRNA (Reverse) | 5'CGAACCTCCGACTTTCGTTCC-3' | |

**Table 6.1** shows the primers used and their expected PCR product size, for Quantitative PCR analysis, designed on the Primer Express software (PE Biosystems).

*RT*

5 µg of RNA extracted from control and growth factor treated LNCaP cells from three independent experiments were reverse transcribed as described in Chapter 2. All cDNAs were screened for gDNA contamination with β-actin primers, which span an intron (Chapter 2), and found to be free of gDNA contamination.

*Quantitative PCR*

PCR was carried out on a PE Biosystems 7000 ABI Prism using the following thermocycling protocol; 95 °C 10 min, 40 cycles of 95 °C 30 sec and 60 °C 1 min with the

fluorescence emitted from the SYBR green being read by the instrument after each thermocycle. The following reaction conditions were used; 2X SYBR Green master mix (PE Biosystems), 50 nM each ADAM-9, ADAM-10, PSA or 18s (housekeeping gene) forward and reverse primer (Table 6.1), 1 µl of cDNA template in a final reaction volume of 20 µl. Each growth factor treatment was run in triplicate for either ADAM-9, -10 or PSA. 18s was also quantitated in the same PCR in triplicate for each growth factor treatment in a 96-well PCR plate format.

*Quantitation of ADAM-9 and -10 mRNA transcript*

Each primer set was validated for quantitation using the 'ct - value' direct comparison method, as per the manufacturer's recommendations. Briefly, cDNA from LNCaP cells was serially diluted and underwent a PCR under the same conditions described above. The ct value was graphed against cDNA concentration and an $R^2$ value of >0.97 was obtained, showing that these primer sets could effectively detect relative changes of target message (ADAM-9, -10, PSA or 18s), in a linear fashion, in the cDNA from the cell line to be used for subsequent mRNA level quantitation.

The ABI-Prism 7000 measures the changes in fluorescence emitted, in this case, from the SYBR green dye bound to the dsDNA PCR product after each PCR cycle. Data are expressed as a cycle threshold (ct) value where the increase in fluorescence above a set background is first detected. The lower the ct-value, the higher the amount of the transcript of interest is present in the starting cDNA sample. The difference in ct-values between the control and each test condition is indicative of the relative changes in mRNA transcript, as a result of the test condition, in this case, hormone/growth-factor treatment. Variations in the amount of mRNA added to the initial RT reaction were corrected by measuring the ct-values for the 18s rRNA housekeeping gene in the same cDNA sample, in the same PCR. Changes in ct-values between the control group and the test group indicate, with the appropriate statistical validation, whether the levels of the transcript of interest are significantly elevated or decreased.

### *6.2.3 Western Blot Analysis*

*Protein extraction – whole cell lysate*

Cell pellets of control or growth factor treated LNCaP cells were resuspended in 500 µl of lysis buffer, processed and quantitated using the BCA protein assay reagent as described in Chapter 2.

*Protein extraction – nuclear fractionation*

Cellular compartmentalisation from control or EGF treated LNCaP cells was achieved by using the NePer nuclear/cytoplasmic fractionation kit (Pierce) as per manufacturer's recommendations, as described in Chapter 2.

*Western blot*

5 µg of protein from each growth factor treated cell pellet was suspended in a reducing loading buffer and boiled for 3 min prior to loading onto a 10 % SDS-PAGE gel, followed by a standard Western blotting procedure (Chapter 2). For ADAM-9Dis and ADAM-10Cterm antibodies, 0.2 µg/ml was used. For the housekeeping gene antibodies, β-Tubulin and PCNA, 0.2 µg/ml were also used.

*Quantitation of signal intensity*

For the housekeeping genes tubulin-β and PCNA, autoradiographic detections were subjected to over- and under-exposures to determine that the signal detected on the X-ray film was in the linear range, and able to be used effectively for accurate densitometric analysis. Densitometric analysis was carried out using a GS-690 image densitometer (Biorad). Signal intensity obtained for ADAM-9 and -10 expression was normalised for the signal obtained for β-tubulin or PCNA for the same sample on the same Western blot. All Western blots were performed on protein samples collected from three separate treated

cell preparations giving an experimental value for each set of treatments of n=3. Western blots for each set of treatments were performed at least in duplicate, unless otherwise indicated, giving possible n values of at least 6 and subsequent densitometric analysis was performed for each control and test concentration in triplicate. Absolute ratios of intensity between control and test concentrations were calculated and the entire data set was subjected to a one-way ANOVA, followed by a Tukey Post-Hoc analysis, or in the cases where just two sets of data were analysed, a Student's T-test, to determine significance between treatments and their respective controls.

## *6.3 Results*

### *6.3.1 LNCaP cell proliferation*

As a proliferative control to test for biological responsiveness of the LNCaP PCa cell model to each of the growth factors used, an MTT cell proliferation assay was performed. As expected, and as shown in Figure 6.1, LNCaP cell proliferation was significantly increased following the addition of DHT (19 % increase), with a further increase in proliferation with the addition of IGF-1 (additional 24 %). IGF-1 alone (in the absence of DHT) had only a minor effect on cell proliferation. For EGF treated cells (Figure 6.2), a significant linear increase in cell proliferation was observed, with a 4-fold increase at the highest concentration tested (50 ng/ml). These findings parallel the same proliferative response found by Iwamura et al. (1993) and Guo et al. (2000) demonstrating the expected biological response to DHT, IGF-1 and EGF in the LNCaP PCa cell model in our hands.

### *6.3.2 Response of PSA mRNA expression to DHT treatment of LNCaP cells*

Quantitative PCR for PSA using SYBR Green assays described above was performed on cDNA reverse transcribed from total RNA extracted from LNCaP cells treated with 10nM DHT. Large, significant, relative changes in PSA transcript levels were shown (Figure 6.3) indicating that the expected response, that is, DHT upregulating PSA, was effectively detected, and further validating the real-time PCR method of quantitation.

**Figure 6.1:** LNCaP cell proliferation in response to DHT and IGF-1

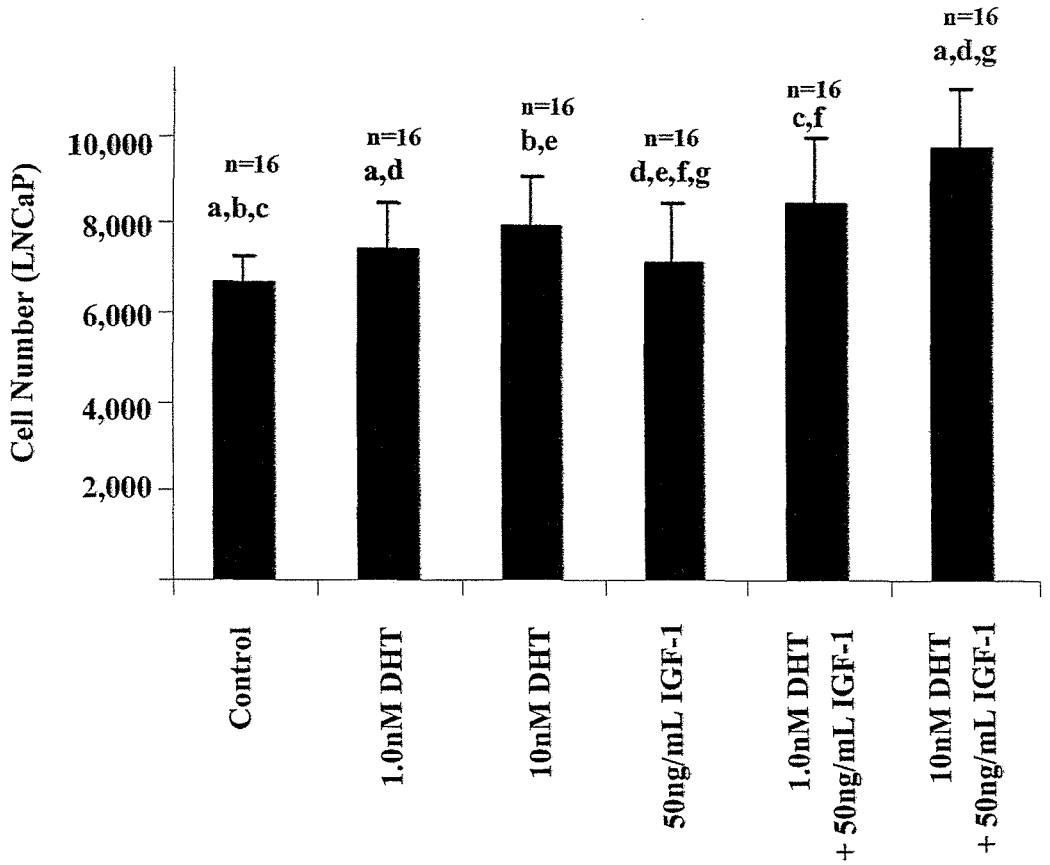


Effects of DHT in the presence or absence of IGF-1 on LNCaP cell proliferation were carried out in 96 well plates, seeding 10,000 cells/well. LNCaP cells were serum starved for 24 h and treated with DHT +/- IGF-1 for a further 96 h. The MTT dye method was used to determine change in cell number. Data shown are derived from a single experiment with each condition replicated in 16 wells on a 96 well plate. Similar results were observed in two subsequent cell proliferation assays. The same letters above each histogram represent statistical significance: $^{b,e}P < 0.05$, $^{a,c,d,f,g}P < 0.01$.

**Figure 6.2:** LNCaP cell proliferation in response to EGF

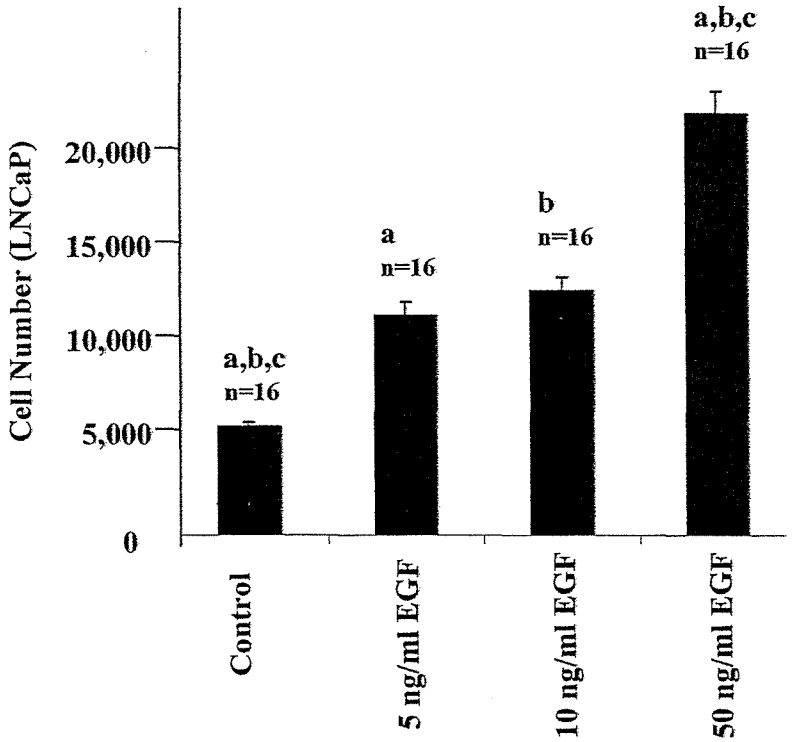


Effect of EGF on LNCaP cell proliferation was carried out in 96 well plates, seeding 10, 000 cells/well. LNCaP cells were serum starved for 24 h and treated with EGF for a further 96 h. The MTT dye method was used to determine change in cell number. Data shown are derived from a single experiment with each condition replicated in 16 wells on a 96 well plate. Similar results were observed in two subsequent cell proliferation assays. The same letters above each histogram represent statistical significance: $^{a,b,c}P < 0.01$.

**Figure 6.3:** The regulation of PSA mRNA by DHT in LNCaP cells

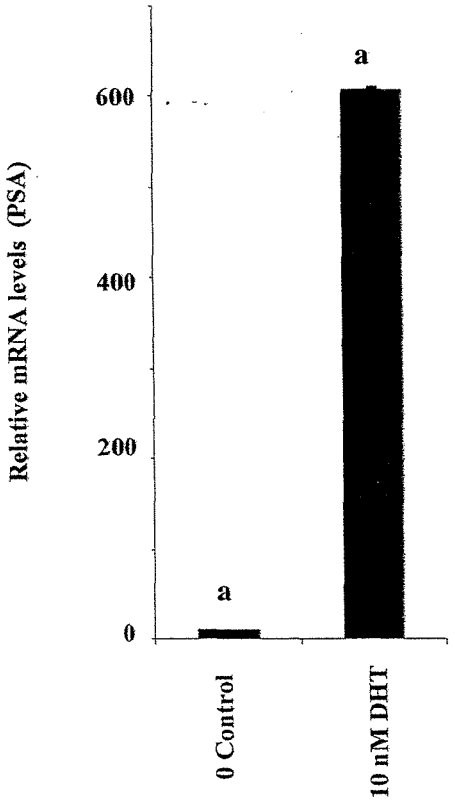


For the mRNA regulation of PSA by DHT, LNCaP cells were treated with 0 (control) or 10 nM DHT and cultured for 48 h. Levels of PSA transcript were determined by quantitative PCR and normalised against 18s rRNA levels. Histograms represent the mean +/- SEM from three independent experiments (n=3) with each treatment sample being quantitated in triplicate in each of two separate PCR reactions. The same letters above each histogram represent statistical significance: $^{a}P<0.01$.

### *6.3.3 Regulation of ADAM-9 mRNA and protein expression in LNCaP cells by DHT, IGF-1, IGF-1 plus DHT and EGF*

*mRNA regulation*

Quantitative PCR using SYBR Green assays described above was performed on cDNA reverse transcribed from total RNA extracted from LNCaP cells treated with IGF-1, DHT, IGF-1 plus DHT or EGF alone. Neither DHT nor IGF-1 regulated ADAM-9 mRNA levels in LNCaP cells (Figure 6.4). However, IGF-1 (50 ng/ml) in the presence of 10 nM DHT significantly up-regulated ADAM-9 mRNA transcript when compared to the 10 nM DHT treatment in the same experiment (Figure 6.4). For EGF regulation, a significant stimulation was also shown in response to 50 ng/ml treatment (Figure 6.5).

*Whole cell lysate protein regulation*

Figure 6.6 shows representative Western blots performed on three separate experiments of whole cell protein extracted from LNCaP cells treated with DHT, IGF-1, or IGF-1 plus DHT. Densitometric analysis, using β-tubulin as a "housekeeping" marker, was used to correct for uneven protein loading between the control and test lanes in each experiment. As shown in the histogram below the Western blots, neither DHT nor IGF-1 alone, regulated levels of the 84 kDa proform form of ADAM-9 protein. However, like the mRNA response, DHT plus IGF-1 significantly increased the proform of 84 kDa ADAM-9 protein levels, ~2-fold. EGF (50 ng/ml), again like the mRNA response, significantly stimulated the expression of unprocessed 84 kDa proform (~1.8 - fold) of ADAM-9 (Figure 6.7). The processed, active ~60 kDa form was not uniformly seen throughout any of the Western blots in these sets of experiments, therefore no analysis of this form of ADAM-9 could be carried out.

*Nuclear protein regulation in LNCaP cells by EGF*

To investigate the effect of EGF on the accumulation of ADAM-9 in the nucleus of LNCaP cells, an experiment whereby LNCaP cells were treated with EGF for 48 h, followed by subcellular fractionation (described in Chapter 2) was performed. EGF alone did not

significantly alter nuclear ADAM-9 unprocessed, 84 kDa protein levels (Figure 6.8), However, a significant but modest up regulation was observed for the presumably processed, active 60 kDa form (~1.5-fold), which unlike LNCaP whole cell lysate preparations, was readily detectable in these particular nuclear preparations. The proliferating cell nuclear antigen (PCNA) was used as a normalisation control in this case as no significant increase in its expression was observed in the growth factor treatment when compared with the no treatment control thus reflecting even protein loading as determined by BCA protein quantitation assays.

**Figure 6.4:** The regulation of ADAM-9 mRNA expression by DHT, IGF-1 or DHT plus IGF-1 in LNCaP cells

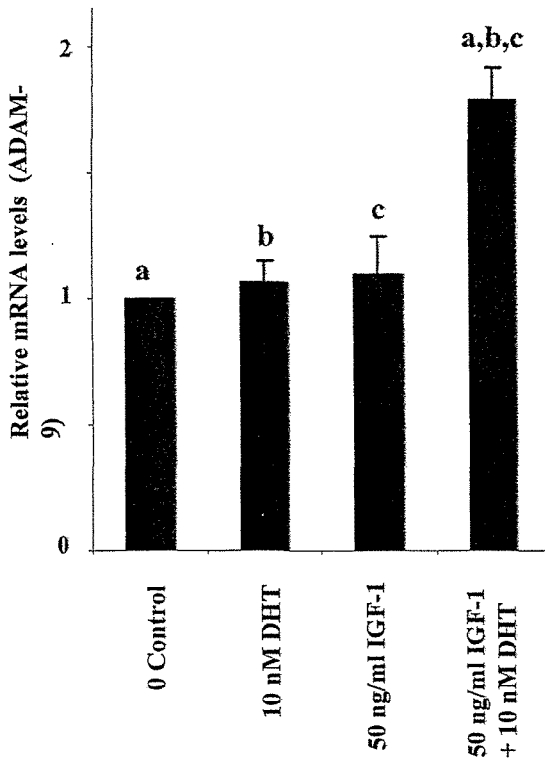


For the mRNA regulation of ADAM-9 by IGF-1 in the presence or absence of DHT, LNCaP cells were treated with 0 (control), 10 nM DHT, 50 ng/ml IGF-1 plus or minus 10 nM DHT and cultured for 48 h. Levels of ADAM-9 transcript were determined by quantitative PCR and normalised against 18s rRNA levels. Histograms represent the mean +/- SEM from three independent experiments (n=3) with each treatment sample being quantitated in triplicate in each of two separate PCR reactions. The same letters above each histogram represent statistical significance: $^{a,b,c}P<0.01$.

**Figure 6.5:** The regulation of ADAM-9 mRNA expression by EGF in LNCaP cells

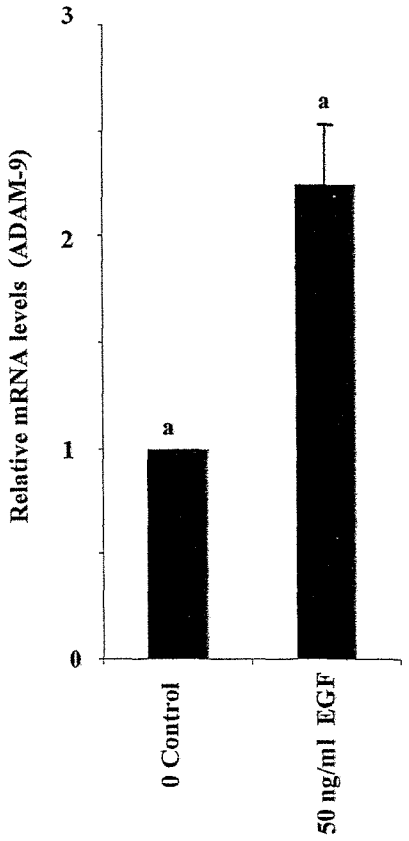


For the mRNA regulation of ADAM-9 by EGF, LNCaP cells were treated with 0 (control) or 50 ng/ml EGF and cultured for 48 h. Levels of ADAM-9 transcript were determined by quantitative PCR and normalised against 18s rRNA levels. Histograms represent the mean +/- SEM from three independent experiments (n=3) with each treatment sample being quantitated in triplicate in each of two separate PCR reactions. The same letters above each histogram represent statistical significance: $^{a}P<0.01$.

**Figure 6.6:** The regulation of ADAM-9 protein expression by DHT, IGF-1 or DHT plus IGF-1 in LNCaP cells

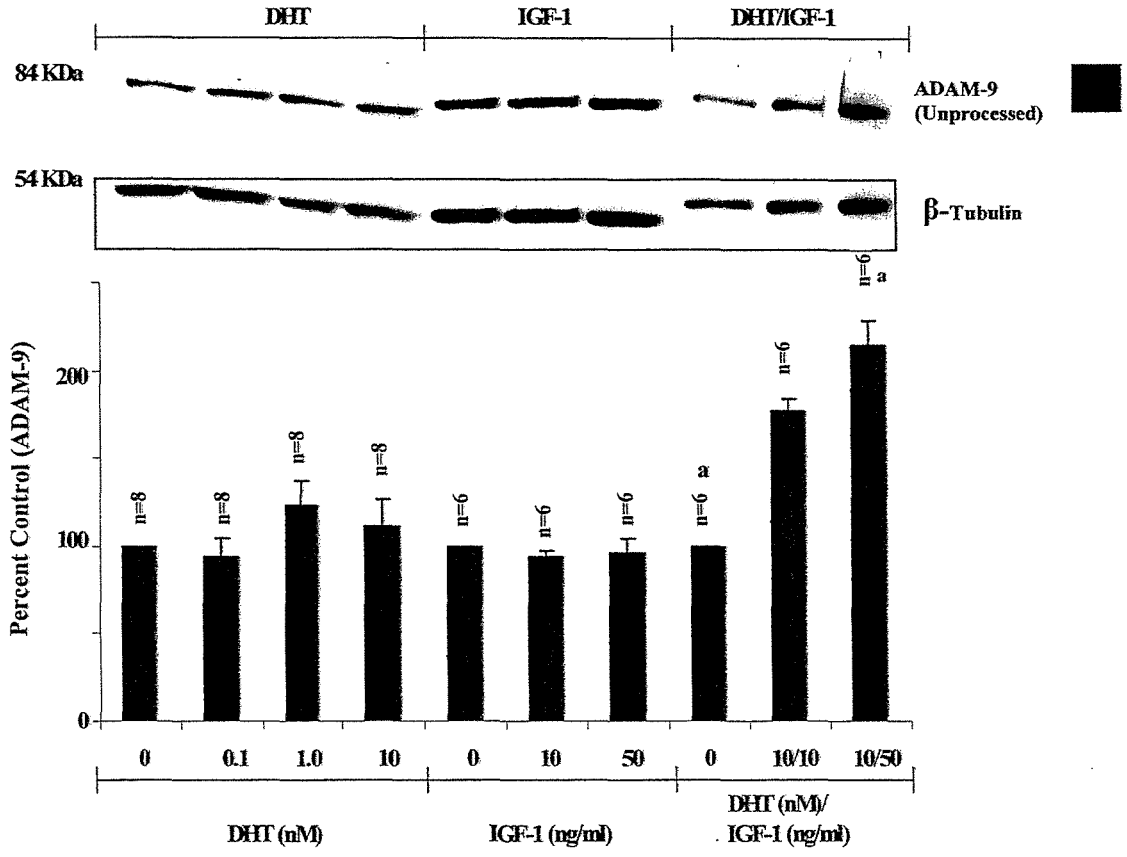


Western blot analysis for ADAM-9 expression in whole cell lysates extracted from LNCaP cells treated with DHT, IGF-1 or IGF-1 in the presence of DHT for 48 h. Quantitative image analysis is shown in the histograms below the Western blots for the 84 kDa, ADAM-9 band. These data are representative of three separate growth factor treated LNCaP whole cell lysate preparations. The signal for ADAM-9 was normalised for protein loading with the signal from β-Tubulin on the same membrane. The same letters above each histogram represent statistical significance:$^{a}P < 0.01$.

**Figure 6.7** The regulation of ADAM-9 protein expression by EGF in LNCaP cells

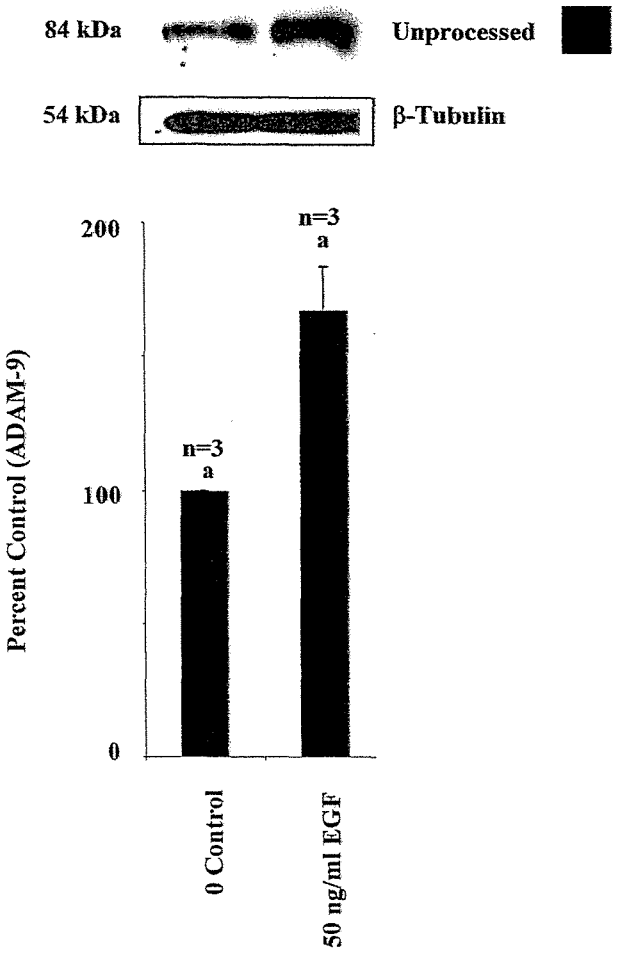


Western blot analysis of ADAM-9 expression in whole cell lysates extracted from LNCaP cells treated with EGF for 48 h. Quantitative image analysis is shown in the histograms below the Western blots for the 84 kDa, ADAM-9 band. These data are representative of a single Western blot of three separate growth factor treated LNCaP whole cell lysate preparations. The signal for ADAM-9 was normalised for protein loading with the signal from β-Tubulin on the same membrane. The same letters above each histogram represent statistical significance: $^{a}P < 0.05$.

**Figure 6.8** The regulation of ADAM-9 nuclear protein expression by EGF in LNCaP cells

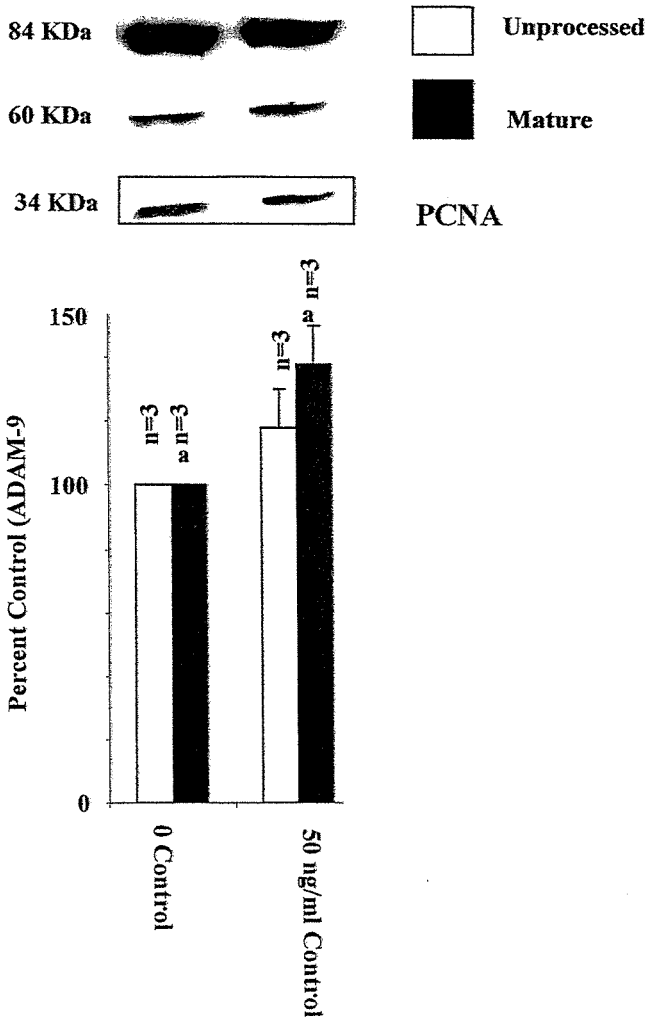


Western blot analysis for ADAM-9 expression in nuclear protein extracts from LNCaP cells treated with EGF for 48 h. Quantitative image analysis is shown in the histograms below the Western blots for the unprocessed 84 kDa, and mature 60 kDa, ADAM-9 band. These data are representative of a single Western blot of three separate growth factor treated LNCaP nuclear protein preparations. The signal for ADAM-9 was normalised for protein loading with the signal from the nuclear marker PCNA on the same membrane. The same letters above each histogram represent statistical significance: $^{a}P < 0.05$.

### *6.3.4 Regulation of ADAM-10 mRNA and protein expression in LNCaP cells by DHT, IGF-1, IGF-1 plus DHT and EGF mRNA regulation*

Quantitative PCR using SYBR Green assays as described above was performed on cDNA reverse transcribed from total RNA extracted from LNCaP cells treated with IGF-1, DHT, IGF-1 plus DHT or EGF. DHT (10 nM) and IGF-1 (50 ng/ml) significantly decreased ADAM-10 mRNA levels in LNCaP cells (Figure 6.9), despite our previous observation that DHT alone increased ADAM-10 mRNA levels in LNCaP cells (McCulloch et al. 2000). Conversely, IGF-1 (50 ng/ml) in the presence of 10nM DHT significantly increased ADAM-10 mRNA when compared to the 10 nM DHT treatment in the same experiment (Figure 6.9). In the case of EGF treatments, ADAM-10 mRNA levels were also significantly elevated in LNCaP cells (Figure 6.10).

*Whole cell lysate protein regulation*

DHT or IGF-1 alone did not significantly alter ADAM-10 protein levels (Figure 6.11). However, IGF-1 (10 or 50 ng/ml) in the presence of 10nM DHT followed the same pattern of response as for mRNA and did up-regulate the unprocessed 100 kDa proform (~2-fold) and significantly increased the levels of processed active 60 kDa form (~4-fold) (Figure 6.11). EGF (50 ng/ml), like the mRNA response, also significantly stimulated the expression of unprocessed 100 kDa proform (~1.5-fold) and the processed 60 kDa processed form (~2-fold) of ADAM-10 (Figure 6.12).

*Nuclear protein regulation in LNCaP cells by EGF*

In an experiment carried out as described for ADAM-9 previously, EGF alone did not significantly alter nuclear ADAM-10 protein levels (Figure 6.13) ($P < 0.07$) although a trend of increased expression across each Western blot was observed, for the unprocessed 100 kDa proform (~2-fold) and the processed, active 60 kDa form (~1.5-fold).

**Figure 6.9:** The regulation of ADAM-10 mRNA expression by DHT, IGF-1, DHT plus IGF-1 in LNCaP cells

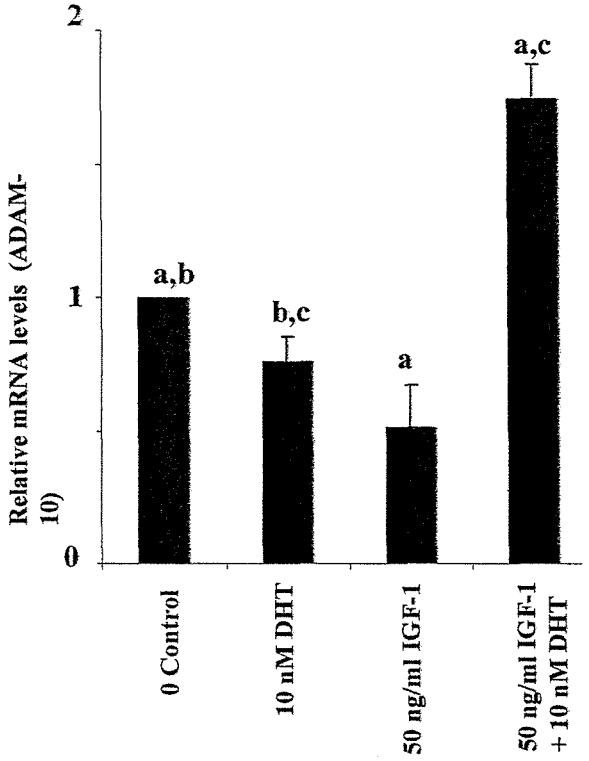


For the mRNA regulation of ADAM-10 by IGF-1 in the presence or absence of DHT, LNCaP cells were treated with 0 (control), 10 nM DHT, 50 ng/ml IGF-1 plus or minus 10 nM DHT and cultured for 48 h. Levels of ADAM-10 transcript were determined by quantitative PCR and normalised against 18s rRNA levels. Histograms represent the mean +/- SEM from three independent experiments (n=3) with each treatment sample being quantitated in triplicate in each of two separate PCR reactions. The same letters above each histogram represent statistical significance: $^{a,c}P<0.01$, $^{b}P<0.05$.

**Figure 6.10:** The regulation of ADAM-10 mRNA expression by EGF in LNCaP cells

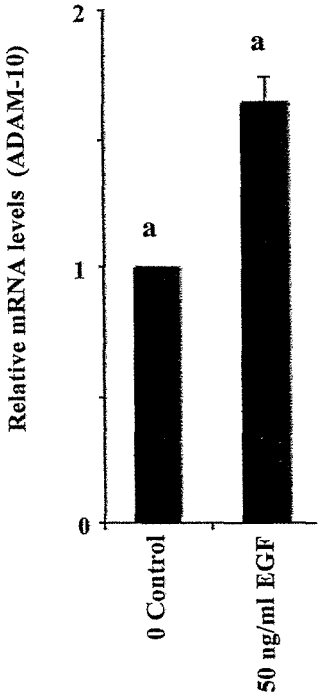


For the mRNA regulation of ADAM-10 by EGF, LNCaP cells were treated with 0 (control) or 50 ng/ml EGF and cultured for 48 h. Levels of ADAM-10 transcript were determined by quantitative PCR and normalised against 18s rRNA levels. Histograms represent the mean +/- SEM from three independent experiments (n=3) with each treatment sample being quantitated in triplicate in each of two separate PCR reactions. The same letters above each histogram represent statistical significance: $^{a}P<0.01$.

**Figure 6.11:** The regulation of ADAM-10 protein expression by DHT, IGF-1, DHT plus IGF-1 in LNCaP cells

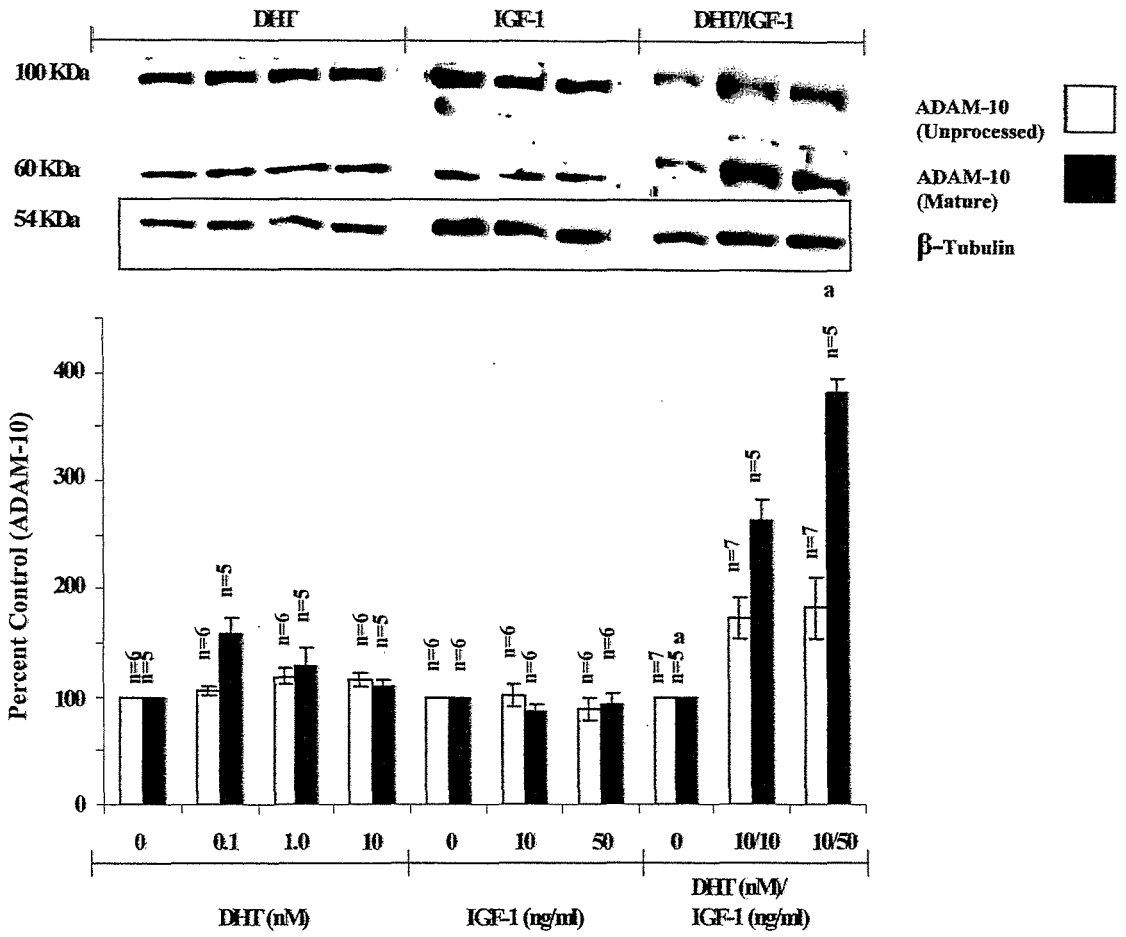


Western blot analysis of ADAM-10 expression in whole cell lysates extracted from LNCaP cells treated with DHT, IGF-1 or IGF-1 in the presence of DHT for 48h. Densitometric analysis is shown in the histograms below the Western blots for the 100 kDa ADAM-10 (pro-enzyme) and the 60 kDa (processed active enzyme) bands. These data are representative of three separate growth factor treated LNCaP whole cell lysate preparations. The signal for ADAM-10 was normalised for protein loading with the signal from β-tubulin on the same membrane. The same letters above each histogram represent statistical significance: $^{a}P<0.05$.

**Figure 6.12:** The regulation of ADAM-10 protein expression by EGF in LNCaP cells

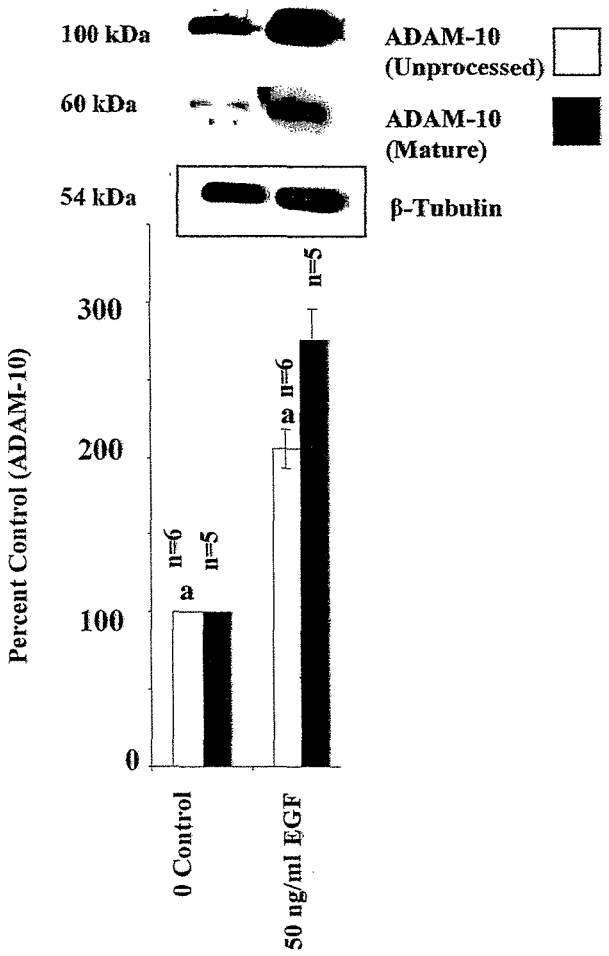


Western blot analysis of ADAM-10 expression in whole cell lysates extracted from LNCaP cells treated with EGF for 48 h. Densitometric analysis is shown in the histograms below the Western blots for the unprocessed 100 kDa and the mature 60 kDa, ADAM-10 bands. These data are representative of two Western blots on three separate growth factor treated LNCaP whole cell lysate protein preparations. The signal for ADAM-10 was normalised for protein loading with the signal from β-tubulin on the same membrane. The same letters above each histogram represent statistical significance: $^{a}P < 0.05$.

**Figure 6.13** The regulation of ADAM-10 nuclear protein expression by EGF in LNCaP cells

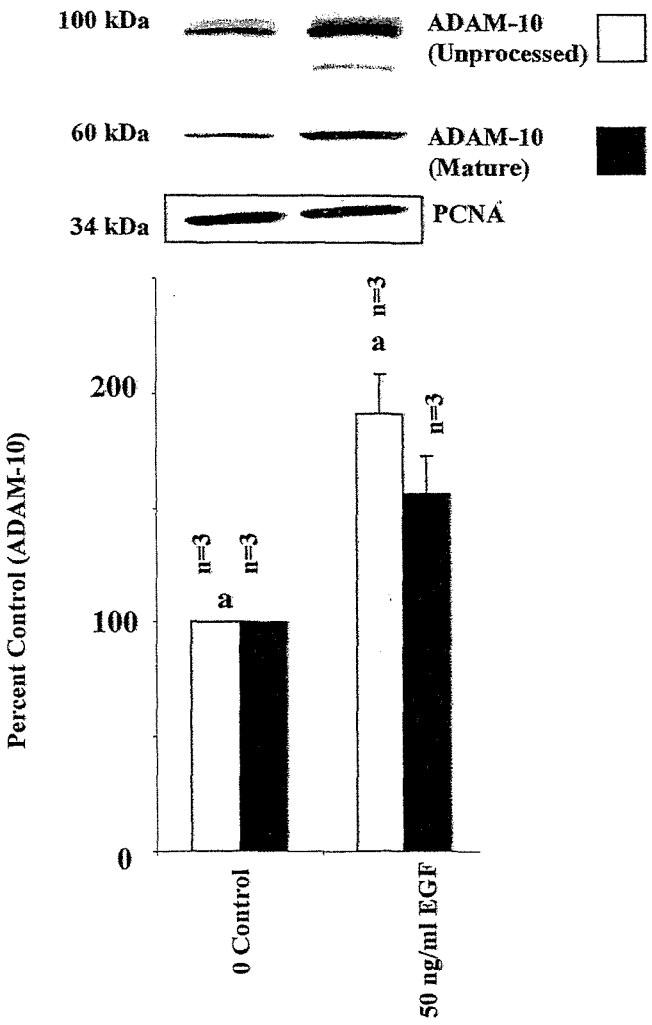


Western blot analysis of ADAM-10 expression in nuclear protein extracts from LNCaP cells treated with EGF. Quantitative image analysis is shown in the histograms below the Western blots for the unprocessed 100 kDa and mature 60 kDa ADAM-10 bands. These data are representative of two Western blots of three separate growth factor treated LNCaP nuclear protein preparations. The signal for ADAM-10 was normalised for protein loading with the signal from PCNA on the same membrane. The same letters above each histogram represent the statistical P - value: $^{a}P < 0.07$.

## *6.4 Discussion*

Previous studies from this laboratory focussed on the regulation of ADAM-9 and -10 mRNA by DHT in the LNCaP cell line (McCulloch et al. 2000). It was found that DHT significantly stimulated both of these ADAM mRNA levels. Thus these studies were extended to more fully describe the regulation of both ADAM-9 and -10 mRNA and protein by each of the prostate growth promoters DHT, IGF-1 and EGF. Because IGF-1 is well documented to act in synergy with DHT (Iwamura et al. 1993), exemplified in this study by IGF-1 stimulating a further increase in LNCaP proliferation in the presence of DHT, but having no effect on cell growth in response to it alone, the regulation of each ADAM by IGF-1 was examined, in the presence and absence of DHT, as well as DHT alone. EGF regulation, on the other hand, was studied as a separate growth factor, as it alone is able to stimulate LNCaP cell proliferation, documented previously (Guo et al. 2000) and illustrated in this study.

### *6.4.1 The regulation of ADAM-9 expression by DHT, IGF-1, DHT plus IGF-1 and EGF*

For ADAM-9, neither IGF-1 nor DHT alone stimulated levels of either mRNA or protein. However, IGF-1 in the presence of DHT significantly stimulated relative levels of ADAM-9 mRNA, and levels of protein in similar fold increments (~2 fold). In the case of EGF stimulation, similar trends of stimulation were also observed for ADAM-9 mRNA and protein (~1.5 to ~2-fold), the latter in both whole cell lysate and nuclear protein fractions.

Although it was anticipated that DHT alone would stimulate ADAM-9 mRNA levels (found previously - McCulloch et al. 2000) in LNCaP cells, this particular study did not replicate this result. Inherent differences in these studies include the use of a different housekeeping gene for normalisation; in this study 18s rRNA was used whilst the previous study used β-actin. Additionally, a different batch and passage number of the LNCaP cell line from American Type Culture Collection (ATCC) was used. This might also contribute to discrepancies leading to conflicting data, as Esquenet et al. (1997) reported that responses to androgens, retinoic acid and vitamin D differed significantly when

proliferation and gene regulation were measured, using two different strains of LNCaP cells from ATCC, which had undergone low or high numbers of passages.

In this current study, however, the regulation of ADAM-9 protein was also examined, and similar trends of synergistic stimulation by IGF-1 and DHT were observed across each of the mRNA and protein levels. Similarly, EGF alone also showed trends of significant stimulation at both the mRNA and protein level, making these new observations consistent within the same cell model. ADAM-9 has three distinct biological roles defined to date; metalloprotease activity due to its active metalloprotease domain (Izumi et al. 1998; Roghani et al. 1999; Schwettmann and Tschesche, 2001), integrin-binding capability, due to its functional integrin-binding loop (Huovila et al. 1996; Zhou et al. 2001) and cell signalling characteristics via its PKA response sites on its cytoplasmic tail (Izumi et al. 1998).

An increase in metalloprotease activity might increase ECM degradation and cell proliferation (Figure 6.14), as active ADAM-9 is able to degrade fibronectin and gelatin *in vitro* (Schwettmann and Tschesche, 2001) and cleave/solubilize membrane bound Hb-EGF (Izumi et al. 1998) (Figure 6.14). This may be pertinent in the transition between androgen-dependent and androgen-independent PCa when, presumably, IGF-1 is acting in synergy with DHT, on tumour cells not yet androgen-insensitive.

Integrin binding and resultant cell signalling events are necessary for cell migration, as well as to re-establish cell-cell and cell-ECM contacts when tumour cells colonise secondary sites within the body. Again, these events are key mechanistic requirements for successful metastasis to occur and may be mediated and intensified by elevated levels of ADAM-9 integrin binding events.

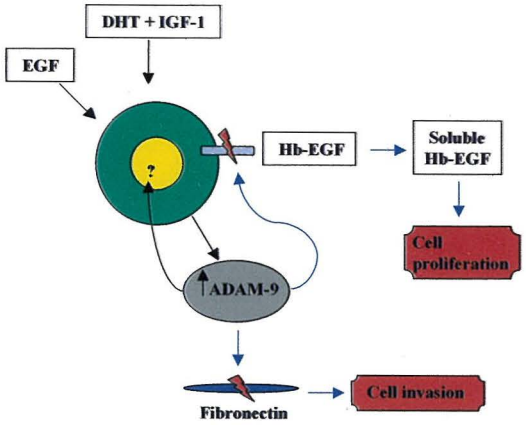


**Figure 6.14:** Schematic diagram, which outlines the possible consequences of elevated levels of ADAM-9 in PCa cells, previously published observations are indicated by blue arrows,**?** indicates that it is not yet known what role ADAM-9 has in the cell nucleus.

It is not yet known what role or effect expression of ADAM-9 in the cell nucleus might have in normal or tumorigenic cells. However, recently a nuclear form of Hb-EGF was described in Transitional Cell Carcinoma (TCC) of the bladder (Adam et al. 2003). Hence, ADAM-9 may carry out proHb-EGF cleavage in the perinuclear/nuclear compartment, releasing active soluble HB-EGF, not unlike its role on the cell membrane. ADAM-9 may also have roles as a nuclear membrane bound receptor, involved in cell signalling through its PKC response sites, or as an active metalloprotease, which might function as a protein/transcription factor activator. Alternatively, ADAM-9 may directly interact with DNA, regulating transcriptional events related to cellular function. Whichever the case, an elevation of levels of this protein in the nucleus may have direct implications in disrupting normal cellular events in tumorigenic cell types.

### *6.4.2 The regulation of ADAM-10 expression by DHT, IGF-1, DHT plus IGF-1 and EGF*

In the case of ADAM-10 mRNA regulation, IGF-1 significantly decreased the relative levels of ADAM-10 mRNA, whilst DHT also slightly decreased the relative levels of mRNA. Conversely, IGF-1 in the presence of DHT significantly stimulated the relative levels of ADAM-10 mRNA. For ADAM-10 protein, neither IGF-1 nor DHT alone had a regulatory effect. However, like the mRNA response, IGF-1 plus DHT increased ADAM-

10 protein levels ~2-fold (unprocessed 100 kDa) and ~4-fold (processed, 60 kDa).

DHT alone did not stimulate ADAM-10 mRNA levels as previously shown, (McCulloch et al. 2000) where a bell-shaped, dose response curve to DHT in LNCaP cells was demonstrated. In the previous study, 10 nM DHT decreased levels of ADAM-10 mRNA from a greater than 4-fold increase, to a smaller than 2-fold increase. It is possible that the deliberate choice of the higher 10 nM stimulatory dose of DHT for the present study (to allow for potential additive effects of IGF-1) may have led to the loss of a DHT stimulatory effect due to the bell-shaped, declining stimulation seen in the previous study. In hindsight, the maximal dose of 1.0 nM DHT may have been preferable, rather than the higher dose of 10 nM. Additional to this, the inherent discrepancies between these two studies discussed above for ADAM-9, still apply in this case and may have compounded the effects of the differential observations.

Of particular note are the preferentially increased levels of mature 60 kDa ADAM-10 (by a factor of 2) compared to unprocessed 100 kDa ADAM-10, in response to IGF-1 plus DHT (whole cell lysate). ADAM-10 has recently been shown to disrupt hemidesmosome linkages between cells and the ECM by the cleavage of the protein L1 (Mechtersheimer et al. 2001). This loss of cell adhesion might assist the cell to migrate through the degraded ECM (Figure 6.15) as in the case of metastasis. The active form of MADM (bovine ADAM-10 orthologue) has potent collagenase activity *in vitro* (Millichip et al. 1998). If the same activity is conserved for human ADAM-10, this may assist cell invasion through the basement membrane (Figure 6.15).

Such hormonal regulation is consistent with the known roles of combined DHT and IGF-1 in the early stages of PCa (Culig et al. 1994). The subsequent loss of androgen-dependence in late-stage PCa might be expected to cause a decrease in ADAM-10, as IGF-1 alone was unable to increase ADAM-10 *in vitro*. However, since ADAM-10 is maintained at equivalent or greater levels in cancer glands *in vivo* (reviewed in Chapter 1) then it would appear that additional regulatory factors like EGF are involved in regulating ADAM-10 expression.

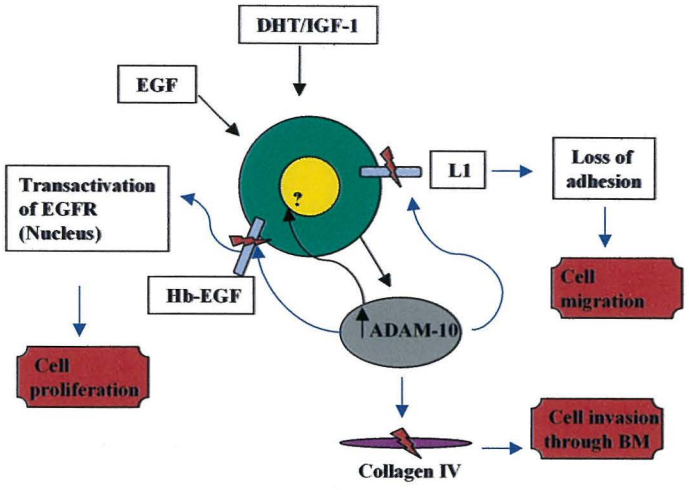


**Figure 6.15:** Schematic diagram of the possible consequences of elevated levels of ADAM-10 in PCa cells, previously published observations are indicated by blue arrows, **?** indicates that it is not yet known what role ADAM-10 has in the cell nucleus.

In the case of EGF, similar trends of stimulation were observed for ADAM-10 mRNA and protein (~1.5 to 2-fold, unprocessed 100 kDa and processed 60 kDa forms) in both whole cell lysate and nuclear fractions. Alongside these observations there is existing immunohistochemical data, which show a high expression profile for nuclear localised ADAM-10, in this study, and EGF in high-grade PCa tumour biopsies (Russell et al. 1998).

A recent study (Yan et al. 2002) linked ADAM-10 to the transactivation of the EGF receptor (EGFR). In this study, the peptide hormone bombesin, through the subsequent activation of G-coupled protein receptors was shown to transactivate the EGFR, with the levels of transactivated EGFR being stimulated when an increase in levels of mouse ADAM-10 were introduced in the cell system. This type of activity may lead to enhanced cell proliferation effects (Figure 6.15). With respect to its nuclear expression, it is not yet known whether ADAM-10 acts as a growth factor activator, a membrane-bound nuclear receptor, or an intermediate cell signal transducer, or directly as a transcription factor.

### *6.4.3 Conclusion*

The synergistic up-regulation by the combined DHT and IGF-1 treatment for both ADAM-9 and -10 proteins supports the hypothesis that these ADAMs may have functional consequences in PCa where these hormone/growth factors have a central role in its development from early stage, androgen sensitive to late stage, androgen insensitive phenotype. This study significantly extends our understanding of the potential roles that ADAM-9 and -10 may have in androgen-sensitive PCa, where IGF-1 can effectively act in synergy, stimulating a plethora of cellular responses. Similarly, the regulation of these two proteins by EGF provides further regulation data, again suggesting a role for both of these ADAMs in PCa, especially where elevated levels of EGF have been shown. This study shows for the first time, evidence that, at the protein level, ADAM-9 and -10 can be regulated by growth factors involved in PCa development. Ongoing studies are now clearly needed to link these observations to the functional consequences of ADAM protein expression in metastatic cancer types.

# CHAPTER SEVEN

## 7.0 GENERAL DISCUSSION

## *7.1 Introduction*

At the outset of this study, little was known with respect to most of the members of the ADAMs family in any cancer type. This family of proteins has since expanded to 34 members characterised thus far. There were a few studies implicating ADAM expression in some cancer cell types, in haematological malignancies (Wu et al. 1997), for example, and in our own laboratory, in choriocarcinoma cell lines (Whiteside et al. Unpublished). Before commencing this major study, one year of research for preliminary evidence to connect the ADAMs to PCa development and progression was carried out. These studies found that ADAM-9, -10, -11, -15 and -17 were expressed in PCa cell lines representing androgen-dependent and androgen-independent PCa (McCulloch et al. 2000). Further regulation analysis provided evidence that ADAM-9 and -10 mRNA levels were elevated by dihydrotestosterone (DHT). Given this information and the potential 'dual' nature of the ADAMs, that is, potential mediators of cell-cell and cell-ECM contacts and active metalloprotease activity, capable of degrading ECM components, it was hypothesised that ADAMs, -9 and -10 may be implicated in the progression, maintenance and survival of PCa by way of hormonal/growth factor regulation.

An additional novel observation that emerged early in the time frame of this larger study was that of the nuclear localisation of ADAM-10 in high-grade PCa. This study, carried out as an honours year project by Pascal Akl (2000), involved an IHC study of the cellular localisation of ADAMs -10 and -17 in pathology sections of tissue from men with prostate disease. A major finding was the dramatic change in localisation of ADAM-10 and -17 from the membrane and cytoplasm of benign secretory and basal epithelial cells of the prostate, to nuclear localisation in secretory cells of tumorigenic glands (See Chapter 1). ADAM-17 had been previously reported to be perinuclear/nuclear localised (Schlondorff et al. 2000) and although this was not in a tumorigenic cell type, it gave some strength to the observations in our laboratory. It was decided to extend these findings in normal prostate and PCa cell lines since it raised particular and novel questions about the possible roles of the cancer specific, nuclear ADAMs. Those nuclear roles would presumably be quite

distinct from the classically recognised roles of cell-cell and cell-ECM attachment, ECM-degradation, and membrane-bound sheddase activity.

The **aims** of this study were **1)** to further characterise the cellular expression of both ADAM-9 and -10 in various prostate pathologies including prostate cell lines and prostate secondary tumour metastases **2)** to generate an ADAM-10 over-expressing prostate cell line model, with a view to assessing their roles in the prostate via functional assays such as cell migration, attachment and invasion, and **3)** to choose a growth-factor responsive model to assess the regulation status of both ADAMs in response to hormones and growth factors, which are highly implicated in prostate growth, specifically DHT, IGF-1 and EGF. By obtaining extensive information with respect to cellular localisation, expression levels, effects on cell behaviour, and growth factor regulation, major advances may be possible in our understanding of the functions of ADAM-9 and -10 in PCa.

### *7.2 The Expression of ADAM-9 and -10 in PCa*

It was found that both ADAM-9 and -10 had readily detectable levels of mRNA and protein expression across cell models which represented normal pathology and low through high-grade metastatic PCa. The abovementioned primary tumour expression study was extended to bone metastases from patients undergoing biopsies, these metastases showed differential membrane/cytoplasmic and nuclear staining for both ADAMs. An expression profile such as this, found for both ADAMs in bone metastases suggests ADAM-9 and -10 may be involved in the local colonisation of PCa tumour cells after the event of migration.

Since both of these ADAMs are active metalloproteases, it is possible that their metalloprotease activity will be involved in the degradation of the surrounding tissue environment to allow for the tumour cell mass to expand. Additionally, the cleavage, solubilisation and activation of growth factors and cytokines may contribute by maintaining the levels of such growth factors, so that additional growth can occur. Specifically, ADAM-9 has recently been found to cleave IGF-BPs in a bone-derived cell line *in vitro* (Mohan et al. 2002), and such activity in bone metastases could readily free biologically

active IGF-1 so that its well known mitogenic effect can be exerted on cells in the surrounding bone environment. Increased bioavailability of growth factors such as IGF-1 might also contribute to enhanced, abnormal osteoblast and osteoclast activation and regulation, hence bone turnover. Increases in these activities are already well documented in the case of other bone metastases such as those from the breast (Mundy and Yoneda, 1996), for example, where abnormal amounts of MMP activity are thought to contribute to this process (Okada et al. 1995). The differential membrane/cytoplasm and nuclear expression demonstrated between cells in the same metastasis illustrated in this study, might reflect the tumour cells undergoing a transformation to a phenotype that is colonising a tumour, rather than 'breaking free' from a primary tumour cell mass, as reflected in high-grade primary tumour cells in which ADAM-10 is predominately nuclear localised.

For *in vitro* cellular localisation data, cell lines were examined by subcellular fractionation, leading to the finding that both ADAMs had representative forms in each of the cell line's nuclear fractions. Further to this, ADAM-10 had two isoforms of its presumably active enzyme, which were differentially expressed in the cell cytoplasm and the cell nucleus. The difference in size of these two isoforms was ~2 kDa and may reflect differential N- or O-glycosylation as a result of differential proximity and processing through the Golgi apparatus. Additionally, the presumably active form of ADAM-9 was also readily detectable in the cell nucleus. The presence of both the pro- and active form of both ADAMs in the cell nucleus raises new questions as to what role/s these particular ADAMs may have, and how they are distinct from classical membrane sheddase activity.

These roles, to date are unclear, however it is hypothesised that the ADAMs could be involved in the activation of nuclear-localised growth factors such as proHb-EGF, for example, which is another example of a classically membrane-bound protein that has been recently found in the cell nucleus (Adam et al. 2003). Both ADAM-9 and -10 metalloprotease activities have the capability to activate Hb-EGF on the cell surface *in vitro* (Izumi et al. 1998; Yan et al. 2002) and it is therefore entirely possible that the same role is carried out in a different location within the cell. Another role for the ADAMs might be that of protein/DNA interaction, where one or both ADAMs may act on DNA directly as an

additional transcription factor. Interestingly, ADAM-10 has a proline rich sequence, C-terminally located, which is a typical feature of the trans activation domain for transcription factors. Such DNA binding activity can be tested by the co-transfection of fragments of ADAM-9 or -10, fused to a Gal-4 DNA binding domain vector (Kato et al., 1990) and a luciferase reporter gene vector containing Gal-4 binding sites. Transcriptional transactivation can be subsequently tested using a luminometer (Kato et al. 1990).

Further examination, in this study, of the expression of both ADAM-9 and -10 by Laser Capture Microdissection (LCM), in homogenous populations of epithelial cells from benign and malignant prostate glands was performed. Although the data were limited, it was concluded that the smaller ADAM-10 isoform, which appears to be nuclear localised *in vitro,* is indeed present, with the larger isoform, in epithelial cells of the prostate and may be the isoform that is predominantly expressed in high-grade PCa in primary tumours as shown by IHC (See Chapter 1). Molecular weight bands similar to those observed *in vitro* in cytoplasmic and nuclear cellular fractions were also shown for ADAM-9. An assay for the detection of differences in mRNA and protein expression of both ADAMs across benign, low through high-grade PCa pathologies was successfully developed and may now be undertaken, once enough material becomes available to substantiate this study.

Technology that has some advantages over LCM is now available and is known as the "Pulse Assisted Laser Microbeam" (PALM) catapulting system (Arcturis Engineering) With this technique, like LCM, a laser pulse guides the removal of homogeneous cell types from a heterogenous tissue, but it does not rely on a flat surface, making micro-dissection accessible to metastatic tissue samples such as those from the bone where calcification particularly contributes to an uneven surface. Using this technology, further expression data can be generated from metastatic biopsies to give a more complete expression profile of the ADAMs.

To better understand the importance and role of nuclear ADAMs, further studies to elucidate the mechanism by which ADAM-9 and -10 are imported into the cell nucleus, would prove valuable. Evidence for possible implication of the α/β importin system in this

mechanism was presented by finding appropriate Nuclear Localisation Sequences (NLS) in the primary amino acid sequence of ADAM-9 and, moreso, in ADAM-10. Studies which knockout the α/β importin system by way of inactivating antibodies or antisense oligonucleotides (Palacios et al. 1997), followed by subcellular fractionation and ADAM-9 and -10 Western blot analysis should show whether or not these ADAMs are imported to the nucleus via these mechanisms.

This study also reported the observation that protein bands corresponding to the Mr of both ADAM-9 and -10 pro- and active forms could be detected in the extracellular environment in membrane vesicles shed from the cell surface of PCa cell lines. This experiment was based on a study by Taraboletti et al. (2002) who outlined the presence and phenomena of membrane vesicle budding. Membrane vesicles are released, or bud, from the cell membrane into the medium and contain cellular and membrane-associated proteins. Active MMP expression was found in these membrane vesicles (Taraboletti et al. 2002) and further, such vesicles facilitate the migration of other cell types, when added in cell culture media in *in vitro* cell migration assays (Angelucci et al. 2000).

The role that active ADAM-9 and -10 may have in the extracellular environment could be to degrade ECM proteins such as collagen and fibronectin, thus facilitating cell invasion in metastasis. Alternatively, given the ECM is rich in growth factors, ADAMs such as -9 and -10 might serve as growth-factor activators or binding protein proteases such as the IGF-BPs or growth hormone BPs. These actions would release or make available high levels of biologically active growth factors to exert their mitogenic affects, thereby stimulating further proliferation of tumorigenic cells. Further studies measuring the activity of both ADAMs in the extracellular environment using fluorogenic peptide substrates (such as those described by Vankemmelbeke et al. 2003 for ADAM-10) might confirm that such ADAM activity is indeed present in membrane vesicles shed from the cell surface of PCa cell lines.

*7.3 Over-expression of ADAM-10 in prostate cell lines:*

To examine the functional consequences of ADAM-10 expression in PCa, the process of constructing ADAM-10 mammalian expression vectors was carried out, in the hope that stably transfected normal prostate and PCa cell lines might over-express ADAM-10, whereby functional cell-based assays could prevail. Three different expression vectors containing full length ADAM-10 inserts (two in this study and one in another study in this laboratory - Dr. Dimitri Odorico) were not capable of achieving significant over-expression of ADAM-10 protein in each of the prostate cell lines tested in this study and additional cell lines tested by Dr. Dimitri Odorico, by way of transient transfection.

As outlined in Chapter 5, the natural Kozak sequence for human ADAM-10 (hADAM-10) was used as the crucial DNA base-positions for the strong promotion of translation within a Kozak sequence (A at -3, and G at +4) (Kozak, 1997) were conserved. Other studies that have examined the function of ADAM-10 using mammalian expression vectors (Anders et al. 2001) have utilised bovine ADAM-10 (MADM). This particular study demonstrated an increase in β-APP processing with an increase in MADM expression, by measuring the levels of secreted β-APP. Interestingly, this study only showed MADM expression using a Hemagglutinin-tag antibody in Western immunoblots, however, there was no indication of a fold increase of overall ADAM-10 production. In our cell system, translation of ADAM-10 from our vector templates may well have taken place, however the vector in this study did not contain a tag for this kind of analysis. Nonetheless, marked over-expression was not observed. Another recent study (Yan et al. 2002) used an expression construct with full-length mouse ADAM-10, which has a Kozak sequence almost identical to MADM but also differs in the same place as hADAM-10 (Chapter 5). This study found that the over expression of MADM but not human ADAM-9 lead to an increase in the trans-activation of the EGFR. However, no indication of the overall changes of levels of MADM was indicated. Yet another group (Franzke et al. 2002) introduced human ADAM-9, mouse ADAM-17 and the bovine ADAM-10 orthologue, MADM to assess the expression in a keratinocyte cell line, which in the case of all three ADAMs, lead to the enhanced cleavage of Collagen XVII. To test for ADAM-10 over-expression, immunofluorescence using the

same ADAM-10Cterm antibody did confirmed over-expression in HaCat cells transiently transfected with high levels of construct DNA using electroporation. No full-length human ADAM-10 mammalian expression vector, to date, to our knowledge, is available for this kind of research.

The difficulties associated with ADAM-10 over expression need further attention so that the functional consequences of the expression of both ADAMs, an original part of this study, can effectively be assessed *in vitro*. Different approaches need to be undertaken whereby a full consensus Kozak sequence, or that homologous to the bovine and mouse ADAM-10 orthologues, both successful in ADAM-10 protein induction (Franzke, et al. 2002; Yan et al. 2002) is introduced 5' to the translation start site, instead of the naturally occurring human ADAM-10 Kozak sequence. Also, the use of a tagged vector system such as pcDNAHis, for example, might show whether the introduced vector stimulates ADAM-10 levels. Additionally, a non-ADAM-10 expressing cell line would be useful, so that a comparison between endogenous and introduced levels of ADAM-10 protein expression can be made.

Once an ADAM-10 over-expressing PCa cell system is ultimately established, cell based assays can be performed, including cell attachment, migration and invasion assays, whereby, the PCa cells are seeded onto synthetic ECM (Matrigel) or components of the ECM such as Fibronectin, Vitronectin and various types of Collagen. These types of assays are well established and have been used successfully for some years by other members of this laboratory (Leavesley et al. 1993; Leavesley et al. 1994). Over time, cellular behaviour can be monitored so that a change in ADAM-10 expression may be correlated with a change in cellular behaviour and properties. Also, the same *in vitro* cell based assays can be performed on PCa cells, in which endogenous levels of ADAM-10 have been knocked out, for example, with morpholino antisense oligonucleotides, as used in previous ADAM-10 studies (Yan et al. 2002), or the utilisation of the newly developed small interference RNAs (siRNAs) technology. Once these experiments are performed, important data pertaining to the functional consequence of ADAM-10 protein expression in PCa cells can be obtained.

### *7.4 The regulation of ADAM-9 and -10 by DHT, IGF-1 and EGF*

The final part of this study focussed on the regulation of both ADAM-9 and -10 by the PCa growth promoters DHT, IGF-1 in the presence or absence of DHT, or EGF alone. The expression of both ADAM-9 and -10 mRNA and protein was synergistically stimulated by IGF-1 and DHT, and elevated by EGF alone. Preliminary nuclear regulation data also showed that EGF stimulates the levels of these proteins, which reside in the cell nucleus. A synergistic regulation in response to IGF-1 plus DHT suggests that both ADAMs are elevated in androgen sensitive PCa, where IGF-1 is able to exert its biological affects synergistically. The regulation of both ADAMs by EGF suggests that elevated levels of this growth factor, as shown with increasing PCa severity (Russel et al. 1998), might maintain protein levels such as ADAM-9 and -10.

An increase in the metalloprotease activity of ADAM-9 and -10, as a result of elevated levels of active enzyme, might increase ECM and basement membrane degradation. As outlined previously in Chapter 6, active ADAM-9 is able to degrade fibronectin and gelatin (Schwettmann and Tschesche, 2001) and the active form of MADM (bovine ADAM-10 orthologue) has potent collagenase activity, *in vitro* (Millichip et al. 1998) and it is likely that human ADAM-10 has the same activity. An additional role for both of these ADAMs is the cleavage and solubilisation of proHb-EGF, which is known to promote cell proliferation through signalling via the EGFR pathway. Elevated levels of ADAM-10 have also been linked to the transactivation of the EGF receptor (EGFR) (Yan et al. 2002), and this type of activity may also lead to enhanced cell proliferation.

With respect to the consequences of elevated levels of ADAM-9 and -10 in the cell nucleus, shown in this study in response to EGF treatment, recently a nuclear form of Hb-EGF was described in Transitional Cell Carcinoma (TCC) of the bladder (Adam et al. 2003). Therefore, it is likely that Hb-EGF will be nuclear localised in PCa, hence ADAM-9 and/or -10 protease activity may carry out increased proHb-EGF cleavage in the perinuclear/nuclear compartment, releasing active soluble HB-EGF, not unlike its role on the cell membrane, again leading to an increase in cell proliferation through nuclear

localised EGFR (Yan et al. 2002).

Integrin binding and resultant cell signalling events are necessary for cell migration, as well as to re-establish cell-cell and cell-ECM contacts when tumour cells colonise secondary sites within the body. These events are key mechanistic requirements for successful metastasis to occur and may be mediated and intensified by elevated levels of ADAM-9 integrin binding events. ADAM-10, on the other hand, has no documented interaction with integrins but has recently been shown to disrupt hemidesmosome linkages between cells and the ECM by the cleavage of the protein L1 (Mechtersheimer et al. 2001). This loss of cell adhesion might assist the cell to migrate through the degraded ECM in the case of metastasis.

Future studies are now required to confirm the regulation of ADAM-9 and -10 in the nucleus and elucidate a function for each of these ADAMs in the nuclear compartment. Also, additional studies are needed to fully characterise the responsiveness of membrane vesicle shedding, and the subsequent levels and activity of ADAM-9 and -10, to DHT, IGF-1 and EGF. As outlined earlier, similar studies, which have measured MMP activity, suggest hormones and growth factors are able to stimulate membrane shedding events in as little as 4 hours (Taraboletti et al. 2002) in cells. The employment of specific ADAM activity substrates alongside Western blot analysis might, after growth factor treatment, give an indication of possible changes in ADAM levels and activity in the extracellular environment, potentially contributing to ECM proteolysis and growth factor activation, hence metastasis.

### *7.5 Conclusion*

This study has extensively characterised the expression and hormonal/growth-factor responsiveness in PCa of ADAM-9 and -10, two ADAMs in an extended family of 34 members. Due to their pattern of expression from early through late stage, metastatic disease, and their elevated levels in response to hormones and growth factors that mediate

PCa progression, ADAM-9 and -10 are likely candidates for the assistance of PCa growth and development.

This study provides novel data, which builds a strong basis for further research, with respect to the functional consequences of ADAM-9 and -10, and other ADAMs in PCa, as well as in other cancers that are aggressive and metastatic in nature. The identification and characterisation of such candidate proteins, in a study such as this, is important in acquiring a full understanding of the underlying mechanisms of cancer progression. Once these mechanisms are fully understood, effective treatment regimens can be developed for the prevention, survival and improvement of the quality of life of sufferers with cancers such as that which originates from the prostate gland.

# APPENDIX ONE

## A) Table of common MMPs, their synonyms and extrtacellular matrix substrates:

| Enzyme | Synonym | Molecular Weight (Latent/Active) | Collagen Substrates | Additional Substrates |
|---|---|---|---|---|
| MMP-1 | Collagenase-1, Fibroblast Collagenase, Interstitial Collagenase, Tissue Collagenase | 55,000/45,000 | I,II,III,VII,VIII,X | Aggrecan, Gelatin, MMP-2, MMP-9 |
| MMP-2 | 72 kDa Gelatinase, 72 kDa Gelatinase/Type IVCollagenase, Gelatinase A, TBE-1 | 72,000/66,000 | I, II, III, IV, V, VII, X, XI | Aggrecan, Elastin, Fibronectin, Gelatin, Laminin, MMP-9, MMP-13 |
| MMP-3 | Procollagenase, PTR1 protein, SL-1, Stromelysin-1, Transin-1 | 57,000/45,000 | II, III, IV, IX, X, XI | Aggrecan, Elastin, Fibronectin, Gelatin, Laminin, MMP-7, MMP-8, MMP-13 |
| MMP-7 | Matrilysin, Matrin, PUMP-1 Protease, Uterine Metalloproteinase | 28,000/19,000 | IV, X | Aggrecan, Elastin, Fibronectin, Gelatin, Laminin, MMP-1, MMP-2, MMP-9 |
| MMP-8 | Collagenase–2, Neutrophil Collagenase, | 75,000/58,000 | I, II, III, V, VII, VIII, X | Aggrecan, Elastin, Fibronectin, Gelatin, Laminin |
| MMP-9 | 92 kDa Gelatinase, 92 kDa Gelatinase/Type IV Collagenase, Gelatinase B | 92,000/86,000 | IV, V, VII, X, XIV | Aggrecan, Elastin, Fibronectin, Gelatin |
| MMP-10 | SL-2, Stromelysin-2, Transin-2 | 57,000/44,000 | III, IV, V | Aggrecan, Elastin, Fibronectin, Gelatin, Laminin, MMP-1, MMP-8 |
| MMP-11 | SL-3, Stromelysin-3, ST-3 | 54,000/45,000 and 22,000 | IV | Elastin, Fibronectin, Gelatin, Laminin |
| MMP-13 | Collagenase-3 | 60,000/48,000 | I, II, III, IV | Aggrecan, Gelatin |
| MMP-18 | *Xenopus* Collagenase-4, xCol4 | 70,000/53,000 | | |
| MMP-19 | RASI-1 | 54,000/45,000 | IV | Fibronectin, Aggrecan, COMP, Laminin, Gelatin |
| MMP-20 | Enamelysin | 54,000/22,000 | | Aggrecan, Amelogenin, COMP |
| MMP-23 | CA-MMP | | | |
| MMP-26 | Matrilysin-2, Endometase | 28,000/19,000 | IV | Gelatin, Fibronectin |
| MMP-28 | Epilysin | | | |
| MT1-MMP | MMP-14, Membrane-Type Metalloproteinase-14 | 66,000/56,000 | I, II, III | Aggrecan, Elastin, Fibronectin, Gelatin, Laminin, MMP-2, MMP-13 |
| MT2-MMP | MMP-15, Membrane-Type Metalloproteinase-15 | 72,000/60,000 | | Fibronectin, Gelatin, Laminin, MMP-2 |

| Enzyme | Synonym | Molecular Weight (Latent/Active) | Collagen Substrates | Additional Substrates |
|---|---|---|---|---|
| MT3-MMP | MMP-16, Membrane-Type Metalloproteinase-16 | 64,000/52,000 | | MMP-2 |
| MT4-MMP | MMP-17, Membrane-Type Metalloproteinase-17 | 57,000/53,000 | | Fibrin, Gelatin |
| MT5-MMP | MMP-24 | –/62,000 | | |
| MT6-MMP | MMP-25, Leukolysin | | IV | Gelatin, Fibronectin, Laminin-I |

(Calbiochem - Oncogene Research Products, Volume 2, January 2002; www.calbiochem.com)

**B) Illustration comparing the typical domain structure of an MMP and an ADAM:**

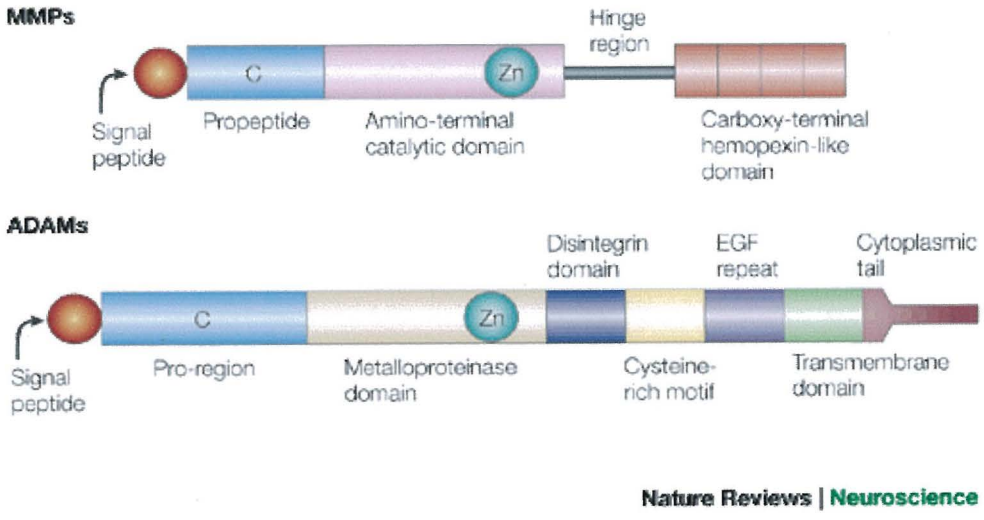


*Nature Reviews Neuroscience* 2:502-511 (2001)

## C) Table of the ADAMs, their synonyms and their expression/functions known to date:

| ADAM | Synonym | Expression/Function |
|---|---|---|
| **ADAM1** | Fertilin α<br>PH-30 α | Subunit of a sperm surface protein involved in sperm-egg fusion; pseudo gene in human |
| **ADAM2** | Fertilin β<br>PH-30 β | Essential for fertilization in mice; interacts with egg integrin $\alpha_6\beta_1$, a sperm receptor |
| **ADAM3A** | Cyritestin 1 (CYRN1)<br>tMDC I | Two human genes (ADAM3A and ADAM3B) and one mouse gene (ADAM3) encoding cyritestin, a sperm protein involved in gamete interaction and sperm-egg plasma membrane adhesion and fusion |
| **ADAM3B** | Cyritestin 2 (CYRN2) | Cyristestin is a polymorphic protein that consists of both membrane-anchored and soluble forms |
| **ADAM4** | tMDC V | ADAMs 4-6 cloned from a mouse testis cDNA library; primarily expressed in testis |
| **ADAM5** | tMDC II | Primarily expressed in testis |
| **ADAM6** | tMDC IV | Primarily expressed in testis |
| **ADAM7** | EPA I | A mammalian epididymal protein that may play a role in sperm maturation |
| **ADAM8** | CD156 MS2 | Expressed in myelomonocytes and may play a role in extravasation of leukocytes |
| **ADAM9** | MDC9 Meltrin γ | Widely expressed, interacts with SH3 proteins; cleaves insulin B-chain and several synthetic peptides; has α-secretase activity |
| **ADAM10** | Kuzbanian (KUZ) MADM | Widely expressed, processes NOTCH and mediates lateral inhibition in neurogenesis; cleaves TNF, myelin basic protein, type IV collagen; has α-secretase activity |
| **ADAM11** | MDC | The gene is somatically rearranged in two primary breast cancers |
| **ADAM12** | Meltrin α | Cleave $\alpha_2$-macroglobulin; has IGFBP-3 protease activity; binds to α-actinin-2; participates in myoblast fusion |
| **ADAM13** | | A Xenopus gene most closely related to mouse ADAM12; located to somitic mesoderm and cranial neural crest cells |
| **ADAM14** | ADM-1 | Expressed in syncytial organs, sperm and sheath cells of sensory organs |
| **ADAM15** | MDC15 Metargidin | RGD-containing ADAM15 interacts with αvβ3 integrin; more than half of mature mouse protein is intracellular |
| **ADAM16** | MDC16 | Interaction of ADAMs, 16, 9 and 13 with integrin receptors may be necessary for frog fertilization |
| **ADAM17** | TACE | Processes TNF, TNF receptor, Notch 1 receptor, L-selectin, TRANCE and HER4 JM-a; has α-secretase activity |
| **ADAM18** | tMDC III ADAM27 | Protein processed on the sperm surface during epididymal transit |
| **ADAM19** | Meltrin β | A novel marker for dendritic cell differentiation and may play a role in osteoblast differentiation |
| **ADAM20** | | Testis-specifically expressed gene without intron |
| **ADAM21** | | Testis-specifically expressed gene without intron |
| **ADAM22** | MDC2 | Expressed predominantly in brain |
| **ADAM23** | MDC3 | Expressed predominantly in brain |
| **ADAM24** | Testase-1 | Testis-specifically expressed gene |
| **ADAM25** | Testase-2 | Testis-specifically expressed gene |
| **ADAM26** | Testase-3 | Testis-specifically expressed gene |
| **ADAM28** | MDC-Lm MDC-Ls eMDCII | Expressed in human lymphocytes and possesses autocatalytic activity to remove the pro domain |
| **ADAM29** | | Testis-specifically expressed gene |
| **ADAM30** | | Testis-specifically expressed gene |
| **ADAM31** | | Highly expressed in specialized epithelia |
| **ADAMTS1** | METH1 | An active protease associated with ECM and essential for normal growth, fertility, and organ morphology and function; cleaves aggrecan at Glu1871 and Leu1872; cleaves $\alpha_2$-macroglobulin |
| **ADAMTS2** | PCNP | Procollagen N-proteinase involved in collagen biosynthesis and may play a role in development |
| **ADAMTS3** | | Cloned from brain |

| ADAM | Synonym | Expression/Function |
|---|---|---|
| **ADAMTS4** | Aggrecanase-1 | Cleaves aggrecan at Glu373 and Ala374; cleaves brevican, a brain specific ECM protein, at Glu395 and Ser396 |
| **ADAMTS5** | Aggrecanase-2 ADAMTS11 | Cleaves aggrecan at Glu373 and Ala374 |
| **ADAMTS6** | | Expressed at low levels, primarily in placenta |
| **ADAMTS7** | | Widely expressed |
| **ADAMTS8** | METH-2 | ADAMTs 8 and 1 disrupt angiogenesis *in vivo* |
| **ADAMTS9** | | Expressed in all fetal tissues examined and some adult tissues |
| | SUP-17 | May be ADAM10 in *C. elegans* and play a role in LIN-12/NOTCH signaling |
| | MIG-17 | A protease in *C. elegans* that directs migration of distal tip cells by remodeling the basement membrane |
| | Decysin | Highly expressed in mature dendritic cells |

(http://www.rndsystems.com/asp/g_SiteBuilder.asp?BodyID=303)

## APPENDIX TWO

**A) PGEMTeasy (Promega) - an intermediate vector used for full length ADAM-10 sub-cloning into the mammalian expression vectors below.**

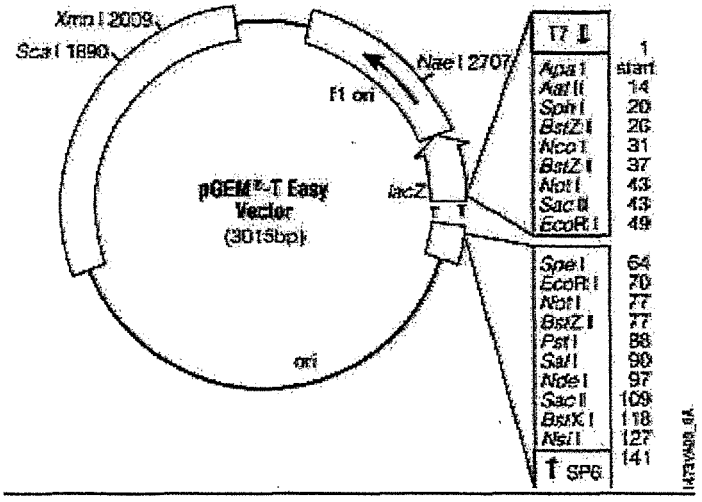


**B) pcDNA3.1 (Invitrogen) – a mammalian expression vector, driven by the CMV promoter, full length ADAM-10 was cloned in the forward (+) direction using the BamH1 restriction digest site.**

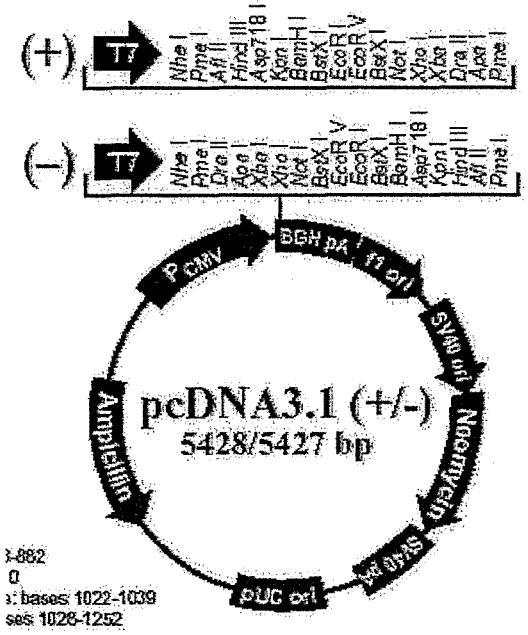

**C) pMEP4 (Invitrogen) - a mammalian expression vector, driven by the inducible metallothionine (phMTIIA) promoter, full length ADAM-10 was cloned in the forward direction using the BamH1 restriction digest site.**

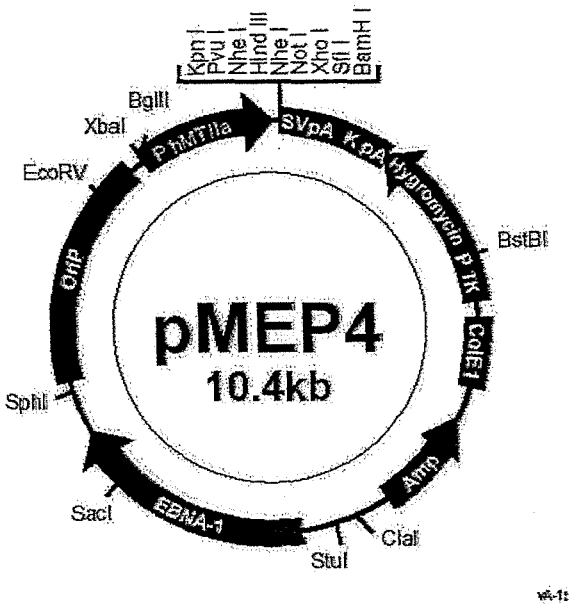

## REFERENCES


Adam, R.M., Danciu, T., McLellan, D.L., Borer, J.G., Lin, J., Zurakowski, D., Weinstein, M.H., Rajjayabun, P.H., Mellon, J.K. and Freeman, M.R. (2003) A nuclear form of the heparin-binding epidermal growth factor-like growth factor precursor is a feature of aggressive transitional cell carcinoma. **Cancer Res** 63, 484-490.

Adler, H.L., McCurdy, M.A., Kattan, M.W., Timme, T.L., Scardino, P.T., and Thompsom, T.C. (1999) Elevated levels of circulating interleukin-6 and transforming growth factor-beta 1 in patients with metastatic prostatic carcinoma. **J Urol** 161, 182-187.

Adolfsson, J. (1993) Deferred treatment of low grade stage T3 prostate cancer without distant metastasis. **J Urol** 149, 326-329.

Alexander, C.M., Hansell, E.J., Behrendtsen, O., Flannery, M.L., Kishnani, N.S., Hawkes, S.P. and Werb, Z. (1996) Expression and function of matrix metalloproteinases and their inhibitors at the maternal-embryonic boundary during mouse embryo implantation. **Development** 122, 1723 - 1736.

Alfandari, D., Wolfsberg, T. G., White, J. M. and Douglas, W. (1997) ADAM 13: A novel ADAM expressed in somitic mesoderm and neural crest cells during *xenopus laevis* development. **Dev Biol** 182, 314 - 330.

Amour, A., Slocombe, P.M., Webster, A., Butler, M., Knight, C.G., Smith, B.J., Stephens, P.E. and Hutton, S.E. (1998) TNF α converting enzyme (TACE) is inhibited by TIMP-3. **FEBS Letters** 435, 39 - 44.

Amour, A., Knight, G., Webster, A., Slocombe, P.M., Stephens, P.E., Knauper, V., Docherty, A.J.P., and Murphy, G. (2000) The in vitro activity of ADAM-10 is inhibited by TIMP-1 and TIMP-3. **FEBS Letters** 473, 275 - 279.

Amour, A., Knight, C.G., English, W.R., Webster, A., Slocombe, P.M., Knauper, V., Docherty, A.J., Becherer. J,D., Blobel, C.P. and Murphy, G. (2002) The enzymatic activity of ADAM8 and ADAM-9 is not regulated by TIMPs. **FEBS Letters** 524, 154-158.

Anders, A., Gilbert, S., Garten, W., Postina, R. and Fahrenholz, F. (2001) Regulation of the α-secretase ADAM10 by its prodomain and proprotein convertases. **FASEB J** 15, 1837-1839.

Angelucci, A., D'Ascenzo, S., Festucci, C., Gravina, G.L., Bologna, M., Dolo, V. and Pavan, A. (2000) Vesicle-associated urokinase plasminogen activator promotes invasion in prostate cancer cell lines. **Clin Exp Met** 18, 163 - 170.

Azuma, M., Aota, K., Tamatan, T., Motegi, K., Yamashita, T., Harada, K., Hayashi, Y., Sato, M. (2000) Suppression of tumor necrosis factor alpha-induced matrix metalloproteinase 9 production by the introduction of a super-repressor form of inhibitor of nuclear factor kappa B alpha complementary DNA into immortalized human salivary gland acinar cells. Prevention of the destruction of the acinar structure in Sjogren's syndrome salivary glands. **Arthrit & Rheum** 43, 1756-1767.

Bader, P., Burkhard, F.C., Markwalder, R. and Studer, U.E. (2003) Disease progression and survival of patients with positive lymph nodes after radical prostatectomy. Is there a chance of cure? **J Urol** 169, 849-854.

Baxter, R.C. (2001) Inhibition of the insulin-like growth factor (IGF)-IGF-binding protein interaction. Review. **Hormone Res** 55 (Suppl 2), 68-72.

Beckett, R. P. (1996) Recent advances in the field of matrix metalloprotienase inhibitors. **Exp.Opin.Ther.Patents** 6, 1305-1315.

Bello, D., Webber, M.M., Kleinman, H.K., Wartinger, D.D. and Rhim, J.S. (1997) Androgen responsive adult human prostatic epithelial cell lines immortalized by human

papillomavirus 18. **Carcin** 18, 1215-1223.

Benbow, U., Buttice, G., Nagase, H. and Kurkinen, M. (1996) Characterisation of the 46-kDa intermediates of matrix metalloproteinase 3 (stromelysin 1) obtained by site directed mutation of phenylalanine 83. **J Biol Chem** 271, 10715 - 10722.

Bentel, J.M. and Tilley, W.D. (1996) Androgen receptors in prostate cancer. **J Endo** 151, 1-11.

Bergers, G. and Coussens, L.M. (2000) Extrinsic regulators of epithelial tumor progression: metalloproteinases. **Curr Opin Genet Dev** 10, 120 - 127.

Bergers, G., Brekken, R., McMahon, G., Vu, T. H., Itoh, T., Tamaki, K., Tanzawa, K., Thorpe, P., Itohara, S., Werb, Z. and Hanahan, D. (2000) Matrix metalloproteinase-9 triggers the angiogenic switch during carcinogenesis. **Nat Cell Biol** 2, 737-744.

Blavier, L., Henriet, P., Imren, S. and Declerck, Y.A. (1999) Tissue inhibitors of matrix metalloproteinases in cancer. **Annals New York Acad Sci** 878, 108 – 119.

Blelloch, R., Anna-Arriola, S.S., Gao, D., Li, Y., Hodgkin, J. and Kimble, J. (1999) The gon-1 gene is required for gonadal morpho-genesis in *Caenorhabditis elegans*, **Dev Biol** 216, 382–393.

Blobel, C. P. (1997) Metalloprotease-disintegrins: Links to cell adhesion and cleavage of TNF α and notch. **Cell** 90, 589 - 592.

Bonaccorsi, L., Carloni, V., Muratori, M., Salvadori, A., Giannini, A., Carini, M., Serio, M., Forti, G. and Baldi, E. (2000) Androgen receptor expression in prostate carcinoma cells suppresses alpha6beta4 integrin-mediated invasive phenotype. **Endocrinology** 141, 3172-3182.

Boyle, P. (1994) New Insights in the epidemiology and natural history of benign prostatic hyperplasia. **Prog Clin Biol Res** 386, 3-18.

Brooks, P.C., Strömblad, S., Sanders, L.C., von Schalscha, T.L., Aimes, R.T., Stetler-Stevenson, W.G., Quigley, J.P. and Cheresh, D.A. (1996) Localization of Matrix Metalloproteinase MMP-2 to the Surface of Invasive Cells by Interaction with Integrin alphaVbeta 3. **Cell** 85, 683-693.

Bubley, G.J., Balk, S.P., Regan, M.M., Duggan, S., Morrissey, M.E., Dewolf, W.C., Salgami, E. and Mantzoros, C. (2002) Serum levels of insulin-like growth factor-1 and insulin-like growth factor-1 binding proteins after radical prostatectomy. **J Urol** 2002 168, 2249-2252.

Butler, G.S., Will, H., Atkinson, S.J. and Murphy, G. (1997) Membrane-type-2 matrix metalloproteinase can initiate the processing of progelatinase A and is regulated by the tissue inhibitors of metalloproteinases. **Eur J Bioch** 244, 653 - 657.

Buxbaum, J.D., Kang-Nian, L., Luo, Y., Slack, J.L., Stocking, K.L., Peschon, J.J., Johnson, R.S., Castner, B.J., Cerretti, D.P. and Black, R.A. (1998) Evidence that tumor necrosis factor alpha converting enzyme is involved in regulated alpha-secretase cleavage of the Alzheimer amyloid protein precursor. **J Biol Chem** 43, 27665 - 27767.

Cal, S., Freije, J.M., Lopez, J.M., Takada, Y. and Lopez-Otin, C. (2000) ADAM 23/MDC3, a human disintegrin that promotes cell adhesion via interaction with the alphavbeta3 integrin through an RGD-independent mechanism. **Mol Biol Cell** 11, 1457-1469.

Cal, S., Arguelles, J.M., Fernandez, P.L. and Lopez-Otin, C. (2001) Identification, characterization, and intracellular processing of ADAM-TS12, a novel human disintegrin with a complex structural organization involving multiple thrombospondin-1 repeats. **J Biol Chem** 276, 17932-17940.

Cameron, P.M., Marcy, A. I., Rokosz, L. L. and Hermes, J.D. (1995) Use of an active site inhibitor of stromelysin to elucidate the mechanism of prostromelysin activation. **Bioorg Chem** 23, 415 – 426.

Carlin, B.I. and Andriole, G.L. (2000) The natural history, skeletal complications, and management of bone metastases in patients with prostate carcinoma. **Cancer**. 88(12 Suppl), 2989-2994.

Castro, M.G., Cowen, R., Williamson, I.K., David, A., Jimenez-Dalmaroni, M.J., Yuan, X., Bigliari, A., Williams, J.C., Hu, J. and Lowenstein, P.R. (2003) Current and future strategies for the treatment of malignant brain tumors. **Pharmacol Ther** 98, 71-108.

Catalona, W.J., Smith, D.S., Ratliff, T.L. and Basler, J.W. (1993) Detection of organ-confined prostate cancer is increased through use of prostate-specific antigen-based screening. **JAMA** 270, 948-954.

Catimel, B., The, T., Fontes, M.R, Jennings, I.G., Jans, D.A., Howlett, G.J., Nice, E.C. and Kobe, B. (2001) Biophysical characterization of interactions involving importin-alpha during nuclear import. **J Biol Chem** 276, 34189-34198.

Cerretti, D.P. (1999) Characterisation of the tumour necrosis factor α - converting enzyme TACE/ADAM17. **Biochem Soc Trans** 27, 219 - 223.

Chan, J.M., Stampfer, M.J., Giovannucci, E., Gann, P.H., Ma, J., Wilkinson, P., Hennekens, C.H., Pollak and M. 1998. Plasma insulin like growth factor-I and prostate cancer risk: a prospective study. **Science** 279, 563 - 566.

Chang, C. and Werb, Z. (2001) The many faces of metalloproteases: cell growth, invasion, angiogenesis and metastasis. Review. **Trends in Cell Biol** 11, S37-43.

Chen, M.S., Almeida, E.A., Huovila, A.P., Takahashi, Y., Shaw, L.M., Mercurio, A.M. and White, J. (1999) Evidence that distinct states of the integrin alpha6beta1 interact with

laminin and an ADAM. **J Cell Biol** 144, 549 – 561.

Cho, C., Primakoff, P., White, J.M. and Myles, D.G. (1996) Chromosomal assignment of four testis-expressed mouse genes from a new family of transmembrane proteins (ADAMs) involved in cell-cell adhesion and fusion. **Genomics** 34, 413 - 417.

Chodak, G.W., Thisted, R.A., Gerber, G.S., Johansson, J.E., Adolfsson, J., Jones, G.W., Chisholm, G.D., Moskovitz, B., Livne, P.M. and Warner, J. (1994) Results of converative management of clinically localized prostate cancer. **N Engl J Med** 330, 242-248.

Chung, L.W.K., Gleave, M.E., Hsieh, J., Hong, S.J. and Zhau, H.E. (1991) Reciprocal mesenchymal-epithelial interaction affecting prostate tumor growth and hormonal responsiveness. **Cancer Surv** 11, 91-119.

Chung, L.W., Kao, C., Sikes, R.A. and Zhau, H.E. (1997) Human prostate cancer progression models and therapeutic intervention. **Acta Urologica Japonica** 43, 815-820.

Chung, T.D., Yu, J.J., Spiotto, M.T., Bartkowski, M. and Simons, J.W. (1999) Characterisation of IL-6 in the progression of prostate cancer. **Prostate** 38, 199 – 207.

Clements, J., Mukhtar, A., Yan, S. and Holland, A. (1997) Kallikreins and kinins in inflammatory-like events in the reproductive tract. **Pharm Res** 35, 537 – 540.

Cohen, P., Peehl, D.M. and Rosenfeld, R.G. (1994) The IGF axis in the prostate. **Horm Metab Res** 26, 81 – 8 4.

Colciaghi, F., Borroni, B., Pastorino, L., Marcello, E., Zimmermann, M., Cattabeni, F., Padovani, A. and Di, Luca. M. (2002) [alpha]-Secretase ADAM10 as well as [alpha]APPs is reduced in platelets and CSF of Alzheimer disease patients. **Mol Med** 8, 67 - 74.

Cornwall, G.A. and Hsia, N. (1997) ADAM 7, a member of the ADAM (A Disintegrin And

Metalloproteinase) gene family is specifically expressed in the mouse anterior pituitary and epididymis. **Endocrinology** 138, 4262 - 4272.

Coussens, L. M., Fingleton, B. and Matrisian, L. M. (2002) Matrix metalloproteinase inhibitors and cancer: trials and tribulations. **Science** 295, 2387-2392.

Culig, Z., Hobisch, A., Cronauer, M.V., Radmayr, C., Trapman, J., Hittmair, A., Bartsch, G. and Klocker, H. (1994) Androgen receptor activation in prostatic tumor cell lines by insulin-like growth factor-I, keratinocyte growth factor, and epidermal growth factor. **Cancer Res** 54, 5474 - 5478.

Dallas, D.J., Genever, P.G., Patton, A.J., Millichip, M.I., Mckie, N. and Skerry, T.M. (1999) Localization of ADAM10 and Notch Receptors in Bone. **Bone** 25, 9-15.

Das, S.K., Yano, S., Wang, J., Edwards, D.R., Nagase, H. and Dey, S.K. (1997) Expression of matrix metalloproteinases and tissue inhibitor of matrix metalloproteinases in the mouse uterus during the peri-implantation period. **Dev Gen** 21, 44 – 54.

Daughady, W.H. and Rotwein, P. (1989) Insulin-like growth factors 1 and 2, peptide, messenger ribonucleic acid and gene structures, serum and tissue concentrations. **Endocr Rev** 10, 68-91.

Doedens, J.R. and Black, R.A. (2000) Stimulation-induced down-regulation of tumor necrosis factor-alpha converting enzyme. **J Biol Chem** 275, 14598-14607.

Duivenvoorden, W.C., Hirte, H.W., Singh, G. (1999) Transforming growth factor beta1 acts as an inducer of matrix metalloproteinase expression and activity in human bone-metastasising cancer cells. **Clin Exp Met** 17, 27-34.

Edelman, G. M. (1984) Cell adhesion and morphogenesis: the regulatory hypothesis. **Proc**

**Natl Acad Sci USA** 81, 1460-1464.

Egeblad, M. and Werb, Z. (2002) New functions for the matrix metalloproteinases in cancer progression. **Nat Rev Cancer** 2, 161 – 174.

Emi, M., Katagari, T., Harada, Y., Saito, H., Inazawa, J., Ito,I., Kasumi, F. and Nakamura, Y. (1992) A novel metalloprotease/disintegrin-like gene at 17q21.3 is somatically rearranged in two primary breast cancers. **Nat Genet** 5, 151 - 157.

Esquenet, M., Swinnen, J.V., Heyns, W. and Verhoeven, G. (1997) LNCaP prostatic adenocarcinoma cells derived from low and high passage numbers display divergent responses not only to androgens but also to retinoids. **J Steroid Biochem Mol Biol** 62, 391-399.

Eto, K., Puzon-McLaughlin, W., Sheppard, D., Sehara-Fujisawa, A., Zhang, X.P. and Takada, Y. (2000) RGD-independent binding of integrin alpha9beta1 to the ADAM-12 and -15 disintegrin domains mediates cell-cell interaction. **J Biol Chem** 275, 34922-34930.

Farnsworth, W.E. (1999) Prostate stroma: physiology. **Prostate** 38, 60-72.

Felding-Habermann, B. and Cheresh, D.A. (1993). VN and its receptors. **Curr Opin Cell Biol** 5, 864-868.

Fidler, I. J. and Ellis, L. M. (1994) The implications of angiogenesis for the biology and therapy of cancer metastasis. **Cell** 79, 185 - 188.

Folkman, J. and Klagsburn, M. (1987) Angiogenic factors. **Science** 235, 442 - 447.

Folkman, J. (1990) What is the evidence that tumours are angiogenesis dependent? **J Natl Cancer Inst** 82, 4-6.

Fong, C.J., Sherwood, E.R., Mendelsohn, J., Lee, C. and Kozlowski, J.M. (1992) Epidermal growth factor receptor monoclonal antibody inhibits constitutive receptor phosphorylation, reduces autonomous growth, and sensitises androgen-independent prostatic carcinoma cells to tumour necrosis factor alpha. **Cancer Res** 52, 5887 - 5892.

Fowlkes, J.L., Suzuki, K., Nagase, H. and Thrailkill, K.M. (1994) Proteolysis of insulin like growth factor binding protein-3 during rat pregnancy: a role for matrix metallproteinases. **Endocrinology** 135, 2810 - 2813.

Fowlkes, J.L., Thrailkill, K.M., Serra, D.M., Suzuki, K. and Nagase, H. (1995) Matrix metalloproteinases as insulin-like growth factor binding protein-degrading proteinases. **Prog Growth Factor Res** 6, 255 - 263.

Fowlkes, J.L., Thrailkill, K.M., Serra, D.M. and Nagase, H. (1997) Insulin-like growth factor binding protein (IGFBP) substrate zymography. A new tool to identify and characterize IGF-BP-degrading proteinases. **Endocrine** 7, 33 - 36.

Franzke, C.W., Tasanen, K., Schacke, H., Zhou, Z., Tryggvason, K., Mauch, C., Zigrino, P., Sunnarborg, S., Lee, D.C., Fahrenholz, F. and Bruckner-Tuderman, L. (2002) Transmembrane collagen XVII, an epithelial adhesion protein, is shed from the cell surface by ADAMs. **EMBO J** 21, 5026-35.

Gall, A-L., Ruff, M., Kannan, R., Cuniasse, P., Yiotakis, A., Dive, V., Rio, M-C., Basset, P. and Moras, D. (2001) Crystal Structure of the Stromelysin-3 (MMP-11) Catalytic Domain Complexed With a Phosphinic Inhibitor Mimicking the Transition-state. **J Mol Biol** 307, 577-586.

Gallegos, N.C., Smales, C., Savage, F.J., Hembry, R.M. and Boulos, P.B. (1995) The distribution of matrix metalloproteinases and tissue inhibitor of metalloproteinases in colorectal cancer. **Surg Oncol** 4, 21 - 29.

Gilpin, B.J., Loechel, F., Mattei, M., Engvall, E., Albrechtsen, R. and Wewer, U.M. (1998) A novel form of human ADAM 12 (meltrin α) provokes myogenisis *in vivo*. **J Biol Chem** 273, 157 - 166.

Gleason, D.F. (1966) Classification of prostatic carcinomas. **Cancer Chemother Rep** 50(3), 125-128.

Glynne-Jones, E., Goddard, L. and Harper, M.E. (1996) Comparative analysis of mRNA and protein expression for epidermal growth factor receptor and ligands relative to the proliferative index in human prostate tissue. **Human Path** 27, 688-694.

Goldberg, G.I., Marmer, B.L., Grant, G.A., Eisen, A.Z., Wilhelm, S. and He, C.S. (1989) Human 72-kilodalton type IV collagenase forms a complex with a tissue inhibitor of metalloproteases designated TIMP-2. **Proc Natl Acad Sci USA** 86, 8207 - 82011.

Goldberg, G.I., Strongin, A., Collier, I.E., Genrich, L.T. and Marmer, B.L. (1992) Interaction of 92-kDa type IV collagenase with the tissue inhibitor of metalloproteinases prevents dimerisation, complex formation of interstitial collagenase, and activation of the proenzyme with stromelysin. **J Biol Chem** 267, 4583-4591.

Gorlich, D. (1998) Transport into and out of the cell nucleus. **EMBO J** 17, 2721-7.

Gottschalk, C., Malberg, K., Arndt, M., Schmitt, J., Roessner, A., Schultze, D., Kleinstein, J. and Ansorge, S. (2000) Matrix metalloproteinases and TACE play a role in the pathogenesis of endometriosis. **Adv Exp Med Biol** 477, 483-6.

Gronberg, H. (2003) Prostate Cancer Epidemiology. **The Lancet** 361, 859-864.

Gumbiner, B.M. (1996) Cell adhesion: the molecular basis of tissue architecture and morphogenesis. **Cell** 84, 345 - 357.

Guo, C., Luttrell, L.M. and Price, D.T. (2000) Mitogenic signaling in androgen sensitive and insensitive prostate cancer cell lines. **J Urol** 163, 1027-32.

Haas, G.P. and Sakr, W.A. (1997) Epidemiology of Prostate Cancer. **Cancer J Clin** 47, 273-278.

Hans, H. G. (1995) Signal transduction mechanisms in cancer. **R. G. Landes Co., USA.**

Harper, M.E., Goddard, L., Glynne-Jones, E., Wilson, D.W., Price-Thomas, M., Peeling, W.B. and Griffiths, K. (1993) An immunochemical analysis of TGF-alpha expression in benign and malignant prostate. **Prostate** 23, 9-23.

Haywood-Reid, P.L., Zipf, D.R. and Springer, W.R. (1997) Quantification of integrin subunits on human prostatic cell lines-comparison of nontumorigenic and tumorigenic lines. **Prostate** 31, 1-8.

Holly, S.P., Larson, M.K. and Parise, L.V. (2000) Multiple roles of integrins in cell motility. Review. **Exp Cell Res** 261, 69-74.

Hooft van Huijsduijnen, R. (1998) ADAM 20 and 21; two novel human testis-specific membrane metalloproteases with similarity to fertilin-alpha. **Gene** 206, 273 - 282.

Horton, M.A. (1997). The alpha v beta 3 integrin "vitronectin receptor". **Int J Biochem Cell Biol** 29, 721-725.

Horwitz, A.R. and Parsons, J.T. (1999) Cell migration--movin' on. **Science.** 286, 1102 - 1103.

Humphrey, P.A., Keetch, C.W., Smith, D.S. and Catalona, W.J. (1996) Prospective characterization of pathologic features of prostate carcinomas detected via serum prostate specific antigen based screening. **J Urol** 155,816-20.

Huovila, A. J., Almeida, E. A. C. and White, J. M. (1996) ADAMs and cell fusion. **Curr Opin Cell Biol** 8, 692 - 699.

Hynes, R.O. (1992) Integrins: versatility, modulation and signalling in cell adhesion. **Cell** 69, 11 - 25.

Iba, K., Reidar, A., Gilpin, B.J., Loechel, F. and Wewer, U.W. (1999) Cysteine-Rich Domain of Human ADAM 12 (Meltrin α) Supports Tumor Cell Adhesion. **Amer J Path**, 154, 1489-1501.

Iba, K., Albrechtsen, R., Gilpin, B., Frohlich, C., Loechel, F., Zolkiewska, A., Ishiguro, K., Kojima, T., Liu, W., Langford, J.K., Sanderson, R.D., Brakebusch, C., Fassler, R., Wewer, U.M. (2000) The cysteine-rich domain of human ADAM 12 supports cell adhesion through syndecans and triggers signalling events that lead to beta1 integrin-dependent cell spreading. **J Cell Biol** 149, 1143-56.

Inoue, D., Reid, M., Lum, L., Kratzschmar, J., Weskamp, G., Myung, Y.M., Baron, R. and Blobel, C.P. (1998) Cloning and initial characterisation of mouse meltrin β and analysis of the expression of four metalloprotease-disintegrins in bone cells. **J Biol Chem** 273, 4180 - 4187.

Inoue, K., Slaton, J.W., Eve, B.Y., Kim, S.J., Perrotte, P., Balbay, M.D., Yano, S., Bar-Eli, M., Radinsky, R., Pettaway, C.A. and Dinney, C.P. (2000) Interleukin 8 expression regulates tumorigenicity and metastases in androgen-independent prostate cancer. **Clin Cancer Res** 6, 2104-19.

Iwamura, M., Sluss, P.M. and Casamento, J.B. (1993) Insulin-like growth factor 1: action and receptor characterisation in human prostate cancer cell lines. **Prostate** 22, 243 - 252.

Izumi, Y., Hirata, M., Hasuwa, H., Iwamoto, R., Umata, T., Miyado, K., Tamai, Y., Kurisaki, T., Sehara-Fujisawa, A., Ohno, S. (1998) A metalloprotease–disintegrin,

MDC9/meltrin-g/ADAM-9 and PKC are involved in TPA-induced ectodomain shedding of membrane-anchored heparin-binding EGF-like growth factor. **EMBO J** 17, 7260-7272.

Jarrad, D.F., Blitz, B.F., Smith, R.C., Patai, B.L. and Rukstalis, D.B. (1994) Effects of epidermal growth factor on prostate cancer line PC-3 growth and invasion. **Prostate** 24, 46-53.

Jeziorska, M., Haboubi, N.Y., Schofield, P.F., Ogata, Y., Nagase, H. and Woolley, D.E. (1994) Distribution of gelatinase B (MMP-9) and type IV collagen in colorectal carcinoma. **Int J Colorectal Dis** 9, 141 - 148.

Jia, L., Shimokawa, K., Bjarnason, J. B. and Fox, J.W. (1996) Snake venom metalloproteinases: Structure, function and relationship to the ADAMs family of proteins. **Toxicon** 34, 1269 - 1276.

Johansson, J.E., Holmberg, L., Johansson, S., Bergstrom, R. and Adami, H.O. (1997) Fifteen-year survival in prostate cancer: a prospective population-based trail in Sweden. **JAMA** 277, 467-471.

Jones, J.I., Gockerman, A., Busby, W.H.Jr., Wright, G. and Clemmons, D.R. (1993) Insulin like binding protein 1 stimulates cell migration and binds to the alpha5beta1 integrin by means of its Arg-Gly-Asp sequence. **Proc Natl Acad Sci USA** 90, 10553 - 10557.

Kadota, N., Suzuki, A., Nakagami, Y., Izumi, T. and Endo, T. (2000) Endogenous meltrin alpha is ubiquitously expressed and associated with the plasma membrane but exogenous meltrin alpha is retained in the endoplasmic reticulum. **J Biochem (Tokyo)** 128, 941 – 9.

Kawamata, H., Kawai, K., Kameyama, S., Johnson, M.D., Stetler-Stevenson, W.G., Oyasu, R. (1995) Over expression of tissue inhibitor of matrix metalloproteinases (TIMP1 and TIMP2) supresses extravasation of pulmonary metastasis of rat bladder carcinoma. **Int J**

**Cancer** 63, 680 - 687.

Kazmi, M.A., Dubin, R.A., Oddoux, C. and Ostrer, H. (1996) High-Level Inducible Expression of Visual Pigments in Transfected Cells. **Biotechniques** 21, 304-311.

Keck, P. J., Hauser, S. D., Krivi, G., Sanzo, K., Wqrren, T., Feder, J. and Connolly, D.T. (1989) Vascular permeability factor, and endothelial cell mitogen related to PDGF. **Science** 246, 1309 - 1312.

Kheradmand, F. and Werb, Z. (2002) Shedding light on sheddases: role in growth and development. **Bioessays** 24, 8-12.

Kim, J., Luo, W., Chen, D.T., Earley, K., Tunstead, J., Yu-Lee, L.Y. and Lin, S.H. (2003) Antitumor activity of the 16-kDa prolactin fragment in prostate cancer. **Cancer Res** 63, 386-393.

Kim, S.J., Uehara, H., Karashima, T., Shepherd, D.L., Killion, J.J. and Fidler, I.J. (2003) Blockade of Epidermal Growth Factor Receptor Signaling in Tumor Cells and Tumor-associated Endothelial Cells for Therapy of Androgen-independent Human Prostate Cancer Growing in the Bone of Nude Mice. **Clin Cancer Res** 9, 1200-1210.

Kini, R. M. and Evans, H. J. (1992) Structural domains in venom proteins: Evidence that metalloproteinases and nonenzymatic platelet aggregation inhibitors (disintegrins) from snake venom are derived by proteolysis from a common precursor. **Toxicon** 30, 265 - 293.

Klein, R.D., Maliner-Jongewaard, M.S., Udayakumar, T.S., Boyd, J.L., Nagle, R.B. and Bowden, G.T. (1999) Promatrilysin expression is induced by fibroblast growth factors in the prostatic carcinoma cell line LNCaP but not in normal primary prostate epithelial cells. **Prostate** 41, 215-23.

Kleiner, D.E. and Stetler-Stevenson, W.G. (1999) Matrix metalloproteinases and

metastasis. **Cancer Chemother Pharmacol** 43, S42 - S51.

Knauper, V., Wilhhelm, S. M., Seperack, P. K., DeClerck, Y. A., Langley, K. E., Osthues A. and Tsheshe, H. (1993) Direct activation of human neutrophil procollagenase by recombinant stromelysin. **Biochem J** 295, 581 - 586.

Koklitis, P. A., Murphy, G., Sutton, C. (1991) Purification of recombinant human prostromelysin. Studies on heat activation to give high-Mr and low-Mr active forms, and a comparison of recombinant with natural stromelysin activities. **Biochem J** 276, 217 - 221.

Kornberg, L.J. (1998) Focal adhesion kinase and its potential involvement in tumor invasion and metastasis. **Head Neck** 8, 745-52.

Kostenuik, P.J., Singh, G. and Orr, F.W. (1997). Transforming growth factor beta upregulates the integrin-mediated adhesion of human prostatic carcinoma cells to type I collagen. **Clin Exp Met** 15, 41-52.

Kouji, K., and Kouji, M. (1998) ADAMTS-1 protein anchors at the extracellular matrix through the thrombospondin type 1 motifs and its spacing region. **J Biol Chem** 273, 13912 – 13917.

Kozak, M. (1984) Compilation and analysis of sequences upstream from the translational start site in eukaryotic mRNAs. **Nucleic Acids Res** 12, 857-872.

Kozak, M. (1997). Recognition of AUG and alternative initiator codons is augmented by G in position 14 but is not generally affected by the nucleotides in positions 15 and 16. **EMBO J** 16, 2482–2492

Kubler, B., Cowell, S., Zapf, J. and Braulke, T. (1998) Proteolysis of insulin-like growth factor binding proteins by a novel 50-kilodalton metalloproteinase in human pregnancy serum. **Endocrinology** 139, 1556 - 1563.

Kuniyasu, H., Troncoso, P., Johnston, D., Bucana, C.D., Tahara, E., Fidler, I.J. and Pettaway, C.A. (2000) Relative expression of type IV collagenase, E-cadherin, and vascular endothelial growth factor/vascular permeability factor in prostatectomy specimens distinguishes organ-confined from pathologically advanced prostate cancers. **Clin Cancer Res** 6, 2295-2308.

Kuno, K., Kanada, N., Nakashima, E., Fujiki, F., Ichimura, F. and Matsushima, K. (2000) Molecular cloning of a gene encoding a new type of metalloproteinase-disintegrin family protein with thrombospondin motifs as an inflammation associated gene. **J Biol Chem.** 272, 556-62.

Labrie, F., Candas, B., Cusan, L., Gomez, J.L., Diamond, P., Suburu, R. and Lemay, M. (1996) Diagnosis of advanced or noncurable prostate cancer can be practically eliminated by prostate-specific antigen. **Urology** 47, 212-217.

Labrousse, A.L., Buisson-Legendre, N., Hornebeck, W. and Bernard, P. (2002) The metalloprotease-directed shedding of BP 180 (collagen XVII) from human keratinocytes in culture is unaffected by ceramide and cell-matrix interaction. **Eur J Dermatol** 12, 240-6.

Lalani, E.N., Stubbs, A. and Stamp, G.W.H. (1997) Prostate cancer; the interface between pathology and basic scientific research. **Cancer Biol** 8, 53 - 59.

Lammich, S., Kojro, E., Postina, R., Gilbert, S., Pfeiffer, R., Jasionowski, M., Haass, C. and Fahrenholz, F. (1999) Constitutive and regulated alpha-secretase cleavage of Alzeimer's amyloid precursor protein by a disintegrin metalloprotease. **Proc Natl Acad Sci USA** 96, 3922 - 3927.

Leavesley, D.I., Schwartz, M.A., Rosenfeld, M. and Cheresh, D.A. (1993). Integrin β1- and β3-mediated endothelial cell migration is triggered through distinct signalling mechanisms. **J Cell Biol** 121, 168–170.

Leavesley, D.I, Oliver, J.M., Swart, B.W., Berndt, M.C., Haylock, D.N. and Simmons, P.J. (1994) Signals from platelet/endothelial cell adhesion molecule enhance the adhesive activity of the very late antigen-4 integrin of human CD34+ hemopoietic progenitor cells. **J Immunol** 153, 4673-4683.

Lee, C. (1996) Role of androgen in prostate growth and regression: stromal-epithelial interaction. **Prostate** 6(Suppl), 52-56.

Leventhal, P.S. and Feldman, E.L. (1997) Insulin like growth factor as regulators of cell motility. **Transmission Electron Microscopy** 8, 1 - 6.

Levi, F., Lucchini, F., Negri, E., Boyle, P. and La Vecchia, C. (2003) Mortality from major cancer sites in the European Union, 1955-1998. **Ann Oncol** 14, 490-495.

Liao, X, Thrasher, J.B., Pelling, J., Holzbeierlein, J., Sang, Q.X. and Li, B. (2003) Androgen stimulates matrix metalloproteinase-2 expression in human prostate cancer. **Endocrinology** 144, 1656-1663.

Loechel, F., Gilpin, B.J., Engvall, E., Albrechtsen, R. and Wewer, U.M. (1998) Human ADAM 12 (meltrin alpha) is an active metalloprotease. **J Biol Chem** 273, 16993 - 16997.

Loechel, F., Overgaard, M.T., Oxvig, C., Albrechtsen, R. and Wewer, U.M. (1999) Regulation of human ADAM 12 protease by the prodomain. Evidence for a functional cysteine switch. **J Biol Chem** 174, 13427 - 13433.

Loechel, F., Fox, J.W., Murphy, G., Albrechtsen, R., Wewer, U.M. (2000) ADAM 12-S cleaves IGFBP-3 and IGFBP-5 and is inhibited by TIMP-3. **Biochem Biophys Res Comm** 278, 511-515.

Long, L., Navab, R. and Brodt, P. (1998) Regulation of the Mr 72,000 type IV collegenase by the type I insulin like growth factor receptor. **Cancer Res** 58, 3243 - 3247.

Mackay, A.R., Ballin, M., Pelina, M.D., Farina, A.R., Nason, A.M., Hartzler, J.L. and Thorgeirsson, U.P. (1992) Effect of phorbol ester and cytokines on matrix metalloproteinase and tissue inhibitor of metalloproteinase expression in tumor and normal cell lines. **Inv & Met** 12, 168 - 84.

Mahimkar, R.M., Baricos, W.H., Visaya, O., Pollock, A.S., Lovett, D.H. (2000) Identification, cellular distribution and potential function of the metalloprotease-disintegrin MDC9 in the kidney. **J Am Soc Nephrol** 11, 595-603.

Marcelli. M., Ittmann, M., Mariani, S., Sutherland, R., Nigam, R., Murthy, L., Zhao, Y., DiConcini, D., Puxeddu, E., Esen, A., Eastham, J., Weigel, N.L. and Lamb, D.J. (2000) Androgen receptor mutations in prostate cancer. **Cancer Res** 60, 944-949.

Maskos, K., Fernandez-Catalan, C., Huber, R., Bourenkov, G.P., Bartunik, H., Ellestad, G.A., Reddy, P., Wolfson, M.F., Rauch, H.T., Castner, B.J., Davis, R., Clarke, H.R.G.,

Matrisian, L.M., (1990) Metalloproteinases and their inhibitors in matrix remodelling. **Trends Genet** 6,121 - 125.

Matsumoto, K., Ziober, B.L., Yao, C. and Kramer, H. (1995) Growth factor regulation of integrin mediated cell motility. **Cancer Met Rev** 14, 205 - 217.

McCulloch, D.R., Harvey, M. and Herington, A.C. (2000) Expression of the ADAMs family of proteases in prostate cancer cell lines and their regulation by dihydrotestosterone. **Mol Cell Endo** 167, 11-21.

Mechtersheimer, S., Gutwein, P., Agmon-Levin, N., Stoeck, A., Oleszewski, M., Riedle, S., Postina, R., Fahrenholz, F., Fogel, M., Lemmon, V. and Altevogt, P. (2001) Ectodomain shedding of L1 adhesion molecule promotes cell migration by autocrine binding to integrins. **J Cell Biol** 155, 661 - 673.

Mettlin C, Murphy GP, Lee F, Littrup PJ, Chesley A, Babaian R, Badalament R, Kane RA, Mostofi FK (1994) Characteristics of prostate cancer detected in the American Cancer Society National Prostate Cancer Detection Project. **J Urol** 152, 1737-1740.

Meyer-Siegler, K. (2000) Macrophage migration inhibitory factor increases MMP-2 activity in DU-145 prostate cells. **Cytokine** 12, 914-21.

Mignatti, P. and Rifkin, D. (1993) Biology and biochemistry of proteinases in tumour invasion. **Physiol Rev** 73, 161 – 195.

Milla, M., Clay, W.C., Carter, H.L., Miller, A.B., Su, J., Lambert, M.H., Willard, D.H., Sheeley, D.M., Kost, T.A., Burkhart, W., Moyer, M., Blackburn, R.K., Pahel, G.L., Mitchell, J.L., Hoffman, C.R. and Becherer, J.D. (1999) Specific sequence elements are required for the expression of functional tumour necrosis factor enzyme (TACE). **J Biol Chem** 43, 30563 - 30570.

Millichip, M. I., Dallas, D. J., Wu, E., Dale, S. and McKie, N. (1998) The metallo-disintegrin ADAM 10 (MADM) from bovine kidney has type IV collagenase activity *in vitro*. **Biochem Biophys Res Comm** 245, 594 - 598.

Mohan, S., Thompson, G.R., Amaar, Y.G., Hathaway, G., Tschesche, H. and Baylink, D.J. (2002) ADAM-9 is an insulin-like growth factor binding protein-5 protease produced and secreted by human osteoblasts. **Biochemistry** 41, 15394-403.

Moll, U.M., Youngleib, G.L., Rosinski, K.B. and Quigley, J.P. (1990) Tumour promoter-stimulated Mr 92,000 gelatinase secreted by normal and malignant human cells:isolation and characterisation of the enzyme from HT1080 tumour cells. **Cancer Res** 50, 6162 - 6170.

Montgomery, B.T., Young, C.Y.F., Bilhartz, D.L., Andrews, P.E., Prescott, J.L., Thompson, N.F. and Tindall, D.J. (1992). Hormonal regulation of prostate specific antigen

(PSA) glycoprotein in the human prostate adenocarcinorna cell line, LNCaP. **Prostate** 21, 63-73.

Mundy, G. R. and Yoneda, T. (1996) Mechanisms of Bone Metastasis In: F. W. O. a. G. Singh (ed.), Bone metastasis - Mechanisms and Pathophysiology. **Austin: R.G. Landes.**

Murphy, G., Ward, R., Hembry, R.M., Reynolds, J.J., Kuhn, K. and Tryggvason, K. (1989) Characterisation of gelatinase from pig polymorphonuclear leucocytes. A metalloproteinase resembling tumour type IV collagenase. **Biochem J** 258, 463 - 472.

Murphy, G. and Docherty, J.P. (1992) The matrix metalloproteases and their inhibitors. **Amer J Resp Cell Mol Biol** 7, 120 - 125.

Nagakawa, O., Murakami, K., Yamaura, T., Fujiuchi, Y., Murata, J., Fuse, H., Saiki, I. (2000) Expression of membrane-type 1 matrix metalloproteinase (MT1-MMP) on prostate cancer cell lines. **Cancer Lett** 155, 173-9.

Nagase, H., Enghild, J.J., Suzuki, K. and Salvesen, G. (1990) Stepwise activation mechanisms of the precursor of matrix metalloproteinase 3 (stromelysin) by proteinases and (4-aminophenyl)mercuric acetate. **Biochemistry** 29, 5783 – 5789.

Nagase, H. (1997) Activation mechanisms of matrix metalloproteinases. **Biol Chem** 378, 151 - 160.

Nagle, R.B., Knox, J.D., Wolf, C., Bowden, G.T. and Cress, A.E. (1994) Adhesion molecules, extracellular matrix, and proteases in prostate carcinoma. **J Cell Biochem** Supp(19), 232 – 237.

Nagle, R.B., Hao, J., Knox, D., Dalkin, B.L., Clark, V. and Cress, A.E. (1995) Expression of Hemidesmosomal and Extracellular Matrix Proteins by Normal and Malignant Human Prostate Tissue. **Amer J Path** 146, 1498 - 1507.

Nath, D., Slocombe, P.M., Stephens, P.E., Warn, A., Hutchinson, G.R., Yamada, K.M., Docherty, A.J. and Murphy, G. (1999) Interaction of metargidin (ADAM-15) with alphaVbeta3 and alpha5beta1 integrins on different haemopoetic cells. **J Cell Sci** 112, 579 - 587.

Nomura, H., Sato, H., Seiki, M., Mai, M. and Okada, Y. (1995) Expression of membrane type metalloprotease in human gastric carcinomas. **Cancer Res** 55, 3263-3266.

Ohuchi, E., Imai, K., Fujii, Y., Sato, H., Seiki, M., Okada, Y. (1997) Membrane type 1 matrix metalloproteinase digests interstitial collagens and other extracellular matrix macromolecules. **J Biol Chem** 272, 2446-51.

Okada, Y., Harris, E.D., Jr. and Nagase, H. (1988) The precursor of a metalloendopeptidase from human rheumatoid synovial fibroblasts. Purification and mechanisms of activation by endopeptidases and 4-aminophenylmercuric acetate. **Biochem J** 254, 731-741.

Optenberg, S.A. and Thompson, I.M. (1990) Economics of screening for carcinoma of the prostate. **Urol Clin North Am** 17, 719-1737.

Orio, F., Terouanne, B., Georget, V., Lumbroso, S., Avances, C., Siatka, C. and Sultan, C. (2002) Potential action of IGF-1 and EGF on androgen receptor nuclear transfer and transactivation in normal and cancer human prostate cell lines.
**Mol Cell Endo** 198:105 - 114.

Ornstein, D.K., Gillespie, J.W., Paweletz, C.P., Duray, P.H., Herring, J., Vocke, C.D., Topalian, S.L., Bostwick, D.G., Linehan, W.M., Petricoin, E.F. 3rd. and Emmert-Buck, M.R. (2000) Proteomic analysis of laser capture microdissected human prostate cancer and in vitro prostate cell lines. **Electrophoresis** 21, 2235-2242.

Pajouh, M.S., Nagle, R.B., Breathnach, R., Finch, J.S., Brawer, M.K. and Bowden, G.T.

(1991) Expression of metalloproteinase genes in human prostate cancer **J Cancer Res Clin Oncol** 117, 144-150.

Palacios, I., Hetzer, M., Adam, S.A. and Mattaj, I.W. (1997) Nuclear import of U snRNPs requires importin beta. **EMBO J** 16, 6783-6792.

Paweletz, C.P., Liotta, L.A. and Petricoin, E.F. 3rd (2001) New technologies for biomarker analysis of prostate cancer progression: Laser capture microdissection and tissue proteomics. **Urology** 57(4Suppl 1), 160-163.

Peng, L., Tang, S., Xie, J., Luo, T. and Dai, B. (2002) Quantitative analysis of IGF-I and its application in the diagnosis of prostate cancer. **Hua Xi Yi Ke Da Xue Xue Bao** 33, 137-139.

Pepper, M. S., Belin, P., Montesano, R., Orci, L. and Vassalli, J.D. (1990) Transforming growth factor β1 modulates fibroblast growth factor induced proteolytic and angiogenic properties of endothelial cells *in vitro*. **J Cell Biol** 111, 743 - 755.

Petersen, M., Fitzner, J.N., Ceretti, D.P., March, C.J., Paxton, R.J., Black, R.A. and Wolfram, B. (1998) Crystal structure of the catalytic domain of human tumour necrosis factor-alpha-converting enzyme. **Proc Natl Acad Sci USA** 95, 3408 - 3412.

Presta, M., Maier, J. A. and Ragnotti, G. (1989) The mitogenic signalling pathway but not the plasminogen activator-inducing pathway of basic fibroblast growth factor is mediated through protein kinase C in fetal bovine aortic endothelial cells. **Mol Cell Biol** 109, 1877 - 1884.

Primakoff, P. and Myles, D.G. (2000) The ADAMs gene family: surface proteins with adhesion and protease activity. **Trends Genet** 16, 83 - 87.

Pusztai, L., Lewis, C. E. and Yap, E. (1996) Cell proliferation in cancer. **Oxford**

**University Press Inc., USA.**

Pyke, C., Ralfkiaer, E., Tryggvason, K. and Dano, K. (1993) Messenger RNA for two type IV collagenases is located in stromal cells in human colon cancer. **Amer J Pathol** 142, 359 - 365.

Rabbani, S.A., Harakidas, P., Guo, Y., Steinman, D., Davidsen, S.K. and Morgan, D.W. (2000) Synthetic inhibitor of matrix metalloproteases decreases tumor growth and metastases in a syngeneic model of rat prostate cancer in vivo. **Int J Cancer** 87, 276-282.

Rabinovitz, I., Nagle, R.B. and Cress, A.E. (1995) Integrin alpha 6 expression in human prostate carcinoma cells is associated with a migratory and invasive phenotype in vitro and in vivo. **Clin Exp Metastasis** 13, 481-91.

Rajah, R., Valentinis, B. and Cohen, P. (1997) Insulin-like growth factor (IGF)- binding protein-3 induces apoptosis and mediates the effects of transforming growth factor-beta1 on programmed cell death through a p53- and IGF-independent mechanism. **J Biol Chem** 272, 12181-12188.

Reinikainen, P., Palvimo, J.J. and Janne, O.A., 1996. Effects of mitogens on androgen receptor-mediated transactivation. **Endocrinology** 137, 4351- 4357.

Reinmer, P., Grams, F., Huber, R., Kleine, T., Schnierer, S., Piper, M., Tschesche, H. and Bode, W. (1994) Structural implications for the role of the N terminus in the 'superactivation' of collagenases. A crystallographic study. **FEBS Letters** 338, 227 - 223.

Roghani, M.J., Becherer, D., Moss, M.L., Atherton, R.E., Erdjument-Bromage, H., Arribas, J., Blackburn, R.K., Weskamp, G., Tempst, P. and Blobel, C.P. (1999) Metalloprotease-Disintegrin MDC9: Intracellular Maturation and Catalytic Activity. **J Biol Chem** 274, 3531-3540.

Roodman, G.D. (2001) Biology of osteoclast activation in cancer. **J Clin Oncol** 19(15), 3562 - 3571.

Rosendahl, M. S., Ko, S. C., Long, D. L., Brewer, M.T., Rosenweig, B., Hedl, E., Anderson, L., Pyle, S.M., Moreland, J., Meyers, M.A., Kohno, Y., Lyons, D. and Lichenstein, H.S. (1997) Identification and characterisation of a pro-tumour necrosis factor-α-processing enzyme from the ADAM family of zinc metalloproteases. **J Biol Chem** 272, 24588 - 24593.

Rubens, R. D. (1998) Bone metastases - the clinical problem. **Eur J Cancer**, 34, 210-213.

Rubin, M.A. (2001) Use of laser capture microdissection, cDNA microarrays, and tissue microarrays in advancing our understanding of prostate cancer. **J Pathol**.195, 80-6.

Rucklidge, G.J., Edvardsen, K. and Bock, E. (1994) Cell-adhesion molecules and metalloproteinases: a linked role in tumour cell invasiveness. **Biochem Soc Trans** 22, 63 - 8.

Russell, P.J., Bennett, S. and Stricker, P. (1998) Growth factor involvement in progression of prostate cancer. **Clin Chem** 44, 705 - 723.

Sanchez-Sweatman, O.H., Orr, F.W. and Singh, G. (1999) Human metastatic prostate PC3 cell lines degrade bone using matrix metalloproteinases. **Inv & Met** 18, 297-305.

Sato, Y. and Rifkin, D. B. (1988) Autocrine activities of basic fibroblast growth factor: Regulation of endothelial cell movement, plasminogen activator synthesis and DNA synthesis. **J Cell Biol** 107, 1199 - 1205.

Sato, H., Takino, T., Okada, Y., Cao, J., Shinagawa, A., Yamamoto, E. and Seiki, M. (1994) A matrix metalloprotease expression on the surface of invasive tumour cells. **Nature** 370, 61-65.

Sato, T., del Carmen, O. M., Hou, P., Heegaard, A. M., Kumegawa, M., Foged, N. T. and Delaisse, J. M. (1997) Identification of the membrane-type matrix metalloproteinase MT1-MMP in osteoclasts. 110, 589-596.

Scaletscky, R., Koch, M.O., Eckstein, C.W., Bicknell, S.L., Gray, G.F. Jr. and Smith, J.A. Jr. (1994) Tumor volume and stage in carcinoma of the prostate detected by elevations in prostate specific antigen. **J Urol** 152, 129-131.

Schlondorff, J., Becherer, J.D. and Blobel, C.P. (2000) Intracellular maturation and localization of the tumour necrosis factor alpha convertase (TACE) **Biochem J** 347, 131 - 138.

Schvartz, I., Seger, D. and Shaltiel, S. (1999) Vitronectin. **Int J Biochem Cell Biol** 31, 539-544.

Schwettmann, L. and Tschesche, H. (2001) Cloning and Expression in *Pichia pastoris* of Metalloprotease Domain of ADAM 9 Catalytically Active against Fibronectin. **Prot Exp Pur** 21, 65–70.

Shalinsky, D. R., Brekken, J., Zou, H., McDermott, C. D., Forsyth, P., Edwards, D., Margosiak, S., Bender, S., Truitt, G., Wood, A., Varki, N. M. and Appelt, K. (1999) Broad antitumor and antiangiogenic activities of AG3340, a potent and selective MMP inhibitor undergoing advanced oncology clinic al trials. **Ann N Y Acad Sci** 878, 236-270.

Siegsmund, M.J., Yamazaki, H. and Pastan, I. (1994). Interleukin 6 receptor mRNA in prostate carcinomas and benign prostate hyperplasia. **J Urol** 151, 1396-1399.

Skovronsky, D.M., Blaine Moore, D., Milla, M.E., Doms, R.W. and Lee, V. M-Y. (2000) Protein Kinase C-dependent α-Secretase Competes with β-Secretase for Cleavage of Amyloid-β Precursor Protein in the Trans-Golgi Network. **J Biol Chem** 275, 2568-2575.

Springman, E.B., Angelton, E.L., Birkedl-Hanson, H. and Van Wart, H.E. (1990) Multiple modes of activation of latent human fibroblast collegenase: evidence for the role of $cys^{73}$ active-site Zn complex in latency and a cysteine switch mechanism for activation. **Proc Natl Acad Sci USA** 87, 364 - 368.

Stearns, M.E. and Wang, M. (1998). Alendronate blocks metalloproteinase secretion and bone collagen I release by PC-3 ML cells in SCID mice. **Clin Exp Met** 16, 693-702.

Steiner, H., Godoy-Tundidor, S., Rogatsch, H., Berger, A.P., Fuchs, D., Comuzzi, B., Bartsch, G., Hobisch, A. and Culig, Z. (2003) Accelerated in vivo growth of prostate tumors that up-regulate interleukin-6 is associated with reduced retinoblastoma protein expression and activation of the mitogen-activated protein kinase pathway. **Amer J Pathol** 162, 655-663

Sternlicht, M.D. and Bergers, G. (2000) Matrix metalloproteinases as emerging targets in anticancer therapy: status and prospects. **Emerging Therapeutic Targets** 4, 609-633.

Steinman, D.H., Curtin, M.L., Garland, R.B., Davidsen, S.K., Heyman, R.R., Holms, J.H., Albert, D.H., Magoc, T.J., Nagy, I.B., Marcotte, P.A., Li, J., Morgan, D.M., Hutchins, C. and Summers, J.B. (1998). The design, synthesis and structure activity relationships of a series of macrocyclic MMP inhibitors. **Bioorg Medical Chem Lett** 8, 2087-2092.

Stetler-Stevenson, W.G., Hewitt, R. and Corcoran, M. (1996) Matrix metalloproteinases and tumor invasion: from correlation and causality. **seminars in Cancer Biology** 7, 147 - 154.

Still, K., Robson, C.N., Autzen, P., Robinson, M.C. and Hamdy, F.C. (2000) Localization and quantification of mRNA for matrix metalloproteinase-2 (MMP-2) and tissue inhibitor of matrix metalloproteinase-2 (TIMP-2) in human benign and malignant prostatic tissue. **Prostate** 42, 18-25.

Sugiura, T. and Berditchevski, F. (1999) Function of alpha3beta1-tetraspanin protein

complexes in tumour cell invasion. Evidence for the role of the complexes in production of matrix metalloproteinase 2 (MMP-2). **J Cell Biol** 146, 1375 - 1389.

Sumitomo, M., Tachibana, M., Nakashima, J., Murai, M., Miyajima, A., Kimura, F., Hayakawa, M. and Nakamura, H. (1999) An essential role for nuclear factor kappa B in preventing TNF-alpha induced cell death in prostate cancer. **J Urol** 161, 674 - 679.

Sundareshan, P., Nagle, R.B. and Bowden, G.T. (1999) EGF induces the expression of matrilysin in the human prostate adenocarcinoma cell line, LNCaP. **Prostate** 40, 159 – 166.
Suzuki, K., Enghild, J.J., Morodomi, T., Salvesen, G. and Nagase, H. (1990) Mechanisms of activation of tissue procollagenase by matrix metalloproteinase 3 (stromelysin). **Biochemistry** 29, 10261 - 10270.

Tang, B.L. (2001) ADAMTS: a novel family of extracellular matrix proteases. **Int J Biochem Cell Biol** 33, 33–44.

Taraboletti, G., C'Ascenzo, S.D., Borsotti, P., Giavazzi, R., Pavan, A. and Dolo, V. (2002) Shedding of the Matrix Metalloproteinases MMP-2, MMP-9 and MT1-MMP as Membrane Vesicle Associated Components by Endothelial Cells. **Amer J Path** 160, 673-680.

Telford, N.A., Hogan, A., Franz, C.R. and Schultz, G.A. (1990) Expression of genes for insulin and insulin-like growth factors and receptors in early postimplantation mouse embryo and embryonal carcinoma cells. **Mol Reprod Develop** 26, 81-92.

Thin, T.H., Wang, L., Kim, E., Collins, L.L., Basavappa, R. and Chang, C. (2003) Isolation and characterization of androgen receptor mutant, AR(M749L), with hypersensitivity to 17-beta estradiol treatment. **J Biol Chem** 278, 7699-7708.

Trikha, M., Timar, J., Lundy, S.K., Szekeres, K., Tang, K., Grignon, D., Porter, A.T. and Honn, K.V. (1996) Human prostate carcinoma cells express functional alphaIIb(beta)3 integrin. **Cancer Res** 56, 5071-5078.

Ueda, Y., Imai, K., Tsuchiya, H., Fujimoto, N., Nakanishi, I., Katsuda, S., Seiki, M. and Okada, Y. (1996) Matrix metalloproteinase 9 (gelatinase B) is expressed in multinucleated giant cells of human giant cell tumour of bone and is associated with vascular invasion. **Amer J Path** 148, 611 - 622.

Ueda, T., Bruchovsky, N. and Sadar, M.D. (2001) Activation of the androgen receptor N-terminal domain by IL-6 via MAPK and STAT3 signal transduction pathways. **J Biol Chem.** 277, 7076-7085.

Upadhyay, J., Shekarriz, B., Nemeth, J.A., Dong, Z., Cummings, G.D., Fridman, R., Sakr, W., Grignon, D.J. and Cher, M.L. (1999) Membrane type 1-matrix metalloproteinase (MT1-MMP) and MMP-2 immunolocalization in human prostate: change in cellular localization associated with high-grade prostatic intraepithelial neoplasia. **Clin Cancer Res** 5, 4105-10.

van Bokhoven, A., Varella-Garcia, M., Korch, C. and Miller, G.J. (2001) TSU-Pr1 and JCA-1 cells are derivatives of T24 bladder carcinoma cells and are not of prostatic origin. **Cancer Res** 61, 6340-6344.

Vankemmelbeke, M.N., Jones, G.C., Fowles, C., Ilic, M.Z., Handley, C.J., Day, A.J., Knight, C.G., Mort, J.S. and Buttle DJ. (2003) Selective inhibition of ADAMTS-1, -4 and -5 by catechin gallate esters. **Eur J Biochem** 270, 2394-2403.

Van Wart, H.E. and BirkDal-Hansen, H. (1990) The cysteine switch: A principle of regulation of metalloproteinase activity with potential applicability to the entire matrix metalloproteinase gene family. **Proc Natl Acad Sci USA** 87, 5578 - 5582.

Veldscholte, J., Ris-Stalpers, C., Kuiper, G.G., Jenster, G., Berrevoets, C., Claassen, E., van Rooij, H.C., Trapman, J., Brinkmann, A.O. and Mulder, E. (1990) A mutation in the ligand binding domain of the androgen receptor of human LNCaP cells affects steroid binding characteristics and response to anti-androgens. **Biochem Biophys Res Comm** 173, 534-

540.

Vihko, P., Kontturi, M., Lukkarinen, O., Ervasti, J. and Vihko, R. (1985) Screening for carcinoma of the prostate: rectal examination and enzymatic radioimmunologic measurements of serum acid phosphatase compared. **Cancer** 56, 173-177.

Vile, R. G. (1995) Cancer metastasis: From mechanisms to therapies. **Jacaranda Wiley Ltd. Australia.**

Vincent, B., Paitel, E., Saftig, P., Frobert, Y., Hartmann, D., De Strooper, B., Grassi, J., Lopez-Perez, E. and Checler, F. (2001). The disintegrins ADAM-10 and TACE contribute to the constitutive and phorbol-esters-regulated normal cleavage of the cellular prion protein. **J. Biol. Chem.** 276, 37743-37746.

Ware, J.L. (1994) Prostate cancer progression. Implications of histopathology. **Amer J Pathol** 145, 983-993.

Warner, J. and Whitmore, W.F. Jr. (1994) Expectant management of clinically localized prostate cancer. **J Urol** 152, 1757-1760.

Wayner, E.A., Carter, W.G., Piotrowicz, R.S. and Kunicki, T.J. (1988) The function of multiple extracellular matrix receptors in cell adhesion to the extracellular matrix: Preparation of monoclonal antibodies to the fibronectin receptor that specifically inhibit cell adhesion to fibronectin and react with platelet glycoproteins Ic-IIa. **J Cell Biol**107, 1881 - 1889.

Wayner, E.A., Orlando, R.A. and Cherish, D.A. (1991) Integrins $\alpha V\beta 3$ and $\alpha V\beta 5$ contribute to cell attachment to vitronectin but differentially distribute on the cell surface. **J Cell Biol** 113, 919 - 929.

Weskamp, G., Krätzschmar, J.R., Reid, M. and Blobel, C.P. (1996). MDC9, a widely

expressed cellular disintegrin containing cytoplasmic SH3 ligand domains. **J Cell Biol** 132, 717-726.

Whiteside, E.J., Boucaut, K.J., Jackson, M.M., Teh, A., Herington, A.C. and Harvey, M.B. (1998), Expression of members of the ADAMS gene family in placental tissues. **Biol Reprod** 58 (Suppl.1), 96.

Whiteside, E.J., Jackson, M.M., Herington, A.C., Edwards, D.R. and Harvey, M.B. (2001) Matrix metalloproteinase-9 and tissue inhibitor of metalloproteinase-3 are key regulators of extracellular matrix degradation by mouse embryos. **Biol Reprod** 64, 1331-1337.

Will, H., Atkinson, S.J., Butler, G.S., Smith, B. and Murphy, G. (1996). The soluble catalytic domain of membrane type 1 matrix metalloproteinase cleaves the propeptide of progelatinase A and initiates autoproteolytic activation-regulation by TIMP-2 and TIMP-3. **J Biol Chem** 271, 17119 - 17123.

Wolfsberg, T. G., Primakoff, P., Myles, D. G. and White, J.M. (1995) ADAM, a novel family of membrane proteins containing A Disintgrin And Metalloprotease Domain: Multipotential functions in cell-cell and cell-matrix interactions. **J Cell Biol** 131, 275 - 278.

Wu, H.C., Hseih, J.T., Gleave, M.E., Brown, N.M., Pathak, S. and Chung, W.K. (1994) Derivation of androgen-independent human LNCaP prostatic cancer cell sublines: role of bone stromal cells **Int J Cancer** 57, 406-412.

Wu, E., Croucher, P.I. and Mckie N. (1997) Expression of members of the novel membrane linked metalloproteinase family ADAM in cells derived from a range of haematological malignancies. **Biochem Biophys Res Comm** 235, 437 - 442.

Xu, B.J., Caprioli, R.M., Sanders, M.E. and Jensen, R.A. (2002) Direct analysis of laser capture microdissected cells by MALDI mass spectrometry. **J Am Soc Mass Spectrom** 13,

1292-1297.

Yacoub, A., McKinstry, R., Hinman, D., Chung, T., Dent, P. and Hagan, M. P. (2003) Epidermal Growth Factor and Ionizing Radiation Up-regulate the DNA Repair Genes XRCC1 and ERCC1 in DU145 and LNCaP Prostate Carcinoma through MAPK Signaling. **Radiat Res** 159, 439-452.

Yamagata, S., Yoshii, Y., Suh, J.G., Tanaka, R. and Shimizu, S. (1991) Occurrence of an active form of gelatinase in human gastric and colorectal carcinoma tissues. **Cancer Letters** 59, 51 - 55.

Yan, Y., Shirakabe, K. and Werb, Z. (2002) The metalloprotease Kuzbanian (ADAM10) mediates the transactivation of EGF receptor by G protein-coupled receptors. **J Cell Biol** 158, 221-226

Yu, Q. and Stamenkovic, I. (1999) Localisation of matrix metalloprotease 9 to the cell surface provides a mechanism for CD44-mediated tumour invasion. **Genes Dev** 13, 35-48.

Zeng, Z.S. and Guillem, J.G. (1995) Distinct pattern of matrix metalloproteinase 9 and tissue inhibitor of metalloproteinase 1 mRNA expression in human colorectal cancer and liver metastases. **British J Cancer** 72, 575 - 582.

Zern, A. Z. and Reid, L. M. (1993) Extracellular matrix. **Marcel Dekker Inc., USA.**

Zhang, X., Kamata, T., Yokoyama, K., Puzon-McLaughlin, W. and Takada, Y. (1998) Specific interaction of the recombinant disintegrin-like of MDC-15 (metargidin, ADAM 15) with integrin $\alpha 5\beta 3$. **J Biol Chem** 273, 7345 - 7350.

Zhang, Y., Jiang, J., Black, R.A., Baumann, G. and Frank, S.J. (2000) Tumor necrosis factor-alpha converting enzyme (TACE) is a growth hormone binding protein (GHBP) sheddase: the metalloprotease TACE/ADAM-17 is critical for (PMA-induced) GH receptor

proteolysis and GHBP generation. **Endocrinology** 141, 4342-4348

Zhau, H.E., Li, C.L. and Chung, L.W. (2000) Establishment of human prostate carcinoma skeletal metastasis models. **Cancer** 88(12 Suppl), 2995-3001.

Zheng, D.Q., Woodard, A.S., Fornaro, M., Tallini, G. and Languino, L.R. Prostatic (1999) carcinoma cell migration via alpha(v)beta3 integrin is modulated by a focal adhesion kinase pathway. **Cancer Res** 59, 1655-64.

Zhou, M., Graham, R., Russell, G. and Croucher, P.I. (20001) MDC-9 (ADAM-9/Meltrin gamma) functions as an adhesion molecule by binding the alpha(v)beta(5) integrin. **Biochem Biophys Res Comm** 280, 574 - 580.

Zhu, H.J., Ross, F.P. and Teitelbaum, S.L. (1996) Phorbol myristate acetate transactivates the avian beta 3 integrin gene and induces alpha V beta 3 integrin expression. **J Cell Biochem** 61, 420 - 429.

Zolkiewska, A. (1999) Disintegrin-like/cysteine-rich region of ADAM 12 is an active cell adhesion domain. **Exp Cell Res** 252, 423-31.

Zucker, S., Lysik, R.M., Zarrabi, M.H., and Moll, U. (1993) Mr 92,000 type IV collagenase is increased in plasma of patients colon cancer and breast cancer. **Cancer Res** 53, 140 -146.

Zucker, S., Cao, J. and Chen, W. T. (2000) Critical appraisal of the use of matrix metalloproteinase inhibitors in cancer treatment. **Oncogene** 19, 6642-6650.